

Dissertation

Zur Erlangung des Doktorgrades der Fakultät für Chemie und
Pharmazie der Ludwig-Maximilians-Universität zu München



Precise Oligoethylenimine-based Carriers for Nucleic
Acid Delivery

Development of a Novel Solid-Phase Polymer Synthesis Platform

Vorgelegt von
David Henning Schaffert
aus Wesel

2010

Aus dem Leben eines Taugenichts
Joseph von Eichendorff

Erklärung

Diese Dissertation wurde im Sinne von § 13 Abs. 3 bzw. 4 der Promotionsordnung vom 29. Januar 1998 von Professor Dr. Ernst Wagner betreut.

Ehrenwörtliche Versicherung

Diese Dissertation wurde selbständig, ohne unerlaubte Hilfe erarbeitet.

München, am 10.08.2010

.....
(Unterschrift des Autors)

Dissertation eingereicht am 10.08.2010

1. Gutacher: Prof. Dr. Ernst Wagner
2. Gutacher: Prof. Dr. Franz Paintner

Mündliche Prüfung am 21.10.2010

Meinen Eltern

1 Table of Contents

1	Table of Contents	5
2	Introduction.....	9
2.1	Brief History of Macromolecular Therapy.....	9
2.2	Barriers in Macromolecular Drug Delivery	12
2.3	Delivery Systems for Nucleic Acids	16
2.4	Design and Synthesis of Programmable Polymeric Carrier Systems by Solid-Phase Synthesis and CombiChem	19
2.5	Sequence Defined Polymers Allow Detailed Structure-Activity Relationship Studies.....	20
2.6	Aims of the Thesis	22
3	Materials and Methods	24
3.1	Chemicals and Reagents.....	24
3.2	DMF Purification	25
3.3	Quantification Assays	25
3.4	Chromatography	26
3.4.1	Analytical RP-HPLC	26
3.4.2	Analytical IEX-HPLC.....	26
3.4.3	Desalting.....	27
3.4.4	Thin Layer Chromatography (TLC).....	27
3.4.5	Flash Column Chromatography (FCC)	28
3.4.6	Dry Column Vacuum Chromatography (DCVC)	28
3.5	Spectroscopy and Spectrometry.....	29
3.5.1	NMR Spectroscopy Instrumentation	29
3.5.2	Mass Spectrometry Instrumentation	29
3.6	LPEI-Conjugate Synthesis.....	30
3.6.1	Synthesis of LPEI 22 kDa x HCl/Free Base.....	30
3.6.2	Removal of Low M_w Impurities From LPEI and brPEI	30
3.6.3	Synthesis of 3-(Pyridin-2-ylsulfanyl)-propionic acid	31
3.6.4	Synthesis of N-Succinimidyl-3-(2-pyridyldithio)-propionate (SPDP)	32
3.6.5	Synthesis of mEGF-SH.....	33
3.6.6	Synthesis of LPEI-PEG-OPSS Conjugates	33
3.6.7	Attachment of mEGF-SH to LPEI-PEG-OPSS Conjugates	33

3.6.8	Synthesis of brPEI Tetraconjugate (Mel-brPEI-PEG-mEGF).....	34
3.7	Solid-Phase Synthesis Building blocks.....	35
3.8	Solid-Phase Protocols	41
3.8.1	Analytical Procedures.....	41
3.8.2	General Procedure for 2-Chlorotrityl-Resin Loading.....	42
3.8.3	Downsizing of Resin Load for MAP-System Synthesis.....	43
3.8.4	Solid-Phase Synthesis Cycles	43
3.9	General Cleavage Procedures	44
3.10	General Procedures Solid-Phase Synthesis.....	45
3.10.1	Synthesis of N-Terminal Stp-Modified Peptides	45
3.10.2	General Procedure: Synthesis of Stp-Chains	45
3.10.3	General Procedure: Synthesis of i-Shapes with one FA: HO-K-Stp ₁ -FA ₁	46
3.10.4	General Procedure: Synthesis of i-Shapes with two FAs: HO-K-Stp ₁ -K-FA ₂	46
3.10.5	General Procedure: Synthesis of i-Shapes with a Single Coupling Domain: HO-C-Stp ₁ -K-FA ₂	47
3.10.6	General Procedure: Synthesis of i-Shapes with Two Coupling Domains: HO-C-Stp ₃ -C-K-FA ₂	47
3.10.7	Synthesis of t-Shapes with One FA: HO-C-Stp ₁ -K(FA)-Stp ₁ -C-H	48
3.10.8	Synthesis of t-Shapes with Two FAs: HO-C-Stp ₁ -K(K-FA ₂)-Stp ₁ -C-H	49
3.11	Biophysical and Biological Methods	50
3.11.1	Polyplex Formation.....	50
3.11.2	Size and Zetapotential Measurements	51
3.11.3	Gel-Shift Assays	51
3.11.4	Erythrocyte Leakage Assay	52
3.11.5	Cell Viability Assay (MTT Assay).....	52
3.11.6	Luciferase Gene Silencing.....	53
3.11.7	Luciferase Reporter Gene Expression.....	53
3.11.8	poly(I:C) Cell Culture and Cell Killing Assay <i>in vitro</i>	54
3.11.9	poly(I:C) <i>in vivo</i> Study.....	55
3.12	Statistical Analysis.....	55
4	Results	56

4.1	Poly(I:C) Mediated Tumor Growth Suppression in EGF-receptor Overexpressing Tumors Using EGF-Polyethylene Glycol - Linear Polyethylenimine as Carrier.....	56
4.1.1	Introduction.....	56
4.1.2	Synthesis of LPEI-PEG Conjugates	57
4.1.3	Polyplex Formation and Biophysical Characterization.....	58
4.1.4	<i>In vitro</i> Antitumoral Activity of poly(I:C) Polyplexes.....	60
4.1.5	<i>In vivo</i> Anti-Tumor Activity	64
4.2	Protocols and Building Blocks for the Solid-Phase Assisted Synthesis of Defined Polyamidoamines	67
4.2.1	Introduction.....	67
4.2.2	Application of an Alternating Condensation Approach to Ethylenimine-based PAAs	69
4.2.3	PAA Synthesis Using Polyamino Acid Building Blocks.....	72
4.2.4	Application of Fmoc-Stp(boc) ₃ -OH to PAA and Peptide Synthesis.....	75
4.3	Design and Evaluation of a Library of Precise, Sequence-defined Oligoamidoamines for Nucleic Acid Delivery	77
4.3.1	Introduction.....	77
4.3.2	Structural Overview and Rationale	78
4.3.3	Lytic Activity.....	80
4.3.4	Correlation of Cytotoxicity with Unspecific Lysis Activity	82
4.3.5	Structure-Activity Relationships in Nucleic Acid Binding.....	83
4.3.6	Impact of the Different Domains on Nucleic Acid Delivery.....	86
4.4	Evaluation of Different PAA Families for <i>in vitro</i> DNA Delivery.....	90
4.4.1	Introduction.....	90
4.4.2	<i>in vitro</i> DNA Delivery	90
4.4.3	DNA Delivery Using Non-thiol Containing Chains and i-shapes.....	91
4.4.4	Influence of a Dimerization Anchor on Transfection Efficiency.....	93
4.4.5	DNA Delivery Using Crosslinking i-Shape Structures.....	96
4.4.6	DNA Delivery Using PAAs With t-Shape Topology.....	98
5	Discussion	102
5.1	Poly(I:C) Mediated Tumor Killing by LPEI-PEG-EGF Complexation	102
5.2	Development of a Synthesis Platform for the Production of Defined Polyamidoamines	104

5.3	Design and Biophysical Evaluation of a PAA-Library for Nucleic Acid Delivery.....	105
5.4	Evaluation of Different Stp-based PAA Families for <i>in vitro</i> DNA Delivery.....	107
6	Summary.....	109
7	References.....	111
8	Appendix.....	126
8.1	List of Used Polymers.....	126
8.2	Abbreviations.....	128
8.3	Buffer List.....	131
8.4	Supporting Information Chapter 4.1.....	132
8.5	Supporting Information Chapter 4.4.....	134
8.6	Used Protective Groups and Polymer Nomenclature.....	135
8.7	Analytical Data.....	137
8.8	Publications.....	156
8.9	Curriculum Vitae.....	158
8.10	Acknowledgements.....	159

2 Introduction

2.1 Brief History of Macromolecular Therapy

Most of the therapeutic drugs on market today are small molecules. But the advent of recombinant DNA technology¹⁻³ and an increasing molecular knowledge of metabolism and cause of many diseases slowly shifted the focus of development towards macromolecular therapy options.

Insulin was the first clinically used macromolecular therapeutic and was commercialized as extract of bovine pancreas in the early 1930s by Lilly. It's role in diabetes was well known from 1922⁴ and the successful application as therapeutic drug laid the foundations for a slow paradigm shift in drug development. As a consequence of the successful elucidation of its molecular mechanism medical research focused on the molecular basis of human metabolism and its connection to diseases. The focused work of the 1940–1960s resulted in the identification of many endogenous proteins with therapeutic potential⁵⁻⁶. But only the rapid advances in biotechnological production⁷ and protein design technologies⁸⁻⁹ allowed the explosion of the biopharmaceutical market we see today.

Macromolecules differ from the classical small drug therapeutics in various ways. Small molecules are generally produced by direct chemical synthesis and obey to Lipinski's "rule of five"¹⁰ stating that most of the therapeutically used drugs possess a $M_w < 500$ Da, contain only a small number of hydrogen bond donors/acceptors, and a partition coefficient which allows diffusion through lipid bilayers. Biogenic macromolecules on the other hand are large (>1000 Da), often multiple charged and in most cases do not enter cells readily. These properties render most intracellular targets inaccessible therefore the majority of the used macromolecular drugs are either surface receptor ligands¹¹⁻¹² or antibodies targeting extracellular targets¹³ and surface proteins¹⁴. With the growing knowledge of genetics and protein expression the idea of treating diseases at their molecular root got more and more attention. The original concept of gene therapy¹⁵ is straightforward and elegant: genetic disorders are the result of a loss of genetic function either by a mutation in the protein-encoding gene (examples include Duchenne muscle dystrophy and cystic fibrosis) or by a mutation-impaired regulatory sequence. Stable replacement of the deficient gene

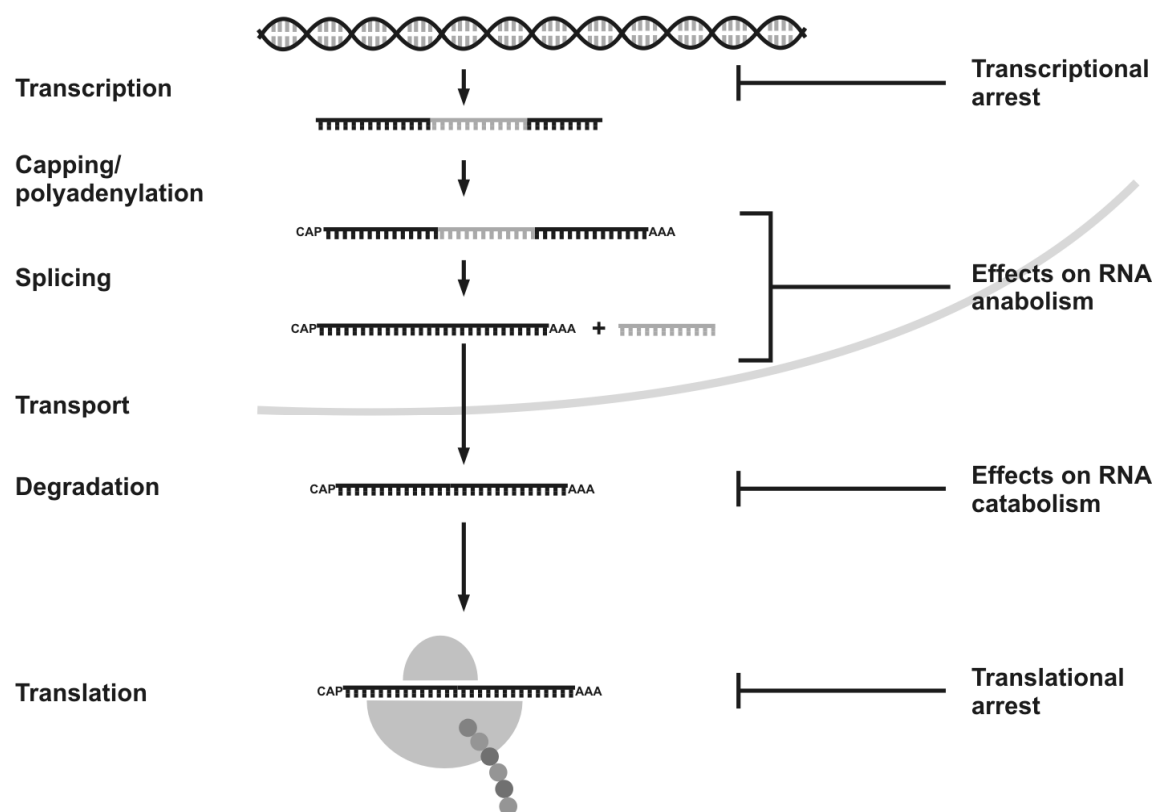


Figure 2.1: RNA intermediary metabolism. Different steps in transcription and processing are shown (introns in grey, 5'-cap and poly(A) tail as plain text). Possible intervention sites using antisense approaches are labeled by arrows (adapted from¹⁶)

(gene transfer) with a functional copy in the affected cell would restore the original function thereby serving a therapeutic goal¹⁷.

The concept has been studied using viral delivery systems for various monogenetic disease model systems (Hemophilia A and B, cystic fibrosis, severe combined immunodeficiency syndrome¹⁸) and extended by including tissue engineering¹⁹, DNA vaccination²⁰, infectious disease treatment and suicide gene cancer therapy²¹. But despite the persuasive ideas and first successful applications there still are a lot of technical problems to solve before gene therapy will be an standard option for medical treatment.

In recent years antisense technology (**Figure 2.1**) received increasing attention due to its complementary approach and the belief that there is a somehow reduced set of problems connected to it. As for gene therapy the basic concept of antisense is intriguing, the activity of antisense drugs stems from complementary Watson-Crick hybridization²² allowing the generation of gene-specific drugs. Antisense therapies do not deliver new genetic information but are able to regulate gene expression by degrading target mRNA or regulating RNAs (**Figure 2.1**). While plasmid based gene

therapy has to reach the nucleus to express a therapeutic gene or achieve stable integration into the genome without causing mutagenesis²³ the majority of antisense nucleic acids attack different sites of the mRNA metabolism in the cytosol (**Figure 2.1**). One of the first reported approaches was the use of 13-25 bases long, complementary antisense oligodeoxynucleotides (asODN) to inhibit the translation of a mRNA transcript resulting in a target protein knockdown²⁴. The expected mechanism was hypothesized as steric block through complementary Watson-Crick base pairing thereby inhibiting access of the translational machinery to the mRNA²⁵⁻²⁶. The discovery of the RNase H pathway²⁷ as a DNA-RNA duplex dependent protein translation inhibiting mechanism led to a detailed examination of the molecular basis of antisense activity. RNase H is able to recognize DNA-RNA duplexes and specifically cleaves the RNA thereby freeing the asODN resulting in a repetitive, catalytic process of duplex formation and degradation. This mechanism was exploited in the majority of the first generation antisense therapeutics²⁸. A related mechanism is the dsRNA induced gene-silencing mechanism. In 1998 Fire and Mello reported that introduction of exogenous dsRNA into cells of *Caenorhabditis elegans* inhibited cellular protein expression²⁹ but additional experiments with human cells using synthetic dsRNAs (78 bp) only showed an interferon-induced non-specific response³⁰. Three years later Tuschl et al. could demonstrate that use of small 21 – 23 bp long dsRNAs (siRNAs) causes effective, sequence specific RNA interference in mammalian cells without significant side effects³¹⁻³². The siRNAs are incorporated into a multi-protein complex known as RNA-induced silencing complex (RISC). During assembly of the complex the siRNA is further processed, resulting in release of the passenger strand and binding of the guide strand to the Ago2 protein³³. This strand is used by the RISC as template to destroy complementary target RNA via an embedded RNase activity of the Ago2 protein³⁴. These discoveries led to a surge in interest to harness RNAi for biomedical research and drug development.

While most of the used, antisense based therapeutic approaches aim at inhibiting protein expression they can also be used to correct splicing errors in the pre-mRNA³⁵ or to increase gene activity by degradation of regulatory RNA³⁶. But despite the assumed advantages of antisense technology over gene therapy or their mechanistic differences they share one trait; without effective delivery their therapeutic use is limited.

2.2 Barriers in Macromolecular Drug Delivery

Successful application of nucleic acids (NAs) in a therapeutic setting is strongly dependent on successful delivery of the nucleic acid payload into the target cell. The rather low efficiency of non-viral vectors stems from the numerous extracellular and intracellular barriers (**Figure 2.2**) entrapping or destroying significant amounts of the payload before entering the cell. In contrast to peptides and proteins, which show reasonable stability in circulation, nucleic acids are characterized by a rather short half-life due to rapid degradation by nucleases³⁷ making efficient protection of the nucleic acid mandatory. Most non-viral delivery systems, including cationic lipids, polymers such as polyethyleneimine (PEI) or dendrimers, achieve this by compacting the nucleic acid payload through electrostatic interactions of the cationic carriers with the negatively charged nucleic acid. But the resulting positive net charge of many non-viral delivery systems is partly responsible for additional deleterious effects of the extracellular environment. Positive net charge of polyplexes increases unspecific, electrostatically induced interactions with negatively charged components of the biological environment like cell membranes and proteins. These interactions result in a number of side effects with reduction of effective therapeutic dose being the most prominent, followed by cytotoxic effects³⁸ and stimulation of the immune system.

To overcome these problems strategies like dextran modification of the polycation³⁹, hydrophobic backbone modifications⁴⁰⁻⁴¹ or conversion of the polymeric backbone into a polyanion⁴² were reported. The most common and versatile solution is PEGylation of the carrier systems. Polyethylene glycol (PEG), a hydrophilic, uncharged polymer with excellent solvatization properties was described for the generation of less immunogenic proteins, characterized by extended circulation times⁴³. PEGylation of liposomes is a long known strategy to reduce unspecific interactions during circulation and was transferred to PEI-based carrier systems by Ogris et al.⁴⁴. The PEGylation of PEI results in reduced interactions with blood components and the innate immune system. Recently the beneficial role of PEGylation for polymeric oligonucleotide (ON) delivery systems in siRNA/PEI delivery was examined in more detail by using radioactively labeled compounds for a detailed study of the pharmacokinetics⁴⁵.

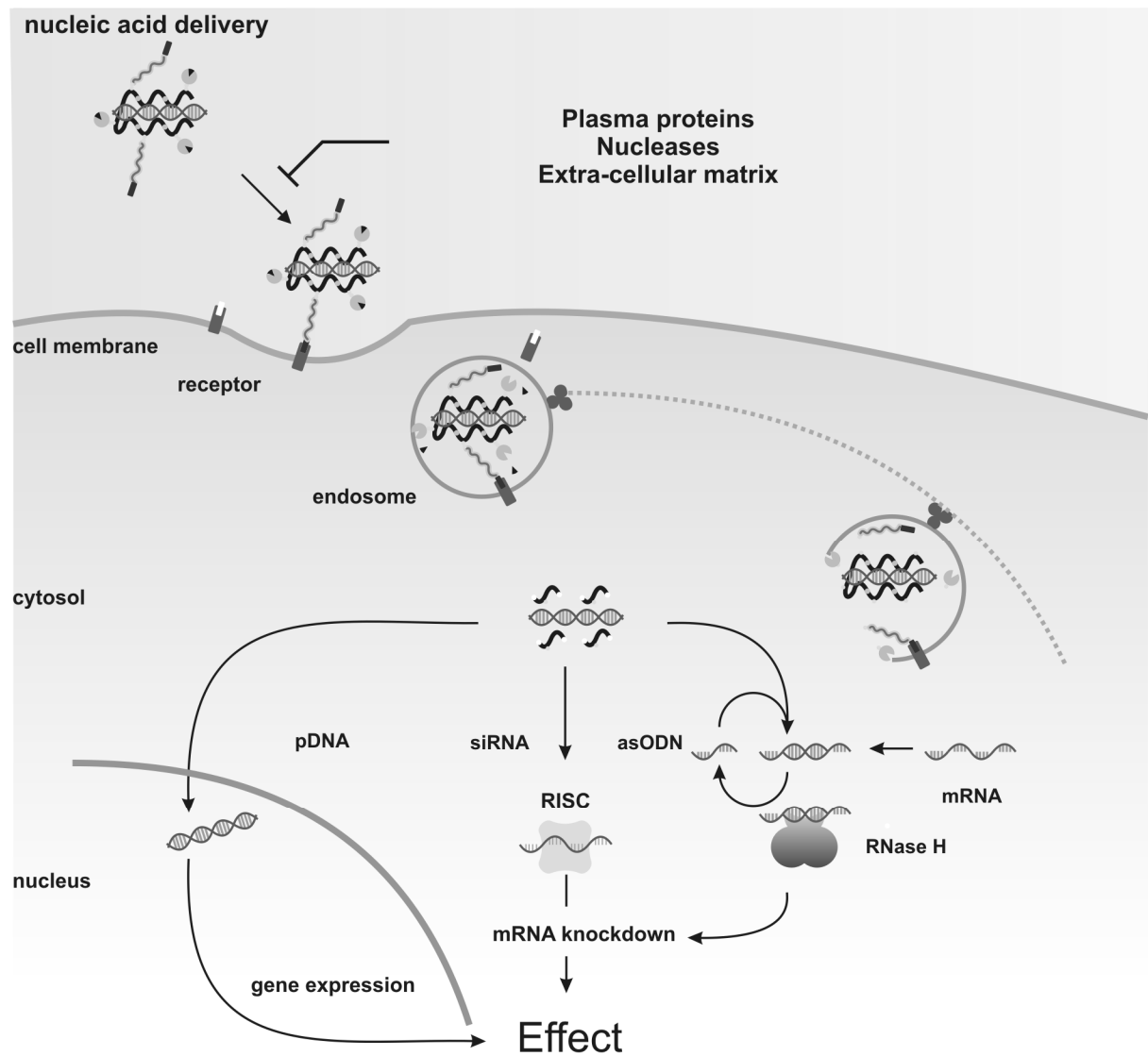


Figure 2.2: Bottlenecks in macromolecular delivery exemplified for a bioresponsive NA delivery system. After docking to the cell by ligand–receptor interaction, the vector is internalized into an endosomal vesicle which can be actively transported to the perinuclear region by microtubules. The acidic pH-shift in the maturing endosome unmasks a domain which disrupts the endosomal membrane releasing the particles into the cytoplasm. Vector unpacking by degradation of the polymeric backbone (disulfide, ester bonds) may occur in a time- and environment-dependent fashion either in the cytosol or in the nucleus. Depending on the form of nucleic acid, the payload is processed in the cytosol (siRNA and asODN) or has to enter the nucleus (pDNA).

After successful passage through the circulation the polyplex has to extravasate in the vicinity of the target cell and cross the extra-cellular matrix (ECM) to deliver its payload to the cell surface and into the cytosol. The ECM is a network of different, charged macromolecular species and able to disrupt electrostatically stabilized polymer-NA formulations⁴⁶⁻⁴⁷ resulting in a profound impact on delivery efficiency. Apart from being a physical barrier for successful delivery to cells the composition of the ECM can influence the gene expression itself⁴⁸.

Incorporation of targeting into a delivery platform improves the specificity of the carrier for certain tissues or organs and supports the uptake of the delivery systems resulting in improved delivery efficiency. To achieve this goal different passive and active targeting concepts were developed. Due to the abnormal neovascularization and an inadequate lymphatic drainage tumor vasculature generally is characterized by an increased leakiness resulting in enhanced permeability and retention (EPR) for macromolecular drug entities⁴⁹. This effect can be exploited to enrich nucleic acid formulations in tumor tissue. The EPR-targeting effect is mostly dependent on the molecular weight (>50 kDa) of the used polymer or the size of the resulting nanoparticles and can be improved by increasing M_w and hydrophilicity of the carrier via PEGylation. By covalently attaching ligands to the carrier it is possible to improve uptake into cells specifically expressing or over-expressing the target receptor. Active targeting for nucleic acid formulations was introduced in 1987 by Wu et al.⁵⁰ for hepatocyte targeting and has been used extensively for the generation of carrier systems with an increased specificity for certain cell types. Prominent examples for this ligand-driven strategy are the use of transferrin⁵¹, EGF⁵¹, folate⁵² and peptides like RGD, GE11⁵³ or B6⁵⁴. Active targeting is also used to improve the cellular uptake of PEGylated formulations and was combined with reversible PEGylation to escape the PEG-dilemma⁵⁵.

After successful internalization several intracellular bottlenecks such as endosomal escape, cytosolic transport and successful vector unpacking have to be resolved by a pDNA delivery system. In contrast to pDNA-delivery systems, nuclear localization is irrelevant for most of the antisense therapeutics. However, in either case the formulation has to escape the endosomal compartment which will otherwise degrade the payload over time. While certain polymeric carriers like PEI or PAMAM-dendrimers can utilize their high, intrinsic buffer capacity to cause an osmotic burst of the endosome⁵⁶ their efficiency of escaping the endosomal entrapment is still low.

Lipid-based formulations are not able to induce an osmotic burst but can escape the endosomal pathway by destabilizing the endosomal membrane⁵⁷. This process is enhanced by the inclusion of helper lipids in cationic polymer formulations or lipid modification of cationic polymers.

Another frequently used strategy is the modification of polymeric carriers with membrane disrupting agents. One of the most prominent examples is melittin, the major component of the bee venom. This pH-independent, strongly lytic peptide inserts into biological membranes and induces pore formation causing effective vesicle rupture. Modification of polymeric vectors with melittin increases their delivery efficiency but also increases cytotoxicity⁵⁸. To circumvent the problem of unspecific lytic activity various peptide-based membrane active agents were developed, mimicking the endosomal escape strategies of viruses or certain bacteria. Peptides like the influenza peptide respond to the acidification of the endosome by a conformational shift which results in increased membrane destabilization. This concept was adapted for the design of membrane active synthetic peptides like GALA/KALA⁵⁹. These amphipathic peptides change their conformation in acidic environment from random coil to an alpha-helical structure able to interact with lipid membranes, leading to membrane rupture and subsequent release of vesicle contents into the cytosol.

Following the successful escape out of the endosomal pathway pDNA-based formulations have to be efficiently trafficked to the nucleus, followed by release from the carrier for successful gene expression. In case of non-dividing cells the pDNA payload has to pass the nuclear pore complex (NPC). These pores possess an inner diameter of ~ 9 nm making free diffusion of the carrier-NA complex into the nucleus a unlikely process. Proteins containing an exposed nuclear localization sequence (NLS) are recognized by importin, a cytosolic heterodimer carrier protein, dock to the NPC and are actively transported into the nucleus⁶⁰. Most of the known NLS are characterized by clusters of basic amino acids that are recognized by the importins. By attaching the M9 sequence to a peptidic scaffold Subramanian et al.⁶¹ could demonstrate an increase nuclear import of pDNA resulting in a tenfold increase of expression. Zanta and coworkers⁶² demonstrated that covalent attachment of a single NLS to a plasmid was sufficient for increased nuclear entry while attachment of several NLS inhibited the transport.

In conclusion, polymeric carriers have to cope with apparently contradictory demands: to stabilize the nucleic acid against degradation, but release it at its biological site of action; to shield the polyplex during circulation in the blood stream, but to deshield it upon cell entry; to leave the cell membranes intact, but to rapidly destabilize the endosomal membrane. It is unlikely that a simple homopolymer is up to these tasks. Dynamic, multi-domain delivery systems may be a more promising answer to this challenge.

2.3 Delivery Systems for Nucleic Acids

A major aim for any nucleic acid delivery strategy is efficient payload delivery into the target cell resulting in a therapeutic effect. This is a challenging task because of the unfavorable properties of the nucleic acid payload and the numerous extracellular and intracellular barriers preventing easy delivery. Administration of naked pDNA or RNAs did only in a few exceptional and not generally useful cases⁶³⁻⁶⁵ result in effective *in vivo* delivery. The limitation is due to the fast degradation of either DNA or RNA in *in vivo* settings by nucleases³⁷ and limited extravasation⁶⁶. Although gene expression/silencing can be achieved by either intramuscular/intratumoral⁶⁷⁻⁶⁸ injection or physically assisted methods like electroporation⁶⁹ or hydrodynamic delivery⁷⁰ these methods miss general applicability or are characterized by a rather low efficiency.

Viral vectors are considered to be the most efficient vector systems and are used in the majority of clinical gene therapy studies⁷¹. Due to their long evolution they are exceptionally suited to transport nucleic acids into foreign cells. By replacing viral genetic information with therapeutic nucleic acids viral systems can be used for effective delivery into target cells. But despite their advantageous properties it was a long way from the first, failed study in 1973 using Shope papilloma virus to treat hyper-arginaemia by an *ex vivo* approach⁷² to the successful delivery of genetic material into humans in 1990⁷³. Despite their advantages in terms of efficiency viral delivery systems have disadvantages originating from their parent wild-type viruses. Major parts of the properties of a viral delivery system are defined by the wild-type they originate from, including loading capacity, tropism, maintenance of transgene expression, immunogenicity and inflammatory potential⁷⁴. This results in difficulties

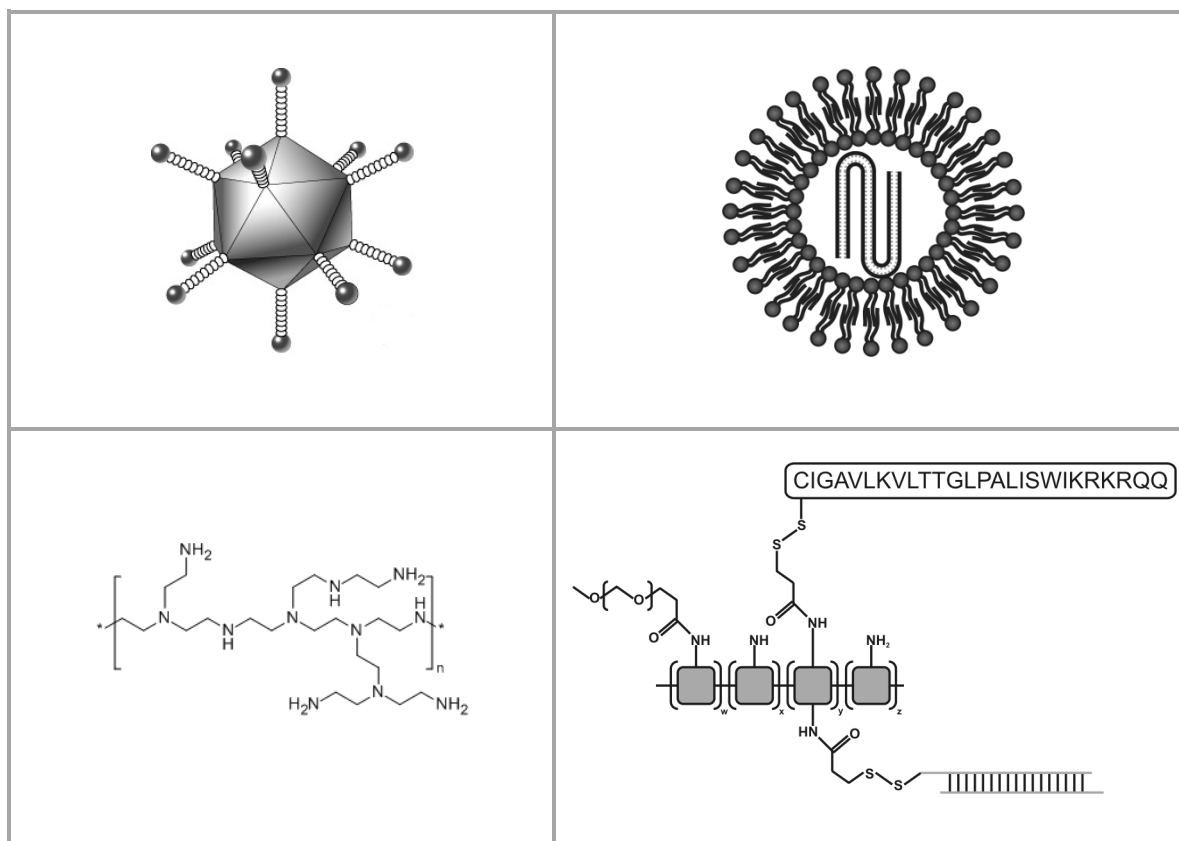


Figure 2.3: Schematic representations of the four major delivery system classes. A: adeno virus; B: cationic lipid/liposome; C: cationic polymeric delivery system; D: dynamic polymeric delivery system, reproduced from⁷⁵⁻⁷⁶.

regarding retargeting, potentially severe immune responses and the problem of mutagenesis. In general viruses are superior delivery systems but expensive in production, possess only a limited flexibility and are quite complicated in handling.

In 1987 Felgner et al.⁷⁷ described a new class of transfection reagents which complex DNA through charged, liposomal structures and were able to transfect cells in a reliable, efficient way. These so called lipoplexes are electrostatically stabilized complexes made from cationic lipids like DOTAP or DOPE and negatively charged nucleic acids. The lipid components spontaneously form micellar structures with cationic surfaces in aqueous environment. The cationic surface interacts with negatively charged nucleic acids to form complexes which enter cells via endocytosis. Internalized lipoplexes are able to escape the endosomal pathway by interactions with the endosomal membrane⁷⁸⁻⁷⁹. Published reports suggest that the cationic lipids interact with the negatively charged endosomal membrane causing membrane perturbations resulting in a breakdown of the membrane and subsequent release of the complexed nucleic acids into the cytoplasm⁵⁷. Despite their high *in*

vitro efficiency the susceptibility towards serum proteins restricts extensive use *in vivo*. Nevertheless cationic lipids are considered to be one of the best non-viral delivery systems and have already been tested in clinical trials⁷¹.

Similar to liposomes, polymers offer some practical advantages over viral delivery systems. Polymeric delivery vehicles are cheap in production, easy to modify, not recognized by the immune system and show no size limitations for their payload. Over the last 15 years polyethylenimine advanced to the most used member of this class⁸⁰. PEI polymers contain primary, secondary and, in case of branched PEI, tertiary amines which are only partially protonated under physiological conditions. This structural feature results in a high intrinsic buffer capacity and allows the compaction of nucleic acids into small nanoparticles (50-500 nm). These properties result in an exceptionally high *in vitro* efficiency compared to other polymeric vectors and also some *in vivo* efficacy. But despite its efficiency PEI has some disadvantages. Its transfection efficiency is only moderate compared to viral delivery systems. Major drawback of PEI-based delivery vehicles is a pronounced *in vitro* and *in vivo* toxicity⁸¹⁻⁸⁴, mainly caused by the positive net charge of PEI polyplexes resulting in unspecific interactions^{44,85} with the biological environment. In contrast to peptide based delivery systems or polyarginine/-lysine polymers, PEI is not biodegradable resulting in inefficient metabolization and elimination. This property can lead to PEI accumulation in cells and organs, limiting its usefulness for repeated application.

The limitations of homopolymers like PEI and the resulting problems led to the development of increasingly complex polymeric systems which are able to react to external stimuli. Modifications include improved biodegradability resulting in reduced toxicity⁸⁶⁻⁸⁷, targeted delivery using shielded formulations⁸⁸ and carriers with covalently attached payload which is only released in the cytosol⁷⁵⁻⁷⁶. These systems are the first versions of the so called programmable polymeric delivery systems (PPDS), dealing with the contradicting requirements of successful delivery.

2.4 Design and Synthesis of Programmable Polymeric Carrier Systems by Solid-Phase Synthesis and CombiChem

Polymer design for nucleic acid delivery suffers from the vast potential combinations of variables and the complex biological environment in which the carriers are employed. Furthermore, recent studies emphasize the need for specialized systems, as not every carrier is appropriate for every task and there is an increasing need for adaptive polymers which can deal with changing biochemical environments.^{46,75,89} Combinatorial chemistry can drastically shorten the development cycles by producing a large set of system descriptors (chemical structures, physical properties and biological characteristics associated with these structures) which can be used for rational vector design. The concept of high throughput combinatorial chemistry was introduced to the gene therapy field by the Robert Langer lab, synthesizing a library of 2350 single entity poly(β -amino esters)⁹⁰ (PAEs). The information derived from this library was subsequently used in several applications, for example by Green et al.⁹¹ to construct optimized PAEs for human endothelial cell transfections in high serum conditions. Starting with low-molecular weight 0.42 kDa and 1.8 kDa PEI and 24 bi- and oligo-acrylate esters, Thomas et al.⁹² developed a 144-member library. *In vitro* and *in vivo* screening identified nine effective polymers, of which two showed systemic *in vivo* gene delivery to the lung with reduced toxicity compared to PEI. To take full advantage of the potential of such encouraging combinatorial approaches, further optimization of polymer chemistry and purification, resulting in libraries of monodisperse polymers with defined size and topology, better models to correlate *in vitro* and *in vivo* efficacy, as well as computational assistance for elucidating structure-activity relations will be necessary. One has to emphasize that any high-throughput screening which only uses standard *in vitro* test systems would not necessarily select candidate vectors with highest *in vivo* efficacy.

2.5 Sequence Defined Polymers Allow Detailed Structure-Activity Relationship Studies

For better defined copolymer structures and libraries with defined molecular weight and topology,⁹²⁻⁹⁵ meaningful structure/transfection correlations are possible. However, more detailed studies are not possible, even with such systems, due to the limited design space and/or their polydispersity. This limitation may be circumvented by alternative chemistry methodologies, including for example dendrimer⁹⁶⁻⁹⁷ synthesis and/or solid-phase synthesis⁹⁸ (**Figure 2.4**), which provide defined monodisperse products by control of position and structure of every unit in a polymer. Hartmann et al.⁹⁹⁻¹⁰⁰ adopted standard solid phase chemistry to build up a small library of monodisperse, sequence-defined poly(amidoamine) (PAA) polymers.

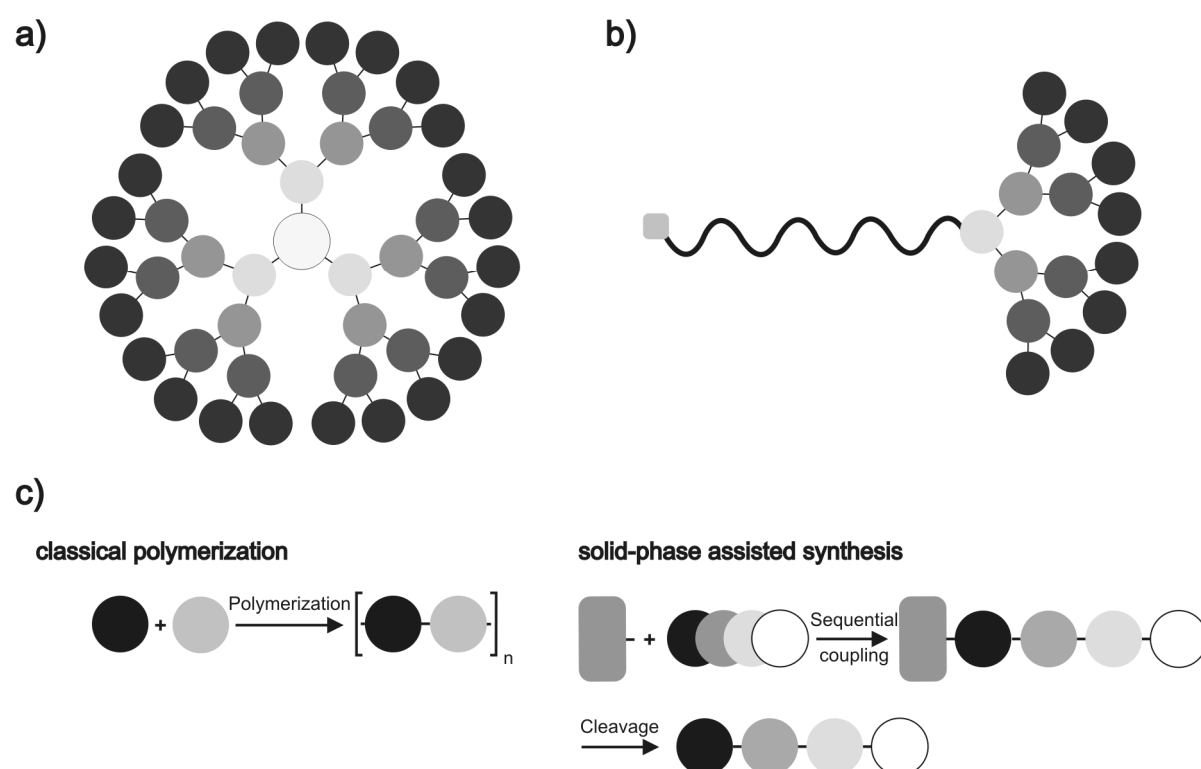


Figure 2.4: Schematic representations of defined, monodisperse polymeric delivery systems.

(a) Generation 4 dendrimer, consisting of a trivalent core and four layers of bivalent building blocks. (b) Modular linear dendritic hybrid, consisting of targeting ligand, linear shielding domain and attached generation 3 dendron for binding and compaction of nucleic acids. (c) Comparison of classical polymerization and solid-phase methodology; classical polymerization results in disperse systems with its design space limited to the starting materials. Solid-phase supported synthesis allows the sequence-specific synthesis of monodisperse polymers with absolute control of position and composition of every monomer by sequential elongation of the polymeric chain.

Defined incorporation of PEG or oligopeptide blocks was possible. Different PEG-PAA copolymers were synthesized, where the cationic nature of the PAA segments was systematically varied. This modulated the structure of the resulting polyplexes, ranging from extended ring-like structures to highly compact toroidal structures. Importantly, stable single-polynucleotide complexes could be generated, as described similarly for sequence-defined synthetic peptide-based block copolymers by DeRouchey et al.⁴⁷ or previous published work for synthetic poly(lysine)-PEG conjugates.

These reports demonstrate the slow shift of the field of polymeric delivery towards the increasingly complex systems of bio-responsive, programmable polymers and to the application of increasingly sophisticated chemical methods and strategies in the development of new carrier systems.

2.6 Aims of the Thesis

The innovation speed of small molecule therapeutics decreased in the last years but the number of EMEA approved biologicals is on a steady rise for the last 15 years. It is only a question of time until the first intracellular targeted therapeutic options will arrive on the market. But the success of these concepts is closely connected to the development of efficient, reliable, non-toxic carrier systems - without an efficient mode of intracellular entry no effective therapeutic can enter the market. A major drawback of the established polymeric delivery systems is their heterogeneity in terms of molecular weight, the limited freedom in their molecular design and the resulting problems for synthesis of defined batches for clinical testing and controlled modification of the systems. The sometimes ambiguous results in biological assay systems and the lack of information for precise structure-activity relationships imposes further restrictions on the development of new carrier systems.

While numerous literature examples show improvements of polymeric delivery efficacy¹⁰¹ most of these approaches rely on chemical modification of polydisperse polymer precursors. But due to the heterogenic nature of the starting material every modification results in an even more complex product. Aim of the first part of this thesis was the simplification and subsequent optimization of an already described efficient, modular, brPEI-based delivery system¹⁰². This previous delivery system was a tetraconjugate, composed of compaction (brPEI 25 kDa), targeting/shielding (EGF coupled to 3.2 kDa PEG) and lytic domains (all-D-Melittin). Despite its nucleic acid delivery efficiency, synthesis was too complex for further refinement and the overall yield was low. By development of a new synthetic strategy and a simplified modular setup in the current work we aimed at a better control over the production process and increased flexibility for ligand attachment.

The second aim of the thesis was the development of a solid-phase synthesis platform for the rapid synthesis of sequence-defined, polyamine-based cationic carrier systems. Novel protected building blocks had to be synthesized and the solid-phase assembly process to be optimized. Polymers derived with this method by nature of the synthetic approach should be monodisperse. The molecular precision of the assembly should allow the introduction of multiple chemical modifications which are compatible with the specific reaction conditions of the used solid-phase

chemistry. These polymers should allow the study of structure-activity relationships (SAR) in more detail and offer increased control over the polymer and thereby the possibility of fine-tuning their properties.

The third aim of the thesis was the application of the novel solid-phase assisted method in the design and synthesis of precise polymers with nucleic acid carrier activity. The synthesized polymers had to be evaluated in biophysical assays (NA binding and lytic activity) and *in vitro* systems (pDNA and siRNA delivery) to construct SARs which can be used for further optimization of the polymers.

Aim of the fourth part of the thesis was the more detailed design and analysis of the precise polymers as pDNA transfection agents. By screening them for *in vitro* transfection capabilities and correlating these to their biophysical parameters, first useful SARs and promising lead candidates should be identified.

3 Materials and Methods

3.1 Chemicals and Reagents

Fmoc-amino acids and resins (base resins and preloaded resins) were bought from IRIS Biotech, Marktredwitz and Novabiochem GmbH, Darmstadt. Pybop® was bought from Multisynth GmbH, Witten. DCM, MeOH, THF were bought from Merck and distilled before use. DMSO, EtOH, ACN were bought in the highest quality available from Sigma and used without further purification. ACN for RP-chromatography was HPLC quality and bought from Merck. Water was used as purified, deionized water.

Branched polyethylenimine (PEI; average MW = 25 kDa) and poly(2-ethyl-2-oxazoline) (PEOZ) 50 kDa, DTT, deuterated solvents and MTT bromide were obtained from Sigma-Aldrich (Munich, Germany). All small molecule reagents were bought from Sigma-Aldrich unless stated otherwise. PEG derivatives were custom synthesized by Rapp Polymere, Tübingen.

Recombinant murine epidermal growth factor (mEGF) was obtained from Peprotech Germany (Hamburg, Germany). Cysteine-modified melittin (Mel) was obtained from IRIS Biotech GmbH (Marktredwitz, Germany). Mel had the sequence CIGA VLKV LTTG LPAL ISWI KRKR QQ (all-*D*-configuration), the C-terminal amino acid was introduced as carboxylic acid, the N-terminal amino acid as amine.

Plasmid pEGFP_{Luc} (encoding a fusion of enhanced green fluorescent protein (EGFP) and *Photinus pyralis* luciferase under control of the CMV promoter) was produced with the Qiagen Plasmid Giga Kit (Qiagen, Hilden, Germany) according to the manufacturer recommendations.

Ready to use siRNA duplexes were synthesized by Dharmacon (Lafayette, USA), namely GL3 luciferase duplex: 5'-CUUACGCUGAGUACUUCGAdTdT-3' (sense), 5'-UCGAAGUACUCAGCGUAAGdTdT-3' (antisense) and control-siRNA: siCONTROL 3 5'-AUGUAUUGGCCUGUAUUAGUU-3' (sense), 5'-CUAAUACAGGCCAAUACAUUU-3' (antisense).

Cell culture media, antibiotics, and fetal calf serum were purchased from Invitrogen (Karlsruhe, Germany). Luciferase cell culture lysis buffer and D-luciferin sodium salt were obtained from Promega (Mannheim, Germany).

3.2 DMF Purification

DMF was further purified due to the slow decomposition on storage. To entrap amine impurities and residual water 100 g of freshly activated molecular sieve (4 Å pore diameter) were added to 1 L of DMF p.a. and the bottle stored in the cold room for 7 days before use.

To check for amine impurities a bromophenol assay was performed. 1 mL DMF was pipetted into an eppendorf tube and 6 µL of a freshly prepared bromophenol blue solution (5 mg/mL) were added. If the color of the solution was not yellow the DMF was additionally purified by distillation.

3.3 Quantification Assays

Ellman's Assay¹⁰³

The DTNB working solution contained 60 µl DTNB stock solution and 2440 µl of Ellman's buffer. For a calibration curve cysteine solution with concentrations from 0.0 to 0.5 µmol/ml were prepared freshly for each measurement. The cysteine solutions were diluted in Ellman's buffer. A solution with 0.25 µmol/ml of the test substance in HBG (pH 7.1), Tris (10 mM, pH 8.0) or acetic acid (10 mM, pH 2) was prepared. For the measurement 30 µl of the test substance or of the cysteine solutions were diluted in 170 µl DTNB-working solution. After incubating for 15 min at room temperature the content of free thiol groups was determined at A_{412} via calibration curve.

Quantitative Analysis of brPEI¹⁰⁴

The concentration of PEI was measured by TNBS assay. Standard brPEI solutions and brPEI containing test solutions were serially diluted in 0.1 M sodium tetraborate buffer to a final volume of 100 µl using a 96 well plate, resulting in e.g. brPEI concentrations of 10 to 60 µg/ml. To each well 2.5 µl of TNBS (75 nmol, 22 µg; diluted in water) were added. After 5 - 20 minutes incubation time at RT (depending on the strength of the developed colour) the absorption was measured at 405 nm using a microplate reader (Spectrafluor Plus, Tecan Austria GmbH).

Quantitative Analysis of LPEI¹⁰⁵

Content of linear PEI in the conjugates after size exclusion chromatography was measured performing a copper assay. PEI was mixed with copper (II) ions for formation of dark blue cuprammonium complexes. These complexes were detected by UV-VIS spectrometry measuring absorption at 285 nm. For this purpose first a calibration curve was established. Linear PEI22 was diluted in water to a final volume of 100 μ l and added to 100 μ l of a 2.25 M copper solution, 0.1 M sodium acetate pH 7.4. Finally the conjugates were diluted, mixed with CuSO₄ solution and A₂₈₅ nm was measured.

3.4 Chromatography

3.4.1 Analytical RP-HPLC

Analytical HPLC runs were done using a Waters HPLC System consisting of a P-900 gradient pump system and a 996 Photodiode array detector under the control of the Millenium software. Analytical columns were either a C18-RP-Phase (Waters Symmetry C₁₈, 3.9 x 150 mm) or a C4-RP-Phase (YMC C₄, 4.0 x 150 mm). All peptides were analyzed using an exploratory Water/ACN (buffered with 0.1% TFA) gradient starting at 95:5 reaching 0:100 in 45 min.

3.4.2 Analytical IEX-HPLC

Analytical IEX-HPLC runs were done on a GE Healthcare ÄKTA Basic system consisting of a P-900 dual-pump, a UV-900 three-channel UV-detector and F-950 fraction collector under the control of the UNICORN software version 4.11. All analytical runs were done on a Resource S 1 mL column using a salt gradient starting at 5 mM reaching 3 M over 30 min in a 10 mM HCl buffer (pH 1.9) 30% ACN.

3.4.3 Desalting

Desalting was done using a 10/30 G-10 column connected to an Äkta Basic System. Procedure for a typical desalting run: 10-30 mg of compound were dissolved in 1 mL of a 10 mM HCl buffer (pH 1.9) containing 30% ACN. The sample was applied to the column and the major peak ($A_{214,280}$) collected.

3.4.4 Thin Layer Chromatography (TLC)

Silica gel coated glass (Merck, silica gel 60 F₂₅₄) were used for thin layer chromatography. Detection methods were UV-detection at 254 nm or different staining baths.

Cerium Stain (All Purpose Stain)

15.0 g of ammonium cerium nitrate ($(\text{NH}_4)_2\text{Ce}(\text{NO}_3)_6$) and 15.0 g of ammonium heptamolybdate ($(\text{NH}_4)_6\text{Mo}_7\text{O}_{24}$) were covered with 270 mL distilled water. After the addition of 30 mL concentrated sulfuric acid (98 %) the resulting suspension was stirred at 50 °C for 30 min and filtered.

Potassium Permanganate Stain (Oxidative Stain)

3.0 g KMnO_4 and 20.0 g K_2CO_3 were dissolved in 400 mL of MilliQ Water under addition of 2.5 mL of 10 % (w/v) NaOH.

Ninhydrin Stain (Primary Amine Stain)

0.8 g Ninhydrin p.a were dissolved in 400 mL of a mixture of n-butanol/water/acetic acid (100:4.5:0.5).

Iodine Vapor Stain (Oxidative Stain/PEG Stain)

A sufficient amount of iodine was loaded onto silica gel and stored in a stoppered flask.

3.4.5 Flash Column Chromatography (FCC)

Flash chromatography was used like described by Still et al.¹⁰⁶. Stationary phase was silica gel with a mean diameter of 0.035 – 0.073 mm unless otherwise stated. Column height and diameter were chosen in accordance to the general guidelines of the published method.

3.4.6 Dry Column Vacuum Chromatography (DCVC)

Dry column vacuum chromatography was performed like described by Pedersen et al.¹⁰⁷. A sintered glass funnel (porosity of sinter filter: P3) of appropriate size was filled with about 6-7 cm of loose silica (Silica gel 60[®], mean diameter 15-40 µm) and tapped to give a level surface. Vacuum was applied and the surface was pressed firmly to form a well compacted bed. The column was checked for voids and channels by pouring *n*-heptane onto the silica bed while vacuum was applied. The bed was covered with a filter paper of appropriate size to prevent disruption of the silica bed when charging it.

The raw product mixture was dissolved in an appropriate amount of a low boiling solvent like DCM, methanol or ethyl acetate, and preabsorbed on Celite[®] 500 fine, followed by removal of solvent by evaporation. The loaded Celite[®] was grinded to a fine powder in a mortar and added as a thin, uniform layer on top of the column and vacuum was applied to compact the column. The column was then gradient-eluted with a suitable solvent system. Mixtures of *n*-heptane, chloroform, ethyl acetate and methanol were used, starting with the least polar solvent mixture, followed by solvent fractions typically with 1-10 % increments in the polar component. The fractions with a volume of 5-100 ml were monitored by TLC and product containing fractions were pooled and concentrated.

3.5 Spectroscopy and Spectrometry

3.5.1 NMR Spectroscopy Instrumentation

The ^1H -NMR spectra were recorded using a JNMR-GX 400 (400 MHz) or a JNMR-GX 500 (500 MHz) unit manufactured by Jeol. The coupling constant had an accuracy of 0.3 Hz. Deuterated chloroform or water were used as solvents as well as internal standards. The spectra were analyzed using the NMR-software packages NUTS (2 D professional version 20020107 by Acron NMR, 2002), MestreNova (Ver. 5.2.5-4119 by Mestrelab Research) or Delta NMR processing and control software (version 4.3.1 by Jeol).

3.5.2 Mass Spectrometry Instrumentation

ESI-MS were measured on a ThermoScientific LTQ-FT Mass Spectrometer or on a Bruker Maxis ESI. MALDI-MS analysis was performed on a Bruker Autoflex MALDI-TOF system.

3.6 LPEI-Conjugate Synthesis

3.6.1 Synthesis of LPEI 22 kDa x HCl/Free Base

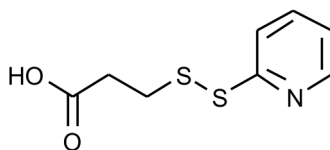
Synthesis of LPEI was performed analogous to published procedures¹⁰⁸ with modifications. Poly(2-ethyl-2-oxazoline) 50 kDa (5 g) were suspended in 50 ml of 30% hydrochloric acid. The mixture was refluxed for 48 h yielding a fine white precipitate. The solid was isolated by filtration and washed four times using 30% HCl to remove traces of propionic acid. The resulting LPEI hydrochloride was air-dried over night, dissolved in 200 ml distilled water and freeze-dried. Yield: 3.5 g, 85% (¹H-NMR, D₂O, 400 MHz: broad singlett 3.5 ppm)

LPEI hydrochloride (2.5 g) were dissolved in 75 ml of 1 M NaOH at 100 °C. The solution was cooled to room temperature and the resulting LPEI precipitate isolated. The gel-like precipitate was washed 3 times with 75 ml 1 M NaOH and 5 times with 75 ml distilled water. The resulting viscous gel was transferred into a round bottom flask, shock frosted using liquid nitrogen and lyophilized yielding 1 g (76%) of a white, fluffy lyophilizate.

3.6.2 Removal of Low M_w Impurities From LPEI and brPEI

50 mg of LPEI (hydrochloride) or brPEI (free base) were dissolved in 1 ml water and the pH was adjusted to 7.0 using NaOH or HCl respectively. Small molecular weight fractions of the polymer were removed by SEC chromatography using a G-25 preparative grade Sephadex column and a 20 mM HEPES (pH 7.4) buffer for elution. The PEI containing fractions were pooled and concentrated. PEI concentrations were determined using photometric copper assay (see 3.3) for LPEI, or TNBS-assay (see 3.3) for brPEI, respectively.

3.6.3 Synthesis of 3-(Pyridin-2-ylsulfanyl)-propionic acid



Dithiopyridine (3.770 g, 17.11 mmol, 2 eq) was dissolved in 30 mL EtOH abs. and 0.4% (v/v) acetic acid. A solution of 3-mercaptopropionic acid (0.900 g, 8.48 mmol, 737 μ L, 1 eq) in 20 mL EtOH abs. and 0.4% acetic acid was added dropwise over the course of 1 h. After 2 h of stirring the solvent was evaporated and the resulting yellowish oil was purified by DCVC using basic alumina as stationary phase (diameter 4 cm, h = 7 cm). Column was conditioned with CHCl_3 , the oil was loaded using $\text{CHCl}_3/\text{MeOH}$ 8:2 and eluted until the collected fractions were colorless. Product was eluted by including 4% acetic acid in the solvent. Product containing fractions were pooled and solvent remnants removed by HV treatment for 48 h.

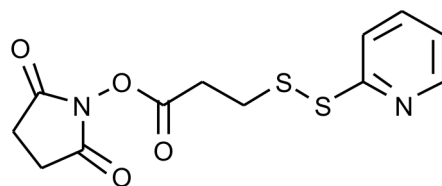
$\text{C}_8\text{H}_9\text{NO}_2\text{S}_2$: 1.6436 g (90%). Colorless to yellowish oil.

TLC: R_f = 0.84 ($\text{CH}_2\text{Cl}_2/\text{EtOH}$ = 3:2 + 4 % CH_3COOH).

^1H NMR (500 MHz, CD_3OD , 19.2 $^\circ\text{C}$): δ = 2.71 (t, J = 6.8 Hz, 2 H, CH_2S), 3.04 (t, J = 6.9 Hz, 2 H, CH_2COOH), 7.20 – 7.26 (m, 1 H, $\text{H}_{\text{arom.}}$), 7.77 – 7.89 (m, 2 H, $\text{H}_{\text{arom.}}$), 8.40 (ddd, J = 4.9/1.8/0.9 Hz, 1H, $\text{H}_{\text{arom.}}$) ppm.

MS (ESI); m/z = 260.0068 [$\text{M} + \text{HCOOH}$] $^+$, 216.0145 [$\text{M} + \text{H}$] $^+$ ($\text{C}_8\text{H}_{10}\text{O}_2\text{N}_1^{32}\text{S}_2$).

3.6.4 Synthesis of N-Succinimidyl-3-(2-pyridyldithio)-propionate (SPDP)



3-(Pyridin-2-ylsulfanyl)-propionic acid (1.643 g, 7.634 mmol, 1 eq) was dissolved in dry DCM under nitrogen atmosphere. N-Hydroxysuccinimide (1.000 g, 8.688 mmol, 1.1 eq) was added and after complete dissolution DCC (1.7505 g, 8.688 mmol, 1.1 eq) was added. After 4 h the resulting DCU was filtered off and the solution concentrated, yielding a yellowish waxy solid. The solid was further purified by DCVC ($\varnothing = 4.5$ cm, $h = 5$ cm, $\text{CH}_3\text{Cl}/\text{MeOH}$ gradient, 50 mL fractions, MeOH 0-15%, 1% steps), followed by recrystallization from EtOH (50 °C to -20 °C). The product was isolated by filtration and the recrystallization solution was concentrated and recrystallized again.

$\text{C}_{12}\text{H}_{12}\text{N}_2\text{O}_4\text{S}_2$: 1.3355 g (56%). White solid.

TLC: $R_f = 0.75$ ($\text{CH}_2\text{Cl}_2/\text{MeOH} = 10:1$).

^1H NMR (500 MHz, CDCl_3 , 22.9°C): $\delta = 2.84$ (s, 4 H, $\text{COCH}_2\text{CH}_2\text{CO}$), 3.04–3.09 (m, 2 H, $\text{SCH}_2\text{CH}_2\text{CO}$), 3.09 – 3.15 (m, 2 H, $\text{SCH}_2\text{CH}_2\text{CO}$), 7.09–7.14 (m, 1 H, $\text{H}_{\text{arom.}}$), 7.64–7.69 (m, 2 H, $\text{H}_{\text{arom.}}$), 8.48–8.51 (ddd, $J = 4.7/1.3/1.2$ Hz, 1 H, $\text{H}_{\text{arom.}}$) ppm.

^{13}C NMR (100 MHz, CDCl_3 , 20.5°C): $\delta = 25.7$ (t, $\text{COCH}_2\text{CH}_2\text{CO}$), 31.1 (t, $\text{COCH}_2\text{CH}_2\text{S}$), 32.9 (t, $\text{COCH}_2\text{CH}_2\text{S}$), 120.1 (d, $\text{C}_{\text{arom.}}$), 121.2 (d, $\text{C}_{\text{arom.}}$), 137.4 (d, $\text{C}_{\text{arom.}}$), 150.0 (d, $\text{C}_{\text{arom.}}$), 159.3 (s, $\text{C}_{\text{arom.}}$), 167.2 (s, $\text{COCH}_2\text{CH}_2\text{S}$), 169.1 (s, $\text{COCH}_2\text{CH}_2\text{CO}$) ppm.

MS (EI, 70 eV); $m/z = 312.0157$ [M] $^+$, 198.0105 (29), 143.9892, 110.9817. HRMS (EI, 70 eV): [M] $^+$ ber. für $\text{C}_{12}\text{H}_{12}\text{N}_2\text{O}_4\text{S}_2$, 312.0239; found 312.0194. MS (ESI); $m/z = 312.0312$ [$\text{M}+\text{H}$] $^+$

3.6.5 Synthesis of mEGF-SH

Mercapto-modified EGF was synthesized analogously as described by Blessing et al.¹⁰⁹. A solution of 10 mg of EGF (1.65 μ mol, recombinant, murine) in 1.0 ml of 20 mM HEPES buffer pH 7.1 was mixed with a solution of SPDP (5.2 mg, 16.5 μ mol) in 0.5 ml EtOH, resulting in a final concentration of 30% EtOH. After 2 h reaction time the resulting EGF-PDP was purified by SEC using a Sephadex G-25 superfine column and pH 7.1 HEPES/30% EtOH buffer for elution. The product containing fractions were collected and concentrated in a speedvac. Five mg of the resulting EGF-PDP in 2.5 ml of 20 mM HEPES pH 7.1 were treated with a 50-fold molar excess of DTT for 15 min under argon atmosphere. EGF-SH was purified by SEC on a Sephadex G-10 column using 20 mM HEPES pH 7.1 for elution yielding 3.5 mg EGF-SH (determined by A_{280}).

3.6.6 Synthesis of LPEI-PEG-OPSS Conjugates

20 mg of LPEI (free base form, 0.9 μ mol) were dissolved in 1 mL of EtOH by shaking for 30 min at 30 °C. The use of ethanol as solvent was superior over aqueous buffers and various other organic solvents in terms of reproducibility and yield. After complete dissolution 2.25 μ mol of the appropriate NHS-PEG-OPSS or NHS-PEG in DMSO were added and agitated for 3 h. The resulting conjugate was purified using ion-exchange chromatography (20 mM HEPES pH 7.1, Elution with 20 mM HEPES containing 3 M NaCl) followed by dialysis (MWCO: 10 kDa) against 20 mM HEPES pH 7.1. Substitution grade was calculated by A_{343} after DTT induced 2-Pyridinethione release and/or ^1H -NMR Analysis.

3.6.7 Attachment of mEGF-SH to LPEI-PEG-OPSS Conjugates

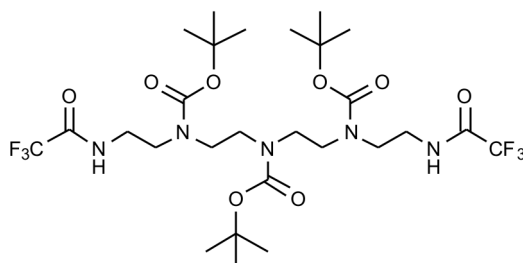
5 mg of LPEI-PEG-OPSS (corresponding to 0.2 μ Mol of OPSS) in 20 mM HEPES pH 7.1 were mixed with a 1.5 molar surplus of mEGF-SH and incubated until A_{343} indicated complete turnover. The resulting conjugate was purified using SEC on a Sephadex G-25 column and concentrated using a speedvac. Concentration was determined by photometric copper assay (see 3.3).

3.6.8 Synthesis of brPEI Tetraconjugate (Mel-brPEI-PEG-mEGF)

EGF-PEG-brPEI-Mel was synthesized like described before¹⁰². Briefly, EGF-SH is anchored to NHS-PEG_{3.4k}-maleinimide, the resulting EGF-PEG_{3.4k}-NHS-Linker is conjugated to brPEI and the resulting conjugate purified by SEC. The construct is subsequently modified with SPDP, purified by SEC and in the last step modified with melittin-SH, followed by SEC purification. This resulted in a conjugate with the nominal composition of EGF: PEG: brPEI: Mel = 2.5 : 2.5 : 1 : 5 .

3.7 Solid-Phase Synthesis Building blocks

Synthesis of Bis-tfa-Tp(boc₃) [Di-*tert*-butyl 5-*tert*-butoxycarbonyl-2,8-bis(trifluoroacetyl-aminoethyl)-2,5,8-triazanonan-1,9-dioate] using Tetraethylenepentamine Penta-hydrochloride



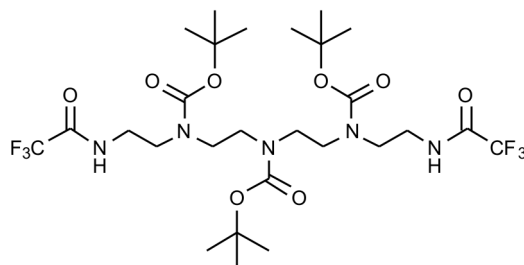
10 g (26.9 mmol, 1 eq) tetraethylenepentamine pentahydrochloride were weighed in a 1 L round bottom flask and dissolved in 250 ml DCM/MeOH (2:1). 18.75 mL (134.5 mmol, 5 eq) TEA were added and after stirring for 2 - 12 h the mixture was cooled down to 0 °C. 6.72 mL (56.3 mmol, 2.1 eq) ethyl trifluoroacetate were diluted in DCM (40 mL) and added dropwise over 2 h at 0 °C. The RBF was allowed to warm to RT after 2 h and was stirred for another hour. Di-*tert*-butyl dicarbonate (23.4 g, 107.6 mmol, 4 eq) was dissolved in 40 ml DCM and added dropwise over one hour. Afterwards 15 ml of triethylamine (107 mmol, 4 eq) were added and the mixture was stirred over night. The organic phase was reduced to approximately 150 mL and washed three times with saturated sodium bicarbonate, followed by three times 5 % sodium citrate solution and finally three times with water. The organic phase was dried over sodium sulfate and the solvent was evaporated to a yellowish viscous, waxy solid. The residue was recrystallised: for this purpose it was dissolved in the minimal amount of DCM (37 mL) which was heated to reflux. Then slowly *n*-hexane (65 mL) was added to the boiling DCM till clouding could be observed at the drop-in point. The crystallisation solution was stored over night in a refrigerator at 4 °C. The crystalline residue was filtered, washed with cooled *n*-hexane and dried.

C₂₇H₄₅F₆N₅O₈: 15.23 g (83.0 %)

¹H NMR (500 MHz, CDCl₃, 24.1 °C): δ = 1.39–1.48 (m, 27 H, OC(CH₃)₃), 3.20–3.55 (m, 16 H, CH₂), 7.93 (d, *J* = 46.5, 0.15 H, NH), 8.21 (d, *J* = 41.3, 0.35 H, NH) ppm.

MS (ESI); *m/z* (%) = 699.3527 [M+NH₄]⁺, 682.3268 [M+H]⁺

Synthesis of Bis-tfa-Tp(boc₃) [Di-*tert*-butyl 5-*tert*-butoxycarbonyl-2,8-bis(trifluoroacetylaminoethyl)-2,5,8-triazanonan-1,9-dioate] Using Technical Grade (85%) Tetraethylenepentamine



12 g (53,8 mmol, 1 eq) of tetraethylenepentamine (TEPA) were weighed in a 1 L round bottom flask and dissolved in 500 mL DCM. The mixture was cooled down to 0 °C. Trifluoroacetic ethyl ester (13.45 ml, 16.05 g, 112.6 mmol, 2.1 eq.) was diluted in 220 ml DCM and transferred into a dropping funnel. It was added dropwise to the cooled mixture in the round bottom flask over 2.5 h. After complete addition of the trifluoroacetic ethyl ester the reaction was stirred for an additional hour at RT.

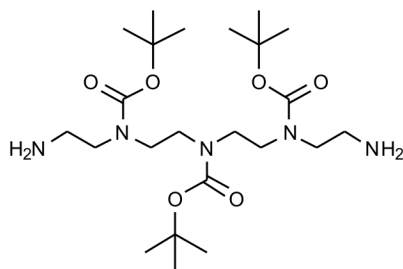
Di-*tert*-butyl dicarbonate (47 g, 215.3 mmol, 4 eq.) was dissolved in 80 ml DCM and added dropwise over one hour. Afterwards 30 ml of triethylamine (21.8 g, 215.2 mmol, 4 eq) were added and the mixture was stirred over night.

The organic phase was reduced to approximately 150 mL and washed three times with saturated sodium bicarbonate, followed by three times 5 % sodium citrate solution and finally three times with water. The organic phase was dried over sodium sulfate and the solvent was evaporated to a yellowish viscous, waxy solid. The oily residue was re-crystallised: for this purpose it was dissolved in the minimal amount of boiling DCM (60 ml). Then *n*-hexane (~ 140 ml) was added to the boiling DCM till clouding was observed at the drop-in site. The crystallisation solution was stored over night in a refrigerator at 4 °C. The microcrystalline residue was filtered, washed with cooled *n*-hexane and dried. Yield = 23.1 g (63%)

C₂₇H₄₅F₆N₅O₈: 23.1 g (63%)

¹H NMR (500 MHz, CDCl₃, 24.0 °C): δ = 1.39–1.48 (m, 27 H, OC(CH₃)₃), 3.20–3.55 (m, 16 H, CH₂), 7.93 (d, J = 46.5, 0.15 H, NH), 8.21 (d, J = 41.3, 0.35 H, NH) ppm.

MS (ESI); *m/z* (%) = 699.3527 [M+NH₄]⁺, 682.3268 [M+H]⁺

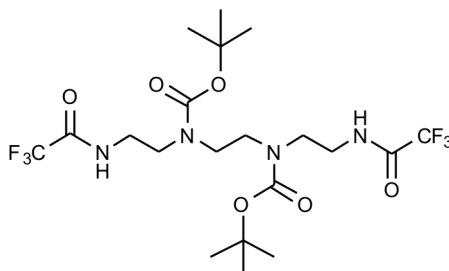
Synthesis of Tp(boc₃) [Di-*tert*-butyl 5-*tert*-butoxycarbonyl-2,8-bis(aminoethyl)-2,5,8-triazanonan-1,9-dioate]

10 g bis-tfa-Tp(boc₃) (14.7 mmol, 1 eq) were suspended in 75 ml ethanol. 100 ml of 3 M aqueous sodium hydroxide (300 mmol, 20 eq) were slowly added via a dropping funnel under stirring. After a reaction time of 6-20 hours the ethanol was evaporated and the aqueous phase was extracted with 3 x 100 ml DCM. The pooled organic phases were dried over sodium sulfate. After evaporation of the solvent and 6 h HV-treatment Tp(boc₃) was isolated as viscous oil which solidified after addition of crystallization seeds and storage at 4 °C.

C₂₃H₄₇N₅O₆: 7.201 g (99.8%)

¹H NMR (400 MHz, CDCl₃, 50.0 °C): δ = 1.40–1.50 (m, 27 H, OC(CH₃)₃), 2.36–2.58 (bs, 4 H, NH₂), 2.79-2.96 (bt, J = 5.1, 4 H, CH₂), 3.21 – 3.41 (m, 12 H, CH₂) ppm.

MS (ESI); *m/z* (%) = 245.6837 [M+2H]⁺, 490.3610 [M+H]⁺

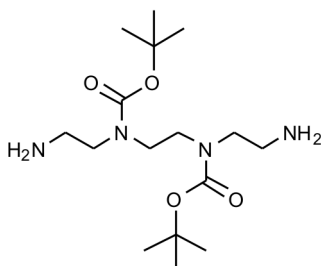
Synthesis of Bis-tfa-Tt(boc₂) [Di-*tert*-butyl 2,5-bis(trifluoroacetylaminoethyl)-2,5-diazahehexan-1,6-dioate]

Triethyltetramine (2.0 g, 13.7 mmol, 2.05 ml, 1 eq) was dissolved in 27 ml CH₂Cl₂. A solution of trifluoroacetic ethyl ester (4.09 g, 28.9 mmol, 3.43 ml, 2.1 eq) in 57 ml CH₂Cl₂ was added dropwise at 0 °C and stirred for 1 h at 0 °C. Triethylamine (2.91 g, 28.8 mmol, 4.00 ml, 2.1 eq) was added and the reaction was brought to RT, followed by dropwise addition of a solution of di-*tert*-butyl dicarbonate (8.9838 g, 41.2 mmol, 3 eq) in 21 ml CH₂Cl₂. The reaction was stirred overnight and washed 3 x 5% NaHCO₃ solution, 3 x 5% citric acid solution and 3 x water dried over Na₂SO₄, filtered and concentrated. The resulting white solid was recrystallized from DCM/hexanes, yielding bis-tfa-Tt(boc₂) as a white solid.

C₂₀H₃₂F₆N₄O₆: 4.829 g (65%)

¹H NMR (400 MHz, CDCl₃, 50 °C): δ = 1.46 (s, 18 H, OC(CH₃)₃), 3.26–3.65 (m, 12 H, CH₂), 7.70 (s_{br}, 0.66 H, NH), 8.84 (s_{br}, 0.67 H, NH) ppm.

MS (ESI); *m/z* = 556.2572 [M+NH₄]⁺, 539.2312 [M+H]⁺

Synthesis of Tt(Boc₂) [Di-*tert*-butyl 2,5-bis(aminoethyl)-2,5-diazahehexan-1,6-dioate]

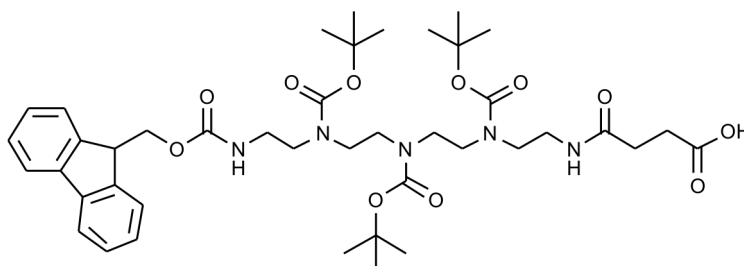
4 g (7.4 mmol, 1 eq) bis-tfa-Tt(boc₂) were suspended in 47 ml EtOH. 50 ml of 3 M aqueous sodium hydroxide (15 mmol, 20 eq) were slowly added via a dropping funnel under stirring. After a reaction time of 6-20 hours the ethanol was evaporated and the aqueous phase was extracted with 3 x 50 ml DCM. The pooled organic phases were dried over sodium sulfate. After evaporation of the solvent and 6 h HV-treatment Tt(boc₂) was isolated as white solid.

C₁₆H₃₄N₄O₄: 1.72 g (66%)

TLC: R_f = 0.23 (CH₂Cl₂/MeOH = 7:3 + 5% Triethylamin).

¹H NMR (400 MHz, CDCl₃, 19.1 °C): δ = 1.24 (s_{br}, 4 H, NH₂), 1.45 (s, 18 H, OC(CH₃)₃), 2.812 (t, J = 6.2 Hz, 4 H, CH₂), 3.25 (t, J = 6.2 Hz, 4 H, CH₂), 3.32 (t, J = 7.5 Hz, 4 H, CH₂) ppm.

¹³C NMR (125 MHz, CDCl₃, 21.3 °C): δ = 28.8 (q, 6 C, C(CH₃)₃), 40.9 (t, 1 C, CH₂), 41.3 (t, 1 C, CH₂), 45.9 (t, 1 C, CH₂), 46.2 (t, 1 C, CH₂), 51.0 (t, 1 C, CH₂), 51.6 (t, 1 C, CH₂), 80.1 (q, 1 C, C(CH₃)₃), 80.2 (q, 1 C, C(CH₃)₃), 156.0 (s, 2 C, C=O) ppm.

Synthesis of Fmoc-Stp-OH [8,11,14-*tert*-Butoxycarbonyl-20-fluoren-9-yl-19-oxa-4,18-dioxo-5,8,11,14,17-pentazaicosanoic acid]

4.0 g of Tp(boc₃) (8.2 mmol, 1 eq) were dissolved in 16.5 mL of THF and cooled to -75 °C. 0.91 g (9 mmol, 1.1 eq) of succinic anhydride were dissolved in 220 mL THF and added dropwise over the course of 2 h. The reaction was stirred for an additional hour at -75 °C and then for 1 h at RT. 4.19 mL DIPEA (3.1 g, 24.1 mmol, 3 eq) were added to the RBF and the reaction mixture cooled to 0 °C. 4.128 g Fmoc-OSu (12.2 mmol, 1.5 eq) were dissolved in a mixture of ACN/THF (25 mL/ 12 mL). This solution was added dropwise to the reaction mixture and stirred over night. The solution was concentrated to approximately 100 mL, mixed with 100 mL of DCM and was washed 5 x with 0.1 M sodium citrate buffer (pH 5.2). The organic phase was dried over NaHCO₃, concentrated and purified by DCVC using a n-Heptane/EtOAc gradient to elute fmoc-byproducts, followed by a EtOAc/MeOH gradient.

C₄₂H₆₁N₅O₁₁: 2.65 g (40%), foamy, off-white solid.

TLC: R_f = 0.63 (CHCl₃/MeOH = 7:3)

¹H-NMR (400 MHz, CDCl₃, 19.1 °C): δ = 7.74 (d, 2H, J=8Hz), 7.56 (d, 2H, J=8Hz), 7.37 (t, 2H, J=8Hz), 7.27 (t, 2H, J=8Hz), 4.40 (m, 2H), 4.20 (t, 1H, J=7Hz), 3.18-3.44 (m, 16H), 2.57-2.70 (m, 2H), 2.37-2.56 (m, 2H), 1.45 (s, 27H) ppm.

¹³C-NMR (100 MHz, CDCl₃, 19.1 °C): δ = 172 (C=O, Suc), 171 (C=O, Suc), 144, 141, 128, 127, 125, 119 (Ar-C-Fmoc), 80 (CH-Fmoc), 60 (OCH₂-Fmoc), 47, 45 (CH₂-Tepa), 35 (CH₂-Suc), 33 (CH₂-Tepa), 28 (CH₃-*tert*-But) ppm.

MS (ESI); m/z = 812.4419 [M+H]⁺, 829.4682 [M+NH₄]⁺, 834.4237 [M+Na]⁺

3.8 Solid-Phase Protocols

3.8.1 Analytical Procedures

Fmoc Quantification

Accurately weighed samples of vacuum-dried resin (10 mg, ~ 1 μ Mol of fmoc) were placed in Eppendorf tubes. 1.0 mL 20 % piperidine in DMF was added to each tube. The tubes were vortexed briefly and agitated at RT for 1.25 h. At the end of this period, the tubes were vortexed and the resin was allowed to settle for approximately 2 min. Aliquots of 50 μ l of the supernatant of each samples, of a positive control (fmoc-Lys(boc)-Wang resin) and of a blank (consisting of 20 % piperidine in DMF) were diluted to 2 ml with DMF (dilution factor 40; see below). A_{301} of each UV sample (duplicates) was determined against the blank solution. The fmoc substitution (mmol/g) was calculated using the following equation:

$$\text{Substitution grade (mmol/ g)} = \frac{1000 \times A_{301}}{m[\text{mg}] \times 7800 \times D}$$

A_{301} is absorbance at 301 nm, m is the mass of the resin, 7800 is the molar extinction coefficient in $\text{L mol}^{-1} \text{ cm}^{-1}$, D is the dilution factor mentioned above.

Kaiser Test¹¹⁰

Solution A: 5% ninhydrin in EtOH (w/v)

Solution B: 80% phenol in EtOH (w/v)

Solution C: KCN in pyridine: 2 mL 0.001 M KCN in 98 mL pyridine

Some beads are transferred into an Eppendorf tube and washed three times with DMF and three times with MeOH. 1-2 drops of each solution are added and the tube placed into a heating block at 100 $^{\circ}\text{C}$ for 4 min. Free amine residues are indicated by intense blue color.

Malachite Green Test¹¹¹

Solution A: 0.025% Malachite Green (w/v) in EtOH abs.

Solution B: Triethylamine

A couple of beads were transferred from the reaction vessel into an eppendorf tube. The beads were washed twice with methanol. 1 ml of Solution A and one drop of Solution B were added. After 2 min the beads were washed with ethanol until the supernatant was clear. Free carboxylic acid residues are indicated by green colored beads.

TNBS Test¹¹²

Solution A: 10 % DIPEA in DMF (v/v)

Solution B: 1% 2,4,6-trinitrobenzenesulfonic acid in MilliQ water (w/v)

A couple of beads were transferred from the reaction vessel into an eppendorf tube. The beads were washed thrice with DMF. Three drops of Solution A and B were added and the tube incubated for 10 min at RT. Orange color of the beads indicated free amines.

3.8.2 General Procedure for 2-Chlorotrityl-Resin Loading

1 g of 2-chlorotrityl chloride resin (Cl-load: 1.6 mmol/g) was weighed into a 50 ml peptide reactor. After adding 10 ml dry DCM and swelling for 10 min 1.25 eq (relative to desired load) fmoc-AA-OH and 2.4 eq DIPEA were added and the reactor was agitated for 1.5 h. The resin was washed four times with DCM and treated with a mixture of DCM/MeOH/DIPEA (10 ml/g, 80/15/5, v/v/v) to cap unreacted 2-chlorotrityl moieties. This step was repeated once. The resin was washed five times with DCM and twice with DMF and was treated twice with 20 % piperidine in DMF for 10/20 min to remove the terminal fmoc-protection group. The resin was washed five times with DMF, twice with DCM and once with n-hexane and dried over KOH in vacuo.

3.8.3 Downsizing of Resin Load for MAP-System Synthesis

0.5 g of Fmoc-Ala-Wang-resin (load = 0.3 to 0.5 mmol/g) were placed in a manual reaction vessel and preswelled in DMF for 1 h. The resin was washed once with DMF and was covered with 4 mL of DMF. 0.065 mmol (38 mg) Fmoc-Lys(Fmoc)-OH, 0.065 mmol (34 mg) PyBOP® and 0.065 mmol HOBt (10 mg) were dissolved in 1 mL DMF, 0.13 mmol DIPEA (23 µL) were added and the solution transferred into the reactor. After 2 h the reactor was drained, washed three times with DMF and 3 times with DCM. The resin was resuspended in 10 mL DCM, followed by the addition of 0.75 mL acetic anhydride and agitated for 1h. Completeness of capping was checked by Kaiser test and the resin washed with DCM (4x), DMF (4x), DCM (4x) followed by hexanes (2x). The low-load resin was transferred into a glass container and dried over night under vacuum.

3.8.4 Solid-Phase Synthesis Cycles

General synthesis protocol A: Coupling Protocol Hartmann Synthesis⁹⁹

Reaction	Description	V [mL/g res]	Repetitions/Time
0 ^a	DCM swell	10	1 x 30 min
(1) ^b	DMF wash	10	3 x 1 min
2 ^c	20% Pip/DMF prewash	10	1 x 5 min
3 ^c	20% Pip/DMF deprotection	10	1 x 20 min
4 ^c	DMF wash	10	5 x 1 min
5	Anhydride coupling (10 eq) in DMF	10	1 x 30 min
6 ^d	Kaiser/Malachit Green test		
7	20% DIPEA wash	10	2 x 3 min
8	DMF wash	10	5 x 1 min
9	Diamine/PyBOP®/HOBt (10 eq) in DMF	10	1 x 30 min
10 ^d	Kaiser/Malachit Green test		
^a Preswelling of trityl based resins before synthesis start			
^b Preswelling of wang based resins before synthesis start			
^c Optional, only if fmoc-protected residue on resin			
^d If Malachit Green/Kaiser test does not show completion of coupling reaction (>99.5), repeat coupling steps			

General synthesis protocol B: Coupling Protocol Polyamidoamine/Peptides

Reaction	Description	V [mL/g res]	Repetitions/Time
0 ^a	DCM swell	10	1 x 30 min
(1) ^b	DMF wash	10	3 x 1 min
2	20% Pip/DMF prewash	10	1 x 5 min
3	20% Pip/DMF deprotection	10	1 x 20 min
4	DMF wash	10	5 x 1 min
5	Preactivated Fmoc-AA (4 eq) in DMF	10	1 x 30 min
6	DMF wash	10	5 x 1 min
7 ^c	Kaiser/TNBS test		
^a Preswelling of trityl based resins before synthesis start ^b Preswelling of wang based resins before synthesis start ^c If Kaiser test does not show completion of coupling reaction (>99.5), repeat 4-7			

Shrinking Protocol for Long Term Resin Storage

Reaction	Description	V [mL/g res]	Repetitions/Time
1	DMF wash	10	5 x 1 min
2	DCM wash	10	3 x 1 min
3	n-hexane wash	10	3 x 1 min

After the last n-hexane wash the resin is predried by suction for 1 min. The damp resin is transferred into an container and dried in vacuo over KOH for 24 h.

3.9 General Cleavage Procedures**General Cleavage Procedure A: Peptides and Non-Oleic Acid Containing PAAs**

The resin was transferred into a syringe reactor of appropriate size and treated with 10 mL/g_(resin) of a TFA/Water/TIS (95:2.5:2.5) mixture for 1-3 h. The resin was filtered and washed twice using pure TFA followed by two DCM washes. The combined filtrates were concentrated using a rotovap and either precipitated by dropwise addition into ice-cold MTBE (50 mL MTBE/1 mL TFA) or other suitable mixtures. If precipitation was not possible the TFA was further concentrated to a glassy film and

washed 3x with ice-cold MTBE. The precipitate/film was dissolved in 2.5% acetic acid, snap-frozen and lyophilized to obtain the crude peptide.

Cleavage Procedure for Oleic Acid Containing PAAs

The resin was transferred into a syringe reactor of appropriate size and treated with 10 mL/g_(resin) of a TFA/Water/EDT (95:2.5:2.5) mixture for 1-2 h. The resin was filtered off and washed twice using pure TFA followed by two DCM washes. The combined filtrates were concentrated in a rotovap and either precipitated by dropwise addition into ice-cold MTBE (50 mL MTBE/1 mL TFA) or other suitable mixtures. The precipitate was collected by centrifugation. If precipitation was not possible the TFA was further concentrated to a glassy film and washed 3x with ice-cold MTBE. The precipitate/film was dissolved in 5% acetic acid, snap-frozen and lyophilized to obtain the crude peptide.

3.10 General Procedures Solid-Phase Synthesis

3.10.1 Synthesis of N-Terminal Stp-Modified Peptides

Peptides were assembled in a fully automatic fashion using fmoc/tBu chemistry on an Applied Biosystems 431A Peptide Synthesizer employing the Applied Biosystems Small Scale FastMoc® protocols. After successful synthesis the resin was transferred to a syringe reactor and was manually modified with Stp-units according to general method **3.8.4.B**

3.10.2 General Procedure: Synthesis of Stp-Chains

An amount of resin corresponding to 25-50 μ mole of loaded amino acid was weighed into a syringe reactor and swelled for 30 min in an appropriate solvent. Briefly, each cycle began with fmoc-removal by treatment with 20% piperidine in DMF followed by DMF washing steps. Coupling was normally done using a mixture of fmoc-AA-OH/PyBOP®/HOBt/DIPEA (4/4/4/8 eq) for 30 min or until complete conversion was indicated by Kaiser test. For a general scheme see Table 3.8.4.B.

3.10.3 General Procedure: Synthesis of i-Shapes with one FA: HO-K-Stp₁-FA₁

After swelling of fmoc-Lys(boc)-Wang resin (0.05-0.20 mmol) in DMF and cleavage of the fmoc protecting group, four equivalents of a solution of fmoc-Stp(boc₃)-OH in DMF, DIPEA (8 eq) and PyBOP®/HOBt (4 eq) were added to the resin and the vessel was agitated until Kaiser test indicated complete conversion (30 min). The reaction solvent was drained and the resin was washed five times with DMF. To cap residual, unreacted primary amino groups before introduction of the fatty acid the resin was acetylated using 5 equivalents of acetic anhydride and 10 equivalents of DIPEA, before the subsequent removal of the fmoc protecting group.

After removal of the fmoc protecting group, the resin was washed three times with DMF followed by three DCM washes. Five equivalents of fatty acid were dissolved in DCM (as concentrated as possible) while 5 equivalents of PyBOP®/HOBt and 10 equivalents of DIPEA dissolved in the smallest possible volume of DMF were added to the resin and the mixture was agitated until Kaiser test did indicate complete conversion (normally 30 min). After completion of the reaction the resin was washed and dried for 12 h over KOH in vacuo. For cleavage conditions see section 3.9.

3.10.4 General Procedure: Synthesis of i-Shapes with two FAs: HO-K-Stp₁-K-FA₂

After swelling of fmoc-Lys(boc)-Wang resin (0.05-0.20 mmol) in DMF and cleavage of the fmoc protecting group, four equivalents of a solution of fmoc-Stp(boc₃)-OH in DMF, DIPEA (8 eq) and PyBOP®/HOBt (4 eq) were added to the resin and the vessel was agitated until Kaiser test indicated complete conversion (30 min). The reaction solvent was drained and the resin was washed five times with DMF. To couple two fatty acids to the N-terminus of the PAA, fmoc-Lys(fmoc)-OH was incorporated before the coupling of the fatty acid. To cap residual, unreacted primary amino groups before introduction of the fatty acid the resin was acetylated using 5 equivalents of acetic anhydride and 10 equivalents of DIPEA, before subsequent removal of the fmoc protecting group.

The resin was washed three times with DMF followed by three DCM washes after removal of the fmoc protecting group. Ten equivalents of the fatty acid were dissolved in DCM while 10 equivalents of PyBOP®/HOBt and 20 equivalents of DIPEA in the smallest possible amount of DMF were added to the resin and the

mixture was agitated until Kaiser test did indicate complete conversion (normally 30 min). After completion of the reaction the resin was washed and dried for 12 h over KOH *in vacuo*. For cleavage conditions see section 3.9.

3.10.5 General Procedure: Synthesis of i-Shapes with a Single Coupling Domain: HO-C-Stp₁-K-FA₂

For PAAs containing a C-terminal cysteine fmoc-Cys(trt)-Wang resin was used. All other steps of the synthesis were performed as described in General Procedure 3.10.3. For cleavage conditions see section 3.9.

3.10.6 General Procedure: Synthesis of i-Shapes with Two Coupling Domains: HO-C-Stp₃-C-K-FA₂

After swelling 0.035 mmol of a fmoc-Cys(trt)-Wang resin in DMF and cleavage of the fmoc protecting group, four equivalents of a solution of fmoc-Stp(boc₃)-OH in DMF, DIPEA (8 eq) and PyBOP®/HOBt (4 eq) were added to the resin and the vessel was agitated until Kaiser test indicated complete conversion (normally 30 min). The reaction solvent was drained and the resin was washed five times with DMF. This cycle was repeated twice. Afterwards the amino acid fmoc-Cys(trt)-OH was coupled. Then, in order to couple two fatty acids to the linear PAA, fmoc-Lys(fmoc)-OH was incorporated *N*-terminal before the coupling of the fatty acid. To cap unreacted primary amino groups, the resin was acetylated using 5 equivalents of acetic anhydride and 10 equivalents of DIPEA, before the subsequent removal of the fmoc protecting group. To couple the fatty acid, the solvent was changed to DCM after fmoc cleavage. Therefore, after removal of the fmoc protecting group, the resin was washed three times with DMF and DCM. 10 equivalents of the fatty acid were dissolved in DCM, 20 equivalents of DIPEA and 20 equivalents of PyBOP®/HOBt in DMF were added to the resin and the mixture was agitated for 30 min. After completion of the reaction the resin was washed and dried over KOH *in vacuo*. For cleavage conditions see section 3.9.

3.10.7 Synthesis of t-Shapes with One FA: HO-C-Stp₁-K(FA)-Stp₁-C-H

After swelling 0.05-0.20 mmol of fmoc-Cys(trt)-Wang resin in DMF for 30 min the fmoc-protection group was cleaved by double treatment with 20% piperidine in DMF. After washing the resin, four equivalents (related to resin loading) of fmoc-Stp(boc₃)-OH, DIPEA (8 eq) and PyBOP®/HOBt (4 eq) were added for 30 min. The reaction solvent was drained and the resin was washed five times with DMF. Reaction progress was monitored by Kaiser test. To introduce a branching point dde-Lys(fmoc)-OH was used in the next coupling step. Dde-Lys(fmoc)-OH (4 eq) solved in DMF, DIPEA (8 eq) and PyBOP®/HOBt (4 eq) solved in DMF were added and the synthesis vessel was agitated for 30 min. After a negative Kaiser test, the resin was washed with DMF. To cap unreacted primary amino groups, the resin was acetylated using 5 equivalents of acetic anhydride and 10 equivalents of DIPEA, before the subsequent removal of the fmoc protecting group. To couple the fatty acid, the solvent was changed to DCM after fmoc-cleavage. Therefore the resin was washed three times with DMF and DCM after removal of the fmoc-protecting group. 5 equivalents of the fatty acid solved in DCM, 10 equivalents of DIPEA and 5 equivalents of PyBOP®/HOBt were added to the resin for 30 min. After completion of the reaction the resin was washed five times with DCM and three times with DMF. The dde-protecting group was cleaved with 2% hydrazine monohydrate in DMF (v/v) (5-10 times for 5 min) till no significant A₃₀₀ was measurable in the deprotection mixture. In-between the deprotection-steps the resin was washed twice with DMF. fmoc-Stp(boc₃)-OH solved in DMF, DIPEA (8 eq) and PyBOP®/HOBt (4 eq) were added for 30 min. After a successful reaction the resin was treated twice with 20% piperidine in DMF. After washing the resin, boc-Cys(trt)-OH (4 eq) solved in DMF, DIPEA (8 eq) and PyBOP®/HOBt (4 eq) were added and the vessel agitated for 30 min. Afterwards the resin was washed and dried over KOH in vacuo. For cleavage conditions see section 3.9.

3.10.8 Synthesis of t-Shapes with Two FAs: HO-C-Stp₁-K(K-FA₂)-Stp₁-C-H

After swelling 0.05-0.20 mmol of fmoc-Cys(trt)-Wang resin in DMF for 30 min the fmoc-protection group was cleaved by double treatment with 20 % piperidine in DMF. After washing the resin, four equivalents (related to resin loading) of fmoc-Stp(boc₃)-OH, DIPEA (8 eq) and PyBOP®/HOBt (4 eq) were added for 30 min. The reaction solvent was drained and the resin was washed five times with DMF. Reaction progress was monitored by Kaiser test. To introduce a branching point dde-Lys(fmoc)-OH was used in the next coupling step. Dde-Lys(fmoc)-OH (4 eq) solved in DMF, DIPEA (8 eq) and PyBOP®/HOBt (4 eq) solved in DMF were added and the synthesis vessel was agitated for 30 min. After a negative Kaiser test, the resin was washed with DMF. After treatment with 20 % piperidine in DMF and washing the resin with DMF, fmoc-Lys(fmoc)-OH (4 eq), DIPEA (8 eq) and PyBOP®/HOBt (4 eq) was added. In order to cap unreacted primary amino groups, the resin was acetylated using 5 equivalents of acetic anhydride and 10 equivalents of DIPEA, before the subsequent removal of the fmoc protecting group. To couple the fatty acid, the solvent was changed to DCM after fmoc-cleavage. Therefore the resin was washed three times with DMF and DCM after removal of the fmoc-protecting group. 10 equivalents of the fatty acid solved in the minimal amount of DCM, 20 equivalents of DIPEA and 10 equivalents of PyBOP®/HOBt were added to the resin for 30 min. After completion of the reaction the resin was washed five times with DCM and three times with DMF.

The dde-protecting group was cleaved with 2% hydrazine monohydrate in DMF (v/v) (5-10 times for 5 min) till no significant A₃₀₀ was measurable in the deprotection mixture. In-between the deprotection-steps the resin was washed twice with DMF. fmoc-Stp(boc₃)-OH solved in DMF, DIPEA (8 eq) and PyBOP®/HOBt (4 eq) were added for 30 min. After successful reaction the resin was treated twice with 20 % piperidine in DMF. After washing the resin, boc-Cys(trt)-OH (4 eq) solved in DMF, DIPEA (8 eq) and PyBOP(R)/HOBt (4 eq) were added for 30 min. Afterwards the resin was washed and dried over KOH in vacuo. For cleavage conditions see section 3.9.

3.11 Biophysical and Biological Methods

3.11.1 Polyplex Formation

DNA Polyplex Formation Using PEI-based Carriers

Polyplex formulations for DNA delivery were prepared as follows: 200 ng of DNA/well and the calculated amount of polymer were diluted in the same volume of HBG (pH 7.1) using separate tubes. The DNA solution was added to the polymer, rapidly mixed by pipetting and incubated for 30-40 min at RT to form the polyplexes necessary for transfection and gel-shift experiments.

poly(I:C)/poly(I) Polyplex Formation Using PEI-based Carriers

Polyplex formulations for p(I:C)/p(I) delivery were prepared as follows: the indicated amount of p(I:C)/p(I) and the calculated amount of polymer were diluted in the same volume of HBG (pH 7.1) using separate tubes. The RNA solution was added to the polymer, rapidly mixed by pipetting up and down and incubated for 30-40 min at RT to form the polyplexes necessary for transfection and gel-shift experiments.

siRNA Polyplex Formation Using PAA-based Carriers

Polyplex formulations for siRNA delivery were prepared as follows: 500 ng of siRNA/well and the calculated amount of PAA were diluted in separate tubes in HBG pH 8.3. The RNA solution was added to the polycations solution, mixed by pipetting and incubated for 30-40 min at RT in order to form the polyplexes necessary for transfection and gel-shift experiments.

DNA Polyplex Formation Using PAA-based Carriers

Polyplex formulations for DNA delivery were prepared as follows: 200 ng of DNA/well and the calculated amount of PAA were diluted in separate tubes in HBG pH 8.3. The DNA solution was added to the polycations solution, mixed by pipetting and incubated for 30-40 min at RT in order to form the polyplexes necessary for transfection and gel-shift experiments.

3.11.2 Size and Zetapotential Measurements

Particle size of siRNA and DNA formulations was measured by laser-light scattering using a Zetasizer Nano ZS (Malvern Instruments, Worcestershire, U.K.). Polyplexes were formed for 30-40 min at RT, containing 10 µg nucleic acid and the corresponding amount of polymer. For measurement of zetapotential polyplexes were diluted with 1 mM NaCl to give a final volume of 1 ml and a nucleic acid concentration of 10 µg/ml. The polyplexes were diluted to 500 µl with HBG or H₂O before measurement.

3.11.3 Gel-Shift Assays

DNA Gel-shift Assay

A 1% agarose gel was prepared by dissolving 1.2 g agarose in 120 ml TBE buffer and heating the mixture to 100 °C. After cooling down to approximately 50 °C, 120 µl Gel-Red (1 mg/mL) were added and the gel was poured in the casting unit. Polyplex-samples containing 100 ng DNA, polymer, HBG-buffer and loading buffer were placed into the pockets after an incubation time of 30 min at RT. Electrophoresis was performed at 120 V for 80 min.

siRNA Gel-shift Assay

A 2.5% agarose gel was prepared by dissolving 3.0 g agarose in 120 ml TBE buffer and heating the mixture to 100 °C. After cooling down to approximately 50 °C, 120 µL Gel-Red (1 mg/mL) were added and the gel was poured in the casting unit. Polyplex-samples containing 500 ng siRNA, polymer, HBG-buffer and loading buffer were placed into the pockets after an incubation time of 30 min at RT. Electrophoresis was performed at 120 V for 40 min.

Polyplex Dissociation Assay

The agarose gels were prepared as described above. The polyplexes contained either 100 ng DNA or 500 ng siRNA and polymer in HBG-buffer. To inhibit electrostatic interactions between the nucleic acid and the polycation, the polyplex samples were incubated with heparin (0.01-0.5 I.U./ 0.5 µg siRNA or 0.1 µg DNA) for

5 min. After adding loading buffer the samples were placed into the gel-pockets. Electrophoresis was performed at 120 V for 40 min (siRNA)/ 80 min (DNA).

3.11.4 Erythrocyte Leakage Assay

Freshly collected, citrate buffered murine blood was washed by four centrifugation cycles, each in phosphate-buffered saline (PBS) at 2000 rpm (600-800 g) at 4 °C for 10 min. The erythrocytes in the pellet were counted. The pellet was then diluted with different PBS buffers (pH 7.4, 6.5 and 5.5) to 5×10^7 erythrocytes/mL. The suspension was always freshly prepared and used within 24 h. 75 µl of the PAA solutions prepared at different concentration and different pH-values were mixed with 75 µl erythrocyte suspension in a 96-well plate (NUNC, V-bottom, Denmark). After incubating the plates under constant shaking at 37 °C for 60 min, intact blood cells and cell debris was removed by centrifugation (4 °C, 600-800 g (2000 rpm), 10 min). 80 µl of the supernatant was transferred to a new 96-well plate (TPP 96F, Trasadingen, Switzerland). Hemoglobin absorption was determined at 405 nm using a microplate reader (Spectrafluor Plus, Tecan Austria GmbH, Grödig, Austria). PBS-buffers with pH-values of 7.4, 6.5 and 5.5 were used as negative control, 1 % TritonX-100 in PBS as positive control. Relative hemolysis was defined as

$$\%[\text{haemolysis}] = \frac{A_{405(\text{PAA})} - A_{405(\text{Buffer})}}{A_{405(\text{TritonX-100})} - A_{405(\text{Buffer})}} \times 100$$

3.11.5 Cell Viability Assay (MTT Assay)

The metabolic activity of the cells was determined using a methylthiazole tetrazolium (MTT)¹¹³ assay as follows: 10 µL per 100 µL of medium of a 5 mg/mL solution of MTT in sterile PBS-buffer was added to each well of the 96-well plate. After incubation for 1-2 h at 37 °C the medium was removed and the cells were frozen at -80 °C for at least 1 h. 200 µl DMSO were added and the samples were incubated under constant shaking at 37 °C for 30 min to dissolve the crystals completely. The optical absorbance was measured at 590 nm with a reference wavelength of 630 nm using a microplate reader (Spectrafluor Plus, Tecan Austria GmbH, Grödig, Austria). The cell viability was defined as percent:

$$\%[\text{viability}] = \frac{A_{590(\text{treated})}}{A_{590(\text{untreated control})}} \times 100$$

3.11.6 Luciferase Gene Silencing

All experiments were performed in stably transfected Neuro2A-eGFPLuc cells. Cells were seeded in 96-well plates (TPP, Trasadingen, Switzerland) using 5000 cells/well 24 h prior to transfection. Transfection complexes containing siRNA were then added to cells in 100 µl culture medium containing 10% serum, 100 U/ml penicillin and 100 µg/ml streptomycin (final siRNA-concentration 367 nM). 48 h after initial transfection medium was removed and cells were lysed in 50 µl 0.5X Promega cell lysis solution to measure the gene expression as described below. Transfections were performed in parallel using a non-specific control siRNA to distinguish between specific gene silencing and unspecific knockdown of protein expression due to carrier toxicity. Qualitative information on the toxicity of the conjugates was obtained by diminution in luciferase expression upon delivery of the non-specific control siRNA compared to the luciferase expression from the same number of untreated control cells.

3.11.7 Luciferase Reporter Gene Expression

Cells were plated in 96 well plates at a density of 10.000 cells per well 24 h prior to transfection. The polyplexes formed using 200 ng of pDNA/well were added to the cells in 100 µl culture medium containing 10% serum, 100 U/ml penicillin and 100 µg/ml streptomycin. 24 h after initial transfection medium was removed and cells were lysed in 50 µl 0.5X Promega cell lysis solution to measure the gene expression. Luciferase activity was measured using a Lumat LB9507 instrument (Berthold, Bad Wildbad, Germany). Luciferase light units were recorded from an 20 µl aliquot of the cell lysate with 10 s integration time after automatic injection of freshly prepared luciferin using the luciferase assay system (LAR, Promega, Mannheim, Germany). Transfection efficiency was evaluated as relative light units (RLU) per number of seeded cells. Two ng of recombinant luciferase (Promega, Mannheim, Germany) corresponded to 10^7 light units.

3.11.8 poly(I:C) Cell Culture and Cell Killing Assay *in vitro*

U87MG and U87MGwtEGFR human glioblastoma cells were cultured on collagen coated flasks in DMEM (1 g of glucose/L) supplemented with 10% fetal calf serum (v/v) and 1% penicillin/streptomycin (v/v). U87MGwtEGFR were maintained under constant G-418 selection pressure. Always two parallel polyplex series were carried out in separate 96-well plates (TPP, Transadingen, Switzerland), one for the determination of cell killing efficacy of poly(I:C) polyplex formulations, and one for the determination of cytotoxicity using analogous polyplexes of poly(I) as control. Cells were seeded 24 h prior to transfection with a density of 1×10^4 cells in 200 μ l of culture medium per well. Immediately before transfection, medium was removed and 100 μ l of a dilution of transfection complexes in serum-containing culture medium were added to the cells. After 4 h of incubation at 37 °C, polyplex containing medium was replaced by 200 μ l of fresh serum-containing medium. All experiments were performed in triplicates. Cell killing was evaluated 48 h after treatment by methylthiazole tetrazolium (MTT)/thiazolyl blue assay as described¹¹³. Optical absorbance was measured at 590 nm (reference wavelength 630 nm) using a micro plate reader (Spectrafluor Plus, Tecan Austria GmbH, Grödig, Austria). Metabolic activity was expressed relative to the metabolic activity of untreated control cells, defined as 100%.

A431 cells were cultured on collagen coated flasks in DMEM (1 g of glucose/L) supplemented with 10% fetal calf serum (v/v) and 1% penicillin/streptomycin (v/v). Two parallel polyplex series were carried out, one for the determination of cell killing efficacy of poly(I:C) polyplex formulations, and one for the determination of cytotoxicity using analogous polyplexes of polyglutamate (poly(Glu)) as control. Cells were seeded 24 h prior to transfection with a density of 4×10^3 cells in 200 μ l of culture medium per well. Immediately before transfection, medium was removed and 100 μ l of a dilution of transfection complexes in serum-containing culture medium were added to the cells. After 4 h of incubation at 37 °C, 100 μ l of fresh serum-containing medium were added. All experiments were performed in duplicates. Cell killing was evaluated by methylthiazole tetrazolium (MTT)/thiazolyl blue assay as described above.

3.11.9 poly(I:C) *in vivo* Study

In vivo anti-tumor activity of EGFR targeted poly(I:C) PEI polyplexes was measured using subcutaneous A431 mouse xenografts. Before the experiment, human epidermoid carcinoma A431 cells were cultured in DMEM supplemented with 10% fetal calf serum (v/v) and 1% penicillin/streptomycin. Two million A431 cells were dissolved in 200 μ l PBS and injected subcutaneously into the right flank of immune compromised female athymic nude mice (Nude-Hsd, 5 weeks old). Volume of the growing tumors was calculated as follows: $V=LW^2/2$ (L=length, W=width). When the tumors reached average volume of 100 mm³, mice were randomly divided into five groups (5 mice per group), and treatment was initiated. The complexes were delivered by intravenous injection every 48 hrs for 2 weeks. The first group received poly(I:C)/Melittin-PEI25-PEG-EGF (p(I:C)/MPPE) polyplexes in HBG buffer at 0.1 μ g poly(I:C)/ μ l buffer (the total dose of poly(I:C) was 10 μ g/injection). The second group received poly(I:C)/LPEI-PEG-EGF (poly(I:C)/PPE) polyplexes in HBG at the same dose and concentration. The control groups (poly(Glu)/MPPE and poly(Glu)/PPE) were treated with the same doses of polymer conjugates but replacing poly(I:C) by polyglutamate poly(Glu). The fifth group did not receive any treatment. Tumor volume was measured twice a week until day 14.

3.12 Statistical Analysis

Results were expressed as a mean \pm standard deviation (SD). One-way analysis of variance (ANOVA) was used for evaluating statistical significance. Statistical analysis was performed with GraphPad Prism 5.0. Statistical significance was set when $P < 0.05$.

4 Results

4.1 Poly(I:C) Mediated Tumor Growth Suppression in EGF-receptor Overexpressing Tumors Using EGF-Polyethylene Glycol - Linear Polyethylenimine as Carrier

4.1.1 Introduction

The rapid progress in cancer therapy over the last years led to the identification of new therapeutic targets, the introduction of new therapeutic technologies like antibody or siRNA treatment and the implementation of personalized treatment regimes in therapy. But despite the effort invested in these new approaches, classical chemotherapeutic agents such as doxorubicin or cisplatin are still widely employed in clinics. The inherent drawbacks of these therapeutic approaches are the sometimes severe side effects and the intrinsic or acquired resistance of cancer cells towards the therapeutic drug. In an ideal therapeutic regime the cancer cells are effectively destroyed by the drug without harming the surrounding cells. This can be achieved by drug-targeting or by targeting cancer-specific cellular pathways.

Hence new, promising nucleic acid based therapeutic concepts like antisense therapy or the application of siRNA have moved into the focus of scientific interest. But the application of gene or oligonucleotide based approaches has its own pitfalls, namely the identification of therapeutic target proteins and the specific delivery of the appropriate nucleic acid into the cancer cells. Especially the delivery is challenging as nucleic acids need lipid-based or polymer-based carrier systems¹¹⁴⁻¹²¹ which protect them in the extracellular environment, effectively transport them to the effector site and facilitate their release into the cytosol.

To circumvent acquired chemoresistance of tumor cells and to increase the therapeutic efficacy, a triple effector strategy has been developed, combining targeted delivery, apoptosis induction and the immunostimulatory properties of the artificial dsRNA poly(I:C)¹⁰². By targeting the EGF receptor which is overexpressed in a variety of tumors a better uptake of poly(I:C) into target cells is possible, followed by interferon induction and apoptosis. Intratumoral application of poly(I:C)/cationic polymer complexes (polyplexes) in an orthotopic glioblastoma model or two other EGF receptor overexpressing tumor models caused complete tumor regression in

nude mice. These very promising therapeutic results were based on poly(I:C) polyplexes with a tetra-component conjugate, consisting of 25kDa branched polyethyleneimine (brPEI), EGF as targeting ligand and polyethylene glycol (PEG) for shielding^{109,122}, and a synthetic derivative of the lytic peptide melittin¹²³⁻¹²⁴. The latter was found to be strictly required for cytosolic delivery of poly(I:C) and therapeutic efficacy. Though effective, the tetraconjugate is not practical for further development due to its complexity. In the current communication we report the synthesis of an improved EGF/PEI based carrier with reduced complexity. The chemically poorly defined brPEI was replaced by the analogous linear 22 kDa polymer (LPEI). LPEI can be synthesized in GMP compatible form¹²⁵, has already been tested in human clinical trials as DNA formulation, and was found to be more effective as brPEI in several applications¹²⁶⁻¹²⁸. The generation of a melittin-free conjugate was possible by selecting an optimized PEG/PEI ratio (equimolar amounts using 2 kDa PEG). The newly developed LPEI based poly(I:C)-carrier system exhibits the key features of the old tetraconjugate, namely EGF receptor targeting and effective payload release into the cytosol of tumor cells. The new conjugate shows an improved therapeutic efficiency combined with a simpler synthesis route, allowing the convenient synthesis of larger amounts of the carrier.

4.1.2 Synthesis of LPEI-PEG Conjugates

A comparison of the chemical syntheses of the LPEI triconjugate and the brPEI tetraconjugate is presented in **Figure 4.1**. LPEI-PEG-EGF conjugates were synthesized by a two step procedure. In the first step NHS-PEG-OPSS is anchored to LPEI via its amine reactive NHS function using EtOH as solvent. The resulting PEGylated carrier can now be modified using any thiol containing ligand using an orthogonal disulfide exchange reaction which can be spectroscopically monitored. The brPEI tetraconjugate (EGF-PEG-brPEI-Mel) synthesis (performed by Wolfgang Rödl, Wagner lab) consists of four consecutive reaction steps with intermediate purification. In the first step EGF-SH is conjugated to NHS-PEG3.4 kDa-maleimide, which is subsequently grafted to brPEI. This conjugate is subsequently modified with SPDP, purified and in the last step modified with melittin-SH.

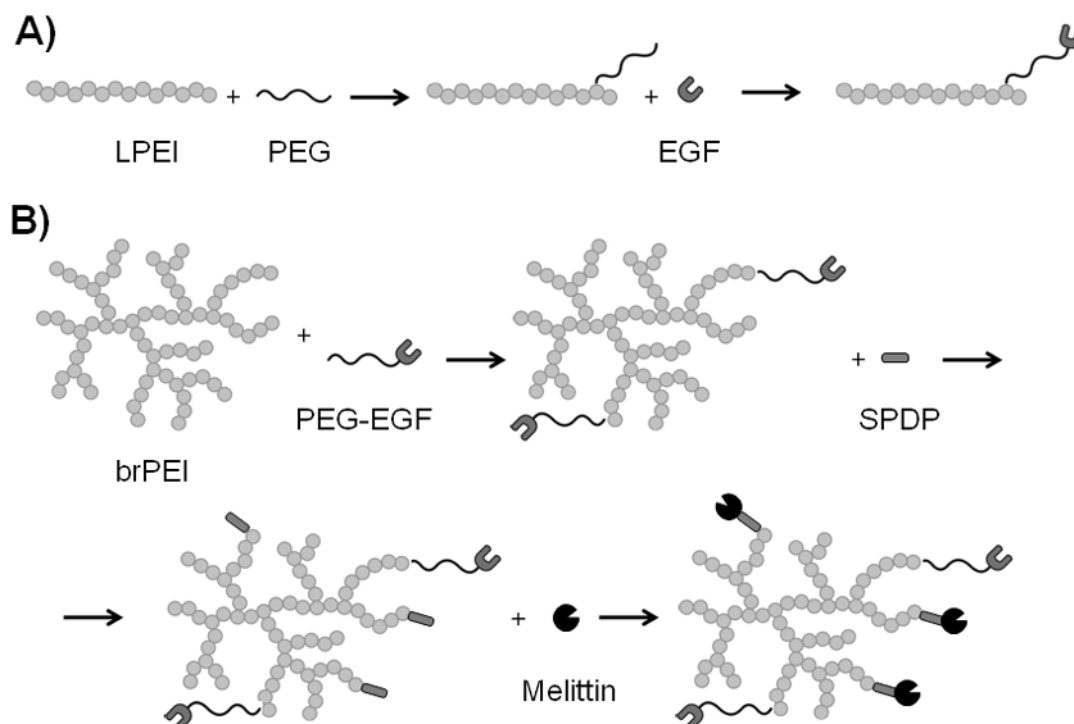


Figure 4.1: Overview of the synthetic strategies for A) EGF-PEG-LPEI triconjugates B) EGF-PEG-brPEI-Mel tetraconjugates.

Conjugate	PEG/PEI ratio	EGF/PEI ratio	Mel/PEI ratio	Linker
brPEI	-	-	-	-
LPEI	-	-	-	-
LPEI-PEG _{10kDa}	1.4	0	-	-
LPEI-PEG _{5kDa}	1.2	0	-	-
LPEI-PEG _{2kDa}	0.9	0	-	-
LPEI-PEG _{10kDa} -EGF	1.4	1.4	-	S-S
LPEI-PEG _{5kDa} -EGF	1.2	1.2	-	S-S
LPEI-PEG _{2kDa} -EGF	0.9	0.9	-	S-S
Mel-brPEI-PEG _{3kDa} -EGF	2.5	2.5	5	Maleimide

Table 4.1: Comparison of the composition of the conjugates.

4.1.3 Polyplex Formation and Biophysical Characterization

The biophysical characteristics of the different conjugates were determined by zeta potential and particle size analysis (**Table 4.2**). Polyplexes prepared by complexation of unmodified PEIs result in well compacted particles (size ~ 120 nm) characterized by relatively high zeta potentials of $\geq +30$ mV. The introduction of a PEG shielding domain leads to significant drop of zeta potential. This was more pronounced for the modification with 10 kDa PEG than for 2 kDa PEG (+11 vs. +24 mV) or 5 kDa PEG (+14 mV). The attachment of EGF leads to a slight increase in zeta potential for polyplexes with all PEGylated PEIs (+17 mV vs. +27 mV vs. +20 mV).

The brPEI tetraconjugate shows a very low zeta potential (+4 mV) and a larger, less uniform diameter (233 ± 122 nm), most probably resulting from the massive modifications of the brPEI backbone (**Table 4.2**). The results are also consistent with the fact that the brPEI conjugate was modified with approximately 2.5 molar equivalents of PEG_{3.4kDa}-EGF chains, as opposed to about one PEG-EGF for the other three conjugates.

The poly(I:C) binding capabilities of the conjugates were comparable as determined in an agarose gel-shift assay (**Appendix 8.4**). A heparin displacement assay (**Appendix 8.4**) revealed small differences between the different polymers. Most significant, a slightly weaker binding of poly(I:C) was found with LPEI (and LPEI conjugates) as opposed to branched brPEI (and the brPEI tetraconjugate). This might have a positive impact on poly(I:C) delivery and intracellular release (see below, next section). PEGylation of LPEI with 2 kDa PEG did not alter poly(I:C) binding, but modification with 10kDa PEG further weakened poly(I:C) binding. The effect of PEGylation however was far less pronounced than the influence of the cationic polymer carrier (LPEI vs. brPEI).

#	Conjugate	Zeta potential [mV]	Size [nm]
1	brPEI	30.0 ± 1.6	120.1 ± 1.1
2	LPEI	31.8 ± 0.8	122.9 ± 2.1
3	LPEI-PEG _{10kDa}	11.1 ± 0.5	114 ± 3.0
4	LPEI-PEG _{5kDa}	14.2 ± 1.3	137.8 ± 2.1
5	LPEI-PEG _{2kDa}	23.9 ± 2.7	121.6 ± 1.9
6	LPEI-PEG _{10kDa} -EGF	16.9 ± 1.4	143.9 ± 33.4
7	LPEI-PEG _{5kDa} -EGF	19.5 ± 0.6	210.5 ± 2.9
8	LPEI-PEG _{2kDa} -EGF	27.3 ± 2.3	210.4 ± 4.1
9	MeI-brPEI-PEG3.4K-EGF	3.5 ± 0.9	233.0 ± 122.0

Table 4.2: Biophysical characterization of the poly(I:C) polyplexes.

4.1.4 *In vitro* Antitumoral Activity of poly(I:C) Polyplexes

Poly(I:C) delivery properties were determined by a cytotoxicity assay using the poly(I:C) sensitive EGF-R overexpressing glioblastoma cell line U87MGwtEGFR. To differentiate between poly(I:C) induced cell death and a potential carrier toxicity, single stranded poly(I) was used as control, as it is reported that the single-strand RNA does not induce apoptosis¹²⁹⁻¹³⁰.

Plain PEI/poly(I:C) polyplexes

To evaluate the suitability of LPEI as a better defined carrier backbone in poly(I:C) delivery, plain LPEI was compared to brPEI without any further modification of the polymers. In the tested poly(I:C) concentration range of 0.25 – 2.5 µg/ml, brPEI/poly(I:C) polyplexes showed no effect on the viability of U87MGwtEGFR cells (**Figure 4.2** top right panel). LPEI demonstrates a superior delivery efficiency at concentrations as low as 0.25 µg/ml, but this is accompanied by a fast shift into unspecific cytotoxicity beginning at 1 µg/ml (**Figure 4.2** top left panel). For DNA transfections routinely a concentration of 0.8 µg/ml is well tolerated with only moderate toxicity, indicating a LPEI independent toxicity mechanism. This effect severely limits the use of unmodified LPEI because of unspecific uptake and a small therapeutic window.

The extent of the far higher potency of LPEI compared to brPEI is surprising, but consistent with previous findings for DNA delivery, for example^{127,131}. A better reversibility of nucleic acid complexation (see also section above) is hypothesized as key issue. Itaka et al.¹³¹ reported on an enhanced intracellular disassembly of LPEI as compared to brPEI DNA polyplexes by intracellular FRET experiments. Intracellular cytosolic release appears to be a critical requirement also for accessibility of poly(I:C).

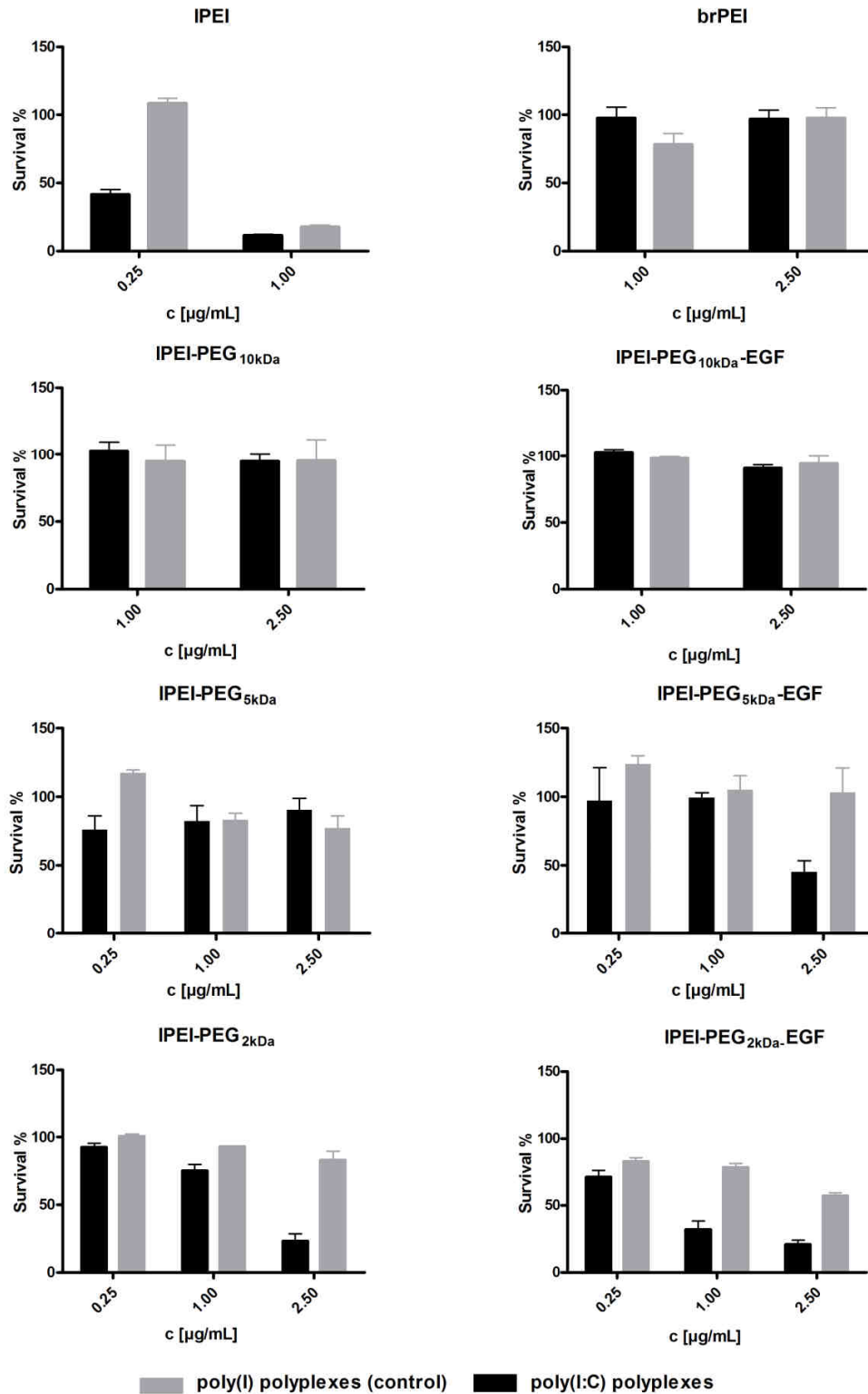


Figure 4.2: *In vitro* antitumoral activity of poly(I:C) polyplexes against U87MGwtEGFR glioma cells. Comparison of brPEI versus LPEI (top panels), LPEI-PEG_{10kDa} versus LPEI-PEG_{5kDa} and PEG_{2kDa} (left panels), and receptor-targeted conjugates LPEI-PEG_{10kDa}-EGF versus LPEI-PEG_{5kDa}-EGF and LPEI-PEG_{2kDa}-EGF (right panels). Please note the different dosages for ineffective conjugates and effective conjugates. For each dosage the same dose of poly(I) polyplexes served as negative control.

PEGylated PEI/ poly(I:C) polyplexes

Various groups described the beneficial role of PEGylation on cytotoxicity of PEI polyplexes, but the grafting of PEG chains onto PEI may also be accompanied by a drop in delivery performance. This has been demonstrated for plasmid DNA delivery^{46,132-137}, the situation may however be different in case of siRNA delivery¹³⁸. Therefore, to evaluate the optimal PEG molecular weight for poly(I:C) delivery, PEG10kDa, PEG5kDa and PEG2kDa were grafted onto the brPEI or LPEI backbone. **Figure 4.2** left panels show a huge impact of PEGylation of LPEI on the delivery efficiency. The attachment of a single PEG10kDa chain to LPEI renders the conjugate inactive. At concentration of 2.5 µg/ml of poly(I:C) or even higher (5 - 10 µg/ml, **Appendix 8.4**) no significant cell killing is observed. Modification with PEG2kDa or PEG5kDa reduces the efficacy and cytotoxicity profile of the corresponding poly(I:C) polyplexes (**Figure 4.2** left panels) considerably.

Targeted EGF-containing PEGylated PEI/poly(I:C) polyplexes

To evaluate the influence of a targeting ligand onto the delivery efficiency of the LPEI-PEG-conjugates, murine EGF was attached at the distal end of the 2 kDa, 5 kDa or 10 kDa PEG spacer. The conjugates were tested as poly(I:C) polyplexes for their cell killing activity (**Figure 4.2** right panels). As expected, introduction of the targeting ligand improved the activity of the PEG2kDa - LPEI conjugate, leading to an increased activity at lower concentrations with more than 60% cell killing at 1 µg/ml (**Figure 4.2** bottom right panel). Cell killing was even more pronounced at 2.5 µg/ml, but poly(I) control polyplexes also triggered some killing. Interestingly, the incorporation of EGF into the PEG10kDa - LPEI conjugate did not recover any significant cytotoxic activity of the LPEI-PEG10kDa-EGF polyplexes (**Figure 4.2** right upper panel), even at a higher dose of 5 µg/ml (**Appendix 8.4**). The LPEI-PEG5kDa-EGF conjugate mediated specific poly(I:C) cell killing, but only at the higher 2.5 µg/ml dose (**Figure 4.2** middle panel, right).

Comparison of the brPEI Tetraconjugate with the LPEI Triconjugate

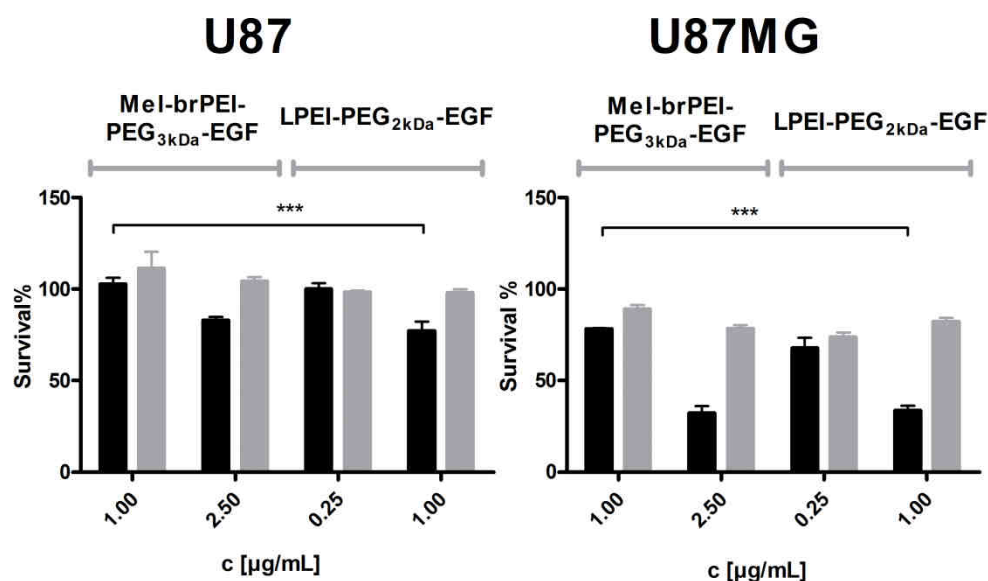


Figure 4.3: In vitro antitumoral activity of poly(I:C) polyplexes. Comparison of the two EGF-conjugates (old tetraconjugate versus new triconjugate LPEI-PEG_{2kDa}-EGF) using U87MG glioma cells with low ('U87MG') or high ('U87MGwtEGFR') levels of EGF receptor. The same doses of poly(I) polyplexes served as negative controls.

The two conjugates, tetraconjugate EGF-PEG-brPEI_{3.4kDa}-Mel and triconjugate LPEI-PEG_{2kDa}-EGF were compared by testing on U87MG (moderate levels of EGFR) and EGFR-over-expressing U87MGwtEGFR cells (receptor levels see **Appendix 8.3**). **Figure 4.3** shows an only limited efficacy on U87MG cells, with marked activity only at higher concentrations of 2.5 µg/ml (data not shown). Testing EGFR over-expressing U87MGwtEGFR cells (**Figure 4.3**) bioactivity was more pronounced with the new triconjugate, resulting in a 60% reduction of cellular viability by treatment at a concentration of 1 µg/ml poly(I:C). On both cell lines, a 2.5-folds higher concentration of the old tetraconjugate had to be applied to obtain a similar cell killing effect. Effects of the poly(I:C) treatment on cell morphology at 48 hours after treatment are shown in **Figure 4.4**.

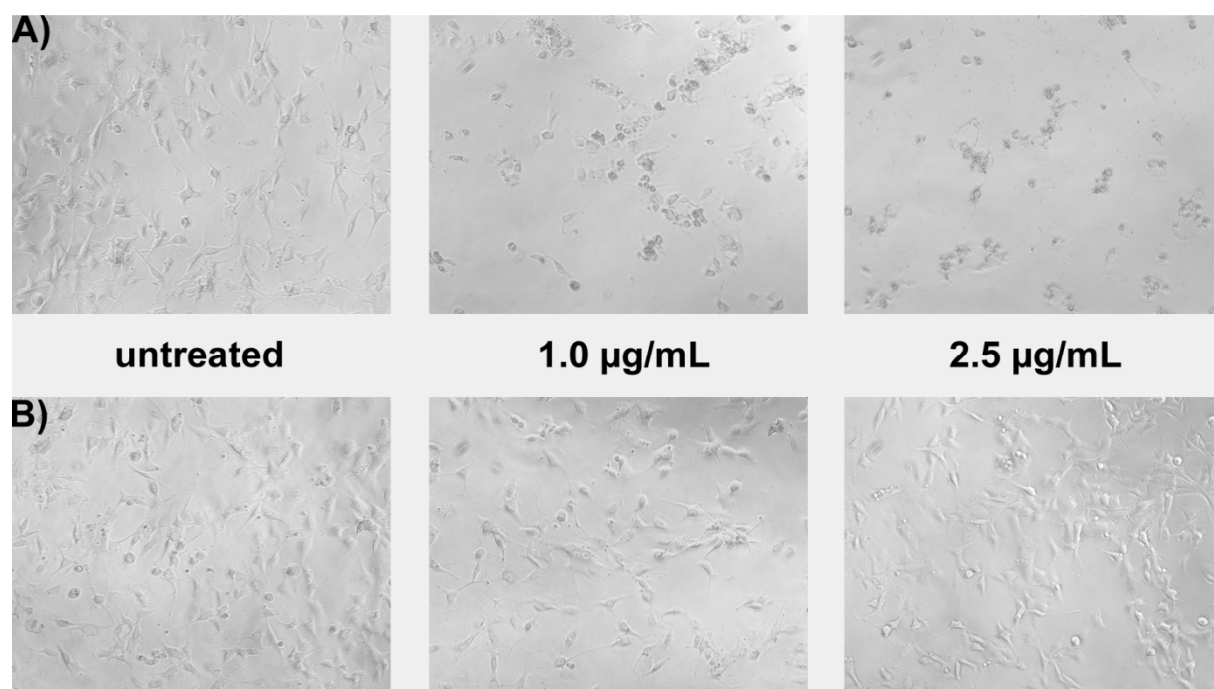


Figure 4.4: Cell morphology of LPEI-PEG2kDa-EGF polyplex treated U87MGwtEGFR cells 48 h after transfection. A: poly(I:C) treated cells; B: poly(I) treated cells (control).

The two conjugates were also compared using the EGFR-overexpressing epidermoid carcinoma cell line A431 (**Figure 4.5**). In these and the following experiments, polyplexes of the nontoxic polyanion polyglutamic acid served as negative control. Efficient and poly(I:C)-specific cell killing was obtained at the lowest tested 1 µg/ml poly(I:C) dose in case of the LPEI-PEG2kDa-EGF conjugate, whereas high doses were required in case of the tetraconjugate.

4.1.5 *In vivo* Anti-Tumor Activity

In vivo anti-tumor activity of EGFR-targeted poly(I:C)/PEI polyplexes was examined using nu/nu mice bearing subcutaneous A431 tumors (performed by Alexei Shir, HU Jerusalem). Conjugate delivery activity was determined by tumor volume analysis after systemic application of tetra- and triconjugate and the control formulations. Intravenous administration of 0.5 mg/kg poly(I:C) started at day 0 and was repeated every second day, for a total of 7 times. Measurement of the average body mass of the mice showed that the mice tolerated the treatment well.

As shown in **Figure 4.6** the tumor volume of control/untreated groups was about 12 times larger than the average tumor volume at day 0, indicating rapid tumor growth

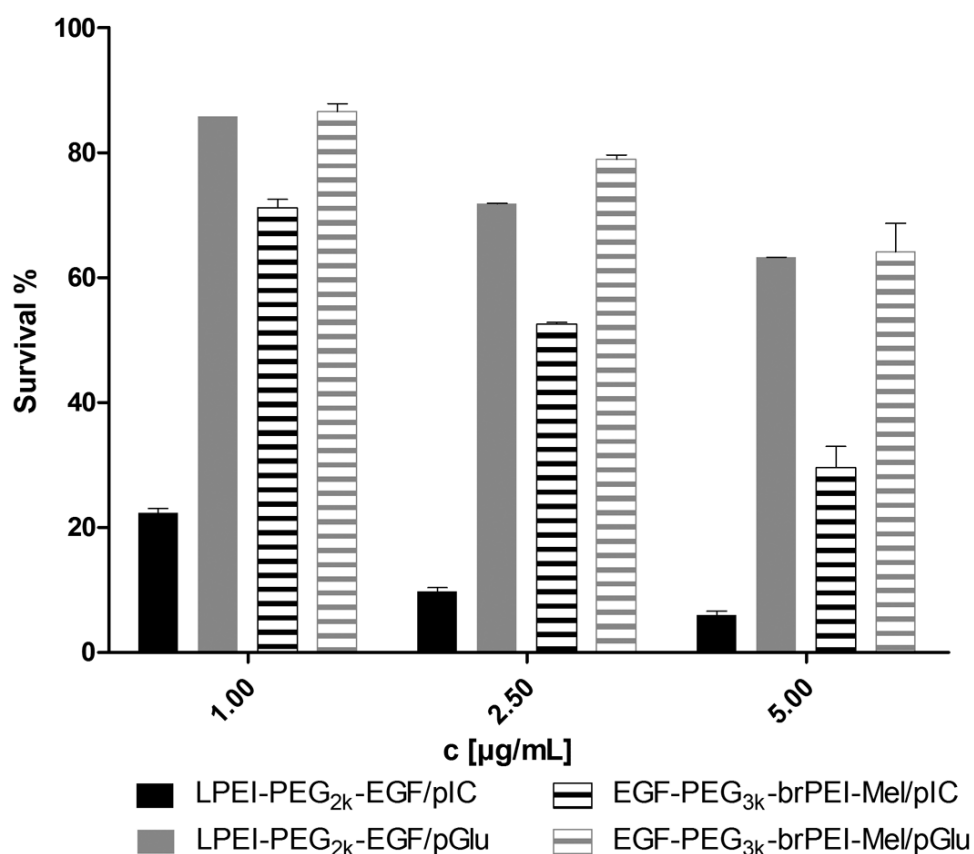


Figure 4.5: *In vitro* antitumoral activity of poly(I:C) polyplexes against A431 cells. Comparison of the two EGF-conjugates (old tetraconjugate versus new triconjugate LPEI-PEG2kDa-EGF). The same doses of poly(Glu) polyplexes served as negative controls (Experiment by A. Shir, HU Jerusalem).

and no tumor growth inhibition by the polyglutamate control polyplexes. Treatment with either EGF triconjugate (EPP_{lin}) or EGF tetraconjugate (MPPE_{br}Mel) resulted in significantly decreased tumor growth speed and tumor end volume. After 14 days of treatment (7 injections) the mean tumor volume of the tetraconjugate group was fourfold increased, while treatment with the triconjugate led to an only doubled tumor volume. The antitumoral effect was only observed in the poly(I:C) groups, showing significantly decreased tumor growth progression compared to the control group.

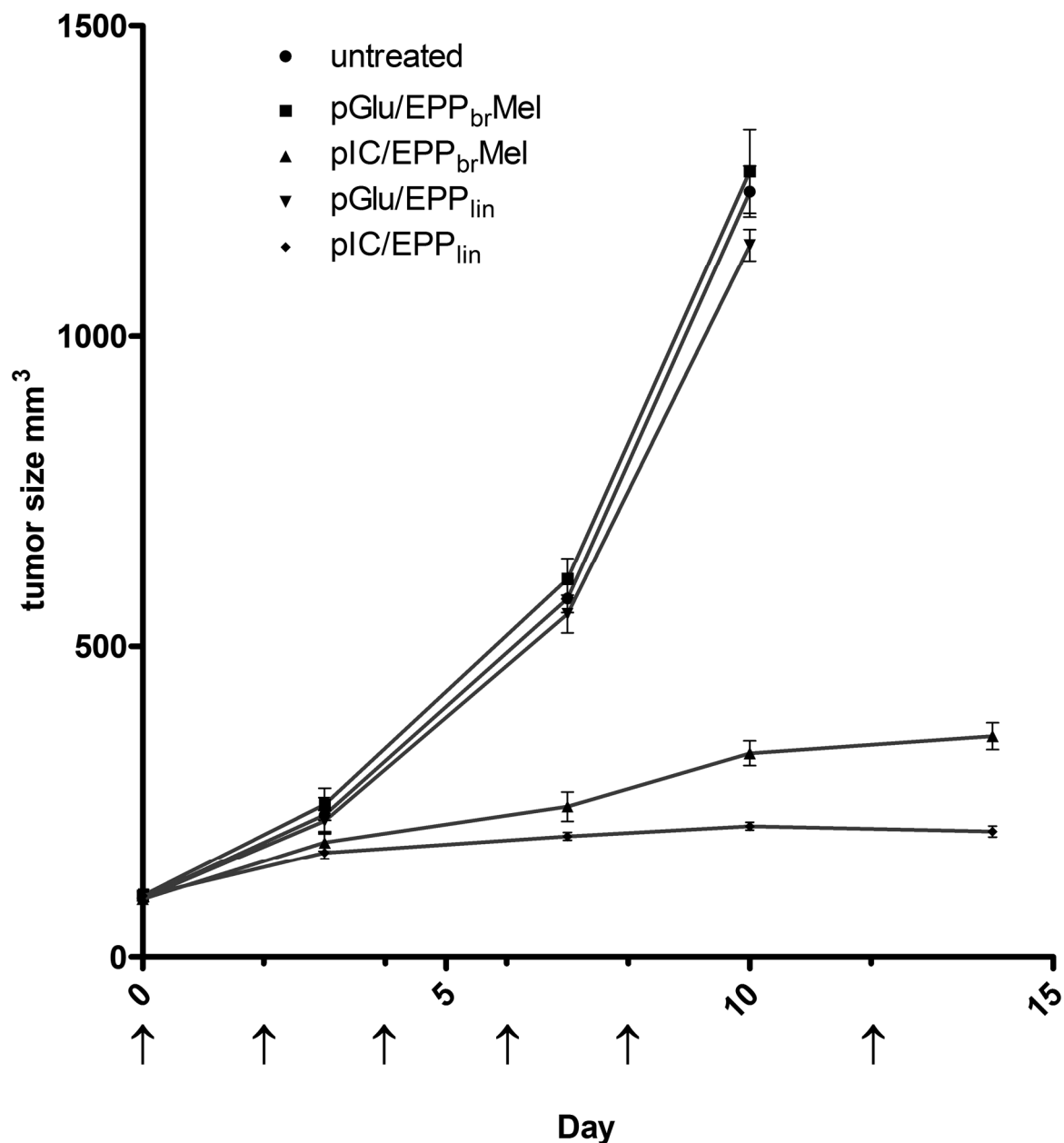


Figure 4.6: *In vivo* anti-tumor activity of EGFR targeted poly(I:C) PEI polyplexes. *In vivo* anti-tumor activity of EGFR targeted poly(I:C) PEI polyplexes was measured using s.c. A431 bearing nude mice. Tumor volume analysis after i.v. injection of the two different formulations of poly(I:C) was done. Each group included 5 mice. Administration of 10 μ g pI:C started on day 0 and was repeated on days 2, 4, 6, 8, 10, 12, for a total of 7 times (indicated by arrows). Tumor volume was measured twice a week until day 14 (Experiment by A. Shir, HU Jerusalem).

4.2 Protocols and Building Blocks for the Solid-Phase Assisted Synthesis of Defined Polyamidoamines

4.2.1 Introduction

Despite the continuous progress in polymeric carrier development there still are inherent limitations which need to be addressed, namely low efficiency and poor definition of currently used polymeric delivery systems. Primary aim of this thesis was the development of solid-phase synthesis protocols to allow the synthesis of sequence-defined polyamidoamines for the delivery of nucleic acids.

Solid-phase synthesis has a long history in the synthesis of peptides, a complex class of macromolecules. Peptides are comparatively short polymers (5-100 units) composed of different amino acids linked by amide bonds. Due to synthetic difficulties caused by their polarity, solubility properties and complex protection strategies the classical solution phase synthesis of peptides is laborious, time consuming and error prone¹³⁹. In 1963 Merrifield⁹⁸ published a landmark article, introducing the concept of peptide synthesis on a solid support. By anchoring the C-terminal amino acid to an adequately functionalized, swellable microgel support it is possible to force amino acid coupling reactions to completion by using large excess of reagents and optimized synthetic protocols. Contaminants, reagents and reaction by-products are removed by a simple filtration step reducing overall synthesis time considerably. Since this breakthrough the field of macromolecular synthesis progressed at high speed, extending from peptides to oligonucleotides and other classes of oligomers. The method found wide acceptance in commercial and academic research and was further improved by the introduction of concepts like combinatorial chemistry¹⁴⁰ and high-throughput screening.

The first reports of application of the methodology to the design of transfection reagents appeared in the early nineties of the last century¹⁴¹⁻¹⁴⁵, but despite apparent advantages the use and development of solid-phase derived polymers was never popular. Apart from precise dendrimer structures generated by solution chemistry¹⁴⁶, ill defined, random polymerized cationic macromolecules continue to be the cutting edge of polymeric transfection reagents. This imbalance is probably the result of the few examples of polyamine and polyamidoamine synthesis in the literature and the

lack of commercial available building blocks. In fact, references to solid-phase derived polyamines are scarce before 1996¹⁴⁷⁻¹⁴⁸.

In 2006 Hartmann et al.⁹⁹ published a solid-phase based method to synthesize linear polyamidoamine (PAA) chains on a PS-PEG-support by a protocol employing alternating condensation steps using cyclic anhydrides and diamines (**Figure 4.7**). The first condensation generates a free carboxylic function on the resin via ring-opening of the cyclic anhydride. The carboxylic function is subsequently activated on solid-phase and the diamine is condensed into the growing PAA chain. 3,3'-diamino-N-methyldipropylamine and protected spermine were used as diamine building blocks. By repetition of this cycle linear PAAs are assembled. As acceptable product purity can only be guaranteed if a conversion $\geq 98\%$ is achieved in every step, constant reaction monitoring is necessary. The procedure allows the synthesis of linear PAAs in a high purity and with absolute control over every monomer unit.

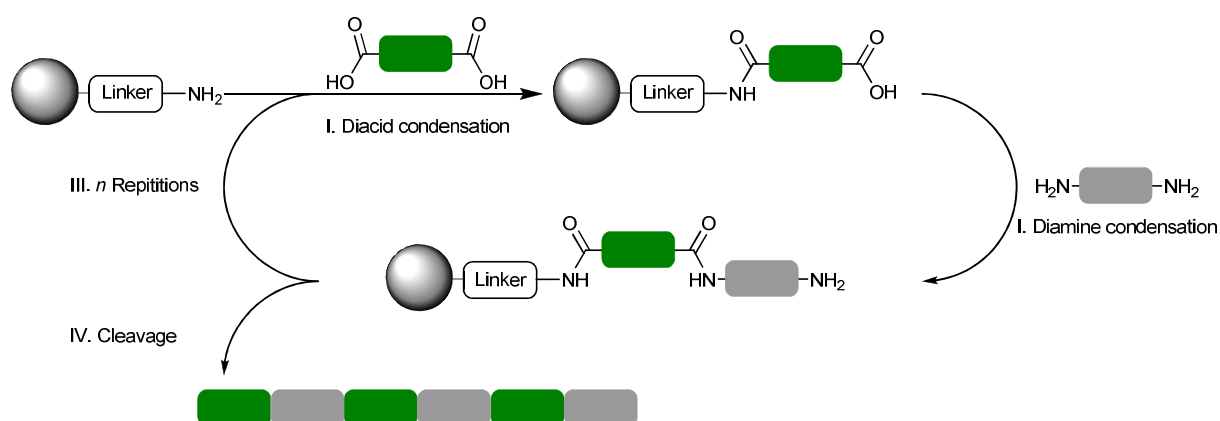


Figure 4.7: PAA solid-phase synthesis concept described by Hartmann et al.⁹⁹

Our initial aim was to adapt the strategy to generate a new polymer library for nucleic acid delivery based on ethylenimine units. Short linear oligoethylenimines instead of propylenimine or spermine should be used as amine building blocks, because oligoethylenimines were previously found to possess superior gene transfer properties¹⁴⁹⁻¹⁵⁰. By using the already published alternating condensation protocols⁹⁹ the problems of developing a new synthetic strategy might have been avoided.

4.2.2 Application of an Alternating Condensation Approach to Ethylenimine-based PAAs

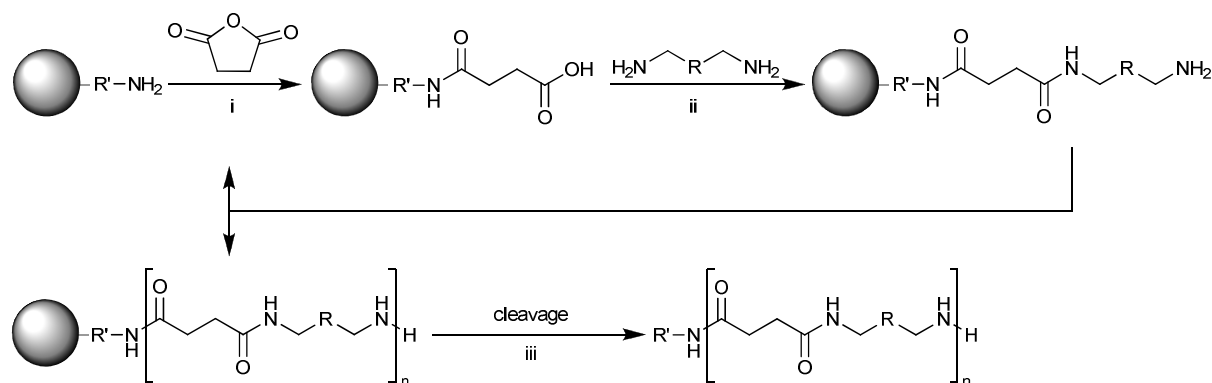


Figure 4.8: Reaction conditions described by Hartman et al.⁹⁹. i: 10 eq succinic anhydride, DMF, 30 min; ii: 10/10/10/20 eq diamine/PyBOP(R)/HOBt/DIPEA, DMF, 30 min; iii: TFA + scavengers, 1 - 2 h

As depicted in **Figure 4.8** the synthetic strategy is based on alternating condensation reactions of cyclic anhydrides and diamines. Variations in the number of repeating units in the oligoethylenimine building blocks (**Figure 4.9**) should have been used to analyze the impact of charge density and buffering capacity on NA delivery.

By employing acid-labile boc-protection to the secondary amines of the oligoethylenimine building blocks they are rendered inaccessible during the PAA synthesis, and possible side reactions are suppressed. Deprotection is achieved by the strongly acidic conditions necessary for the release of the PAA chain from the resin.

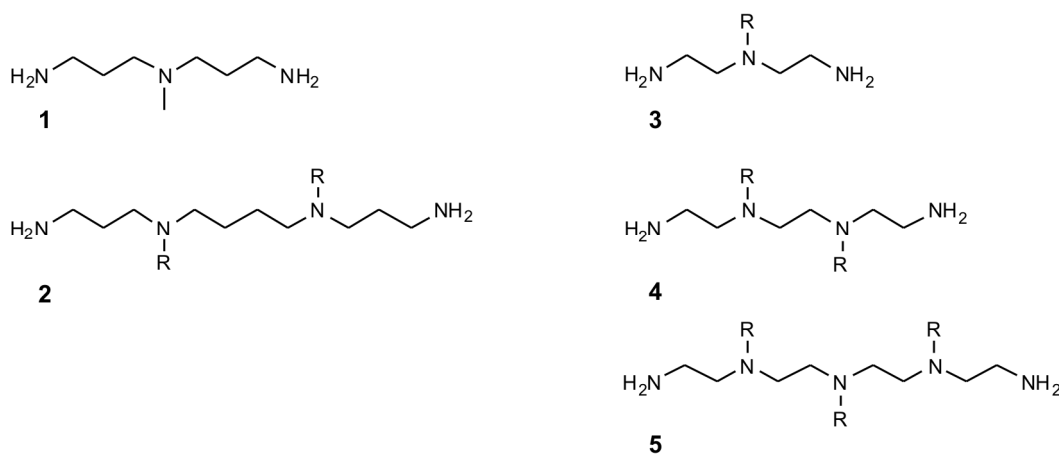


Figure 4.9: Comparison of the used building blocks ($\text{R}=\text{Boc/H}$). left: propylenimine based building blocks: **1** 3,3'-diamino-N-methyldipropylamine, **2** spermine (used by Hartman et al), right: ethylenimine based building blocks: **3** diethylenetriamine (Dt), **4** triethylenetetramine (Tt), **5** tetraethylenepentamine (Tp)

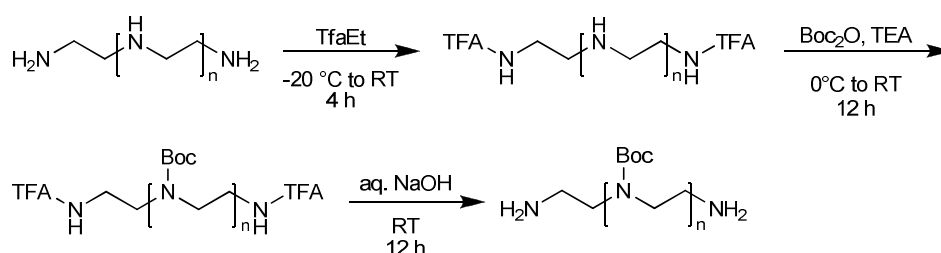


Figure 4.10: General synthetic route for diamine building blocks

The boc-protected diamines were synthesized in a one-pot reaction according to a published method¹⁵¹. The primary amines of the linear oligoethylenimines were selectively¹⁵² protected by acylation using ethyl trifluoroacetate followed by protection of the secondary amines via di-*tert*-butyl dicarbonate. The resulting fully protected amines are readily purified by recrystallization. The trifluoroacetyl groups were removed by alkaline hydrolysis, yielding the pure corresponding diamine in moderate to high overall yields (**Table 4.3**).

ID	backbone	Bistfa _x boc derivative	diamine yield	Overall yield
Dt(boc)	DETA	73 %	63% ^a	46%
Tt(boc₂)	TETA	65 %	66% ^a	43%
Tp(boc₃)	TEPA (x 5 HCl)	83 %	quantitative	83%
Tp(boc₃)	TEPA tech. grade	68 %	quantitative	68%

Table: 4.3 Yields of the boc-protected amine building blocks; ^a not optimized

By this simple three step procedure the diamine building blocks can be produced in large amounts (standard batch size 20 – 40 g) without the need for time-consuming chromatographic purification steps.

Solid-Phase Synthesis:

To establish the solid-phase procedures, the sequence HO-K-Succ-Tp-Succ-Tp-H was chosen as simple model PAA. In-synthesis reaction monitoring showed inconsistent results for the colorimetric assays in every step, accompanied by a lower resin mass gain than calculated. MS-analysis of the cleavage solution revealed the formation of the crosslinked product HO-K-Succ-Tp-Succ-K-OH (**Figure 4.11**).

The incubation of the activated carboxylic acid function with the diamine building block results in crosslinking of a large degree of the adjacent reaction sites,

preventing further chain elongation. Using a Wang-Lys resin with a moderate loading (0.52 mmol/g) a product mixture of crosslinked and desired product could be identified by ESI-MS after the second coupling step, however accompanied by very low yields.

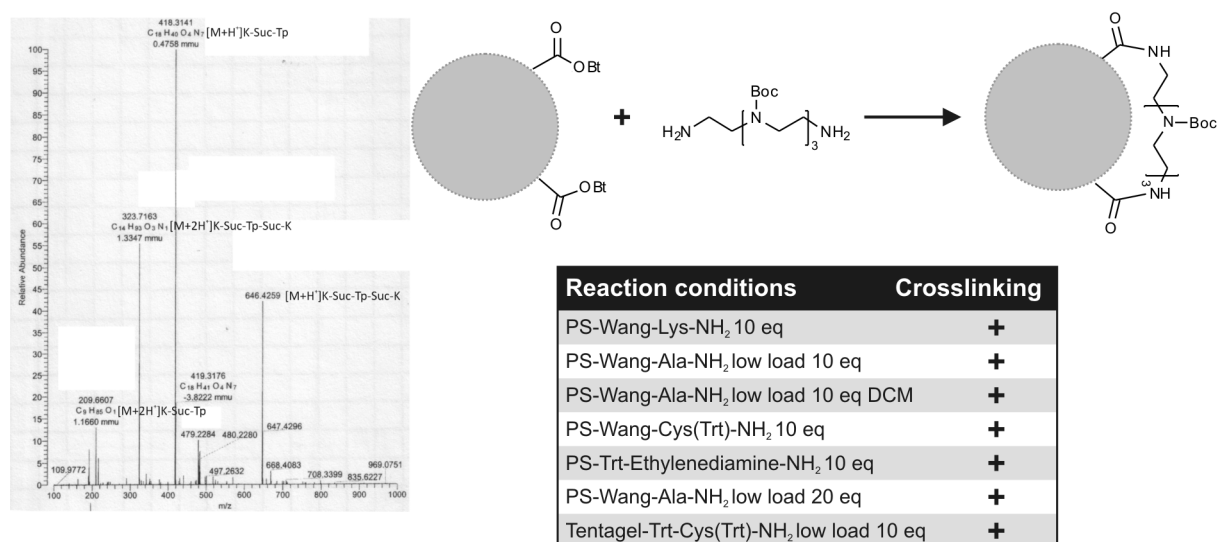


Figure 4.11: Left: Exemplary ESI-MS-spectrum of an alternating condensation reaction using a PS-Wang-K resin. Upper Right: Proposed mechanism for on resin crosslinking Lower right: Formation of crosslinking product in dependency to various reaction conditions

To evaluate the influence of experimental conditions on the formation of crosslinked products, different reaction conditions were tested. In each case the mass increase of the resin was less than predicted and colorimetric assays used for reaction monitoring showed unexpected behavior. The crosslinked product was always present in the different sequences. These results are consistent with reports in literature for on-resin carboxy activation followed by coupling of unprotected diamines. Jørgensen et al.¹⁵³ describe crosslinking up to 60% (per step) of adjacent, activated carboxy sites on solid-phase using a related approach.

Thus, in contrast to the successful application by Hartmann et al. the synthetic strategy yielded no reliable results in our case. Possible explanations include the increased steric requirements of the Tp(boc₃) building block compared to the building blocks used in the original synthesis, changed reaction kinetics by using a Wang-PS resin opposed to Trityl-PEG-PS resin which generally shows faster reaction kinetics¹⁵⁴ and the higher load of most of the used resins.

In addition to the synthetic problems the versatility is limited by technical factors like building block solubility, possible side reactions when using new combinations of

diamines and diacids and the need for complex *in situ* analytics to ensure clean reaction progress. As robust and reliable reactions are a prerequisite to solid-phase assisted library synthesis, the first synthetic route was not further investigated. By adapting the synthetic concept to standard fmoc/tBu peptide synthesis conditions (**Figure 4.12**) it should be possible to use well-established peptide coupling protocols. This would be accompanied by the additional advantage of a decreased error rate resulting from transferring the critical condensation step into the building block synthesis.

4.2.3 PAA Synthesis Using Polyamino Acid Building Blocks

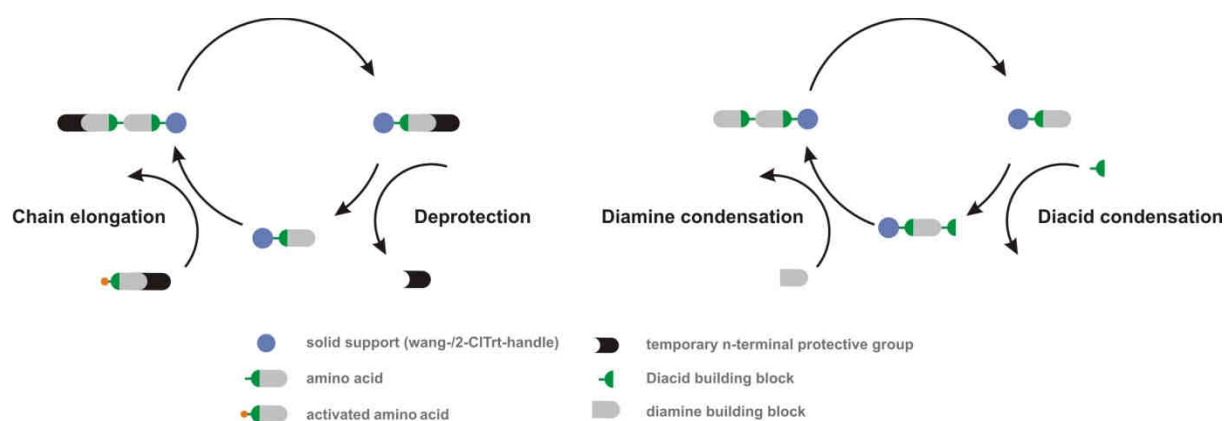


Figure 4.12: Comparison of the two solid-phase PAA synthesis strategies. Left: classical solid-phase peptide synthesis characterized by alternating coupling and deprotection cycles. **Right:** Hartmann PAA synthesis characterized by alternating condensation reactions.

Fmoc/tBu peptide synthesis is characterized by alternating deprotection and elongation cycles. To adapt the PAA synthesis to fmoc/tBu conditions a building block like depicted in **Figure 4.13** was needed. The protection strategy was adapted from fmoc/tBu-amino acids resulting in an orthogonal protected oligoamino acid constructed from diacid component, N-terminal fmoc protection and boc-protected amines. As large scale synthesis was already optimized for Tp(boc₃) we chose that building block as model for the development of the fmoc/tBu building blocks.

Synthesis of the fmoc amino acid building blocks:



Figure 4.13: fmoc-Stp(Boc₃)-OH (n=3, m=2, R=H)

#	Reaction conditions	Yield	Comments
1	1) 1.1 eq Fmoc-Cl, 2 eq DIPEA, DCM -20 °C 12 h 2) 3.0 eq Succinic anhydride, DCM, RT 3 h	30%	two-step synthesis
2	1) 1.1 eq Fmoc-Cl, 2 eq DIPEA, DCM -20 °C 12 h 2) 3.0 eq Succinic anhydride, DCM, RT 3 h	16%	one-pot reaction
3	1) 1.1 eq 9-BBN, Fmoc-Cl, 2 eq DIPEA, DCM -20 °C 12 h 2) 3.0 eq Succinic anhydride, DCM, RT 3 h	20%	<i>in situ</i> complexation (9-BBN)
4	1) 1.1 Succinic anhydride, THF - 20 °C 4h 2) 1.5 eq Fmoc-Cl, 3 eq DIPEA, THF, 0 °C to RT 12 h	40%	one pot-reaction
5	1) 1.1 Succinic anhydride, THF - 70 °C 4h 2) 1.5 eq Fmoc-OSu, 3 eq DIPEA, THF, 0 °C to RT 12 h	46%	less side products

Table 4.4: optimization of product yield/different reaction conditions for fmoc-Stp-OH

The synthetic strategy to convert Tp(boc₃) into the fmoc-Stp(Boc₃)-OH building block required a mono-acylation in the first step, thereby differentiating the two amino functions. Initially that was achieved in a 2-step synthesis by using Fmoc-chloride followed by acylation via succinic anhydride obtaining fmoc-Stp(Boc₃)-OH in an overall yield of 30%.

As the purification of the intermediate fmoc-tp(Boc₃)-NH₂ was quite laborious and time-consuming, the two reaction steps were transferred into a one-pot reaction to ease synthesis and purification. This change was accompanied by a drop of yield to 16%, unacceptable for further use. The yield limiting step was the first mono-acylation, so different conditions were tested for an effective mono-acylation. The most common solution, using a large excess of the diamine¹⁵⁵ was not an option as the protected diamine is the product of a 3 step synthesis and too valuable. The use of temporary protection strategies to selectively shield one amine via protonation¹⁵⁶ or complexation (Table 4.2, entry 3) via 9-BBN¹⁵⁷ did not result in increased yields. In the end, succinic anhydride acylation at -70 °C in THF followed by fmoc introduction using Fmoc-OSu was able to increase the yield to acceptable 40%. Furthermore the use of Fmoc-OSu gave rise to a cleaner raw product as use of Fmoc-Cl is often accompanied by dipeptide formation¹⁵⁸ complicating the purification.

The applicability of the optimized procedure to the synthesis of other oligoamino acids was in the meantime demonstrated by the synthesis of building blocks with close relationship to Stp using educts with varying n/m (unpublished results, Naresh Badgujar). These building blocks offer interesting opportunities to investigate the influence of the polyamine building block on NA complexation and delivery. By using these building blocks it is possible to optimize the resulting PAAs by changing charge density, hydrophobicity or introducing structural strain.

The developed synthetic route thereby provides convenient access to fully protected polyamino building blocks for use in fmoc/tBu solid-phase synthesis.

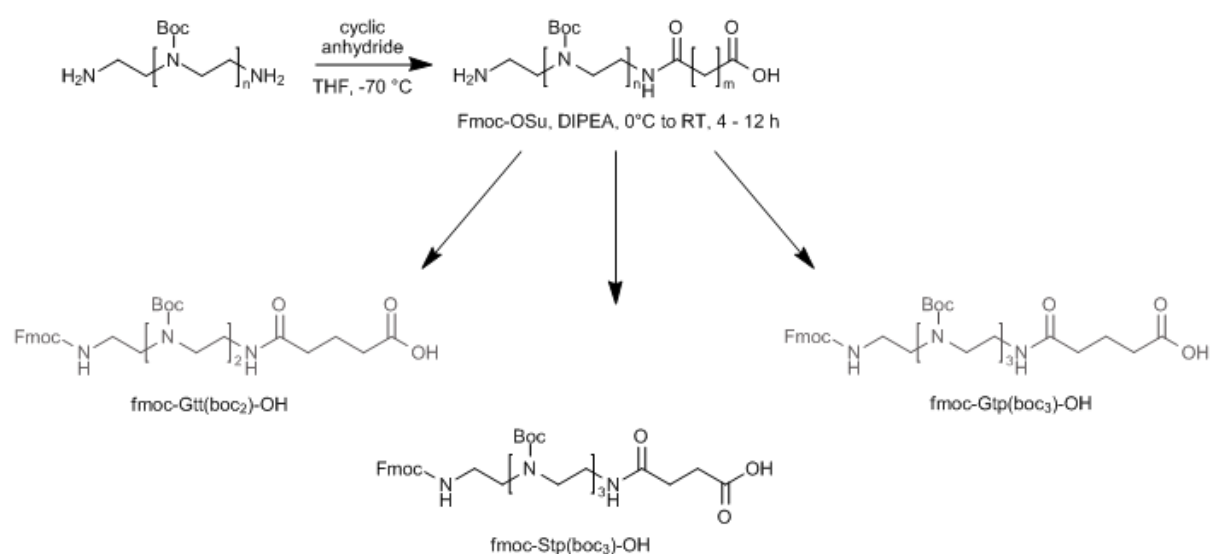


Figure 4.14: Synthetic route to fmoc/tBu-polyamino acids. Optimized synthetic route to fmoc/tBu-polyaminoamido acids, illustrating the general applicability of the synthetic route (Dr. Naresh Badgujar, Wagner lab)

4.2.4 Application of Fmoc-Stp(boc)₃-OH to PAA and Peptide Synthesis

Synthesis of the model PAA HO-K-Stp₄-K-H

To evaluate the usefulness of solid-supported PAA-synthesis using the new fmoc-Stp(boc₃)-OH building block the sequence HO-K-Stp₄-K-H was synthesized (15 charges) using standard PyBOP[®] coupling protocols¹⁵⁹ and subjected to further analysis. RP-HPLC proved altogether to be unsuccessful due to the massive charge and the unpredictable buffering capacity of the PAAs resulting in irreproducible results. These problems are known from literature⁹⁹ and were circumvented by using High Resolution Ion-Exchange HPLC (IEX-HPLC) for analysis. **Figure 4.15** shows an IEX-HPLC trace of crude material after cleavage from the resin. The sequence is an example for one of the longer, unmodified PAAs of the library and shows that the developed coupling protocols work well, resulting in crude product purities > 85%.

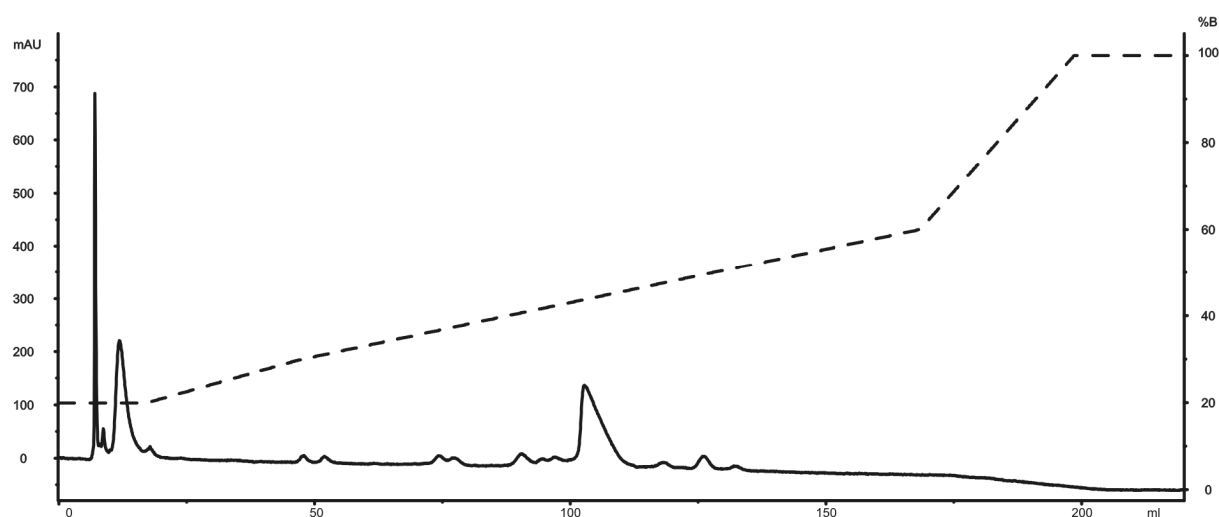


Figure 4.15: IEX-HPLC/UV₂₁₄-trace of crude HO-K-Stp₄-K-H (#18). A cation-exchange Resource S (6 mL) column was used for analysis. Elution by linear gradient over 40 min from 0 to 60% B (A: 20 mM NaCl in 10 mM HCl; B: 3 M NaCl in 10 mM HCl), flow rate 4.0 mL/min

Synthesis of the model Peptide HO-IVNQPTYGYWH-Stp₂-H

To demonstrate the general compatibility of the fmoc-polyamino acid building block to standard fmoc/tBu peptide synthesis the GE11 peptide sequence⁵³ was N-terminal modified with two Stp-units (Sequence: HO-IVNQPTYGYWH-Stp-Stp-H). GE11 is a moderately hydrophobic (GRAVY= -0.700) EGF-R targeting peptide, possessing no charged residues. The initial peptide sequence allows easy purity assessment by RP-HPLC before coupling of the Stp units. N-terminal modification by two Stp units introduces 6 additional positive charges into the peptide, resulting in a drastic change

Results

of chromatographic behavior under IEX conditions. HR-IEX Analytical IEX chromatography of a mini cleavage (**Figure 4.16**) shows a purity > 90 % being consistent to the RP-HPLC run (**insert Figure 4.16**) of the peptide precursor.

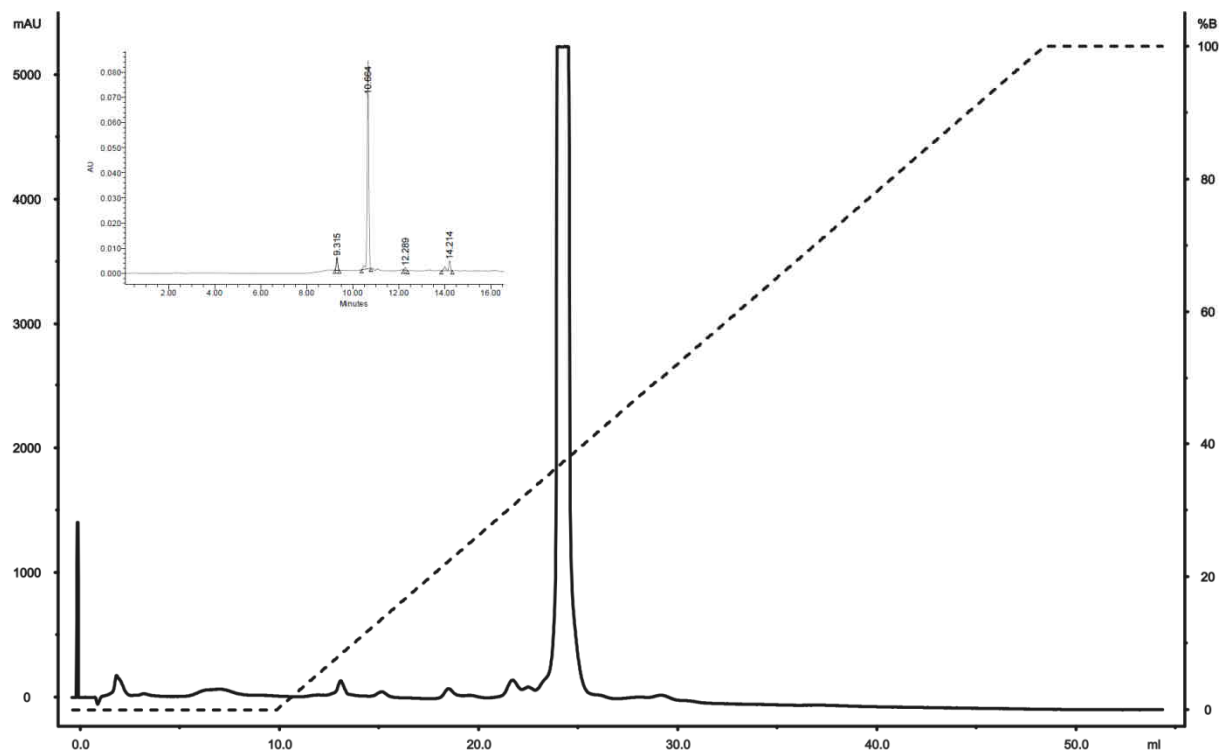


Figure 4.16: IEX-HPLC/UV₂₈₀ trace of crude HO-IVNQPTYGYWH-Stp-Stp-H. A cation-exchange Resource S (1 mL) column was used for analysis. Elution by linear gradient over 40 min from 0 to 100% B (A: 20 mM NaCl in 10 mM HCl; B: 3 M NaCl in 10 mM HCl), flow rate 1.0 mL/min Insert: RP₁₈-HPLC/UV₂₈₀ trace of crude HO-IVNQPTYGYWH-H. Elution by linear gradient over 20 min from 5% A to 100% B (A: Water + 0.1% TFA; B: ACN + 0.1% TFA), flow rate 1.0 mL/min

4.3 Design and Evaluation of a Library of Precise, Sequence-defined Oligoamidoamines for Nucleic Acid Delivery

4.3.1 Introduction

Nucleic acid (NA) delivery systems hold great promise as research tool and in terms of therapeutic application. Nevertheless the development has been slowed down by various problems associated to the effective delivery of NAs into the target cells. Viral delivery, the far most efficient delivery platform, only slowly recovers from a series of serious setbacks associated with inherent safety problems¹⁶⁰⁻¹⁶¹ (immunogenicity, insertional mutagenesis) and will not be applicable for all types of NAs and disease indications. The use of polymeric vectors is impaired by a different set of problems: low efficiency compared to viral systems, ill-defined structures, resulting in problems in structure-activity prediction and evaluation, and synthetic difficulties during the development of increasingly complex multi-domain polymers.

It is questionable if the modification of polymeric macromolecules in a more or less random manner will allow these systems to compete successfully with their viral counterparts. Furthermore the structure activity relationships of polymers modified by these grafting approaches are difficult to analyze due to the large impact of the polymer backbone and their polydispersity. By stripping the used systems down to their essential parts and reassembling them as relatively small, precise polymers one can envision a construction set of functional domains for delivery system development. The different combinations can be screened for synergistic effects resulting in potent delivery vehicles characterized by defined structure and possibility of further extension. It is obvious that traditional polymerization strategies are not suited for this approach, as they cannot deliver the molecular precision necessary for these types of polymers. Reviews¹⁰¹ on the design of polymeric delivery systems agree on a minimal set of necessary structural properties with NA binding/compaction, cell entry, buffering capacity or lytic activity towards cell membranes, and intracellular release of the cargo being the most prominent. An ideal, smart polymeric system would encode these properties in its monomer sequence allowing the programming of properties and behavior during synthesis.

Solid-phase synthesis is an ideal tool for the synthesis of precise, sequence defined polymers and can with the right set of protocols be used for macromolecular synthesis to reach $M_w > 10 \text{ kDa}$ ¹⁶². Aim of this study was the design and evaluation

of a small solid-phase based polymer library to evaluate the influence of different modules in a polymeric NA delivery system. The library is still constrained by its limited design space, but the first results demonstrate the feasibility of the approach. Further development towards more complex modular structures may be able to cope with unsolved bottlenecks in polymeric delivery.

4.3.2 Structural Overview and Rationale

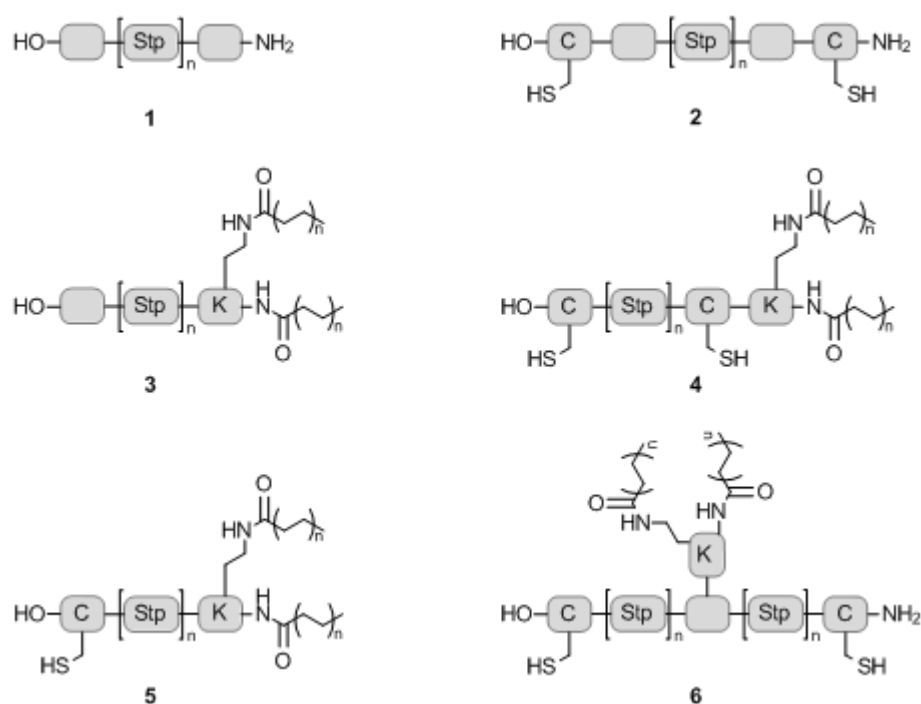


Figure 4.17: Structural overview over the different polymer classes. PAA chain (1), PAA chain with crosslinking cysteines (2); PAA with acylation at N-terminus (i-shape type) without (3), with one dimerizing (5), or with two crosslinking (4) cysteines; PAA with acylation in center (t-shape type) and crosslinking cysteines (6).

The initial library design was governed by the fact that there is only little information on structure-activity relationships in the literature due to the lack of defined polymeric carriers. The few published examples are almost exclusively dendritic structures¹⁶³, small peptides¹⁴³ and PEG-PAAs¹⁰⁰. Even by taking these defined structures into account the design motifs are dominated by M_w (> 10 kDa), variations in charge density and buffering properties. For the first evaluation of the modular solid-phase synthesis platform a big design space had to be covered using a minimal set of building blocks. To evaluate the potential of small PAAs in terms of NA delivery the design parameters were limited to four easily controllable structural parameters:

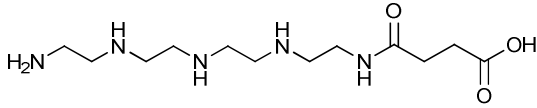
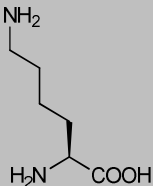
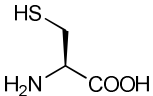
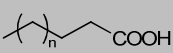
Building block	ID	Introduced Function
	Stp	Nucleic acid binding & buffering
	Lys(K)	Nucleic acid binding & branching point
	Cys(C)	Dimerization/polymerization & possible anchoring point
	Fatty acids (FA)	Polyplex stability & membrane interaction

Table 4.5: Overview over the used building blocks and their function in PAA design.

length of buffering/compaction domain, hydrophilic/lipophilic balance, branching and dimerizing/crosslinking capability (**Table 4.5**).

These four parameters were used to generate a PAA library which can be described by the 6 different families depicted in **Figure 4.17**. The simplest structural family is the PAA chain (**structure 1**), constructed by linear elongation using Stp and/or amino acid units. These structures closely resemble the prominent oligoethyleneimine motif of PEI and were synthesized to support the hypothesis that there is a minimal polymer length necessary for successful delivery of NAs¹⁶⁴. The crosslinking-PAA chain (**structure 2**) is further modified by two cysteine residues and was designed to introduce a dynamic stabilization element into the polyplexes by either stabilizing the formed particle by crosslinking¹⁶⁵ or through increased molecular weight caused by *in situ* polymerization. Both families were hydrophobically modified using fatty acids (FA) at the N-terminus, resulting in the i-shape families (**structures 3 and 4**). The hydrophobic moieties were introduced for two reasons, namely NA binding and membrane interaction⁴⁰. The dimerizing i-shapes (**structure 5**) were synthesized to test polyplex stabilization while the symmetrical t-shapes (**structure 6**) were used to examine the influence of a changed polymer topology on transfection efficacy. To obtain first structure-function relationships in regard to biophysical properties, subsets of the library were tested for NA binding and pH-specificity of lysis.

4.3.3 Lytic Activity

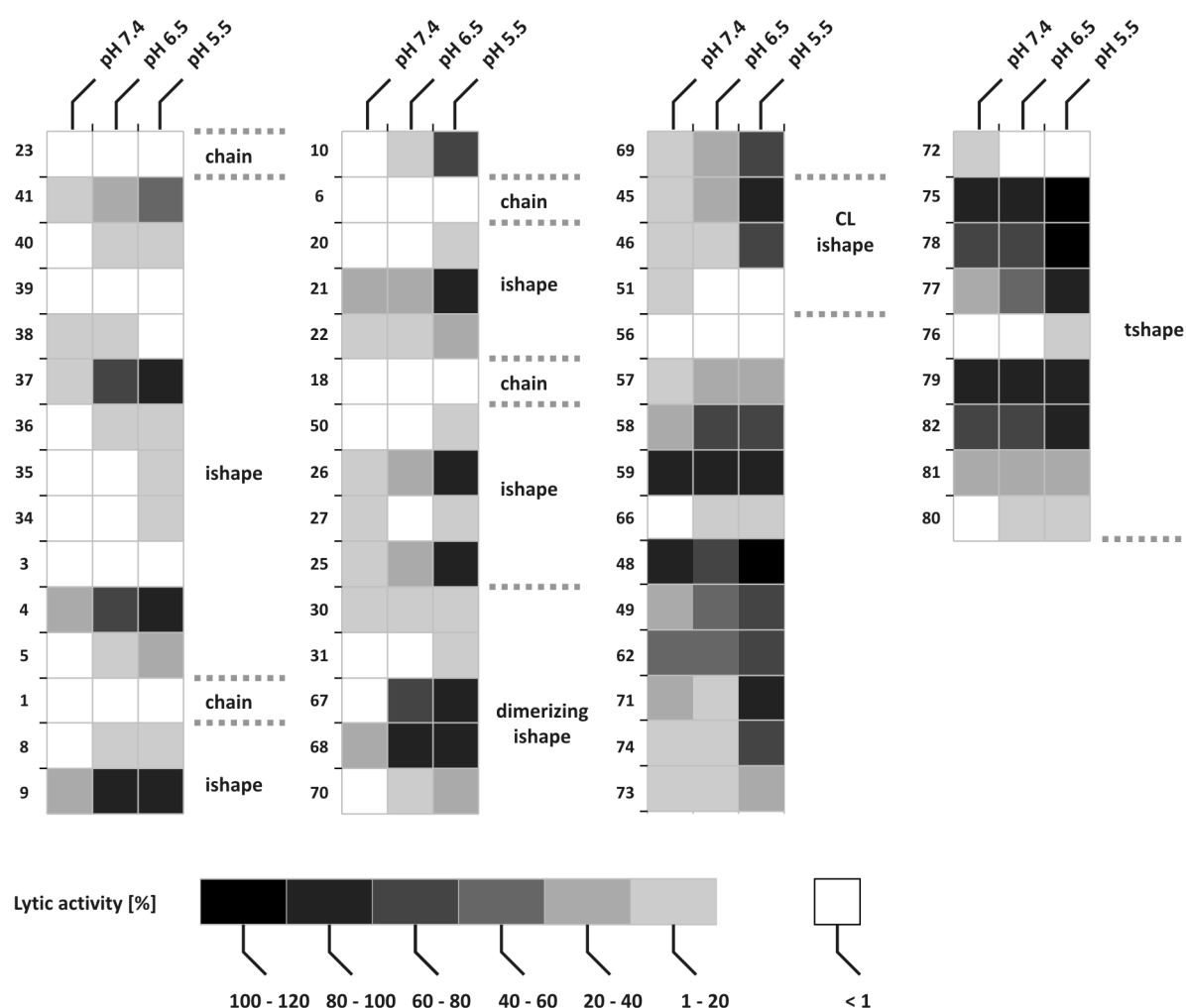


Figure 4.18: Heatmap analysis of the lytic activity of the different sublibraries at a concentration of 5 μ M at different pHs. Determined by erythrocyte leakage assay (synthesis and leakage assay performed by Christina Troiber, master thesis)

To escape endosomal entrapment, an endosomal pH-specific lytic activity is a desired prerequisite for successful delivery of NAs into the cytosol. This is especially true for polymeric vectors without a distinctive proton sponge effect¹²⁴ and has been introduced by attachment of lytic peptides¹⁶⁶ or introduction of hydrophobic residues¹⁶⁷⁻¹⁶⁸. The different polymer families were screened in an erythrocyte leakage assay system¹⁶⁶ to identify structural motifs resulting in a highly pH-specific lytic activity. By assaying the polymers at different pH-values comparable to the pH of different stages of the endosome¹⁶⁹ potent sequences can be identified, which only attack cell membranes at a slightly acidic pH. By using pH-specific lytic delivery systems potential cytotoxic lytic interactions with cell membranes in the beginning of

the transfection process can be reduced, thereby lowering the cytotoxic potential of the carrier.

Lytic activity of the unmodified polymer backbone was analyzed (**Figure 4.18**) using K-Stp₁-K (**#1**), K-Stp₂-K (**#6**); K-Stp₅-K (**#23**) as model sequences. The plain PAA sequences did not express any lytic activity even at concentrations > 5 μ M (data not shown). Introduction of a single N-terminal fatty acid into a K-Stp₂ sequence (**#34 – 37**) showed a slight increase in activity with oleic (**#37**) and myristic acid (**#36**) being the most effective modifications while polymers modified with fatty acids < C₁₄ (**#35, #34**) were essentially non-lytic. A general advantageous trend of an increased activity at lower pH was observed for the fatty acid modified PAAs which is most probably caused by the increased protonation state of the polyamine backbone at endosomal pH and the resulting interaction with negatively charged domains of the cell membranes.

Lytic potency of the polymers was further increased by using an N-terminal lysine as branching point and attaching two fatty acids to the lysine (double fatty acid motif). The increased lytic activity can be attributed to the close vicinity of the fatty acids resembling the general structure of amphipathic lipids. Acylation of the N-terminal lysine using caprylic acid (**#8**) chains did not result in a strong lytic activity, probably due to the rather short alkyl chain. Incorporation of myristyl residues (**#9**) results in a strong, unspecific lysis causing up to 40% of erythrocyte rupture already at neutral pH. Oleic acid modification (**#10**) shows a moderate, highly specific lytic activity rendering this modification the most valuable.

The chain length of the PAA backbone has only a moderate effect on lytic activity (**#22 vs. #10, #9 vs. #21**). Use of a larger backbone normally results in a diminished lytic activity. The most plausible explanation is the reduced molar proportion of lipid in the polymer indicating that 2 – 3 Stp units may be the optimal chain length for lytic activity using i-shape structures.

The introduction of cysteine into the sequence as dimerization/polymerization anchor did not significantly alter the extent and pH-specificity of membrane lysis (**#9, #68, #45 vs. #10, #69, #46**). This finding is especially interesting for the use of the polymers as NA delivery systems, as *in situ* crosslinking polymers may improve polyplex stability but would not cause significant change in cytotoxicity and endosomal escape potency.

4.3.4 Correlation of Cytotoxicity with Unspecific Lysis Activity

The impact of different hydrophobic modifications of a PAA sequence on the cytotoxic potential of the resulting delivery formulation is exemplified in **Figure 4.19**. Modification of the essentially non-toxic sequence K-Stp₂-K (**Figure 4.19, #06**) with a dual fatty acid motif shows an increased cytotoxicity (for fatty acids > C₈) under *in vitro* siRNA-transfection conditions.

In agreement with the observed lytic activity (**Figure 4.19, #08**) the modification with two C₈ residues has no pronounced effect on cellular metabolic activity. If the C₈ residues are substituted with C₁₄ residues (**Figure 4.19, #09**) the use of N/P 12 in the transfection results in a drop of metabolic activity to 30%. Erythrocyte leakage assay (**Figure 4.19, #9**) shows a lytic activity of 20 - 40% already at neutral pH reaching 100% lysis at pH 6.4. The oleic acid modification (**Figure 4.19, #10**) shows a more specific lytic profile reaching 80% lysis not until a pH of 5.5. This is reflected in the relatively late onset of toxicity under *in vitro* conditions, a N/P ratio > 20 is needed for cytotoxic effects.

The toxicity data correlates to the lytic activity of the polymers. Myristic acid modification showed the most potent but nevertheless mostly unspecific lytic activity of all tested polymers. This results in an increased cytotoxic activity when used in a carrier system, severely restricting the use of the myristic acid modification in these types of systems.

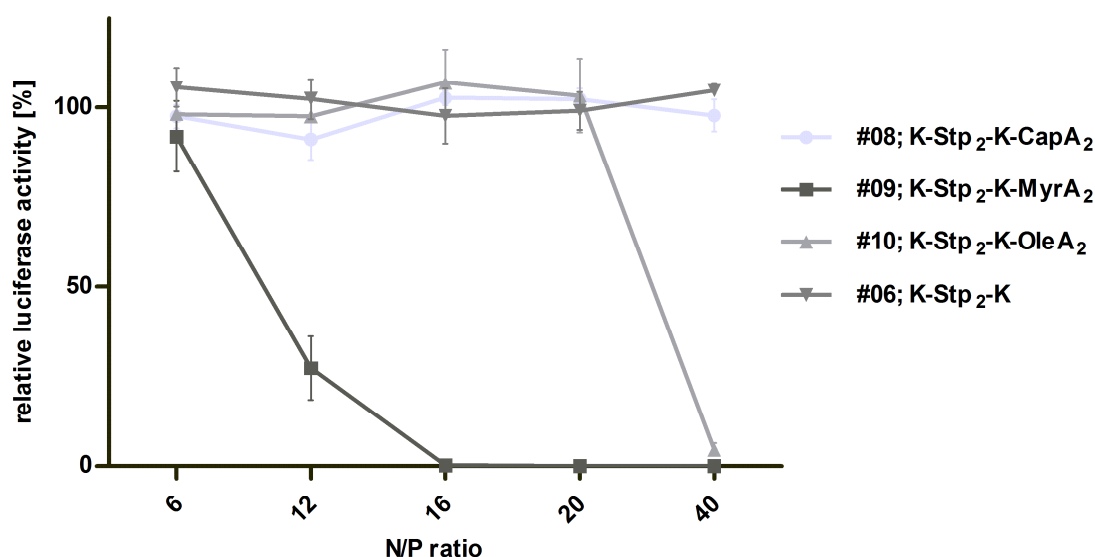


Figure 4.19: Toxicity of siRNA/PAA polyplexes on Neuro2A Luc cells. Cell viability was assessed by measuring luciferase activity after 48 h of incubation with siRNA_(scrambled)/PAA complexes and normalized using the luciferase expression of untreated control.

4.3.5 Structure-Activity Relationships in Nucleic Acid Binding

A principal criterion for the design of polymeric delivery systems is the ability to condense nucleic acids, thereby protecting the payload from degradation and allowing the transport to target cells. This interaction has to be sufficiently stable to withstand competitive interactions from other anionic species in the environment which could result in a premature payload release. The ability of the PAAs to condense NA was studied using an agarose gel shift assay with binding strength correlating to the amount of polymer needed for NA retardation.

As the sequences in the library were too short (< 6 Stp units) to show NA compaction, without additional refinement we were interested in identifying modifications that allow a strong NA compaction using such small backbones. Polymers containing only Stp and a C-terminal lysine were not able to bind either DNA or siRNA in the tested concentrations (**Figure 4.20.1–4, K-Stp₂-K, #6; K-Stp₄-K, #18**). To identify a minimal binding motif for use in nucleic acid delivery systems, a short K-Stp₂ sequence was modified with a single N-terminal fatty acid of differing chain lengths (**Figure 4.21.1–6.; K-Stp₂-OleA, #37; K-Stp₂-MyrA, #36; K-Stp₂-CapA, #35**). The hydrophobic modification had no influence onto the retardation of siRNA, independent of fatty acid chain length. For pDNA compaction the modification with an oleoyl residue showed weak compaction at N/P 40 (**Figure 4.21.4, #37**). This effect was further improved by the introduction of a second FA in close proximity using a N-terminal lysine as branching point. The dual FA motif resulted in strong pDNA polymer interactions with almost complete pDNA retardation at N/P 12 (**Figure 4.21.7–8**) if the fatty acid was either C₁₄ (**#9**) or C₁₈ (**#10**), use of a C₈ (**#8**) modification did not show interactions in the tested concentrations.

For siRNA binding the effect was even more pronounced (**Figure 4.21.7–9**). Single fatty acid modified polymers showed no retardation up to a N/P of 40, while dual FA modified PAAs were able to compact siRNA at a N/P of 12. Interaction of caprylic acid modified PAAs to siRNA was not strong enough to cause retardation.

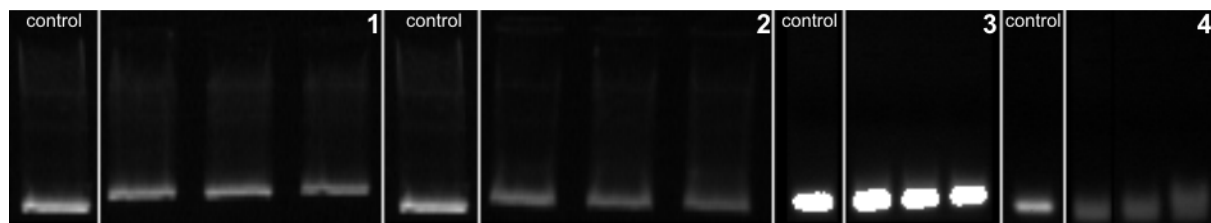


Figure 4.20: Comparison of unmodified PAAs regarding their DNA/siRNA binding in a gel shift assay. Lanes 1 + 2: K-Stp₂-K (#6), K-Stp₄-K (#18) DNA N/P 6/12/20; Lanes 3 + 4: #6, #18 siRNA N/P 12/20/40

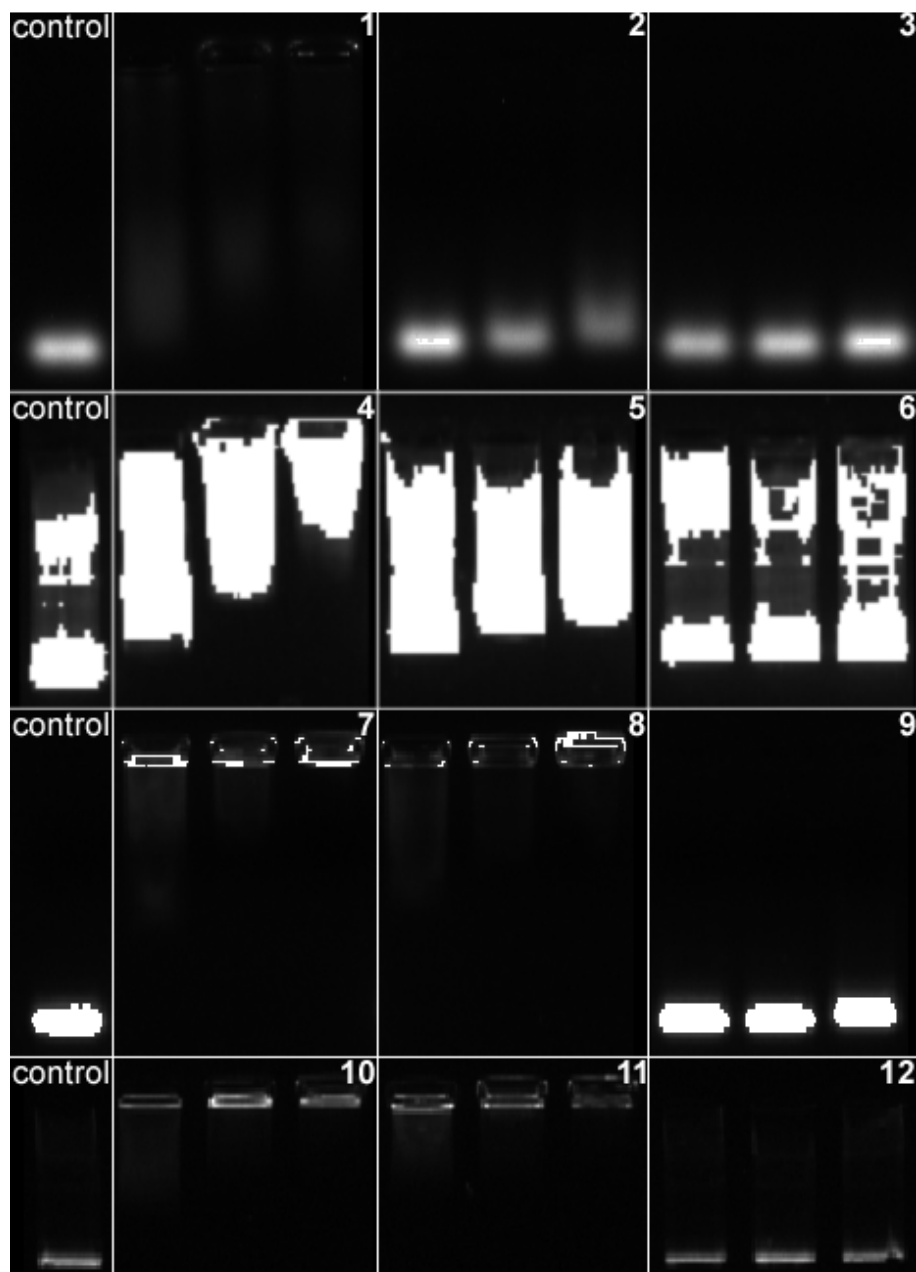


Figure 4.21: Comparison NA interaction of mono or dual fatty acid modified PAAs to siRNA (Row A,C) and pDNA (Row B, D) by agarose gel-shift assay. Row A: siRNA N/P 20/40/60; Row B: DNA N/P 12/20/40 Row C: siRNA N/P 20/40/60; Row D: DNA N/P 12/20/40; 1+4: K-Stp₂-OleA (#37), 2+5: K-Stp₂-MyrA (#36), 3+6: K-Stp₂-CapA (#35), 7+10: K-Stp₂-K-OleA₂ (#10), 8+11: K-Stp₂-K-MyrA₂ (#9), 9+12: K-Stp₂-K-CapA₂ (#8)

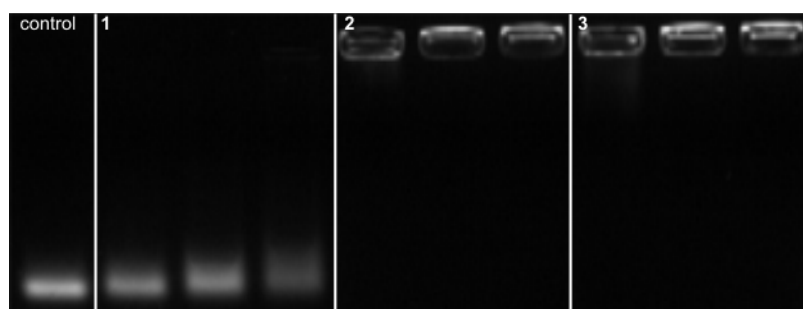


Figure 4.22: siRNA binding capabilities of K-Stp4-K-X2. left column siRNA control, all other columns siRNA complexed with polymer N/P 12/20/40, 1: K-Stp₄-K-CapA₂ (#20); 2: K-Stp₄-K-OleA₂ (#22); 3: K-Stp₄-K-MyrA₂ (#21);

To assess the influence of the PAA backbone length onto NA compaction and to rule out possible destabilization of the polyplexes by a changed hydrophilic-lipophilic ratio a longer, dual-FA modified PAA backbone was assayed for siRNA binding. **Figure 4.22** shows the influence of a longer Stp-sequence on the ability of the K-FA₂ motif to complex siRNA. Oleoyl (**Figure 4.22.2**) and myristyl (**Figure 4.22.3**) modifications result in strong siRNA binding at N/P 12, while the use of caprylic acid (**Figure 4.22.1**) did not result in a better compaction. The introduction of additional Stp units did not improve the binding of the caprylic acid modified PAA, supporting the hypothesis that siRNA binding using PAA systems is mostly governed by hydrophobic interactions.

4.3.6 Impact of the Different Domains on Nucleic Acid Delivery

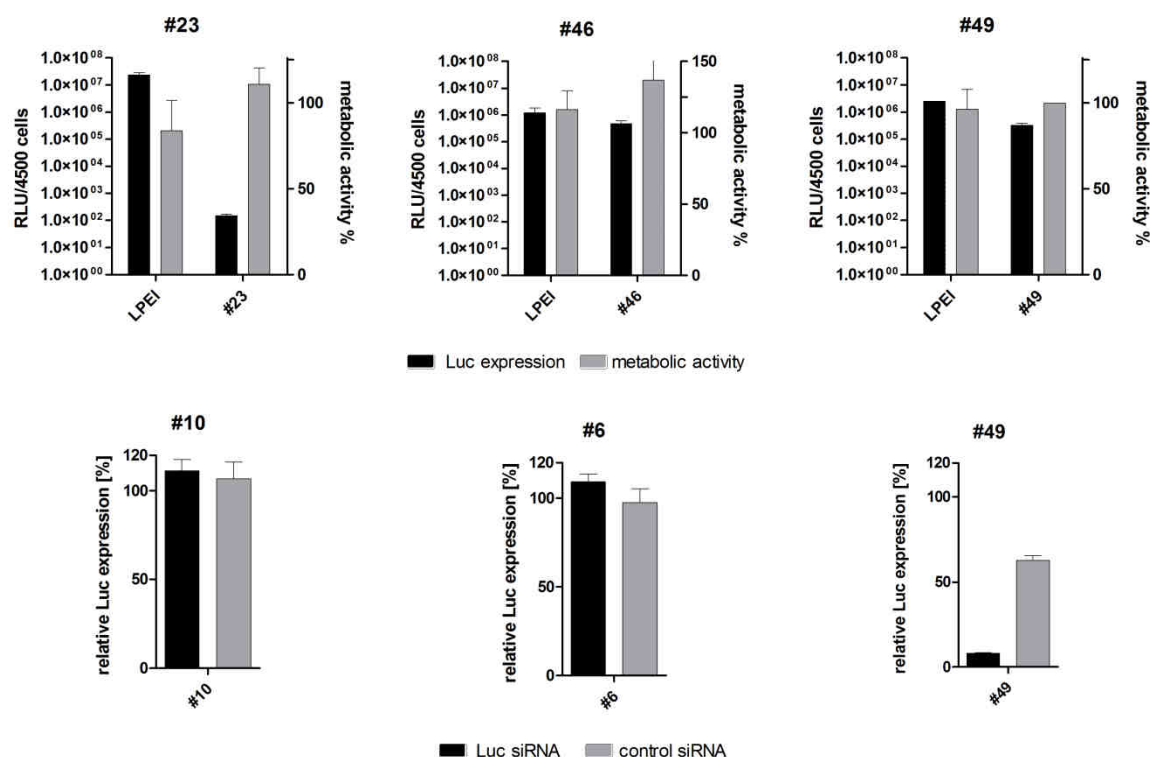


Figure 4.23: Evaluation of different polymers in DNA and siRNA transfer. Upper panel: DNA delivery in Neuro2A cells (1 μ g/mL DNA/well at w/w 10; #23:K-Stp₅-K; #46: C-Stp₃-C-K-OleA₂; #49: C-Stp₂-K-(K-OleA₂)-Stp₂-C) Lower panel: siRNA delivery in Neuro2A/eGFPLuc cells (5 μ g/mL siRNA/well at N/P 12 (~ 10 w/w); #10: K-Stp₂-K-OleA₂; #6: K-Stp₂-K; #49: C-Stp₂-K-(K-OleA₂)-Stp₂-C) (performed by Thomas Fröhlich, Wagner lab)

To identify promising lead structures for subsequent structure activity models library members with differing lytic/binding properties were screened for NA delivery potential in a luciferase reporter gene assay (pDNA delivery) and a Neuro2A/eGFPLuc gene silencing model (siRNA delivery).

Figure 4.23 shows an exemplary comparison of different, modular constructed polymers under optimal experimental conditions. In the upper panel of **Figure 4.23** the pDNA delivery potential and cytotoxicity of different polymers out of the chain, i-shape and t-shape classes is shown. The linear chain K-Stp₅-K (**#23**) is comparable to OEI800 (a rather weak performing member of the PEI family) regarding M_w and number of protonable amines but use of **#23** results in no significant difference of reporter gene expression compared to background expression. Incorporation of a hydrophobic domain and cysteine modification significantly improves the DNA delivery efficiency of the polymers (**#46**, **#49**). While LPEI is still five- to tenfold more efficient in gene delivery both polymers show no apparent effect on the metabolic

activity of the transfected cells and can be further optimized by changes to their structural domains.

The lower panel of **Figure 4.23** shows a comparison of gene silencing and cytotoxic potential of different polymer/siRNA formulations. By comparison of three different classes of polymers (chain (**#6**), i-shape (**#10**), crosslinking t-shape (**#49**)) the synergistic influence of the different domains can be investigated. As already demonstrated for pDNA delivery the use of short unmodified Stp-chains (**#6**) did not result in any significant luciferase knockdown. Use of a dioleoyl modified chain (**#10**) likewise did not result in a significantly increased luciferase knockdown. These results are in line with the data derived from lysis/binding assays. Polymer **#6** shows low lytic activity and forms no stable complexes with siRNA. Polymer **#10** on the other hand has specific lytic activity (80-100% lysis at pH 5.5), forms reasonably stable complexes but fails in delivery. Polymer **#49**, an oleoyl modified t-shape which is further modified by the incorporation of two cysteines demonstrates a potent luciferase knockdown.

#	Sequence	Formula	M _w	protonable amines	Type
1	K-Stp ₁ -K	C ₂₄ H ₅₁ N ₉ O ₅	545,72	6	chain
3	K-Stp ₁ -K-CapA ₂	C ₄₀ H ₇₉ N ₉ O ₇	798,11	4	i-shape
4	K-Stp ₁ -K-MyrA ₂	C ₅₂ H ₁₀₃ N ₉ O ₇	966,43	4	i-shape
5	K-Stp ₁ -K-OleA ₂	C ₆₀ H ₁₁₅ N ₉ O ₇	1074,61	4	i-shape
6	K-Stp ₂ -K	C ₃₆ H ₇₆ N ₁₄ O ₇	817,08	9	chain
8	K-Stp ₂ -K-CapA ₂	C ₅₂ H ₁₀₄ N ₁₄ O ₉	1069,47	7	i-shape
9	K-Stp ₂ -K-MyrA ₂	C ₆₄ H ₁₂₈ N ₁₄ O ₉	1237,79	7	i-shape
10	K-Stp ₂ -K-OleA ₂	C ₇₂ H ₁₄₀ N ₁₄ O ₉	1345,97	7	i-shape
18	K-Stp ₄ -K	C ₆₀ H ₁₂₆ N ₂₄ O ₁₁	1359,80	15	chain
20	K-Stp ₄ -K-CapA ₂	C ₇₆ H ₁₅₄ N ₂₄ O ₁₃	1612,19	13	i-shape
21	K-Stp ₄ -K-MyrA ₂	C ₈₈ H ₁₇₈ N ₂₄ O ₁₃	1780,51	13	i-shape
22	K-Stp ₄ -K-OleA ₂	C ₉₆ H ₁₉₀ N ₂₄ O ₁₃	1888,69	13	i-shape
23	K-Stp ₅ -K	C ₇₂ H ₁₅₁ N ₂₉ O ₁₃	1631,16	18	chain
25	K-Stp ₅ -K-AraA ₂	C ₁₁₂ H ₂₂₇ N ₂₉ O ₁₅	2220,19	16	i-shape
26	K-Stp ₅ -K-MyrA ₂	C ₁₀₀ H ₂₀₃ N ₂₉ O ₁₅	2051,87	16	i-shape
27	K-Stp ₅ -K-OleA ₂	C ₁₀₈ H ₂₁₅ N ₂₉ O ₁₅	2160,05	16	i-shape
30	C-Stp ₁ -K-CapA ₂	C ₃₇ H ₇₂ N ₈ O ₇ S	773,08	3	i-shape
31	C-Stp ₁ -K-SteA ₂	C ₅₇ H ₁₁₂ N ₈ O ₇ S	1053,61	3	i-shape
34	K-Stp ₂ -ButA ₁	C ₃₄ H ₇₀ N ₁₂ O ₇	759,00	7	i-shape
35	K-Stp ₂ -CapA ₁	C ₃₈ H ₇₈ N ₁₂ O ₇	815,10	7	i-shape
36	K-Stp ₂ -MyrA ₁	C ₄₄ H ₉₀ N ₁₂ O ₇	899,26	7	i-shape
37	K-Stp ₂ -OleA ₁	C ₄₈ H ₉₆ N ₁₂ O ₇	953,35	7	i-shape
38	K-Stp ₁ -ButA ₁	C ₂₂ H ₄₅ N ₇ O ₅	487,64	4	i-shape
39	K-Stp ₁ -CapA ₁	C ₂₆ H ₅₃ N ₇ O ₅	543,74	4	i-shape
40	K-Stp ₁ -MyrA ₁	C ₃₂ H ₆₅ N ₇ O ₅	627,90	4	i-shape
41	K-Stp ₁ -OleA ₁	C ₃₆ H ₇₁ N ₇ O ₅	681,99	4	i-shape
45	C-Stp ₃ -C-K-MyrA ₂	C ₇₆ H ₁₅₁ N ₁₉ O ₁₂ S ₂	1587,26	9	i-shape
46	C-Stp ₃ -C-K-OleA ₂	C ₈₄ H ₁₆₃ N ₁₉ O ₁₂ S ₂	1695,44	9	i-shape
48	C-Stp ₂ -K-(K-MyrA ₂)-Stp ₂ -C	C ₉₄ H ₁₈₈ N ₂₆ O ₁₅ S ₂	1986,79	13	t-shape
49	C-Stp ₂ -K-(K-OleA ₂)-Stp ₂ -C	C ₁₀₂ H ₂₀₀ N ₂₆ O ₁₅ S ₂	2094,98	13	t-shape
50	K-Stp ₄ -K-ArA ₂	C ₁₀₀ H ₂₀₂ N ₂₄ O ₁₃	1948,83	13	i-shape
51	C-Stp ₃ -C-K	C ₄₈ H ₉₉ N ₁₉ O ₁₀ S ₂	1166,55	11	chain
56	C-Stp ₂ -K(CapA)-Stp ₂ -C	C ₆₈ H ₁₃₈ N ₂₄ O ₁₃ S ₂	1564,11	13	t-shape
57	C-Stp ₂ -K(MyrA)-Stp ₂ -C	C ₇₄ H ₁₅₀ N ₂₄ O ₁₃ S ₂	1648,27	13	t-shape
58	C-Stp ₂ -K(OleA)-Stp ₂ -C	C ₇₈ H ₁₅₆ N ₂₄ O ₁₃ S ₂	1702,36	13	t-shape
59	C-Stp ₂ -K(ArA)-Stp ₂ -C	C ₈₀ H ₁₆₂ N ₂₄ O ₁₃ S ₂	1732,43	13	t-shape
62	C-Stp ₂ -K(K-ArA ₂)-Stp ₂ -C	C ₁₀₆ H ₂₁₂ N ₂₆ O ₁₅ S ₂	2155,11	13	t-shape
66	C-Stp ₂ -K(K-CapA ₂)-Stp ₂ -C	C ₈₂ H ₁₆₄ N ₂₆ O ₁₅ S ₂	1818,47	13	t-shape
67	C-Stp ₂ -K-MyrA ₂	C ₆₁ H ₁₂₁ N ₁₃ O ₉ S	1212,76	6	i-shape
68	C-K-Stp ₂ -K-MyrA ₂	C ₆₇ H ₁₃₃ N ₁₅ O ₁₀ S	1340,93	7	i-shape
69	C-K-Stp ₂ -K-OleA ₂	C ₇₅ H ₁₄₅ N ₁₅ O ₁₀ S	1449,11	7	i-shape
70	C-Stp ₂ -K-OleA ₂	C ₆₉ H ₁₃₃ N ₁₃ O ₉ S	1320,94	6	i-shape
71	C-Stp ₁ -K(K-MyrA ₂)-Stp ₁ -C	C ₇₀ H ₁₃₈ N ₁₆ O ₁₁ S ₂	1444,07	7	t-shape

72	C-Stp ₁ -K(K)-Stp ₁ -C	C ₄₂ H ₈₆ N ₁₆ O ₉ S ₂	1023,36	9	chain
73	C-Stp ₁ -K(K-SteA ₂)-Stp ₁ -C	C ₇₈ H ₁₅₄ N ₁₆ O ₁₁ S ₂	1556,29	7	t-shape
74	C-Stp ₁ -K(K-OleA ₂)-Stp ₁ -C	C ₇₈ H ₁₅₀ N ₁₆ O ₁₁ S ₂	1552,26	7	t-shape
75	C-Stp ₃ -K(K-MyrA ₂)-Stp ₃ -C	C ₁₁₈ H ₂₃₈ N ₃₆ O ₁₉ S ₂	2529,51	19	t-shape
76	C-Stp ₃ -K(K)-Stp ₃ -C	C ₉₀ H ₁₈₆ N ₃₆ O ₁₇ S ₂	2108,80	19	chain
77	C-Stp ₃ -K(K-SteA ₂)-Stp ₃ -C	C ₁₂₆ H ₂₅₄ N ₃₆ O ₁₉ S ₂	2641,73	17	t-shape
78	C-Stp ₃ -K(K-OleA ₂)-Stp ₃ -C	C ₁₂₆ H ₂₅₀ N ₃₆ O ₁₉ S ₂	2637,69	17	t-shape
79	C-Stp ₄ -K(K-MyrA ₂)-Stp ₄ -C	C ₁₄₂ H ₂₈₈ N ₄₆ O ₂₃ S ₂	3072,23	25	t-shape
80	C-Stp ₄ -K(K)-Stp ₄ -C	C ₁₁₂ H ₂₃₄ N ₄₈ O ₂₁ S ₂	2653,50	27	chain
81	C-Stp ₄ -K(K-SteA ₂)-Stp ₄ -C	C ₁₅₀ H ₃₀₄ N ₄₆ O ₂₃ S ₂	3184,44	25	t-shape
82	C-Stp ₄ -K(K-OleA ₂)-Stp ₄ -C	C ₁₄₈ H ₂₉₈ N ₄₈ O ₂₃ S ₂	3182,39	25	t-shape

Table 4.6: List of tested polymers

4.4 Evaluation of Different PAA Families for *in vitro* DNA Delivery

4.4.1 Introduction

Development and modification of polymeric systems for NA delivery continues to be an attractive field of study as the delivery of genetic information into cells holds great therapeutic promise. Despite the significant maturation of polymer-based gene vectors over the last 20 years, they are still characterized by a rather low efficiency and the potential and the possibilities of modification are far from being fully exploited. Over the time certain design concepts¹⁰¹ were substantiated by numerous reports, including the use of cationic polymers to complex NAs¹⁷⁰⁻¹⁷¹, modification with shielding and targeting domains¹⁷²⁻¹⁷³ and hydrophobic functionalization^{40,121} to promote cellular uptake and endosomal escape. A persisting problem of this classical approach to vector design is the limited information on precise structure-activity relationships. In most investigations the analyzed polymers have been heterogenic systems in terms of molecular weight, grade of polydispersity and sites of conjugations and other modifications. In this regard synthesis and screening of sequence-defined polymers offers the possibility of a more evidence-driven route to the design of polymeric vectors.

The small library of sequence-defined polymers (as described in Chapter 5) was screened for DNA transfection potential. The used luciferase reporter gene system¹⁷⁴ has the advantage of being a positive readout system with a wide detection range, allowing the comparison of carrier efficiencies over more than four log scales. Aim of this first DNA transfection screening was to explore the elementary properties of this new class of sequence-defined polymers, to evaluate their potential as nucleic acid delivery agents and to identify promising lead structures for further optimization. The obtained results provide valuable information for the design of improved DNA transfection polymers, and to some extent also for the delivery of other nucleic acid derivatives (e.g. siRNA, PMOs, PNAs).

4.4.2 *in vitro* DNA Delivery

Following the generic biophysical characterization of the polymers (see Chapter 5) the most promising candidates were screened *in vitro* to identify structural motifs responsible for successful DNA delivery. The PAAs were used to complex a plasmid

encoding an EGFP-luciferase fusion protein (pEGFPLuc) and were screened on cultured Neuro2A murine neuroblastoma cells. Polyplexes were prepared in HBG at a pH of 8.3 (for a survey of the influence of pH on transfection efficiency see **Appendix 8.5**) using w/w ratios from 5 – 40 at a constant DNA dose of 2 µg/mL for transfection and were added to cells in standard serum-containing culture medium. After 24 h luciferase expression and metabolic activity were measured and compared to a LPEI control formulation.

Due to the relatively small size (1-3 kDa) of the screened polymers even small property changes due to an altered polymer sequence will be reflected in transfection efficiency and cytotoxicity, allowing quick assessment of the potential benefit of a modification.

4.4.3 DNA Delivery Using Non-thiol Containing Chains and i-shapes

To evaluate the delivery properties of PAA delivery systems Stp-chains, optionally modified by N-terminal acylation with fatty acids (i-shapes), were screened (see **Figure 4.25**). These families are characterized by a number of 2-5 Stp units in a polymer and, in the case of i-shapes, by fatty acid modification (myristic, oleic, arachidic acid). The influence of the hydrophobic modifications on the NA binding is demonstrated in **Figure 4.24**. Polyplex stability is increased by the incorporation of longer chain fatty acids resulting in stabilization at N/P 6 (**Figure 4.24.2+3 + 4.24.6+7**) while unmodified K-Stp₅-K (**#23**) (**Figure 4.24.1**) shows no DNA binding even at polymer concentrations of N/P 20 (result not shown). The effect of hydrophobic modification on NA compaction is even more pronounced than the number of charges in the single molecule as seen by a comparison of K-Stp₂-K-MyrA₂ (**#9**) and K-Stp₄-K-MyrA₂ (**#21**) (**Figure 4.24.2 and 4.24.5**). To assess delivery capability and toxicity of PAA chains and i-shapes the fatty acid modified sequences were compared to K-Stp₅-K (**#23**) in an *in vitro* transfection assay. The sequence is comparable in M_w and amount of protonable amines to OEI₈₀₀ a rather weak performing member of the PEI family (for a comparison see **Table 4.7**). As shown in **Figure 4.25** even the use of relatively high polymer concentrations (w/w 20) shows no significant increase of luciferase expression compared to untreated cells. This can be explained by inferior condensation properties of the plain PAA sequences compared to the fatty acid modified polymers. Furthermore this is in agreement with results of erythrocyte leakage assays which showed no lytic activity (activity < 10% at

all pHs) for unmodified PAAs thereby reducing the probability of successful endosomal escape. These findings are additionally supported by the absence of toxicity in all tested concentrations (**Figure 4.25**).

The synergistic effect of polyplex stabilization and lytic activity is reflected in the reporter gene expression profiles of the fatty acid modified polymers. Modification of a K-Stp₂-K sequence with either myristic (**#9**) or oleic acid (**#10**) increases the transfection compared to K-Stp₅-K (**#23**) (possessing the double amount of charges) tenfold at a w/w 10. Elongation of the chain by two additional Stp units results in an up to 100-fold increase of reporter gene expression. This is accompanied by an increased cytotoxicity for the myristic acid derivatives in all tested concentrations resulting in a metabolic activity < 10% at a w/w of 40 (**Figure 4.25, #9 + #21**). Oleic acid modification has a comparable effect on the transfection efficiency while the toxicity of the polymers in the tested concentration range is negligible (**Figure 4.25, #10 + #22**).

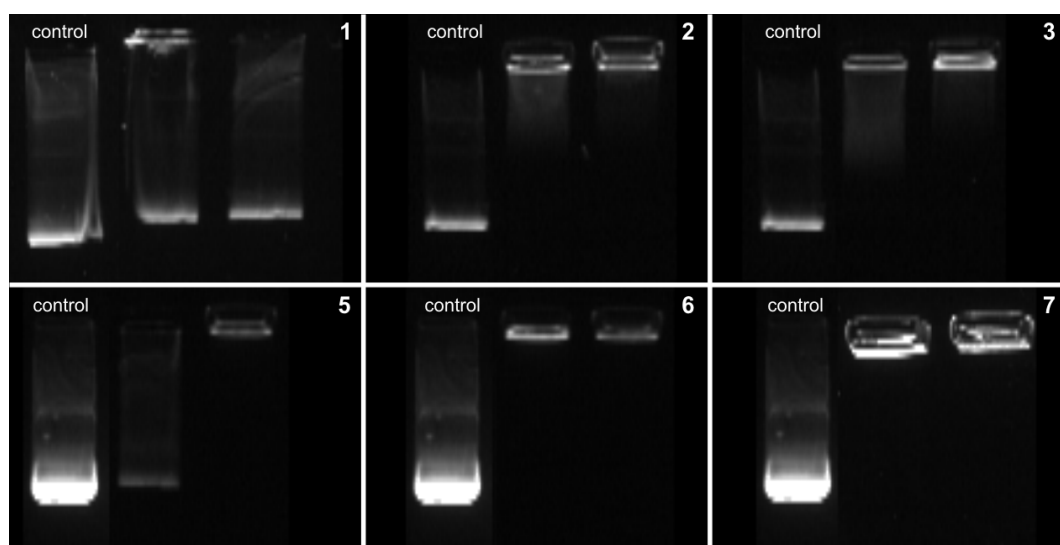


Figure 4.24: DNA binding properties of the PAA chain polymers. 0.1 µg DNA was mixed with polymer at N/P ratios of 6 and 12 (corresponds to a average w/w of 5/10) and analyzed by gel retardation assay. 1: K-Stp₅-K (**#23**); 2: K-Stp₂-K-MyrA₂(**#9**); 3: K-Stp₂-K-OleA₂(**#10**); 4: K-Stp₄-K-MyrA₂(**#21**); 5: K-Stp₄-K-OleA₂(**#22**); 6: K-Stp₄-K-AraA₂ (**#50**)

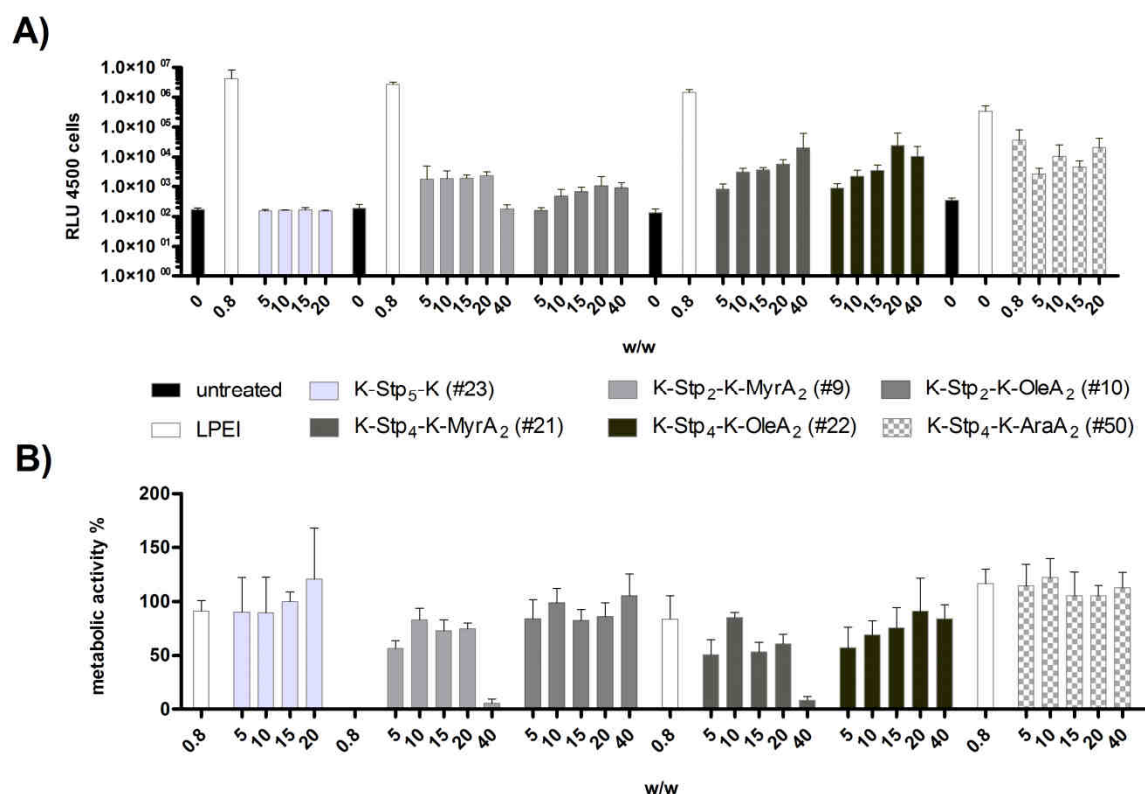


Figure. 4.25: Reporter gene expression and metabolic activity of cells 24 h after transfection using i-shape type PAAs in comparison to a chain type PAA. Neuro2A cells were transfected using 200 ng pCMVLuc (2 μ g/mL DNA) plasmid. Polyplexes were prepared at different w/w ratios and compared to standard LPEI polyplexes. Luciferase reporter gene expression (A) and metabolic activity (MTT Assay, B) are presented as mean value + SD of quintuplicates.

In comparison to LPEI all these structures show 1000-fold lower activity, rendering them useless as gene transfer reagents. Nevertheless, the data demonstrate the beneficial influence of hydrophobic modifications on stability and delivery using small PAA fragments.

4.4.4 Influence of a Dimerization Anchor on Transfection Efficiency

To study the influence of disulfide bridges on polyplex stabilization a C-terminal cysteine was incorporated into an i-shape sequence (**HO-C-Stp_n-K-FA₂**). These structures were initially synthesized to introduce a thiol handle for subsequent bioconjugation to siRNA or proteins, but attempts to prepare lytic siRNAs by direct conjugation to the 5' end (sense strand) of a thiol-modified siRNA duplex were unsuccessful as the lytic activity collapsed (unpublished results Christian Dohmen). The introduction of a C-terminal cysteine showed no significant impact on NA complexation a w/w of 10 was sufficient for complete retardation (**Figure 4.27.1-4**).

Using these dimerizable, fatty acid modified PAAs for DNA delivery had a significant effect on reporter gene expression as shown in **Figure 4.26**. In comparison to their analog sequences K-Stp₂-K-MyrA₂ (**#9**) and K-Stp₂-K-OleA₂ (**#10**) introduction of a C-terminal cysteine (**#67 + #70**) results in a 100-fold increased reporter gene expression at a w/w of 10. To evaluate the possible influence of the primary amine of the lysine residue on DNA delivery sequences without the additional lysine were screened. While the lysine had no significant effect on the oleic acid modified PAAs (**Figure 4.26, #70 vs. #69**) the delivery efficiency of **#68** compared to **#67** was increased 100-fold. Interestingly the toxicity of the myristic acid modified PAAs was not affected in the same manner. While the metabolic activity of cells treated with the non-thiol containing sequence **#9** dropped to 10% (w/w 40), treatment with cysteine modified **#68** only resulted in a decrease to 50% (w/w 40). Oleic acid modification had no pronounced effect on cell viability regardless of sequence composition.

C-terminal cysteine modification seems to be a viable option to increase the delivery capability of short chain PAAs and has the additional benefit of a reducing cellular toxicity in case of myristic acid modified PAAs. Oleic acid modification on the other hand shows a comparable increase in gene expression but without an increased cytotoxicity in the tested concentrations. Myristic acid modified PAAs induce a bell shaped expression profile wherein the reporter gene expression rises with increasing concentration until the onset of toxicity impairs reporter gene expression, while oleic acid modified PAAs reach a more or less stable expression plateau at a w/w of 10.

These results support the hypothesis that the PAA polymers without the ability of disulfide bridge formation suffer from inadequately stabilization of the resulting polyplexes. This problem might be overcome by either synthesizing larger polymers or by using other means of stabilization like *in situ* thiol dimerization or crosslinking.

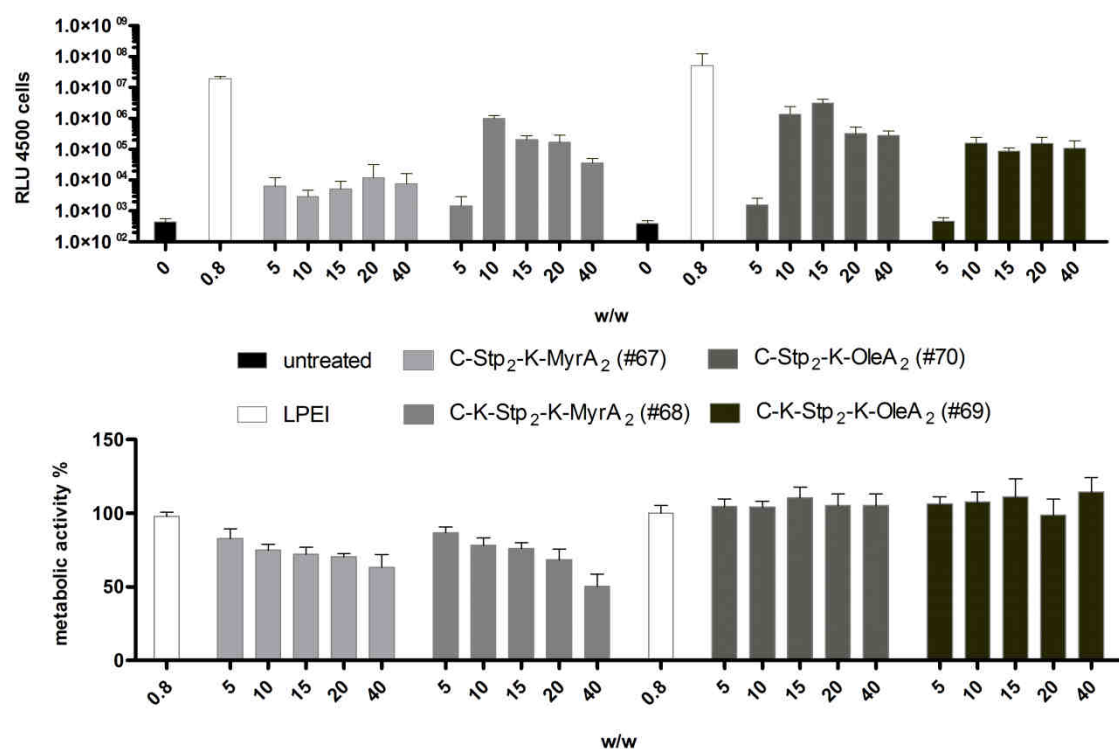


Figure 4.26: Reporter gene expression and metabolic activity of cells 24 h after transfection using dimerizable i-shape type PAAs. Neuro2A cells were transfected using 200 ng pCMVLuc (2 µg/mL DNA) plasmid. Polyplexes were prepared at different w/w ratios and compared to standard LPEI polyplexes. Luciferase reporter gene expression (A) and metabolic activity (MTT Assay, B) are presented as mean value + SD of quintuplicates

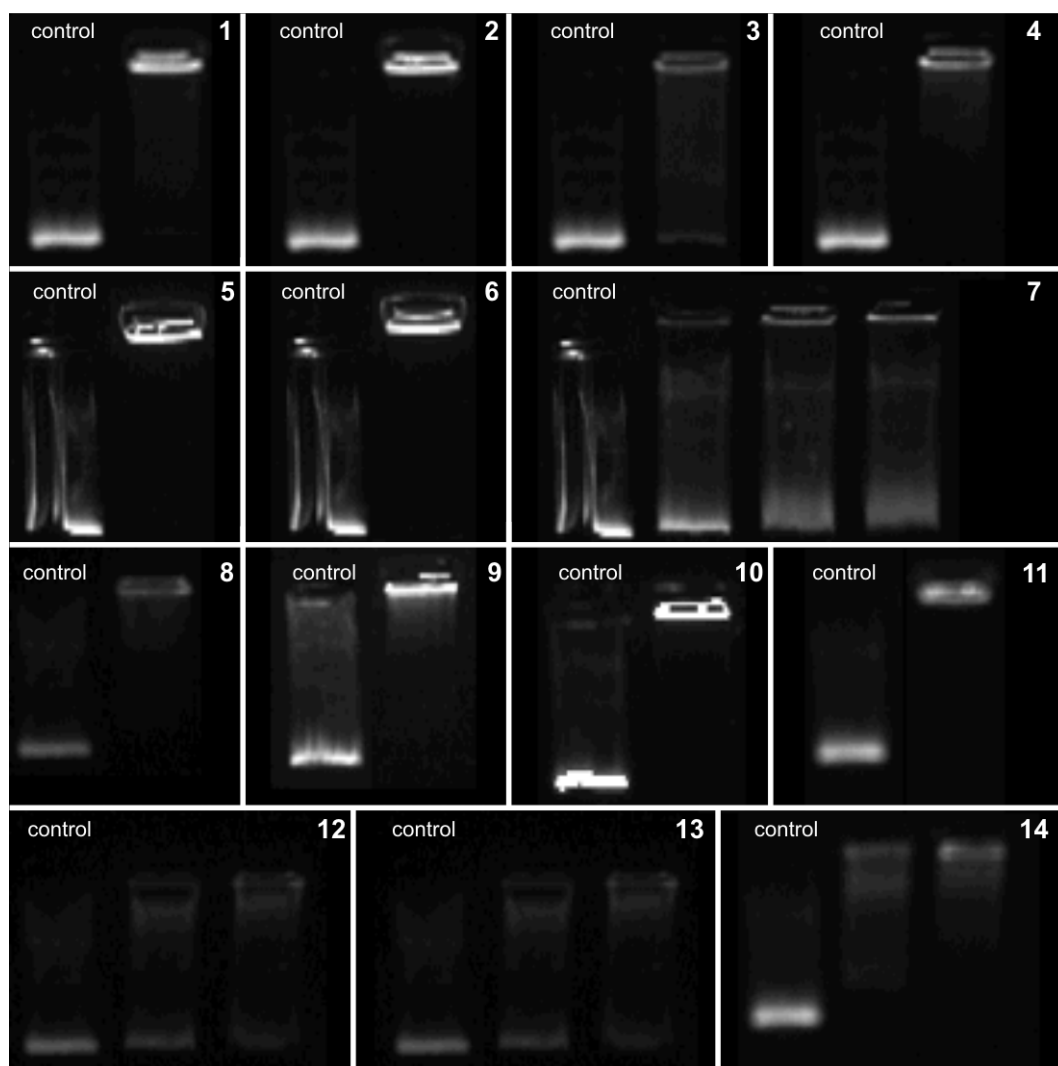


Figure 4.27: Comparison of the gel retardation of DNA of the different PAA families. All polymers were tested at a w/w of 10. Polymers showing no complete retardation at that concentration are shown in increasing concentrations. Picture 1 – 4 dimerizing i-shapes (#67, #68, #70, #69); Picture 5 – 7 i-shape family (#45, #46, #51), w/w 5,10,20; Picture 8 – 11 t-shape family (#74, #49, #78, #82); 12 – 14 crosslinking chains family (#72, #76, #80), w/w 5, 10

4.4.5 DNA Delivery Using Crosslinking i-Shape Structures

By insertion of a second cysteine into the sequence (**HO-C-Stp₃-C-K-FA₂**) the polymers gain the ability of *in situ* polymerization allowing formation of bigger polymeric structures. It was hypothesized that the introduction of crosslinking would be beneficial for NA binding and could further stabilize an already formed complex by crosslinking. Gel retardation assay (**Figure 4.27, #5-7**) shows that in comparison with single cysteine modified PAAs (**Figure 4.27, #1-4**) the NA complexation is improved but still heavily dependent on hydrophobic modifications (**Figure 4.27.7**).

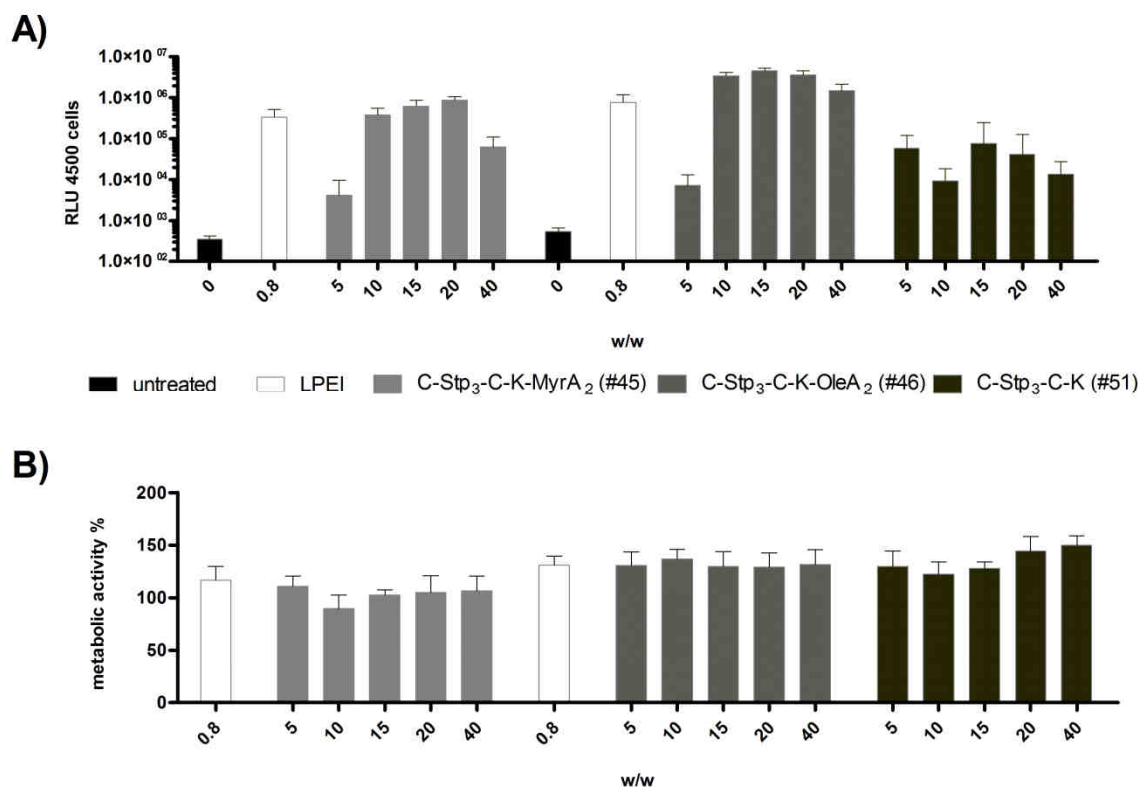


Figure 4.28: Reporter gene expression and metabolic activity of cells 24 h after transfection using crosslinking i-shape type PAAs. Neuro2A cells were transfected using 200 ng pCMVLuc (2 μ g/mL DNA) plasmid. Polyplexes were prepared at different w/w ratios and compared to standard LPEI polyplexes. Luciferase reporter gene expression (A) and metabolic activity (MTT Assay, B) are presented as mean value + SD of quintuplicates.

Figure 4.28 shows the reporter gene expression of crosslinking i-shape formulations with different fatty acid modifications on a HO-C-Stp₃-C-K-H backbone. All tested polymers are able to effectively transfer pDNA into target cells and show a expression profile characterized by a plateau phase beginning with w/w 10. As soon as a critical concentration is reached reporter gene expression is not increased by higher polymer concentrations. For certain other polymeric delivery systems this effect is connected to increasing cytotoxicity at higher concentrations, in these cases MTT assay did not show toxic side effects indicating additional intracellular delivery bottlenecks. Myristic and oleic acid i-shapes are able to compete with the LPEI control demonstrating the delivery potential of these structures.

The use of the backbone control (unmodified N-terminus) resulted in a 10 to 50-fold decrease of efficiency highlighting the importance of the hydrophobic modification. The promising delivery results renders this scaffold into one of the most interesting for further development.

4.4.6 DNA Delivery Using PAAs With t-Shape Topology

By synthesizing a set of symmetrical i-shape polymers with a central hydrophobic domain (t-Shapes) the influence of parameters like the amount of protonable groups per molecule, hydrophilic-lipophilic ratio (HLR) of the molecule and influence of the hydrophobic modification on larger PAA structures were studied.

Figure 4.24 compares the binding capabilities of di-oleoyl modified t-shapes (**#8-11**) with non hydrophobically modified linear chains with terminal cysteines (**#12-14**). The oleoyl t-Shape/DNA complexes are strong enough to prevent migration in the gel at a w/w of 10 while the interaction of the unmodified chains at the same w/w is not strong enough to prevent NA migration. **Figure 4.29** shows the transfection efficiency and cytotoxic potential of oleoyl t-shapes with differing numbers of Stp building blocks per molecule. All tested polymers were synthesized with a dual oleic acid motif at the central lysine, as the oleic acid modification was the most effective modification in terms of toxicity and efficiency in the previous experiments. The balance between hydrophobic and cationic domain has a significant impact on efficacy as seen by comparing the transfection efficiency of **#74** and **#49**. While increasing concentrations of **#74** lead to reporter gene expression almost reaching the LPEI control the use of a polymer containing two additional Stp units results in an early, only moderate plateau of activity. The introduction of additional Stp units didn't improve their overall performance, regardless of the tested concentrations the reporter gene expression was always tenfold lower than the LPEI control. The results indicate a fine balance between hydrophobicity and hydrophilicity as exemplified by **#74**. **#74** has the highest HLR in the screen (**0.341**, **Table 4.7**) and exhibits the strongest activity in terms of expression level. All other t-shape derivatives cannot compete in terms of expression level and reach their maximum level at lower concentrations of w/w 5.

To study the influence of the hydrophobic domain onto the efficiency of the t-shape polymers in more detail, a second set of polymers without hydrophobic modification (crosslinking chains) was synthesized and screened (**Figure 4.30**). Here the trend was reversed **#72**, a structural analogue of **#74** (2 Stp-units) did not show any reporter gene expression while an increase in Stp-building blocks per molecule did result in an increasing gene expression (**#76**, **#80**). Compared to the gene expression levels of the oleoyl t-shapes these polymers have the disadvantage of needing rather high polymer concentrations to achieve a comparable transfection

efficiency. The dual fatty acid motif can increase the delivery efficiency but the influence of the modification diminishes with an increasing number of Stp units in the backbone. This supports earlier findings that the hydrophobic modification is more effective on smaller PAAs and can increase their efficiency dramatically, while an increasing amount of Stp units in a fatty acid-free polymer also results in an improved, but less efficient delivery.

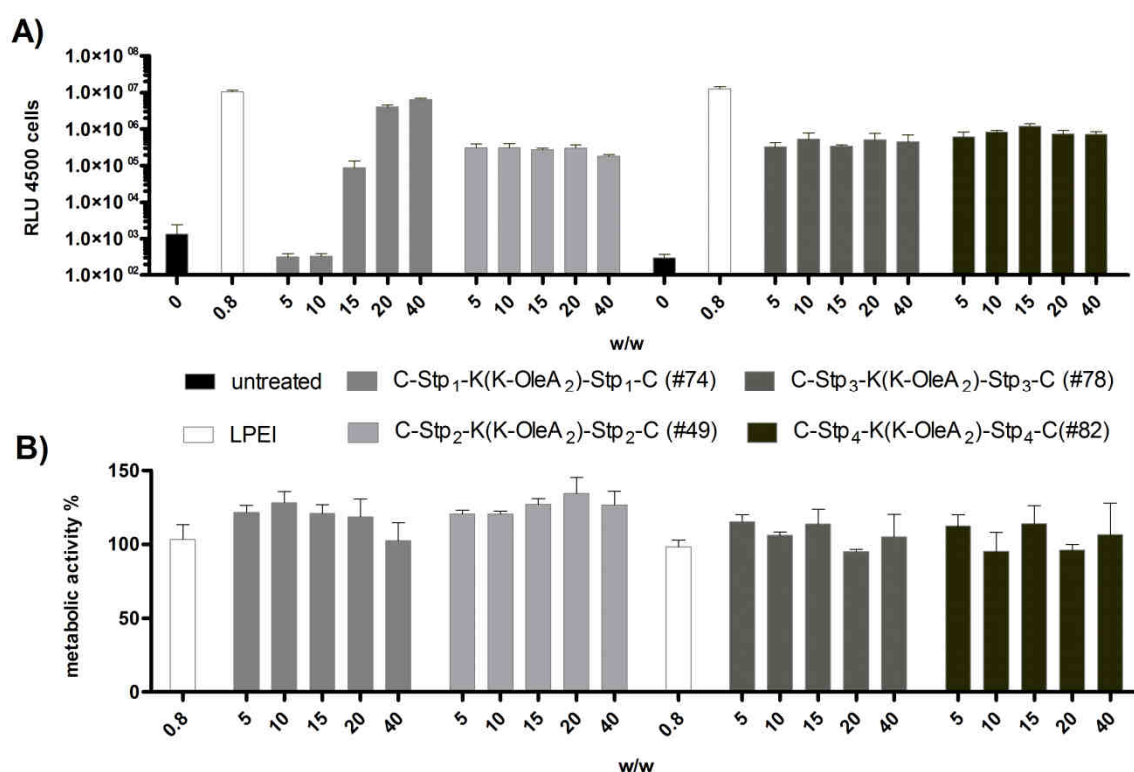


Figure 4.29: Reporter gene expression and metabolic activity of cells 24 h after transfection using t-shape PAAs. Neuro2A cells were transfected using 200 ng pCMVLuc (2 µg/mL DNA) plasmid. Polyplexes were prepared at different w/w ratios and compared to standard LPEI polyplexes. Luciferase reporter gene expression (A) and metabolic activity (MTT Assay, B) are presented as mean value + SD of quintuplicates.

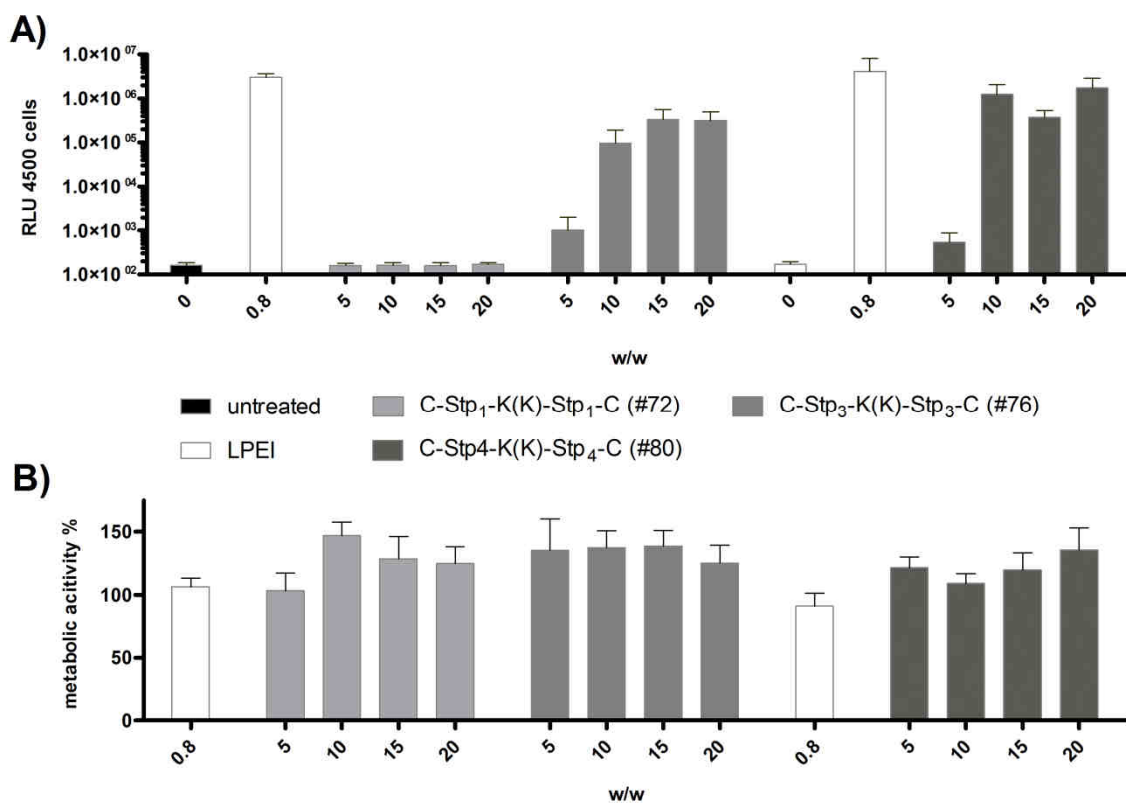


Figure 4.30: Reporter gene expression and metabolic activity of cells 24 h after transfection using non-hydrophobically modified t-shapes. Neuro2A cells were transfected using 200 ng pCMVLuc (2 μ g/mL DNA) plasmid. Polyplexes were prepared at different w/w ratios and compared to standard LPEI polyplexes. Luciferase reporter gene expression (A) and metabolic activity (MTT Assay, B) are presented as mean value + SD of quintuplicates.

#	Sequence	M _w	Prot. Amines	HLR	Charge density [Da/charge]
9	K-Stp ₂ -K-MyrA ₂	1237,8	7	0,340	177
10	K-Stp ₂ -K-OleA ₂	1346,0	7	0,393	192
21	K-Stp ₄ -K-MyrA ₂	1780,5	13	0,236	137
22	K-Stp ₄ -K-OleA ₂	1888,7	13	0,280	145
23	K-Stp ₅ -K	1631,2	18	-	91
45	C-Stp ₃ -C-K-MyrA ₂	1587,3	9	0,265	176
46	C-Stp ₃ -C-K-OleA ₂	1695,4	9	0,312	188
49	C-Stp ₂ -K-(K-OleA ₂)-Stp ₂ -C	2095,0	13	0,252	161
51	C-Stp ₃ -C-K	1166,6	11	-	106
67	C-Stp ₂ -K-MyrA ₂	1212,8	6	0,347	202
68	C-K-Stp ₂ -K-MyrA ₂	1340,9	7	0,314	192
69	C-K-Stp ₂ -K-OleA ₂	1449,1	7	0,365	207
70	C-Stp ₂ -K-OleicA ₂	1320,9	6	0,400	220
72	C-Stp ₁ -K(K)-Stp ₁ -C	1023,4	9	-	114
74	C-Stp ₁ -K(K-OleA ₂)-Stp ₁ -C	1552,3	7	0,341	222
76	C-Stp ₃ -K(K)-Stp ₃ -C	2108,8	19	-	111
78	C-Stp ₃ -K(K-OleA ₂)-Stp ₃ -C	2637,7	17	0,201	155
80	C-Stp ₄ -K(K)-Stp ₄ -C	2653,5	27	-	98
82	C-Stp ₄ -K(K-OleA ₂)-Stp ₄ -C	3182,4	25	0,166	127
Literature examples					
OEI800		800	~ 19		42
LPEI22		22000	~ 500		42
PAMAM G3		6909,0	62		111

Table 4.7: PAA Sequences used in DNA transfections (synthesized by Christina Troiber, master thesis, Wagner lab) in comparison to commonly used transfection reagents.

5 Discussion

5.1 Poly(I:C) Mediated Tumor Killing by LPEI-PEG-EGF Complexation

A virally infected host organism reacts with multiple innate and acquired defense mechanisms to avoid against further virus spread, including humoral and cellular immune responses against proteins and viral particles, and also responses against viral nucleic acid intermediates. A series of toll-like receptors (TLRs) at the cell surface and in endosomal vesicles and also cytosolic factors recognize viral nucleic acids which have different properties as compared to endogenous cellular RNA and DNA. This recognition often triggers inflammatory and interferon responses, shut-down of protein production and suicide of infected cells by apoptosis.

Synthetic viral nucleic acid analogs have been therapeutically applied as immunostimulatory and cytotoxic DNAs and RNAs¹⁷⁵⁻¹⁷⁸. poly(I:C) and analogs thereof^{129,179-181} mimic double-stranded RNA of virus-infected cells which via endosomal toll-like receptor TLR3 and cytosolic helicase mda-5 stimulation activate different pro-apoptotic processes simultaneously. This makes poly(I:C) an interesting tool for cancer treatment because the differently triggered host cell killing mechanisms reduce the probability of developing acquired chemoresistance; they lead to cell death, and the additional expression of anti-proliferative interferons and other cytokines and chemokines inhibits growth of neighbouring cancer cells that have not been “infected” with poly(I:C)¹⁰².

Untargeted poly(I:C) and analogs have already been applied as adjuvants in cancer-directed human immunotherapy studies, with some limited success but by far not all applications¹⁸⁰⁻¹⁸². For example, poly(I:C) stabilized by polylysine and carboxymethylcellulose applied intramuscularly 3 times a week for 4 week as a single agent therapy did not improve progression-free survival of anaplastic glioma patients in a phase II study¹⁸¹. To fully exploit the therapeutic potential of both immune stimulation and tumor cell killing, poly(I:C) has to be delivered intracellularly into endosomes and also the cytosol, in a tumor-targeted fashion. Obviously, delivery presents the major bottleneck. Both liposomal and polymer-based strategies have been developed for poly(I:C). These include MHC antibody-targeted or pH-sensitive liposomes¹⁸³⁻¹⁸⁴, lipoplexes^{129,185}, nontargeted polymer formulations¹⁸⁰ or, as outlined in our previous work, EGF receptor-targeted poly(I:C) polyplexes¹⁰². In the latter paper Shir et al. demonstrated killing of EGFR overexpressing human tumors

including glioblastoma upon local administration. Polyplexes consisted of poly(I:C) complexed with either one or two branched polyethylenimine (brPEI) conjugates comprising recombinant EGF as targeting ligand and PEG as shielding domain^{109,122,186-187}, and synthetic melittin peptide as endosomal release agent. Both targeting and endosomal domain was found to be essential for the observed biological activity¹⁰².

The current work has been based on the task to develop an improved PEI-based carrier for poly(I:C) comprising all the mentioned EGFR targeting, PEG shielding, and endosomal release functions, but providing them within a polymer conjugate of reduced chemical complexity. This was achieved in the following way. At first, the chemically poorly defined brPEI was replaced by the analogous linear 22 kDa polymer LPEI^{122,188} which can be synthesized in GMP compatible form¹²⁵ and has already been tested in human clinical trials for DNA delivery. Due to its higher inherent potency over brPEI^{127,131}, plain LPEI actually mediated *in vitro* cell killing independent of receptor targeting or endosomolytic melittin (**Figure 4.2**). This effect however was accompanied by an unspecific, non-poly(I:C) related cytotoxicity at higher polyplex doses, as demonstrated with poly(I) control polyplexes.

Secondly, LPEI was conjugated with PEG molecules of different molecular weight (2, 5 kDa and 10 kDa). PEGylation strongly reduced the cytotoxicity but also poly(I:C) based cell killing. For 10 kDa PEG and 5 kDa PEG the activity was lost, for 2 kDa PEG only a hint of activity was obtained (**Figure 4.2**). Finally, incorporation of EGF as receptor targeting ligand restored activity for the LPEI-PEG2kDa conjugate but not LPEI-PEG10kDa conjugate (**Figure 4.2**). The LPEI-PEG5kDa mediated moderate activity at a higher dose. Such a “PEG dilemma” (indirect correlation of shielding and efficacy) is consistent with many previous observations by several laboratories^{132,135,189-191} and might be explained by the fact that for endosomal membrane disruption stable PEG-shielding is counter-productive^{55,137,192}. Apparently the window between shielding / targeting specificity and efficient intracellular delivery is narrow.

The newly developed LPEI-PEG2kDa-EGF conjugate exhibits the key features of the old tetraconjugate, namely higher potency on EGFR overexpressing U87MGwtEGFR gliomas as compared to low-expressing U87MG cells (**Figure 4.3**). An approximately 2.5-fold improved therapeutic efficiency was observed *in vitro* in comparison to the old conjugate on U87MGwtEGFR gliomas (**Figure 4.3**). An efficient and specific

poly(I:C) mediated cell killing was also obtained with A431 cells (**Figure 4.5**). These epidermoid carcinoma cells express particularly high levels of EGF receptor. EGFR density is described with 2×10^6 /cell, higher than U87MGwtEGFR (1×10^6 /cell) and much higher than U87MG (1×10^5 /cell)¹⁹³⁻¹⁹⁴. Most encouraging, systemic intravenous administration of poly(I:C) polyplexes were able to strongly retard growth of distant subcutaneous A431 tumors *in vivo*. The treatment was well tolerated by the mice. Once again, the effect was dependent on poly(I:C) as key component of the formulation. Polyplexes made from the novel conjugates showed the best therapeutic effect (**Figure 4.6**).

5.2 Development of a Synthesis Platform for the Production of Defined Polyamidoamines

The development of new strategies for polymer synthesis is a key issue in the field of polymeric delivery. The maturation of the already established systems over the last years resulted in the synthesis of dynamic and increasingly complex systems. But, despite the progress in the development of carrier systems, most of the used polymers continue to be ill-defined due to their synthesis by classical random polymerization methods. Precise incorporation of additional functional domains is not possible, thereby limiting further development of polymeric carriers.

Aim of this study was the development of a solid-phase synthesis platform allowing the synthesis of precise oligoethylenimine-based polymers and integration of the platform into a parallel synthesis setting. In an attempt to use an already published alternating condensation strategy¹⁰⁰ to generate an oligoethylenimine based polyamidoamine library, the corresponding boc-protected oligoethylenimine building blocks were synthesized. But use of these protected oligoethylenimine building blocks together with the published synthesis protocols led to extensive crosslinking of PAA fragments on the resin, severely impeding the use of the synthetic strategy. The alternating condensation strategy is also limited by the need for complex in-reaction monitoring and the extensive MS analysis which has to be performed for every new monomer combination. These findings and concerns regarding limitations of the synthetic versatility of the strategy led us to an adaption of the fmoc/tBu strategy¹⁹⁵⁻¹⁹⁶ for the generation of oligoethylenimine-based libraries.

Use of a polyamino acid for chain elongation circumvents the critical on-resin activation step and through utilization of fmoc-protection for the terminal amine the formation of crosslinking products during the solid-phase synthesis is effectively omitted. 16-Amino-4-oxo-5,8,11,14-tetraazahexadecanoic acid (Stp) was chosen as model building block due to the convenient access to large amounts of the boc-protected precursor and its advantageous properties regarding buffering capabilities and charge density. The synthesized fmoc-Stp(boc₃)-OH building block is fully compatible to standard automated fmoc solid-phase synthesis. The synthesis of pure PAAs and PAA-Peptide chimeras by standard SPS protocols showed acceptable purity of raw product and full compatibility to normal peptide synthesis.

To conclude, a versatile synthetic route for the fast synthesis of defined oligoethylenimine-based PAAs was developed. By using the well established fmoc/tBu SPPS methodology control over every monomer is possible, thereby introducing molecular programmability into the design of delivery vectors. The full compatibility to standard fmoc/tBu peptide synthesis gives access to the vast number of building blocks originally developed for peptide synthesis, allowing introduction of targeting moieties, lytic domains or PEGylation. By combining the synthetic possibilities of the platform with already described dynamic modules the generation of new classes of bio-responsive, dynamic vectors is possible.

5.3 Design and Biophysical Evaluation of a PAA-Library for Nucleic Acid Delivery

Since the formulation of the gene therapy concept in the seventies of the last century¹⁵ the polymeric nucleic acid delivery field matured considerably. But despite the progress in carrier development most of the presently established polymeric carriers are only used in diagnostic settings or for target validation. So far viral vector systems dominate the clinical field of gene therapy⁷¹ but a series of setbacks shed light on inherent safety problems of viral vectors, rendering polymer-based vectors a viable, but until now less efficient alternative. In spite of manifold opportunities for new, effective carrier systems the development of polymeric transfection systems is still characterized by rather low throughput and molecular precision.

The definition of a minimal domain construction set can be achieved by stripping the polymeric delivery system down to its essential parts and using it as template for solid-phase assisted library generation, followed by evaluation in biophysical assays. These domains can subsequently be optimized and used to build new carriers with programmed properties. For a first proof of concept a simple domain model was used to restrict the design space. By limiting the polymer domains to 4 easily controllable structural domains (**Table 4.5**) and incorporation of dynamic stabilization we aimed at a simple, flexible system that allows further optimization of these rather primitive vectors. To construct useful structure-function relationships we defined two key properties (lytic activity, NA binding) as essential biophysical screening parameters for a systematical evaluation of the library.

Poor endosomal escape significantly limits the efficiency of polymeric carriers. Incorporation of either lytic peptides¹⁹⁷ or lipophilic modifications⁴⁰ for increased membrane interactions are often employed to increase the endosomal escape. Initial screens of unmodified PAAs showed that the Stp-backbone has no intrinsic lytic potential and is probably too small for a distinct proton sponge effect. Modification of the Stp backbones with hydrophobic domains resulted in an increased, controllable lytic activity (**Figure 4.18**). In contrast to the only minimal lytic activity of single fatty acid modified PAAs the introduction of a second fatty acid led to a significantly increased lytic activity which can be controlled by type of fatty acid, length of PAA molecule and thiol content. The pH-specificity of the lytic activity can be controlled by careful selection of the hydrophobic modification. The impact of specific lytic activity on the *in vitro* performance of an NA formulation is exemplified in **Figure 4.19** demonstrating that unspecific lytic activity contributes to *in vitro* toxicity.

The second essential property for a nucleic acid delivery system is the ability to bind to the NA payload and to protect it during the transport to the target cell. As the accessible design space of the solid-phase synthesis platform is too big for an exhaustive evaluation we aimed on the fast identification of minimal binding motifs for pDNA and siRNA. The best hits should then serve as lead structures for further delivery system development. As expected, unmodified PAAs ($\text{Stp}_n < 6$) were not able to bind effectively enough to either pDNA or siRNA to prevent migration of NA in a gel-shift assay. To identify a minimal binding motif for hydrophobically modified PAAs a K-Stp₂-K-FA₂ template was systematically acylated with different fatty acids. While introduction of one FA into the template already enabled pDNA binding at high

N/Ps siRNA complexation was not influenced significantly. Use of two FA acids resulted in complete retardation at low N/Ps of siRNA and pDNA if FAs with a chain length > 8 were used. An exemplary comparison of different classes of the polymers in siRNA/DNA delivery (**Figure 4.23**) shows the synergistic effects of the different domains. The most effective polymers are characterized by a hydrophobic domain containing fatty acids with a chain length $> C_8$, at least two Stp units and thiol anchors for stabilization of the resulting polyplexes.

To conclude, parallel synthesis of a modular PAA library followed by biophysical characterization allowed the construction of first PAA SAR models beneficial for the rational development of Stp-based NA delivery vectors. By restricting the library to small polymers with only little variance in their modules it was possible to identify efficient delivery vectors out of the different families. Thus useful domains for further development of programmed polymeric delivery systems could be identified.

5.4 Evaluation of Different Stp-based PAA Families for *in vitro* DNA Delivery

Better defined, modular polymer systems with a diverse and easily accessible design space can open new possibilities for the future development of carrier systems for NA delivery. We used a solid-phase assisted, parallel synthesis approach to generate a small library of defined Stp-Polymers, modified with fatty acids and amino acids. By screening of the library for desirable biophysical characteristics and subsequent *in vitro* evaluation of their DNA delivery capabilities we wanted to demonstrate the potential of modular designed polymers for DNA delivery.

Comparison of four structural different families (cysteine free polymers, chains, i-shapes and t-shapes) regarding DNA binding and transfection efficiency resulted in first SARs for Stp-polymers. **Figures 4.24** and **4.27** show the influence of hydrophobic modifications on the NA binding properties of the PAA systems. Plain Stp-sequences did not condense DNA while polymers containing a dual fatty acid motif (chain length $> C_8$) strongly bound DNA at N/Ps as low as 6. Introduction of two cysteines into linear Stp-sequences for lateral polyplex stabilization via disulfide bridges did not show a comparable impact on NA binding in the gel-shift assay. Even at N/Ps as high as 18, cysteine modified Stp-chains were not able to condense the pDNA completely. Comparison of both stabilization concepts under *in vitro* conditions showed that incorporation of the dual fatty acid motif results in an up to 100-fold

increase of luciferase signal while the cysteine modification results in a 1000-fold increase. The results demonstrate that hydrophobic modification of the polymers using different FAs has a significant impact on NA complexation. Good binding alone, however, does not result in effective transfection. Cysteine containing polymers did not condense DNA as good as the hydrophobically modified polymers, but were able to cause effective pDNA-delivery under *in vitro* conditions.

Combination of hydrophobic and cysteine modification led to the most effective polymer families in terms of binding and *in vitro* performance. Systematic variation of HLR, type of incorporated fatty acid and M_w of the polymers showed that hydrophobic modification is most beneficial for small polymers (**Figure 4.29**) and is the most important contributor to cytotoxicity. While the overall toxicity of the polymers is quite low modification with myristyl residues resulted in significant *in vitro* toxicity, severely limiting the use of this modification in the design of transfection polymers. An increasing number of Stp units in the fatty acid modified polymers leads to no further improvement of transfection efficiency. The transfection efficiency of polymers without fatty acid modification is strongly dependent on the number of Stp-units per molecule. Approximately 6 Stp-units per molecule are required for an activity approaching the LPEI control. Nevertheless, their activity never reaches the level of the best performing i-shapes and t-shapes.

To sum up, we demonstrated that modular design and solid-phase assisted synthesis of Stp-based polymers allows the synthesis of effective delivery systems. We identified two classes of Stp-polymers which were effective in DNA delivery and can serve as template for further development. Due to the variable, modular composition and the already effective delivery, additional domains like targeting ligands or shielding domains can be incorporated for further optimization of the systems.

6 Summary

Polymeric nucleic acid delivery systems have great relevance in the therapeutic delivery of nucleic acids. But despite enormous advances over the last 20 years nucleic acid therapies are far from being a standard option in treatment. One of the biggest obstacles to development of polymeric carriers is the lack of precise design rules and rational design platforms. The almost exclusive use of polydisperse backbones that are modified with additional functional domains, led to increasingly complex, multi-domain polymers requiring complex synthesis routes and characterization efforts.

By the redesign of an efficient, but complex, modular polymeric carrier for the poly(I:C) treatment of glioblastoma we were able to show that decreased complexity can be beneficial in terms of synthesis and efficacy. The new, LPEI-based triconjugate consisting of targeting ligand, PEG-spacer and LPEI-backbone allows the use of GMP grade materials for a more controlled production process amenable to scale-up and shows a significantly improved performance in an *in vivo* setting. Nevertheless, this approach is still biased by the inherent heterogeneity of the used polymeric reactants. This complicates rational conjugate design and exact structure-activity-relationship studies.

As a first step towards the synthesis of programmable polymeric delivery systems, novel polyamino acid building blocks and protocols for the solid-phase synthesis of Stp-polymers were developed. By applying solid-phase synthesis to the production of oligoethylenimine based delivery systems, well defined polymers with programmable properties were synthesized. The solid-phase methodology enables rapid parallel synthesis of PAAs for nucleic acid delivery, allowing library construction for a quick survey of their delivery potential.

The new synthesis platform was used to construct a small library of Stp-based polymers comprising domains with differing properties regarding hydrophobicity, charge density or disulfide formation. The library was restricted to a small M_w range to evaluate the influence of the different domains on core parameters like nucleic acid compaction or lytic activity towards cell membranes. The biophysical screening identified 2 different families (i-shape, t-shape) with interesting properties and siRNA /DNA delivery potential demonstrating the synergistic effect of the different domains

on delivery efficiency. Screening of the library for *in vitro* DNA delivery identified a set of lead structures able to compete with LPEI.

The presented carrier systems are still limited in terms of efficiency and application in therapeutic settings. The polymers developed in this work, however, can be seen as first model systems to increase the knowledge about the rational design of non-viral vectors. The platform itself is a tool allowing the design of cationic polymers with molecular precision. Future development will focus on new building blocks, functional domains and further screening to identify potent sequences. Introduction of other functional domains like targeting ligands, shielding or nuclear localization sequences could allow the design of true PPDS, leading to the elucidation of new delivery bottlenecks and potential therapeutic applications.

7 References

1. Lobban, P.E. and Kaiser, A.D. (1973) Enzymatic end-to end joining of DNA molecules. *J Mol Biol*, **78**, 453-471;
2. Jackson, D.A., Symons, R.H. and Berg, P. (1972) Biochemical method for inserting new genetic information into DNA of Simian Virus 40: circular SV40 DNA molecules containing lambda phage genes and the galactose operon of Escherichia coli. *Proc Natl Acad Sci U S A*, **69**, 2904-2909; Pubmedid:389671
3. Cohen, S.N., Chang, A.C., Boyer, H.W. and Helling, R.B. (1973) Construction of biologically functional bacterial plasmids in vitro. *Proc Natl Acad Sci U S A*, **70**, 3240-3244; Pubmedid:427208
4. Best, C.H. and Scott, D.A. (1923) The preparation of Insuline. *J Biol Chem*, **57**, 709 - 723;
5. Isaacs, A. and Lindenmann, J. (1957) Virus interference. I. The interferon. *Proc R Soc Lond B Biol Sci*, **147**, 258-267;
6. Cohen, S. (1965) The stimulation of epidermal proliferation by a specific protein (EGF). *Dev Biol*, **12**, 394-407;
7. Simonsen, C.C. and McGrogan, M. (1994) The molecular biology of production cell lines. *Biologicals*, **22**, 85-94; doi: S1045-1056(84)71014-1 [pii] 10.1006/biol.1994.1014,
8. Pokala, N. and Handel, T.M. (2001) Review: protein design--where we were, where we are, where we're going. *J Struct Biol*, **134**, 269-281; doi: 10.1006/jsbi.2001.4349, S1047-8477(01)94349-7 [pii],
9. Regan, L. (1991) Protein design. *Curr Opin Biotechnol*, **2**, 544-550;
10. Lipinski, C.A., Lombardo, F., Dominy, B.W. and Feeney, P.J. (2001) Experimental and computational approaches to estimate solubility and permeability in drug discovery and development settings. *Adv Drug Deliv.Rev.*, **46**, 3-26;
11. Bidlingmaier, M. and Strasburger, C.J. (2010) Growth hormone. *Handb Exp Pharmacol*, 187-200; doi: 10.1007/978-3-540-79088-4_8,
12. Merchionne, F. and Dammacco, F. (2009) Biological functions and therapeutic use of erythropoiesis-stimulating agents: perplexities and perspectives. *Br J Haematol*, **146**, 127-141; doi: BJH7702 [pii], 10.1111/j.1365-2141.2009.07702.x
13. Mouser, J.F. and Hyams, J.S. (1999) Infliximab: a novel chimeric monoclonal antibody for the treatment of Crohn's disease. *Clin Ther*, **21**, 932-942; discussion 931; doi: S0149291899800150 [pii],
14. Goldenberg, M.M. (1999) Trastuzumab, a recombinant DNA-derived humanized monoclonal antibody, a novel agent for the treatment of metastatic breast cancer. *Clin Ther*, **21**, 309-318; doi: S0149-2918(00)88288-0 [pii] 10.1016/S0149-2918(00)88288-0,
15. Friedmann, T. and Roblin, R. (1972) Gene therapy for human genetic disease? *Science*, **175**, 949-955;

16. Crooke, S.T. (2008) *Antisense drug technology : principles, strategies, and applications*. 2nd ed. CRC Press, Boca Raton.
17. Edelstein, M.L., Abedi, M.R. and Wixon, J. (2007) Gene therapy clinical trials worldwide to 2007--an update. *J. Gene Med.*, **9**, 833-842;
18. Cavazzana-Calvo, M. and Fischer, A. (2007) Gene therapy for severe combined immunodeficiency: are we there yet? *J Clin. Invest*, **117**, 1456-1465;
19. Salvay, D.M., Zelivyanskaya, M. and Shea, L.D. (2010) Gene delivery by surface immobilization of plasmid to tissue-engineering scaffolds. *Gene Ther*, doi: gt201079 [pii], 10.1038/gt.2010.79,
20. Chiarella, P., Fazio, V.M. and Signori, E. (2010) Application of Electroporation in DNA Vaccination Protocols. *Curr Gene Ther*, doi: ABS-36a [pii],
21. Sawicki, J.A., Anderson, D.G. and Langer, R. (2008) Nanoparticle delivery of suicide DNA for epithelial ovarian cancer therapy. *Adv Exp Med Biol*, **622**, 209-219; doi: 10.1007/978-0-387-68969-2_17,
22. Watson, J.D. and Crick, F.H. (1953) Molecular structure of nucleic acids; a structure for deoxyribose nucleic acid. *Nature*, **171**, 737-738;
23. Check, E. (2002) A tragic setback. *Nature*, **420**, 116-118;
24. Loke, S.L., Stein, C.A., Zhang, X.H., Mori, K., Nakanishi, M., Subasinghe, C., Cohen, J.S. and Neckers, L.M. (1989) Characterization of oligonucleotide transport into living cells. *Proc Natl Acad Sci U S A*, **86**, 3474-3478; Pubmedid:287160
25. Edwards, M.S., Kasper, D.L., Jennings, H.J., Baker, C.J. and Nicholson, W. (1982) Capsular sialic acid prevents activation of the alternative complement pathway by type III, group B streptococci 175. *J Immunol*, **128**, 1278-1283;
26. Dheur, S., Dias, N., van Aerschot, A., Herdewijn, P., Bettinger, T., Remy, J.S., Helene, C. and Saison-Behmoaras, E.T. (1999) Polyethylenimine but not cationic lipid improves antisense activity of 3'-capped phosphodiester oligonucleotides. *Antisense Nucleic Acid Drug Dev*, **9**, 515-525;
27. Crooke, S.T. (2000) Progress in antisense technology: the end of the beginning. *Methods Enzymol*, **313**, 3-45;
28. Agrawal, S. and Kandimalla, E.R. (2000) Antisense therapeutics: is it as simple as complementary base recognition? *Mol Med Today*, **6**, 72-81; doi: S135743109901638X [pii],
29. Fire, A., Xu, S., Montgomery, M.K., Kostas, S.A., Driver, S.E. and Mello, C.C. (1998) Potent and specific genetic interference by double-stranded RNA in *Caenorhabditis elegans*. *Nature*, **391**, 806-811;
30. Caplen, N.J., Fleenor, J., Fire, A. and Morgan, R.A. (2000) dsRNA-mediated gene silencing in cultured *Drosophila* cells: a tissue culture model for the analysis of RNA interference. *Gene*, **252**, 95-105; doi: S0378-1119(00)00224-9 [pii],
31. Elbashir, S.M., Harborth, J., Lendeckel, W., Yalcin, A., Weber, K. and Tuschl, T. (2001) Duplexes of 21-nucleotide RNAs mediate RNA interference in cultured mammalian cells. *Nature*, **411**, 494-498;

32. Tuschl, T. (2001) RNA interference and small interfering RNAs. *Chembiochem.*, **2**, 239-245;
33. Meister, G., Landthaler, M., Patkaniowska, A., Dorsett, Y., Teng, G. and Tuschl, T. (2004) Human Argonaute2 mediates RNA cleavage targeted by miRNAs and siRNAs. *Mol Cell*, **15**, 185-197; doi: 10.1016/j.molcel.2004.07.007, S1097276504004150 [pii],
34. Song, J.J., Smith, S.K., Hannon, G.J. and Joshua-Tor, L. (2004) Crystal structure of Argonaute and its implications for RISC slicer activity. *Science*, **305**, 1434-1437; doi: 10.1126/science.1102514, 1102514 [pii],
35. Ivanova, G.D., Arzumanov, A., Abes, R., Yin, H., Wood, M.J., Lebleu, B. and Gait, M.J. (2008) Improved cell-penetrating peptide-PNA conjugates for splicing redirection in HeLa cells and exon skipping in mdx mouse muscle. *Nucleic Acids Res*, **36**, 6418-6428; doi: gkn671 [pii] 10.1093/nar/gkn671, Pubmedid:2582604
36. Stenvang, J. and Kauppinen, S. (2008) MicroRNAs as targets for antisense-based therapeutics. *Expert Opin Biol Ther*, **8**, 59-81; doi: 10.1517/14712598.8.1.59,
37. Houk, B.E., Hochhaus, G. and Hughes, J.A. (1999) Kinetic modeling of plasmid DNA degradation in rat plasma. *AAPS.PharmSci.*, **1**, E9;
38. Fahrmeir, J., Gunther, M., Tietze, N., Wagner, E. and Ogris, M. (2007) Electrophoretic purification of tumor-targeted polyethylenimine-based polyplexes reduces toxic side effects in vivo. *J.Control Release*, **122**, 236-245;
39. Tseng, W.C. and Jong, C.M. (2003) Improved stability of polycationic vector by dextran-grafted branched polyethylenimine. *Biomacromolecules.*, **4**, 1277-1284;
40. Zintchenko, A., Philipp, A., Dehshahri, A. and Wagner, E. (2008) Simple Modifications of Branched PEI Lead to Highly Efficient siRNA Carriers with Low Toxicity. *Bioconjug Chem*, **19**, 1448-1455;
41. Thomas, M. and Klibanov, A.M. (2002) Enhancing polyethylenimine's delivery of plasmid DNA into mammalian cells 1. *Proc.Natl.Acad.Sci.U.S.A*, **99**, 14640-14645;
42. Dubruel, P., Dekie, L., Christiaens, B., Vanloo, B., Rosseneu, M., Van De, K.J., Mannisto, M., Urtti, A. and Schacht, E. (2003) Poly-l-glutamic acid derivatives as multifunctional vectors for gene delivery. Part B. Biological evaluation. *Biomacromolecules.*, **4**, 1177-1183;
43. Abuchowski, A., McCoy, J.R., Palczuk, N.C., van Es, T. and Davis, F.F. (1977) Effect of covalent attachment of polyethylene glycol on immunogenicity and circulating life of bovine liver catalase. *J.Biol Chem*, **252**, 3582-3586;
44. Ogris, M., Brunner, S., Schuller, S., Kircheis, R. and Wagner, E. (1999) PEGylated DNA/transferrin-PEI complexes: reduced interaction with blood components, extended circulation in blood and potential for systemic gene delivery. *Gene Ther*, **6**, 595-605;
45. Merkel, O.M., Librizzi, D., Pfestroff, A., Schurrat, T., Buyens, K., Sanders, N.N., De Smedt, S.C., Behe, M. and Kissel, T. (2009) Stability of siRNA

- polyplexes from poly(ethylenimine) and poly(ethylenimine)-g-poly(ethylene glycol) under in vivo conditions: effects on pharmacokinetics and biodistribution measured by Fluorescence Fluctuation Spectroscopy and Single Photon Emission Computed Tomography (SPECT) imaging. *J Control Release*, **138**, 148-159; doi: S0168-3659(09)00305-8 [pii] 10.1016/j.jconrel.2009.05.016,
46. Burke, R.S. and Pun, S.H. (2008) Extracellular Barriers to in Vivo PEI and PEGylated PEI Polyplex-Mediated Gene Delivery to the Liver. *Bioconjug Chem*, **19**, 693-704;
 47. DeRouchey, J., Schmidt, C., Walker, G.F., Koch, C., Plank, C., Wagner, E. and Radler, J.O. (2008) Monomolecular assembly of siRNA and poly(ethylene glycol)-peptide copolymers. *Biomacromolecules.*, **9**, 724-732;
 48. Dhaliwal, A., Maldonado, M., Han, Z. and Segura, T. (2010) Differential uptake of DNA-poly(ethylenimine) polyplexes in cells cultured on collagen and fibronectin surfaces. *Acta Biomater*, doi: S1742-7061(10)00173-X [pii] 10.1016/j.actbio.2010.03.038,
 49. Maeda, H. (2001) The enhanced permeability and retention (EPR) effect in tumor vasculature: the key role of tumor-selective macromolecular drug targeting. *Adv Enzyme Regul*, **41**, 189-207;
 50. Wu, G.Y. and Wu, C.H. (1987) Receptor-mediated in vitro gene transformation by a soluble DNA carrier system. *J Biol Chem*, **262**, 4429-4432;
 51. Kircheis, R., Blessing, T., Brunner, S., Wightman, L. and Wagner, E. (2001) Tumor targeting with surface-shielded ligand-polycation DNA complexes. *J Control Release*, **72**, 165-170;
 52. Guo, W. and Lee, R.J. (1999) Receptor-Targeted Gene Delivery Via Folate-Conjugated Polyethylenimine. *AAPS Pharmsci*, **1**, Article 19;
 53. Li, Z., Zhao, R., Wu, X., Sun, Y., Yao, M., Li, J., Xu, Y. and Gu, J. (2005) Identification and characterization of a novel peptide ligand of epidermal growth factor receptor for targeted delivery of therapeutics. *Faseb J*, **19**, 1978-1985;
 54. Xia, H., Anderson, B., Mao, Q. and Davidson, B.L. (2000) Recombinant human adenovirus: targeting to the human transferrin receptor improves gene transfer to brain microcapillary endothelium. *J Virol*, **74**, 11359-11366; Pubmedid:113241
 55. Knorr, V., Allmendinger, L., Walker, G.F., Paintner, F.F. and Wagner, E. (2007) An acetal-based PEGylation reagent for pH-sensitive shielding of DNA polyplexes. *Bioconjug Chem*, **18**, 1218-1225;
 56. Behr, J.P. (1997) The proton sponge: A trick to enter cells the viruses did not exploit. *Chimia*, **51**, 34-36;
 57. Xu, Y. and Szoka, F.C., Jr. (1996) Mechanism of DNA release from cationic liposome/DNA complexes used in cell transfection. *Biochemistry*, **35**, 5616-5623;
 58. Meyer, M., Zintchenko, A., Ogris, M. and Wagner, E. (2007) A dimethylmaleic acid-melittin-polylysine conjugate with reduced toxicity, pH-triggered

- endosomolytic activity and enhanced gene transfer potential. *J. Gene Med.*, **9**, 797-805;
59. Subbarao, N.K., Parente, R.A., Szoka, F.C., Jr., Nadasdi, L. and Pongracz, K. (1987) pH-dependent bilayer destabilization by an amphipathic peptide. *Biochemistry*, **26**, 2964-2972;
60. Nigg, E.A. (1997) Nucleocytoplasmic transport: signals, mechanisms and regulation. *Nature*, **386**, 779-787; doi: 10.1038/386779a0,
61. Subramanian, A., Ranganathan, P. and Diamond, S.L. (1999) Nuclear targeting peptide scaffolds for lipofection of nondividing mammalian cells 920. *Nat. Biotechnol.*, **17**, 873-877;
62. Zanta, M.A., Belguise, V.P. and Behr, J.P. (1999) Gene delivery: A single nuclear localization signal peptide is sufficient to carry DNA to the cell nucleus. *Proc. Natl. Acad. Sci. U.S.A*, **96**, 91-96;
63. Hagstrom, J.E., Hegge, J., Zhang, G., Noble, M., Budker, V., Lewis, D.L., Herweijer, H. and Wolff, J.A. (2004) A facile nonviral method for delivering genes and siRNAs to skeletal muscle of mammalian limbs. *Mol. Ther.*, **10**, 386-398;
64. Sebestyen, M.G., Budker, V.G., Budker, T., Subbotin, V.M., Zhang, G., Monahan, S.D., Lewis, D.L., Wong, S.C., Hagstrom, J.E. and Wolff, J.A. (2006) Mechanism of plasmid delivery by hydrodynamic tail vein injection. I. Hepatocyte uptake of various molecules. *J. Gene Med.*, **8**, 852-873;
65. Suda, T., Suda, K. and Liu, D. (2008) Computer-assisted hydrodynamic gene delivery. *Mol Ther*, **16**, 1098-1104;
66. Lampugnani, M.G. and Dejana, E. (1997) Interendothelial junctions: structure, signalling and functional roles. *Curr. Opin. Cell Biol*, **9**, 674-682;
67. Wolff, J.A., Malone, R.W., Williams, P., Chong, W., Acsadi, G., Jani, A. and Felgner, P.L. (1990) Direct gene transfer into mouse muscle in vivo 726. *Science*, **247**, 1465-1468;
68. Shi, F., Rakhmievich, A.L., Heise, C.P., Oshikawa, K., Sondel, P.M., Yang, N.S. and Mahvi, D.M. (2002) Intratumoral injection of interleukin-12 plasmid DNA, either naked or in complex with cationic lipid, results in similar tumor regression in a murine model. *Mol Cancer Ther*, **1**, 949-957;
69. Takei, Y., Nemoto, T., Mu, P., Fujishima, T., Ishimoto, T., Hayakawa, Y., Yuzawa, Y., Matsuo, S., Muramatsu, T. and Kadomatsu, K. (2008) In vivo silencing of a molecular target by short interfering RNA electroporation: tumor vascularization correlates to delivery efficiency. *Mol Cancer Ther*, **7**, 211-221;
70. Liu, F., Song, Y. and Liu, D. (1999) Hydrodynamics-based transfection in animals by systemic administration of plasmid DNA. *Gene Ther.*, **6**, 1258-1266;
71. <http://www.wiley.co.uk/genetherapy/clinical/>.
72. Rogers, S., Lowenthal, A., Terheggen, H.G. and Columbo, J.P. (1973) Induction of arginase activity with the Shope papilloma virus in tissue culture cells from an argininemic patient. *J Exp Med*, **137**, 1091-1096; Pubmedid:2139227

73. Rosenberg, S.A., Aebersold, P., Cornetta, K., Kasid, A., Morgan, R.A., Moen, R., Karson, E.M., Lotze, M.T., Yang, J.C. and Topalian, S.L. (1990) Gene transfer into humans--immunotherapy of patients with advanced melanoma, using tumor-infiltrating lymphocytes modified by retroviral gene transduction. *N.Engl.J Med.*, **323**, 570-578;
74. Bouard, D., Alazard-Dany, D. and Cosset, F.L. (2009) Viral vectors: from virology to transgene expression. *Br J Pharmacol*, **157**, 153-165; doi: bjp2008349 [pii]
10.1038/bjp.2008.349, Pubmedid:2629647
75. Meyer, M., Dohmen, C., Philipp, A., Kiener, D., Maiwald, G., Scheu, C., Ogris, M. and Wagner, E. (2009) Synthesis and Biological Evaluation of a Bioresponsive and Endosomolytic siRNA-Polymer Conjugate. *Mol Pharm*, **6**, 752-762; doi: 10.1021/mp9000124,
76. Rozema, D.B., Lewis, D.L., Wakefield, D.H., Wong, S.C., Klein, J.J., Roesch, P.L., Bertin, S.L., Reppen, T.W., Chu, Q., Blokhin, A.V. *et al.* (2007) Dynamic PolyConjugates for targeted in vivo delivery of siRNA to hepatocytes. *Proc.Natl.Acad.Sci U.S.A*, **104**, 12982-12987;
77. Felgner, P.L., Gadek, T.R., Holm, M., Roman, R., Chan, H.W., Wenz, M., Northrop, J.P., Ringold, G.M. and Danielsen, M. (1987) Lipofection: A highly efficient, lipid mediated DNA-transfection procedure. *Proc Natl Acad Sci U S A*, **84**, 7413-7417;
78. Hafez, I.M., Maurer, N. and Cullis, P.R. (2001) On the mechanism whereby cationic lipids promote intracellular delivery of polynucleic acids. *Gene Ther*, **8**, 1188-1196;
79. Wattiaux, R., Jadot, M., Warnier-Pirotte, M.T. and Wattiaux-De Coninck, S. (1997) Cationic lipids destabilize lysosomal membrane in vitro 2. *FEBS Lett.*, **417**, 199-202; doi,
80. Lungwitz, U., Breunig, M., Blunk, T. and Gopferich, A. (2005) Polyethylenimine-based non-viral gene delivery systems. *Eur.J.Pharm.Biopharm.*, **60**, 247-266; doi,
81. Hong, S., Leroueil, P.R., Janus, E.K., Peters, J.L., Kober, M.M., Islam, M.T., Orr, B.G., Baker, J.R., Jr. and Banaszak Holl, M.M. (2006) Interaction of polycationic polymers with supported lipid bilayers and cells: nanoscale hole formation and enhanced membrane permeability. *Bioconjug Chem*, **17**, 728-734; doi,
82. Breunig, M., Lungwitz, U., Liebl, R. and Goepferich, A. (2007) Breaking up the correlation between efficacy and toxicity for nonviral gene delivery. *Proc.Natl.Acad.Sci U.S.A*, **104**, 14454-14459; doi,
83. Moghimi, S.M., Symonds, P., Murray, J.C., Hunter, A.C., Debska, G. and Szweczyk, A. (2005) A two-stage poly(ethylenimine)-mediated cytotoxicity: implications for gene transfer/therapy. *Mol Ther*, **11**, 990-995; doi,
84. Chollet, P., Favrot, M.C., Hurbin, A. and Coll, J.L. (2002) Side-effects of a systemic injection of linear polyethylenimine-DNA complexes. *J Gene Med.*, **4**, 84-91; doi,

85. Plank, C., Mechtler, K., Szoka, F.C., Jr. and Wagner, E. (1996) Activation of the complement system by synthetic DNA complexes: a potential barrier for intravenous gene delivery. *Hum. Gene Ther*, **7**, 1437-1446; doi,
86. Gosselin, M.A., Guo, W. and Lee, R.J. (2001) Efficient gene transfer using reversibly cross-linked low molecular weight polyethylenimine. *Bioconjug Chem*, **12**, 989-994; doi,
87. Kloeckner, J., Wagner, E. and Ogris, M. (2006) Degradable gene carriers based on oligomerized polyamines. *Eur. J. Pharm. Sci.*, **29**, 414-425; doi,
88. Philipp, A., Meyer, M. and Wagner, E. (2008) Extracellular targeting of synthetic therapeutic nucleic Acid formulations. *Curr Gene Ther*, **8**, 324-334; doi,
89. Wang, X.L., Jensen, R. and Lu, Z.R. (2007) A novel environment-sensitive biodegradable polydisulfide with protonatable pendants for nucleic acid delivery. *J. Control Release*, **120**, 250-258; doi,
90. Anderson, D.G., Lynn, D.M. and Langer, R. (2003) Semi-Automated Synthesis and Screening of a Large Library of Degradable Cationic Polymers for Gene Delivery. *Angew. Chem. Int. Ed Engl.*, **42**, 3153-3158; doi,
91. Green, J.J., Langer, R. and Anderson, D.G. (2008) A Combinatorial Polymer Library Approach Yields Insight into Nonviral Gene Delivery. *Acc. Chem Res*, **41**, 749-759; doi,
92. Thomas, M., Lu, J.J., Zhang, C., Chen, J. and Klibanov, A.M. (2007) Identification of novel superior polycationic vectors for gene delivery by high-throughput synthesis and screening of a combinatorial library. *Pharm. Res.*, **24**, 1564-1571; doi,
93. Russ, V., Elfberg, H., Thoma, C., Kloeckner, J., Ogris, M. and Wagner, E. (2008) Novel degradable oligoethylenimine acrylate ester-based pseudodendrimers for in vitro and in vivo gene transfer. *Gene Ther*, **15**, 18-29; doi,
94. Lee, Y., Mo, H., Koo, H., Park, J.Y., Cho, M.Y., Jin, G.W. and Park, J.S. (2007) Visualization of the degradation of a disulfide polymer, linear poly(ethylenimine sulfide), for gene delivery. *Bioconjug Chem*, **18**, 13-18; doi,
95. Lee, C.C., Liu, Y. and Reineke, T.M. (2008) General Structure-Activity Relationship for Poly(glycoamidoamine)s: The Effect of Amine Density on Cytotoxicity and DNA Delivery Efficiency. *Bioconjug Chem*, **19**, 428-440; doi,
96. Buhleier, E., Wehner, W. and VÖGtle, F. (1978) "Cascade"- and "Nonskid-Chain-like" Syntheses of Molecular Cavity Topologies. *Synthesis*, **1978**, 155-158; doi,
97. Tomalia, D.A., Baker, H., Dewald, J., Hall, M., Kallos, G., Martin, S., Roeck, J., Ryder, J. and Smith, P. (1985) A New Class of Polymers: Starburst-Dendritic Macromolecules. *Polymer Journal*, **17**, 117-132; doi,
98. Merrifield, R.B. (1963) Solid phase peptide synthesis I. The synthesis of a tetrapeptide. *Journal of the American Chemical Society*, **85**, 5; doi,

99. Hartmann, L., Krause, E., Antonietti, M. and Borner, H.G. (2006) Solid-phase supported polymer synthesis of sequence-defined, multifunctional poly(amidoamines). *Biomacromolecules.*, **7**, 1239-1244; doi,
100. Hartmann, L., Hafele, S., Peschka-Suss, R., Antonietti, M. and Borner, H.G. (2008) Tailor-Made Poly(amidoamine)s for Controlled Complexation and Condensation of DNA. *Chemistry.*, **14**, 2025-2033; doi,
101. Mintzer, M.A. and Simanek, E.E. (2009) Nonviral vectors for gene delivery. *Chem Rev*, **109**, 259-302; doi: 10.1021/cr800409e
10.1021/cr800409e [pii],
102. Shir, A., Ogris, M., Wagner, E. and Levitzki, A. (2006) EGF receptor-targeted synthetic double-stranded RNA eliminates glioblastoma, breast cancer, and adenocarcinoma tumors in mice. *PLoS Med*, **3**, e6; doi,
103. Ellman, G.L. (1959) Tissue sulfhydryl groups. *Archives of Biochemistry and Biophysics*, **82**, 70-77; doi,
104. Habeeb, A.F.S.A. (1966) Determination of free amino groups in proteins by trinitrobenzenesulfonic acid. *Analytical Biochemistry*, **14**, 328-336; doi,
105. Ungaro, F., De Rosa, G., Miro, A. and Quaglia, F. (2003) Spectrophotometric determination of polyethylenimine in the presence of an oligonucleotide for the characterization of controlled release formulations. *J.Pharm.Biomed.Anal.*, **31**, 143-149; doi,
106. Still, W.C., Kahn, M. and Mitra, A. (1978) Rapid chromatographic technique for preparative separations with moderate resolution. *The Journal of Organic Chemistry*, **43**, 2923-2925; doi: 10.1021/jo00408a041,
107. Pedersen, D.S. and Rosenbohm, C. (2001) Dry Column Vacuum Chromatography. *Synthesis*, **2001**, 2431-2434; doi,
108. Jeong, J.H., Song, S.H., Lim, D.W., Lee, H. and Park, T.G. (2001) DNA transfection using linear poly(ethylenimine) prepared by controlled acid hydrolysis of poly(2-ethyl-2-oxazoline) 1. *J Control Release*, **73**, 391-399; doi,
109. Blessing, T., Kurs, M., Holzhauser, R., Kircheis, R. and Wagner, E. (2001) Different strategies for formation of pegylated EGF-conjugated PEI/DNA complexes for targeted gene delivery. *Bioconjug Chem*, **12**, 529-537; doi,
110. Kaiser, E., Colescott, R.L., Bossinger, C.D. and Cook, P.I. (1970) Color test for detection of free terminal amino groups in the solid-phase synthesis of peptides. *Analytical Biochemistry*, **34**, 595-598; doi,
111. Attardi, M.E., Porcu, G. and Taddei, M. (2000) Malachite green, a valuable reagent to monitor the presence of free COOH on the solid-phase. *Tetrahedron Letters*, **41**, 7391-7394; doi,
112. Hancock, W.S. and Battersby, J.E. (1976) A new micro-test for the detection of incomplete coupling reactions in solid-phase peptide synthesis using 2,4,6-trinitrobenzene-sulphonic acid. *Analytical Biochemistry*, **71**, 260-264; doi,
113. Mosmann, T. (1983) Rapid colorimetric assay for cellular growth and survival: Application to proliferation and cytotoxicity assays. *Journal of Immunological Methods*, **65**, 55-63; doi,

114. Felgner, P.L., Barenholz, Y., Behr, J.P., Cheng, S.H., Cullis, P., Huang, L., Jessee, J.A., Seymour, L., Szoka, F., Thierry, A.R. *et al.* (1997) Nomenclature for synthetic gene delivery systems. *Hum Gene Ther*, **8**, 511-512; doi: 10.1089/hum.1997.8.5-511,
115. Duncan, R. (2003) The dawning era of polymer therapeutics. *Nat.Rev.Drug Discov.*, **2**, 347-360; doi,
116. Li, S.D. and Huang, L. (2006) Gene therapy progress and prospects: non-viral gene therapy by systemic delivery. *Gene Ther*, **13**, 1313-1319; doi,
117. Meyer, M. and Wagner, E. (2006) Recent developments in the application of plasmid DNA-based vectors and small interfering RNA therapeutics for cancer. *Hum.Gene Ther*, **17**, 1062-1076; doi,
118. Pack, D.W., Hoffman, A.S., Pun, S. and Stayton, P.S. (2005) Design and development of polymers for gene delivery. *Nat.Rev.Drug Discov.*, **4**, 581-593; doi,
119. Schaffert, D. and Wagner, E. (2008) Gene therapy progress and prospects: synthetic polymer-based systems. *Gene Ther*, **15**, 1131-1138; doi,
120. Wagner, E. (2008) The Silent (R)evolution of Polymeric Nucleic Acid Therapeutics. *Pharm.Res*, **25**, 2920-2923; doi,
121. Love, K.T., Mahon, K.P., Levins, C.G., Whitehead, K.A., Querbes, W., Dorkin, J.R., Qin, J., Cantley, W., Qin, L.L., Racie, T. *et al.* (2010) Lipid-like materials for low-dose, in vivo gene silencing. *Proc Natl Acad Sci U S A*, **107**, 1864-1869; doi: 0910603106 [pii] 10.1073/pnas.0910603106, Pubmedid:2804742
122. Wolschek, M.F., Thallinger, C., Kursa, M., Rossler, V., Allen, M., Lichtenberger, C., Kircheis, R., Lucas, T., Willheim, M., Reinisch, W. *et al.* (2002) Specific systemic nonviral gene delivery to human hepatocellular carcinoma xenografts in SCID mice. *Hepatology*, **36**, 1106-1114; doi,
123. Boeckle, S., Fahrmeir, J., Roedl, W., Ogris, M. and Wagner, E. (2006) Melittin analogs with high lytic activity at endosomal pH enhance transfection with purified targeted PEI polyplexes. *J.Control Release*, **112**, 240-248; doi,
124. Meyer, M., Philipp, A., Oskuee, R., Schmidt, C. and Wagner, E. (2008) Breathing life into polycations: functionalization with pH-responsive endosomolytic peptides and polyethylene glycol enables siRNA delivery. *J Am Chem Soc*, **130**, 3272-3273; doi,
125. Bonnet, M.E., Erbacher, P. and Bolcato-Bellemin, A.L. (2008) Systemic delivery of DNA or siRNA mediated by linear polyethylenimine (L-PEI) does not induce an inflammatory response. *Pharm Res*, **25**, 2972-2982; doi: 10.1007/s11095-008-9693-1,
126. Ferrari, S., Moro, E., Pettenazzo, A., Behr, J.P., Zacchello, F. and Scarpa, M. (1997) ExGen 500 is an efficient vector for gene delivery to lung epithelial cells in vitro and in vivo. *Gene Ther*, **4**, 1100-1106; doi,
127. Wightman, L., Kircheis, R., Rossler, V., Carotta, S., Ruzicka, R., Kursa, M. and Wagner, E. (2001) Different behavior of branched and linear polyethylenimine for gene delivery in vitro and in vivo. *J.Gene Med.*, **3**, 362-372; doi,

128. Thomas, M., Lu, J.J., Ge, Q., Zhang, C., Chen, J. and Klibanov, A.M. (2005) Full deacylation of polyethylenimine dramatically boosts its gene delivery efficiency and specificity to mouse lung. *Proc.Natl.Acad.Sci.U.S.A*, **102**, 5679-5684; doi,
129. Hirabayashi, K., Yano, J., Inoue, T., Yamaguchi, T., Tanigawara, K., Smyth, G.E., Ishiyama, K., Ohgi, T., Kimura, K. and Irimura, T. (1999) Inhibition of cancer cell growth by polyinosinic-polycytidylic acid/cationic liposome complex: a new biological activity. *Cancer Res*, **59**, 4325-4333; doi,
130. Field, A.K., Tytell, A.A., Lampson, G.P. and Hilleman, M.R. (1967) Inducers of interferon and host resistance. II. Multistranded synthetic polynucleotide complexes. *Proc Natl Acad Sci U S A*, **58**, 1004-1010; doi, Pubmedid:335739
131. Itaka, K., Harada, A., Yamasaki, Y., Nakamura, K., Kawaguchi, H. and Kataoka, K. (2004) In situ single cell observation by fluorescence resonance energy transfer reveals fast intra-cytoplasmic delivery and easy release of plasmid DNA complexed with linear polyethylenimine. *J Gene Med*, **6**, 76-84; doi,
132. Erbacher, P., Bettinger, T., Belguise-Valladier, P., Zou, S., Coll, J.L., Behr, J.P. and Remy, J.S. (1999) Transfection and physical properties of various saccharide, poly(ethylene glycol), and antibody-derivatized polyethylenimines (PEI). *J Gene Med*, **1**, 210-222; doi,
133. Kircheis, R. and aso. (2001) TNF alpha. doi,
134. Kircheis, R., Schuller, S., Brunner, S., Ogris, M., Heider, K.H., Zauner, W. and Wagner, E. (1999) Polycation-based DNA complexes for tumor-targeted gene delivery in vivo. *J Gene Med*, **1**, 111-120; doi,
135. Kursa, M., Walker, G.F., Roessler, V., Ogris, M., Roedl, W., Kircheis, R. and Wagner, E. (2003) Novel Shielded Transferrin-Polyethylene Glycol-Polyethylenimine/DNA Complexes for Systemic Tumor-Targeted Gene Transfer. *Bioconjug.Chem.*, **14**, 222-231; doi,
136. Merdan, T., Kunath, K., Petersen, H., Bakowsky, U., Voigt, K.H., Kopecek, J. and Kissel, T. (2005) PEGylation of poly(ethylene imine) affects stability of complexes with plasmid DNA under in vivo conditions in a dose-dependent manner after intravenous injection into mice. *Bioconjug.Chem.*, **16**, 785-792; doi,
137. Walker, G.F., Fella, C., Pelisek, J., Fahrmeir, J., Boeckle, S., Ogris, M. and Wagner, E. (2005) Toward synthetic viruses: endosomal pH-triggered deshielding of targeted polyplexes greatly enhances gene transfer in vitro and in vivo. *Mol Ther*, **11**, 418-425; doi,
138. Malek, A., Czubayko, F. and Aigner, A. (2008) PEG grafting of polyethylenimine (PEI) exerts different effects on DNA transfection and siRNA-induced gene targeting efficacy. *J Drug Target*, **16**, 124-139; doi,
139. Bodanszky, M. (1984) *Principles of peptide synthesis*. Springer-Verlag, Berlin ; New York.

140. Lebl, M. (1998) Parallel Personal Comments on "Classical" Papers in Combinatorial Chemistry. *Journal of Combinatorial Chemistry*, **1**, 3-24; doi: 10.1021/cc9800327,
141. Yingyongnarongkul, B.-e., Howarth, M., Elliott, T. and Bradley, M. (2004) Solid-Phase Synthesis of 89 Polyamine-Based Cationic Lipids for DNA Delivery to Mammalian Cells. *Chemistry - A European Journal*, **10**, 463-473; doi,
142. Wyman, T.B., Nicol, F., Zelphati, O., Scaria, P.V., Plank, C. and Szoka, F.C., Jr. (1997) Design, synthesis, and characterization of a cationic peptide that binds to nucleic acids and permeabilizes bilayers. *Biochemistry*, **36**, 3008-3017; doi,
143. Plank, C., Tang, M.X., Wolfe, A.R. and Szoka, F.C., Jr. (1999) Branched cationic peptides for gene delivery: role of type and number of cationic residues in formation and in vitro activity of DNA polyplexes. *Hum.Gene Ther.*, **10**, 319-332; doi,
144. Chen, Q.R., Zhang, L., Luther, P.W. and Mixson, A.J. (2002) Optimal transfection with the HK polymer depends on its degree of branching and the pH of endocytic vesicles. *Nucleic Acids Res.*, **30**, 1338-1345; doi,
145. Chen, Q.R., Zhang, L., Stass, S.A. and Mixson, A.J. (2001) Branched co-polymers of histidine and lysine are efficient carriers of plasmids. *Nucleic Acids Res.*, **29**, 1334-1340; doi,
146. Kukowska-Latallo, J.F., Bielinska, A.U., Johnson, J., Spindler, R., Tomalia, D.A. and Baker, J.R., Jr. (1996) Efficient transfer of genetic material into mammalian cells using Starburst polyamidoamine dendrimers. *Proc.Natl.Acad.Sci.U.S.A*, **93**, 4897-4902; doi,
147. Nash, I.A., Bycroft, B.W. and Chan, W.C. (1996) Dde -- A selective primary amine protecting group: A facile solid phase synthetic approach to polyamine conjugates. *Tetrahedron Letters*, **37**, 2625-2628; doi,
148. Byk, G., Frederic, M. and Scherman, D. (1997) One pot synthesis of unsymmetrically functionalized polyamines by a solid phase strategy starting from their symmetrical polyamine-counterparts. *Tetrahedron Letters*, **38**, 3219-3222; doi,
149. Russ, V., Gunther, M., Halama, A., Ogris, M. and Wagner, E. (2008) Oligoethylenimine-grafted polypropylenimine dendrimers as degradable and biocompatible synthetic vectors for gene delivery. *J Control Release*, **132**, 131-140; doi,
150. Han, M., Bae, Y., Nishiyama, N., Miyata, K., Oba, M. and Kataoka, K. (2007) Transfection study using multicellular tumor spheroids for screening non-viral polymeric gene vectors with low cytotoxicity and high transfection efficiencies. *J Control Release*, **121**, 38-48; doi,
151. Koscova, Simona, Budesinsky, Milos, Hodacova and Jana, G. (2003). Czechoslovak Academy of Sciences, Institute of Organic Chemistry and Biochemistry, Praha, TCHEQUE, REPUBLIQUE, Vol. 68, pp. 7.

152. Xu, D., Prasad, K., Repic, O. and Blacklock, T.J. (1995) Ethyl trifluoroacetate: a powerful reagent for differentiating amino groups. *Tetrahedron Letters*, **36**, 7357-7360; doi,
153. Jørgensen, M.R., Jaroszewski, J.W., Witt, M. and Franzyk, H. (2005) On-Resin Carboxy Group Activation of ω -Amino Acids in Solid-Phase Synthesis-of Philanthotoxin Analogues. *Synthesis*, **2005**, 2687-2694; doi,
154. Li, W. and Yan, B. (1998) Effects of Polymer Supports on the Kinetics of Solid-Phase Organic Reactions: A Comparison of Polystyrene- and TentaGel-Based Resins. *The Journal of Organic Chemistry*, **63**, 4092-4097; doi: 10.1021/jo9802271,
155. Bender, J.A., Meanwell, N.A. and Wang, T. (2002) The mono-functionalization of symmetrical polyamines. *Tetrahedron*, **58**, 3111-3128; doi,
156. Oganessian, A., Cruz, I.A., Amador, R.B., Sorto, N.A., Lozano, J., Godinez, C.E., Anguiano, J., Pace, H., Sabih, G. and Gutierrez, C.G. (2007) High Yield Selective Acylation of Polyamines: Proton as Protecting Group. *Organic Letters*, **9**, 4967-4970; doi: 10.1021/ol702206d,
157. Zhang, Z., Yin, Z., Meanwell, N.A., Kadow, J.F. and Wang, T. (2003) Selective Monoacylation of Symmetrical Diamines via Prior Complexation with Boron. *Organic Letters*, **5**, 3399-3402; doi: 10.1021/ol0300773,
158. Lapatsanis, L., Milias, George, Froussios, Kleanthis, Kolovos, Miltiadis. (1983) Synthesis of N-2,2,2-(Trichloroethoxycarbonyl)-L-amino Acids and N-(9-Fluorenylmethoxycarbonyl)-L-amino Acids Involving Succinimidoxo Anion as a Leaving Group in Amino Acid Protection *Synthesis*, **8**, 671-673; doi,
159. Chan, W.C. and White, P.D. (2000) *Fmoc solid phase peptide synthesis : a practical approach*. Oxford University Press, New York.
160. Raper, S.E., Chirmule, N., Lee, F.S., Wivel, N.A., Bagg, A., Gao, G.P., Wilson, J.M. and Batshaw, M.L. (2003) Fatal systemic inflammatory response syndrome in a ornithine transcarbamylase deficient patient following adenoviral gene transfer. *Mol Genet.Metab*, **80**, 148-158; doi,
161. Therapy, B.o.t.E.S.o.G.a.C. (2008) Case of Leukaemia Associated with X-Linked Severe Combined Immunodeficiency Gene Therapy Trial in London. *Human Gene Therapy*, **19**, 3-4; doi: 10.1089/hum.2007.1221,
162. Canne, L.E., Botti, P., Simon, R.J., Chen, Y., Dennis, E.A. and Kent, S.B.H. (1999) Chemical protein synthesis by solid phase ligation of unprotected peptide segments. *J. Am. Chem. Soc.*, **121**, 8720; doi,
163. Tomalia, D.A., Naylor, A.M. and Goddard, W.A. (1990) Starburst dendrimers: molecular-level control of size, shape, surface chemistry, topology, and flexibility from atoms to macroscopic matter. *Angew.Chem.Int.Ed.Engl.*, **29**, 138-175; doi,
164. Godbey, W.T., Wu, K.K. and Mikos, A.G. (1999) Size matters: molecular weight affects the efficiency of poly(ethylenimine) as a gene delivery vehicle 2. *J.Biomed.Mater.Res.*, **45**, 268-275; doi,
165. Russ, V., Frohlich, T., Li, Y., Halama, A., Ogris, M. and Wagner, E. (2010) Improved in vivo gene transfer into tumor tissue by stabilization of

- pseudodendritic oligoethylenimine-based polyplexes. *J Gene Med*, **12**, 180-193; doi: 10.1002/jgm.1430,
166. Plank, C., Oberhauser, B., Mechtler, K., Koch, C. and Wagner, E. (1994) The influence of endosome-disruptive peptides on gene transfer using synthetic virus-like gene transfer systems. *J Biol.Chem.*, **269**, 12918-12924; doi,
 167. Wang, X.L., Ramusovic, S., Nguyen, T. and Lu, Z.R. (2007) Novel polymerizable surfactants with pH-sensitive amphiphilicity and cell membrane disruption for efficient siRNA delivery. *Bioconjug Chem*, **18**, 2169-2177; doi,
 168. Philipp, A., Zhao, X., Tarcha, P., Wagner, E. and Zintchenko, A. (2009) Hydrophobically modified oligoethylenimines as highly efficient transfection agents for siRNA delivery. *Bioconjug Chem*, **20**, 2055-2061; doi: 10.1021/bc9001536,
 169. Lee, R.J., Wang, S. and Low, P.S. (1996) Measurement of endosome pH following folate receptor-mediated endocytosis. *Biochimica et Biophysica Acta (BBA) - Molecular Cell Research*, **1312**, 237-242; doi,
 170. Boussif, O., Lezoualc'h, F., Zanta, M.A., Mergny, M.D., Scherman, D., Demeneix, B. and Behr, J.P. (1995) A versatile vector for gene and oligonucleotide transfer into cells in culture and in vivo: polyethylenimine. *Proc.Natl.Acad.Sci.U.S.A*, **92**, 7297-7301; doi,
 171. Bello Roufai, M. and Midoux, P. (2001) Histidylated polylysine as DNA vector: elevation of the imidazole protonation and reduced cellular uptake without change in the polyfection efficiency of serum stabilized negative polyplexes. *Bioconjug Chem*, **12**, 92-99; doi,
 172. Wu, C.H., Wilson, J.M. and Wu, G.Y. (1989) Targeting genes: delivery and persistent expression of a foreign gene driven by mammalian regulatory elements in vivo 939. *J.Biol.Chem.*, **264**, 16985-16987; doi,
 173. Zenke, M., Steinlein, P., Wagner, E., Cotten, M., Beug, H. and Birnstiel, M.L. (1990) Receptor-mediated endocytosis of transferrin-polycation conjugates: an efficient way to introduce DNA into hematopoietic cells. *Proc.Natl.Acad.Sci.U.S.A*, **87**, 3655-3659; doi,
 174. Ow, D.W., JR, D.E.W., Helinski, D.R., Howell, S.H., Wood, K.V. and Deluca, M. (1986) Transient and stable expression of the firefly luciferase gene in plant cells and transgenic plants. *Science*, **234**, 856-859; doi: 234/4778/856 [pii] 10.1126/science.234.4778.856,
 175. Krieg, A.M., Yi, A.K., Matson, S., Waldschmidt, T.J., Bishop, G.A., Teasdale, R., Koretzky, G.A. and Klinman, D.M. (1995) CpG motifs in bacterial DNA trigger direct B-cell activation. *Nature*, **374**, 546-549; doi,
 176. Vollmer, J. and Krieg, A.M. (2009) Immunotherapeutic applications of CpG oligodeoxynucleotide TLR9 agonists. *Advanced Drug Delivery Reviews*, **61**, 195-204; doi,
 177. Poeck, H., Besch, R., Maihoefer, C., Renn, M., Tormo, D., Morskaya, S.S., Kirschnek, S., Gaffal, E., Landsberg, J., Hellmuth, J. et al. (2008) 5[prime]-triphosphate-siRNA: turning gene silencing and Rig-I activation against

- melanoma. *Nat Med*, **14**, 1256-1263; doi: http://www.nature.com/nm/journal/v14/n11/supinfo/nm.1887_S1.html,
178. Besch, R., Poeck, H., Hohenauer, T., Senft, D., Hacker, G., Berking, C., Hornung, V., Endres, S., Ruzicka, T., Rothenfusser, S. *et al.* (2009) Proapoptotic signaling induced by RIG-I and MDA-5 results in type I interferon-independent apoptosis in human melanoma cells. *J Clin Invest*, **119**, 2399-2411; doi: 37155 [pii], 10.1172/JCI37155, Pubmedid:2719920
179. Matsumoto, M. and Seya, T. (2008) TLR3: interferon induction by double-stranded RNA including poly(I:C). *Adv Drug Deliv Rev*, **60**, 805-812; doi: S0169-409X(07)00383-3 [pii], 10.1016/j.addr.2007.11.005,
180. Okada, H. (2009) Brain tumor immunotherapy with type-1 polarizing strategies. *Ann N Y Acad Sci*, **1174**, 18-23; doi: NYAS4932 [pii] 10.1111/j.1749-6632.2009.04932.x,
181. Butowski, N., Lamborn, K.R., Lee, B.L., Prados, M.D., Cloughesy, T., DeAngelis, L.M., Abrey, L., Fink, K., Lieberman, F., Mehta, M. *et al.* (2009) A North American brain tumor consortium phase II study of poly-ICLC for adult patients with recurrent anaplastic gliomas. *J Neurooncol*, **91**, 183-189; doi: 10.1007/s11060-008-9705-3,
182. Jasani, B., Navabi, H. and Adams, M. (2009) Ampligen: a potential toll-like 3 receptor adjuvant for immunotherapy of cancer. *Vaccine*, **27**, 3401-3404; doi: S0264-410X(09)00111-X [pii], 10.1016/j.vaccine.2009.01.071,
183. Milhaud, P.G., Compagnon, B., Bienvenue, A. and Philippot, J.R. (1992) Interferon production of L929 and HeLa cells enhanced by polyribonucleosinic acid-polyribocytidylic acid pH-sensitive liposomes. *Bioconjug Chem*, **3**, 402-407; doi,
184. Milhaud, P.G., Machy, P., Lebleu, B. and Leserman, L. (1989) Antibody targeted liposomes containing poly(rl).poly(rC) exert a specific antiviral and toxic effect on cells primed with interferons alpha/beta or gamma. *Biochim Biophys Acta*, **987**, 15-20; doi: 0005-2736(89)90449-5 [pii],
185. Sakurai, F., Terada, T., Maruyama, M., Watanabe, Y., Yamashita, F., Takakura, Y. and Hashida, M. (2003) Therapeutic effect of intravenous delivery of lipoplexes containing the interferon-beta gene and poly I: poly C in a murine lung metastasis model. *Cancer Gene Ther.*, **10**, 661-668; doi,
186. Kloeckner, J., Boeckle, S., Persson, D., Roedl, W., Ogris, M., Berg, K. and Wagner, E. (2006) DNA polyplexes based on degradable oligoethylenimine-derivatives: Combination with EGF receptor targeting and endosomal release functions. *J.Control Release*, **116**, 115-122; doi,
187. de Bruin, K., Ruthardt, N., von Gersdorff, K., Bausinger, R., Wagner, E., Ogris, M. and Brauchle, C. (2007) Cellular dynamics of EGF receptor-targeted synthetic viruses. *Mol Ther*, **15**, 1297-1305; doi,
188. Boeckle, S., Wagner, E. and Ogris, M. (2005) C- versus N-terminally linked melittin-polyethylenimine conjugates: the site of linkage strongly influences activity of DNA polyplexes. *J Gene Med*, **7**, 1335-1347; doi,

189. Kale, A.A. and Torchilin, V.P. (2007) "Smart" drug carriers: PEGylated TATp-modified pH-sensitive liposomes. *J.Liposome Res.*, **17**, 197-203; doi,
190. Hatakeyama, H., Akita, H., Kogure, K., Oishi, M., Nagasaki, Y., Kihira, Y., Ueno, M., Kobayashi, H., Kikuchi, H. and Harashima, H. (2007) Development of a novel systemic gene delivery system for cancer therapy with a tumor-specific cleavable PEG-lipid. *Gene Ther*, **14**, 68-77; doi,
191. Rudolph, C., Schillinger, U., Plank, C., Gessner, A., Nicklaus, P., Muller, R. and Rosenecker, J. (2002) Nonviral gene delivery to the lung with copolymer-protected and transferrin-modified polyethylenimine 1. *Biochim.Biophys.Acta*, **1573**, 75; doi,
192. Meyer, M. and Wagner, E. (2006) pH-responsive shielding of non-viral gene vectors. *Expert.Opin.Drug Deliv.*, **3**, 563-571; doi,
193. Milas, L., Fan, Z., Andratschke, N.H. and Ang, K.K. (2004) Epidermal growth factor receptor and tumor response to radiation: in vivo preclinical studies. *Int J Radiat Oncol Biol Phys*, **58**, 966-971; doi: 10.1016/j.ijrobp.2003.08.035 S0360301603021047 [pii],
194. Han, Y., Caday, C.G., Nanda, A., Cavenee, W.K. and Huang, H.J. (1996) Tyrphostin AG 1478 preferentially inhibits human glioma cells expressing truncated rather than wild-type epidermal growth factor receptors. *Cancer Res*, **56**, 3859-3861; doi,
195. Chang, C.-d., Felix, A.M., Jimenez, M.H. and Meienhofer, J. (1980) Solid-Phase Peptide Synthesis of Somatostatin Using Milde base Cleavage of Na-9-fluorenylmethyloxycarbonylamino acids. *International Journal of Peptide and Protein Research*, **15**, 485-494; doi,
196. Atherton, E., Bury, C., Sheppard, R.C. and Williams, B.J. (1979) Stability of fluorenylmethoxycarbonylamino groups in peptide synthesis. Cleavage by hydrogenolysis and by dipolar aprotic solvents. *Tetrahedron Letters*, **20**, 3041-3042; doi,
197. Plank, C., Zauner, W. and Wagner, E. (1998) Application of membrane-active peptides for drug and gene delivery across cellular membranes. *Adv.Drug Deliv.Rev.*, **34**, 21-35; doi,

8 Appendix

8.1 List of Used Polymers

#	Sequence	Formula	M _w	protonable amines	Type
1	K-Stp ₁ -K	C ₂₄ H ₅₁ N ₉ O ₅	545,72	6	chain
3	K-Stp ₁ -K-CapA ₂	C ₄₀ H ₇₉ N ₉ O ₇	798,11	4	i-shape
4	K-Stp ₁ -K-MyrA ₂	C ₅₂ H ₁₀₃ N ₉ O ₇	966,43	4	i-shape
5	K-Stp ₁ -K-OleA ₂	C ₆₀ H ₁₁₅ N ₉ O ₇	1074,61	4	i-shape
6	K-Stp ₂ -K	C ₃₆ H ₇₆ N ₁₄ O ₇	817,08	9	chain
8	K-Stp ₂ -K-CapA ₂	C ₅₂ H ₁₀₄ N ₁₄ O ₉	1069,47	7	i-shape
9	K-Stp ₂ -K-MyrA ₂	C ₆₄ H ₁₂₈ N ₁₄ O ₉	1237,79	7	i-shape
10	K-Stp ₂ -K-OleA ₂	C ₇₂ H ₁₄₀ N ₁₄ O ₉	1345,97	7	i-shape
18	K-Stp ₄ -K	C ₆₀ H ₁₂₆ N ₂₄ O ₁₁	1359,80	15	chain
20	K-Stp ₄ -K-CapA ₂	C ₇₆ H ₁₅₄ N ₂₄ O ₁₃	1612,19	13	i-shape
21	K-Stp ₄ -K-MyrA ₂	C ₈₈ H ₁₇₈ N ₂₄ O ₁₃	1780,51	13	i-shape
22	K-Stp ₄ -K-OleA ₂	C ₉₆ H ₁₉₀ N ₂₄ O ₁₃	1888,69	13	i-shape
23	K-Stp ₅ -K	C ₇₂ H ₁₅₁ N ₂₉ O ₁₃	1631,16	18	chain
25	K-Stp ₅ -K-AraA ₂	C ₁₁₂ H ₂₂₇ N ₂₉ O ₁₅	2220,19	16	i-shape
26	K-Stp ₅ -K-MyrA ₂	C ₁₀₀ H ₂₀₃ N ₂₉ O ₁₅	2051,87	16	i-shape
27	K-Stp ₅ -K-OleA ₂	C ₁₀₈ H ₂₁₅ N ₂₉ O ₁₅	2160,05	16	i-shape
30	C-Stp ₁ -K-CapA ₂	C ₃₇ H ₇₂ N ₈ O ₇ S	773,08	3	i-shape
31	C-Stp ₁ -K-SteA ₂	C ₅₇ H ₁₁₂ N ₈ O ₇ S	1053,61	3	i-shape
34	K-Stp ₂ -ButA ₁	C ₃₄ H ₇₀ N ₁₂ O ₇	759,00	7	i-shape
35	K-Stp ₂ -CapA ₁	C ₃₈ H ₇₈ N ₁₂ O ₇	815,10	7	i-shape
36	K-Stp ₂ -MyrA ₁	C ₄₄ H ₉₀ N ₁₂ O ₇	899,26	7	i-shape
37	K-Stp ₂ -OleA ₁	C ₄₈ H ₉₆ N ₁₂ O ₇	953,35	7	i-shape
38	K-Stp ₁ -ButA ₁	C ₂₂ H ₄₅ N ₇ O ₅	487,64	4	i-shape
39	K-Stp ₁ -CapA ₁	C ₂₆ H ₅₃ N ₇ O ₅	543,74	4	i-shape
40	K-Stp ₁ -MyrA ₁	C ₃₂ H ₆₅ N ₇ O ₅	627,90	4	i-shape
41	K-Stp ₁ -OleA ₁	C ₃₆ H ₇₁ N ₇ O ₅	681,99	4	i-shape
45	C-Stp ₃ -C-K-MyrA ₂	C ₇₆ H ₁₅₁ N ₁₉ O ₁₂ S ₂	1587,26	9	i-shape
46	C-Stp ₃ -C-K-OleA ₂	C ₈₄ H ₁₆₃ N ₁₉ O ₁₂ S ₂	1695,44	9	i-shape
48	C-Stp ₂ -K-(K-MyrA ₂)-Stp ₂ -C	C ₉₄ H ₁₈₈ N ₂₆ O ₁₅ S ₂	1986,79	13	t-shape
49	C-Stp ₂ -K-(K-OleA ₂)-Stp ₂ -C	C ₁₀₂ H ₂₀₀ N ₂₆ O ₁₅ S ₂	2094,98	13	t-shape
50	K-Stp ₄ -K-AraA ₂	C ₁₀₀ H ₂₀₂ N ₂₄ O ₁₃	1948,83	13	i-shape
51	C-Stp ₃ -C-K	C ₄₈ H ₉₉ N ₁₉ O ₁₀ S ₂	1166,55	11	chain
56	C-Stp ₂ -K(CapA)-Stp ₂ -C	C ₆₈ H ₁₃₈ N ₂₄ O ₁₃ S ₂	1564,11	13	t-shape
57	C-Stp ₂ -K(Myra)-Stp ₂ -C	C ₇₄ H ₁₅₀ N ₂₄ O ₁₃ S ₂	1648,27	13	t-shape
58	C-Stp ₂ -K(OleA)-Stp ₂ -C	C ₇₈ H ₁₅₆ N ₂₄ O ₁₃ S ₂	1702,36	13	t-shape
59	C-Stp ₂ -K(ArA)-Stp ₂ -C	C ₈₀ H ₁₆₂ N ₂₄ O ₁₃ S ₂	1732,43	13	t-shape
62	C-Stp ₂ -K(K-AraA ₂)-Stp ₂ -C	C ₁₀₆ H ₂₁₂ N ₂₆ O ₁₅ S ₂	2155,11	13	t-shape

66	C-Stp ₂ -K(K-CapA ₂)-Stp ₂ -C	C ₈₂ H ₁₆₄ N ₂₆ O ₁₅ S ₂	1818,47	13	t-shape
67	C-Stp ₂ -K-MyrA ₂	C ₆₁ H ₁₂₁ N ₁₃ O ₉ S	1212,76	6	i-shape
68	C-K-Stp ₂ -K-MyrA ₂	C ₆₇ H ₁₃₃ N ₁₅ O ₁₀ S	1340,93	7	i-shape
69	C-K-Stp ₂ -K-OleA ₂	C ₇₅ H ₁₄₅ N ₁₅ O ₁₀ S	1449,11	7	i-shape
70	C-Stp ₂ -K-OleA ₂	C ₆₉ H ₁₃₃ N ₁₃ O ₉ S	1320,94	6	i-shape
71	C-Stp ₁ -K(K-MyrA ₂)-Stp ₁ -C	C ₇₀ H ₁₃₈ N ₁₆ O ₁₁ S ₂	1444,07	7	t-shape
72	C-Stp ₁ -K(K)-Stp ₁ -C	C ₄₂ H ₈₆ N ₁₆ O ₉ S ₂	1023,36	9	chain
73	C-Stp ₁ -K(K-SteA ₂)-Stp ₁ -C	C ₇₈ H ₁₅₄ N ₁₆ O ₁₁ S ₂	1556,29	7	t-shape
74	C-Stp ₁ -K(K-OleA ₂)-Stp ₁ -C	C ₇₈ H ₁₅₀ N ₁₆ O ₁₁ S ₂	1552,26	7	t-shape
75	C-Stp ₃ -K(K-MyrA ₂)-Stp ₃ -C	C ₁₁₈ H ₂₃₈ N ₃₆ O ₁₉ S ₂	2529,51	19	t-shape
76	C-Stp ₃ -K(K)-Stp ₃ -C	C ₉₀ H ₁₈₆ N ₃₆ O ₁₇ S ₂	2108,80	19	chain
77	C-Stp ₃ -K(K-SteA ₂)-Stp ₃ -C	C ₁₂₆ H ₂₅₄ N ₃₆ O ₁₉ S ₂	2641,73	17	t-shape
78	C-Stp ₃ -K(K-OleA ₂)-Stp ₃ -C	C ₁₂₆ H ₂₅₀ N ₃₆ O ₁₉ S ₂	2637,69	17	t-shape
79	C-Stp ₄ -K(K-MyrA ₂)-Stp ₄ -C	C ₁₄₂ H ₂₈₈ N ₄₆ O ₂₃ S ₂	3072,23	25	t-shape
80	C-Stp ₄ -K(K)-Stp ₄ -C	C ₁₁₂ H ₂₃₄ N ₄₈ O ₂₁ S ₂	2653,50	27	chain
81	C-Stp ₄ -K(K-SteA ₂)-Stp ₄ -C	C ₁₅₀ H ₃₀₄ N ₄₆ O ₂₃ S ₂	3184,44	25	t-shape
82	C-Stp ₄ -K(K-OleA ₂)-Stp ₄ -C	C ₁₄₈ H ₂₉₈ N ₄₈ O ₂₃ S ₂	3182,39	25	t-shape

8.2 Abbreviations

Abbreviation	Meaning
2-CITrt	2-Chlorotrityl
9-BBN	9-Borabicyclo[3.3.1]nonane
AA	Amino acid
ACN	Acetonitrile
asODN	Antisense oligodeoxynucleotide
boc	<i>tert</i> -Butyloxycarbonyl
brPEI	Branched polyethylenimine
CMV	Cytomegalovirus
Da	Dalton
DCM	Dichloromethane
DCU	Dicyclohexylurea
DCVC	Dry column vacuum chromatography
Dde	N-(1-(4,4-dimethyl-2,6-dioxocyclohexylidene)ethyl)
DIPEA	Diisopropylethylamine
DMEM	Dulbecco's modified eagle's medium
DMF	Dimethylformamide
DMSO	Dimethyl sulfoxide
DNA	Deoxyribonucleic acid
DOPE	Dioleoyl-phosphatidylethanolamine
DOTAP	N-[1-(2,3-Dioleoyloxy)propyl]-N,N,N-trimethylammonium
dsRNA	Double-stranded ribonucleic acid
DTNB	Dithionitrobenzoic acid
DTT	DL-Dithiothreitol
ECM	Extracellular matrix
EDT	Ethanedithiol
EDTA	Ethylenediamine tetraacetic acid
EGF	Epithelial growth factor
eGFP	Enhanced green fluorescent protein
EMA	European medicines agency
EPR	Enhanced permeability and retention
ESI-MS	Electrospray ionization mass spectrometry
EtOH	Ethanol
FAB-MS	Fast atom bombardment mass spectrometry
FCS	Fetal calf serum
fmoc/tBu	9-Fluorenylmethyloxycarbonyl/ <i>tert</i> -Butyl
fmoc-AA-OH	Fmoc-amino acid

FRET	Foerster resonance energy transfer
GMP	Good manufacturing practice
HBG	HEPES buffered glucose
HEPES	N-(2-hydroethyl) piperazine-N'-(2-ethansulfonic acid)
HLR	Hydrophilic-hydrophobic ratio
HOBt	1-Hydroxybenzotriazole
HPLC	High-performance liquid chromatography
HV	High vacuum
IEX	Ion-exchange
LPEI	Linear polyethylenimine
Luc	Luciferase
MALDI	Matrix assisted laser desorption ionization mass spectrometry
Mel	Melittin
MeOH	Methanol
mRNA	Messenger RNA
MS	Mass spectrometry
MTBE	<i>tert</i> -Butyl methylether
MTT	Methylthiazolyldiphenyl-tetrazolium bromide
M _w	Molecular weight
N/P ratio	Number of protonable nitrogens to phosphates
NA	Nucleic acid
NHS	N-Hydroxysuccinimide
NLS	Nuclear localization sequence
NMR	Nuclear magnetic resonance
NPC	Nuclear pore complex
OEI	Oligoethylenimine
ON	Oligonucleotide
OPSS	<i>ortho</i> -Pyridyldisulfide
PAA	Polyamidoamine
PAE	Poly(β -amino ester)
PAMAM	Polyamidoamine (in dendrimers nomenclature)
pDNA	Plasmid DNA
PDP	(2-pyridyldithio)-propionoyl modified
PEG	Polyethylene glycol
pEGFPLuc	Plasmid encoding a EGFP-Luciferase fusion
PEI	Polyethylenimine
PEOZ	Poly(2-ethyl-2-oxazoline)
Pip	Piperidine
PMO	Phosphorodiamidate morpholino oligo
Poly(I)	Polyinosinic acid

poly(I:C)	Polyinosinic:polycytidylic acid duplex
PPDS	Programmable polymeric delivery system
PS	Polystyrole
PyBOP®	Benzotriazol-1-yl-oxytripyrrolidinophosphonium hexafluorophosphate
RBF	Round-bottom flask
RISC	RNA-induced silencing complex
RLU	Relative light units
RNA	Ribonucleic acid
RNAi	RNA interference
RP-HPLC	Reversed-Phase High-performance liquid chromatography
RT	Room temperature
SAR	Structure-activity relationship
SEC	Size-exclusion chromatography
siRNA	Small inhibitory RNA
SPDP	N-Succinimidyl-3-(2-pyridyldithio)propionate
Stp	16-Amino-4-oxo-5,8,11,14-tetraazahexadecanoic acid
Succ	Succinyl
TBE	Tris-Boric acid-EDTA Buffer
TEA	Triethylamine
TFA	Trifluoroacetic acid
TfaEt	Ethyl trifluoroacetate
THF	Tetrahydrofuran
TIS	Triisopropylsilane
TLC	Thin layer chromatography
TLR	Toll-like receptor
TNBS	Trinitrobenzenesulfonic acid
UV-VIS	Ultraviolet-Visible spectroscopy

8.3 Buffer List

Buffer	Ingredient	
DMEM LG	Biochrom DMEM medium powder	10.15 g/L
	NaHCO ₃	3.7 g/L
	FCS	10%
	Glucose monohydrate	10 g
	Penicillin	1%
	Streptomycin	1%
	Stable glutamine	1%
	Adjusted to pH 7.4	
DNA Loading Buffer	0.5 M EDTA (pH 8.0) solution	2.4 mL
	Glycerine	12.0 mL
	MilliQ water	5.6 mL
	Bromophenol blue	40 mg
DTNB-Stock Solution	DTNB	4 mg
	MilliQ water	1 mL
Ellman's Buffer	Na ₂ HPO ₄ (0.2 M)	28.4 g/L
	EDTA disodium salt dihydrate	372 mg/L
	Adjusted to pH 8.0	
HBG	HEPES (20 mM)	4.76 g/L
	Glucose monohydrate	50 g/L
	MilliQ	ad 1000 mL
	pH adjusted to 7.1	
LAR	1 M glycylglycine solution (pH 8.0)	2 mL (20 mM)
	100 mM MgCl ₂ solution	1 mL (1 mM)
	0.5 M EDTA solution (pH 8.0)	20 µL (0.1 mM)
	DTT	50.8 mg (3.2 mM)
	ATP	27.8 mg (0.55 mM)
	Coenzyme A	21.3 mg (0.27 mM)
	MilliQ water	Ad 100 mL
	pH adjusted to 8.0	
	Luciferine-Solution	Ad 0.5 mM
PBS	KCl	0.2 g
	KH ₂ PO ₄	0.24 g
	NaCl	8.0 g
	Anhydrous Na ₂ PO ₄	1.15 g
	MilliQ water	Ad 1000 mL
	Adjusted to pH 7.4	
RNA Loading Buffer	0.5 M EDTA (pH 8.0)	2.4 mL
	Glycerine	12.0 mL
	MilliQ water	5.6 mL
	Xylene cyanol	40 mg
TBE Buffer	Trizma base	10.8 g
	Boric acid	5.5 g
	EDTA disodium salt dehydrate	0.75 g
	MilliQ water	Ad 1000 mL

8.4 Supporting Information Chapter 4.1

PEI/poly(I:C) binding

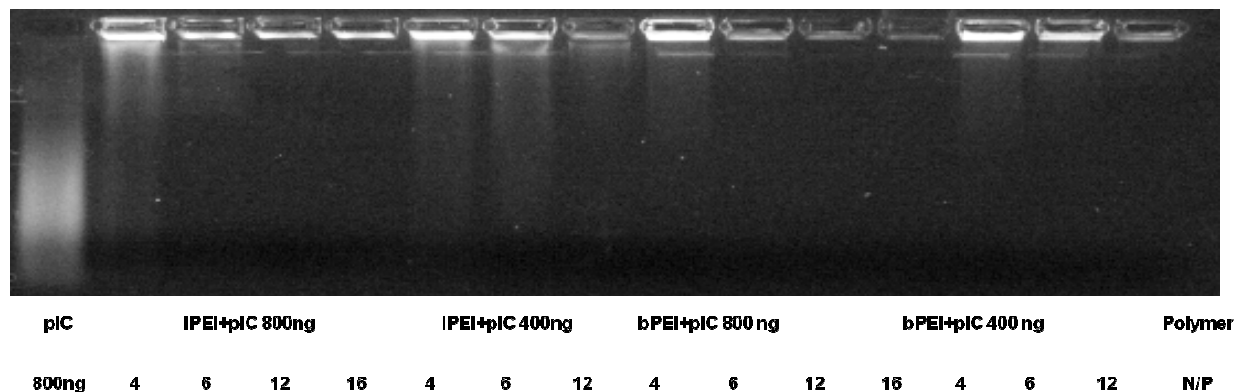


Figure S1. Binding of poly(I:C) to PEI as analyzed by agarose gel shift assay. 400 or 800 ng poly(I:C) were complexed using either LPEI or brPEI and analyzed by gel shift assay. Both polymer backbones were able to efficiently complex poly(I:C) at a minimal N/P ratio of 6.

Heparin Dissociation Assay

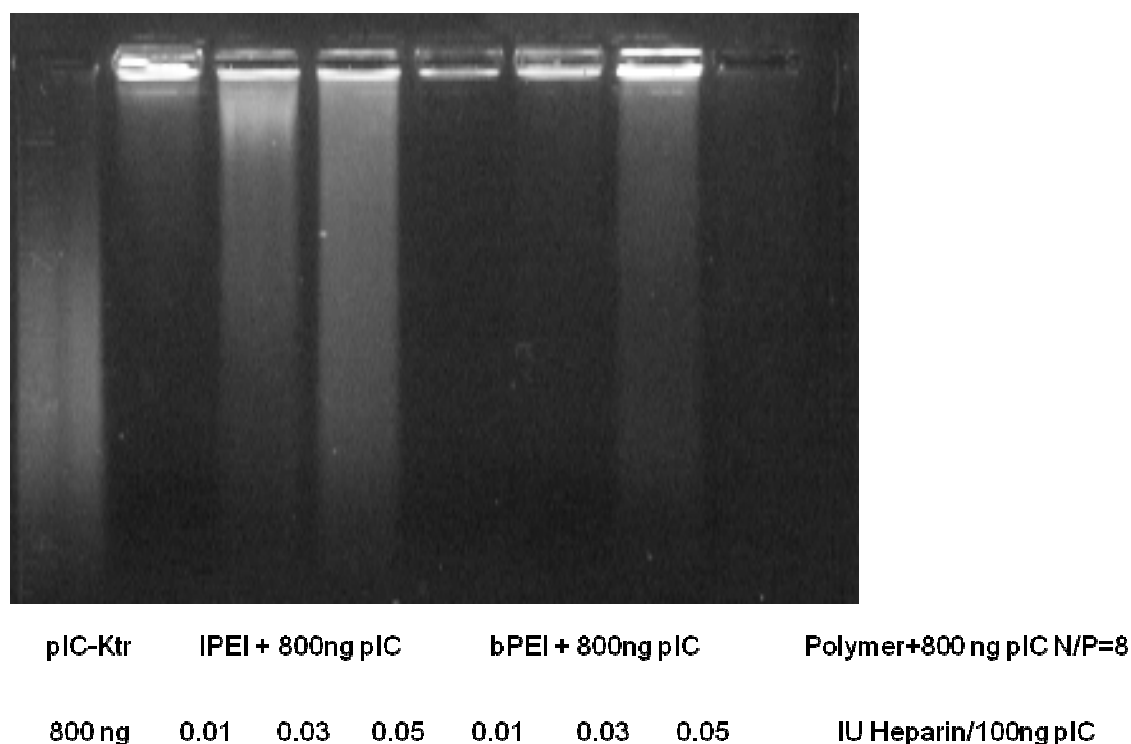


Figure S2: Binding of poly(I:C) to PEI conjugates as analyzed by heparin dissociation and agarose gel shift assay. 800 ng poly(I:C) were complexed using indicated polymers at N/P ratio of 8 and treated with indicated amounts of the polyanion heparin, resulting in partial release of poly(I:C) at higher concentrations.

Determination of the EGFR Count on U87MG/U87MGwtEGFR

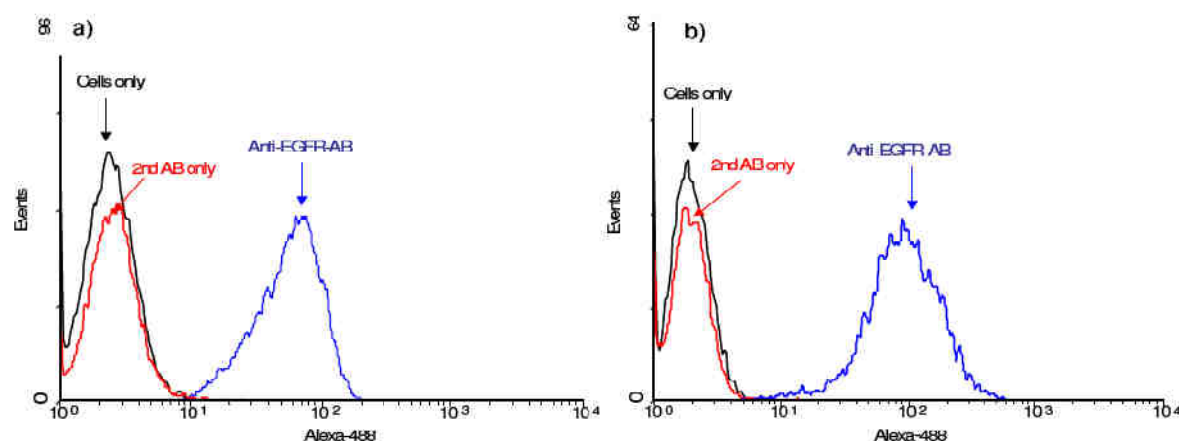


Figure S3: Relative EGF receptor cell surface level on tumor cell lines. U87MG (a), U87MGwtEGFR cells (b) were incubated with a mouse anti-EGFR antibody followed by treatment with an Alexa-488 conjugated secondary polyclonal goat anti-mouse antibody. Untreated cells (cells only) as well as cells, incubated only with secondary antibody (2nd AB only) served as negative control.

Poly(I:C) Dose Titration Using LPEI-PEG_{10kDa}-EGF as Carrier

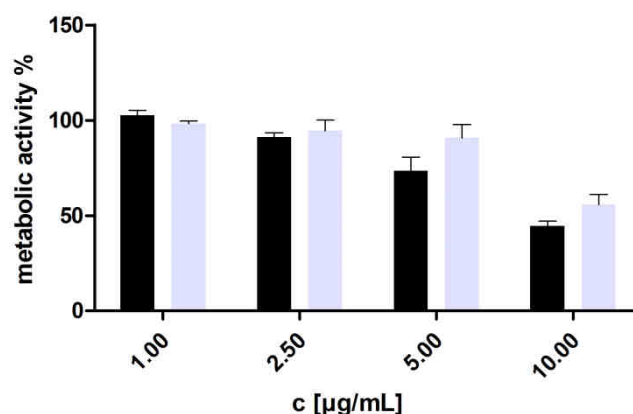


Figure S4: *In vitro* antitumoral activity of poly(I:C) at different concentrations against U87MGwtEGFR glioma cells. Comparison of poly(I:C) [black bars] with poly(I) control [grey bars]. Conditions: 10.000 cells/well, Incubation for 48 h with indicated dose of poly(I:C), poly(I). Metabolic activity was measured by MTT test.

8.5 Supporting Information Chapter 4.4

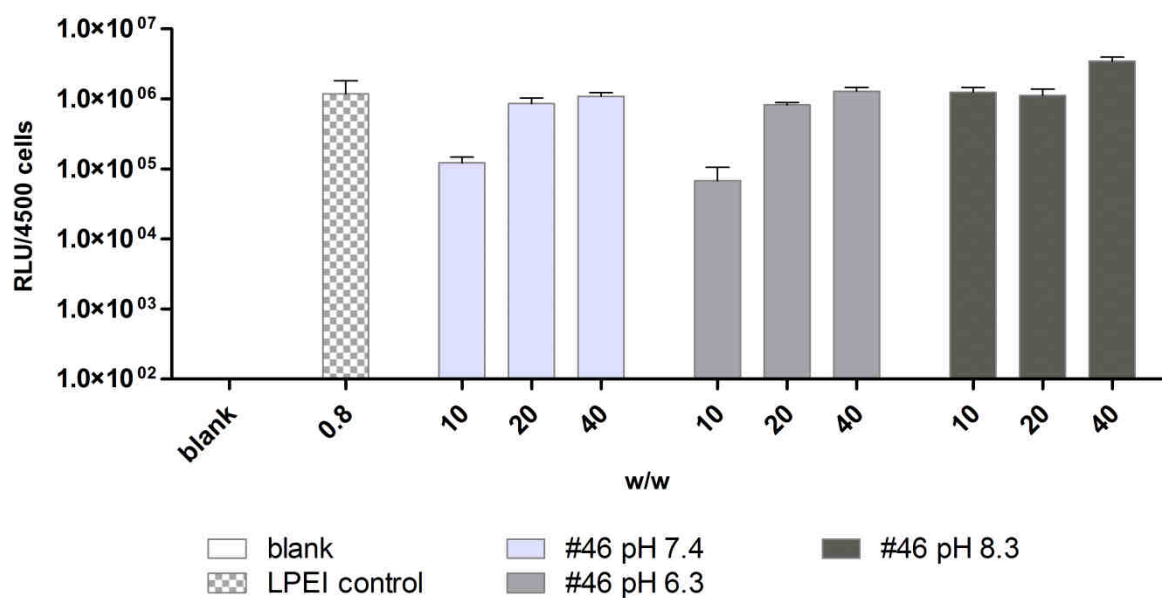


Figure S4. Influence of polyplex formation buffer pH on transfection efficiency.

Conditions: Neuro2A, 10.000 cells/well; polyplexes formed with pDNA(EGFP_{Luc}) and polymer in pH adjusted buffer (HBG titrated with HCl/NaOH). Polyplexes were formed by mixing equal volumes of pDNA/Polymer solution, incubated for 30 min and added to the cells 20 μ L on 80 μ L and incubated for 24 h. Experiment shows pH dependency of the transfection protocol. Differences between pH 6.3 and pH 8.3 are highly significant.

8.6 Used Protective Groups and Polymer Nomenclature

Amino acid	Three letter code	One letter code	Used prot. group	Residue weight (-H ₂ O)	Charge
β-Alanine	βAla	-	-	71.08	0
Alanine	Ala	A	-	71.08	0
Arginine	Arg	R	Pbf	156.19	+1
Asparagine	Asn	N	Trt	114.11	0
Aspartic acid	Asp	D	OtBu	115.09	-1
Cysteine	Cys	C	Trt StBu	103.15	0
Glutamic acid	Glu	E	OtBu	129.12	-1
Glutamine	Gln	Q	Trt	128.13	0
Glycine	Gly	G	-	57.05	0
Histidine	His	H	Trt	137.14	0/+1
Isoleucine	Ile	I	-	113.16	0
Leucine	Leu	L	-	113.16	0
Lysine	Lys	K	Boc	128.18	+1
Methionine	Met	M	-	131.20	0
Phenylalanine	Phe	F	-	147.18	0
Proline	Pro	P	-	97.12	0
Serine	Ser	S	tBu	87.08	0
Threonine	Thr	T	tBu	101.11	0
Tryptophan	Trp	W	Boc	186.22	0
Tyrosine	Tyr	Y	tBu	163.18	0
Valine	Val	V	-	99.13	0
SuccTEPA	Stp	-	Boc	281.21	+3

Fatty acid	Four letter code	Residue weight (-H ₂ O)	C:D	n-x	Δ ^x
Acetic acid	AceA	42.03	2:0	-	-
Butyric acid	ButA	70.09	4:0	-	-
Caprylic acid	CapA	126.19	8:0	-	-
Myristic acid	MyrA	210.35	14:0	-	-
Oleic acid	OleA	264.44	18:1	n-9	cis-Δ ⁹
Arachidic acid	AraA	294.51	20:0	-	-

General Nomenclature of Synthesized PAAs and Peptides

- Contrary to IUPAC peptide nomenclature all sequences are written in C→N direction, the carboxy terminal residue is indicated by the HO-prefix and N-terminal residue (if present) is labeled with -H
- Standard amino acids are always written in single letter code (e.g. A, K, C)
- Polyaminoacids and all non-natural amino acids are always written using three letter code (eg. Stp, Dha)
- Fatty acids are always written in 4 letters (eg. LinA, OleA) where the forth letter is always an A
- Polyaminoacid abbreviations are build with the following rules:
 1. Letter: Acid component → succinic acid → S
 2. Letter: Amine component → spacer unit part → tetraethylene → t
 3. Letter: Amine component → number of amines → pentamine → p
- Branching is indicated by the use of round brackets followed by an index for the number of branches

8.7 Analytical Data

Sequence: HO-K-Stp₁-K-H

#: 01

Molecular formula:

C₂₄H₅₁N₉O₅M_w 545.72

MALDI:

546.9

546.4 [M+H] calc.

NMR:

¹H-NMR (400 MHz, D₂O, 17.0 °C): δ = 1.29 - 1.48 (m, 4H, γ-CH₂-, Lys), 1.54 - 1.68 (m, 4H, δ-CH₂-, Lys), 1.69 - 1.93 (m, 4H, β-CH₂-, Lys), 2.42 - 2.52 (m, 2H, O=C-CH₂-, Stp), 2.52 - 2.62 (m, 2H, O=C-CH₂-, Stp), 2.87 - 2.94 (t, J=7.6 Hz, 4H, ε-CH₂-, Lys), 3.15 - 3.32 (m, 4H, N-CH₂-, Stp), 3.35 - 3.55 (m, 12H, N-CH₂-, Stp), 3.89 - 3.99 (t, J=6.64 Hz, 1H, O=C-C(R)H-NH-, Lys), 4.20 - 4.25 (dd, J=5.3, 8.8, 1H, O=C-C(R)H-NH-, Lys) ppm.

Sequence: HO-K-Stp₁-K-CapA₂

#: 03

Molecular formula:

C₄₀H₇₉N₉O₇M_w 798.11

MALDI:

799.1

798.6 [M+H] calc.

NMR:

¹H-NMR (400 MHz, D₂O, 17.0 °C): δ = 0.73 - 0.83 (m, 6H, -CH₃, CapA), 1.11 - 1.27 (m, 16H, -CH₂-, CapA), 1.28 - 1.90 (m, 16H, δ-CH₂/γ-CH₂/β-CH₂, Lys; O=C-CH₂-CH₂-, CapA), 2.10 - 2.32 (m, 4H, O=C-CH₂, CapA), 2.45 - 2.52 (m, 2H, O=C-CH₂-, Stp), 2.52 - 2.59 (m, 2H, O=C-CH₂-, Stp), 2.88 - 2.96 (t, J=7.8 Hz, 2H, ε-CH₂, Lys), 3.07 - 3.14 (m, 2H, ε-CH₂, Lys), 3.16 - 3.25 (m, 4H, N-CH₂-, Stp), 3.37 - 3.56 (m, 12H, N-CH₂-, Stp), 4.07 - 4.16 (m, 1H, O=C-C(R)H-NH-, Lys), 4.18 - 4.29 (m, 1H, O=C-C(R)H-NH-, Lys) ppm.

Sequence: HO-K-Stp₁-K-MyrA₂

#: 04

Molecular formula:

C₅₂H₁₀₃N₉O₇M_w 966.43

MALDI:

967.4

967.4 [M+H] calc.

NMR:

¹H-NMR (400 MHz, D₂O, 17.0 °C): δ = 0.71 - 0.86 (m, 6H, -CH₃, MyrA), 1.02 - 1.31 (bs, 44H, -CH₂-, MyrA), 1.31 - 2.05 (m, 16H, δ-CH₂/γ-CH₂/β-CH₂, Lys; O=C-CH₂-CH₂-, MyrA), 2.06 - 2.38 (m, 4H, O=C-CH₂, MyrA), 2.41 - 2.52 (m, 2H, O=C-CH₂-, Stp), 2.52 - 2.65 (m, 2H, O=C-CH₂-, Stp), 2.88 - 2.97 (t, J=7.8 Hz, 2H, ε-CH₂, Lys), 3.15 - 3.29 (m, 2H, ε-CH₂, Lys), 3.15 - 3.29 (m, 4H, N-CH₂-, Stp), 3.36 - 3.62 (m, 12H, N-CH₂-,

Stp), 4.04 – 4.16 (m, 1H, O=C-C(R)H-NH-, Lys), 4.18 – 4.34 (m, 1H, O=C-C(R)H-NH-, Lys) ppm.

Sequence: HO-K-Stp₁-K-OleA₂

#: **05**

Molecular formula: C₅₈H₁₁₁N₉O₇

M_w 1074.61

MALDI: Not determined

NMR: ¹H-NMR (400 MHz, D₂O, 16.9 °C): δ = 0.67 – 0.88 (m, 6H, -CH₃, OleA), 0.91 – 1.93 (m, 64H, -CH₂-, OleA; β-CH₂-, δ-CH₂-, γ-CH₂-, Lys; -CH₂-CH=CH-CH₂-, O=C-CH₂-CH₂-, OleA), 2.06 – 2.38 (bm, 4H, O=C-CH₂-, OleA), 2.41 – 2.65 (m, 4H, O=C-CH₂-, Stp), 2.87 – 2.99 (m, 4H, ε-CH₂-, Lys), 3.14 – 3.27 (m, 4H, N-CH₂-, Stp), 3.29 – 3.62 (m, 12H, N-CH₂-, Stp), 4.02 – 4.09 (m, 1H, O=C-C(R)H-NH-, Lys), 4.24 – 4.34 (m, 1H, O=C-C(R)H-NH-, Lys) ppm.

Sequence: HO-K-Stp₂-K-H

#: **06**

Molecular formula: C₃₆H₇₆N₁₄O₇

M_w 817.07

MALDI: Not determined

NMR: ¹H-NMR (400 MHz, D₂O, 16.8 °C): δ = 1.29 – 1.46 (m, 4H, γ-CH₂-, Lys), 1.56 – 1.76 (m, 4H, δ-CH₂-, Lys), 1.76 – 1.92 (m, 4H, β-CH₂-, Lys), 2.43 – 2.51 (m, 6H, O=C-CH₂-, Stp), 2.52 – 2.62 (m, 2H, O=C-CH₂-, Stp), 2.87 – 2.95 (t, *J*=7.6 Hz, 4H, ε-CH₂-, Lys), 3.13 – 3.29 (m, 8H, N-CH₂-, Stp), 3.35 – 3.55 (m, 24H, N-CH₂-, Stp), 3.89 – 3.99 (t, *J*=6.64 Hz, 1H, O=C-C(R)H-NH-, Lys), 4.20 – 4.25 (dd, *J*=5.2, 8.8, 1H, O=C-C(R)H-NH-, Lys) ppm.

Sequence: HO-K-Stp₂-K-CapA₂

#: **08**

Molecular formula: C₅₂H₁₀₄N₁₄O₉

M_w 1068.81

MALDI: 1070.5 1069.8 [M+H] calc.

NMR: ¹H-NMR (400 MHz, D₂O, 16.9 °C): δ = 0.72 – 0.81 (m, 6H, -CH₃, CapA), 1.09 – 1.25 (m, 16H, -CH₂-, CapA), 1.26 – 1.90 (m, 16H, δ-CH₂-, γ-CH₂-, β-CH₂-, Lys; O=C-CH₂-CH₂-, CapA), 2.08 – 2.32 (m, 4H, O=C-CH₂-, CapA), 2.42 – 2.50 (m, 6H, O=C-CH₂-, Stp), 2.52 – 2.59 (m, 2H, O=C-CH₂-, Stp), 2.87 – 2.95 (t, *J*=7.7 Hz, 2H, ε-CH₂-, Lys), 3.06 – 3.13 (m, 2H, ε-CH₂-, Lys)

Lys), 3.14 – 3.25 (m, 8H, N-CH₂-, Stp), 3.33 – 3.56 (m, 24H, N-CH₂-, Stp), 4.06 – 4.16 (m, 1H, O=C-C(R)H-NH-, Lys), 4.17 – 4.24 (m, 1H, O=C-C(R)H-NH-, Lys) ppm.

Sequence: HO-K-Stp₂-K-MyrA₂

#: **09**

Molecular formula: C₆₄H₁₂₈N₁₄O₉

M_w 1237.78

MALDI: Not determined

NMR: ¹H-NMR (400 MHz, D₂O, 16.8 °C): δ = 0.72 – 0.85 (m, 6H, -CH₃, MyrA), 1.06 – 1.28 (m, 40H, -CH₂-, MyrA), 1.26 – 1.90 (m, 16H, γ-CH₂/δ-CH₂/β-CH₂, Lys; O=C-CH₂-CH₂-, MyrA), 2.08 – 2.32 (m, 4H, O=C-CH₂, MyrA), 2.42 – 2.53 (m, 6H, O=C-CH₂-, Stp), 2.53 – 2.63 (m, 2H, O=C-CH₂-, Stp), 2.87 – 2.98 (t, J=7.6 Hz, 2H, ε-CH₂, Lys), 3.04 – 3.14 (m, 2H, ε-CH₂, Lys), 3.15 – 3.28 (m, 8H, N-CH₂-, Stp), 3.33 – 3.58 (m, 24H, N-CH₂-, Stp), 4.05 – 4.22 (m, 2H, O=C-C(R)H-NH-, Lys) ppm.

Sequence: HO-K-Stp₂-K-OleA₂

#: **10**

Molecular formula: C₇₂H₁₄₀N₁₄O₉

M_w 1345.97

MALDI: Not determined

NMR: ¹H-NMR (400 MHz, D₂O, 16.9 °C): δ = 0.69 – 0.82 (m, 6H, -CH₃, OleA), 0.99 – 1.30 (m, 40H, -CH₂-, OleA), 1.32 – 1.91 (m, 24H, β-CH₂/δ-CH₂/γ-CH₂, Lys; -CH₂-CH=CH-CH₂, O=C-CH₂-CH₂-, OleA), 1.92 – 1.99 (m, 4H, O=C-CH₂, OleA), 2.42 – 2.51 (m, 6H, O=C-CH₂-, Stp), 2.51 – 2.60 (m, 2H, O=C-CH₂-, Stp), 2.87 – 2.99 (m, 4H, ε-CH₂, Lys), 3.14 – 3.26 (m, 8H, N-CH₂-, Stp), 3.35 – 3.55 (m, 24H, N-CH₂-, Stp), 4.11 – 4.31 (m, 2H, O=C-C(R)H-NH-, Lys) ppm.

Sequence: HO-K-Stp₄-K-H

#: **18**

Molecular formula: C₆₀H₁₂₆N₂₄O₁₁

M_w 1359.79

MALDI: 1360.0 1630.0 [M+H] calc.

NMR: ¹H-NMR (400 MHz, D₂O, 16.7 °C): δ = 1.30 – 1.45 (m, 4H, γ-CH₂-, Lys), 1.54 – 1.68 (m, 4H, δ-CH₂-, Lys), 1.69 – 1.93 (m, 4H, β-CH₂-, Lys), 2.40 – 2.51 (m, 14H, O=C-CH₂-, Stp), 2.51 – 2.59 (m, 2H, O=C-CH₂-, Stp), 2.86 – 2.95 (t, J=7.6 Hz, 4H, δ-CH₂-, Lys), 3.09 – 3.30 (m, 16H, N-CH₂-,

Stp), 3.30 – 3.53 (m, 48H, N-CH₂-, Stp), 3.89 – 3.99 (t, $J=6.64$ Hz, 1H, O=C-C(R)H-NH-, Lys), 4.20 – 4.25 (dd, $J=5.2, 8.8$, 1H, O=C-C(R)H-NH-, Lys) ppm.

Sequence: HO-K-Stp₄-K-CapA₂

#: **20**

Molecular formula:

C₇₆H₁₅₄N₂₄O₁₃

M_w 1612.19

MALDI:

1611.8

1612.2 [M+H] calc.

NMR:

¹H-NMR (400 MHz, D₂O, 16.8 °C): δ = 0.72 – 0.83 (m, 6H, -CH₃, CapA), 1.12 – 1.25 (m, 16H, -CH₂-, CapA), 1.26 – 1.88 (m, 16H, δ -CH₂/ γ -CH₂/ β -CH₂, Lys; O=C-CH₂-CH₂-, CapA), 2.10 – 2.29 (m, 4H, O=C-CH₂, CapA), 2.42 – 2.52 (m, 14H, O=C-CH₂-, Stp), 2.52 – 2.59 (m, 2H, O=C-CH₂-, Stp), 2.88 – 2.95 (t, $J=7.8$ Hz, 2H, ϵ -CH₂, Lys), 3.06 – 3.14 (m, 2H, ϵ -CH₂, Lys), 3.14 – 3.25 (m, 16H, N-CH₂-, Stp), 3.32 – 3.56 (m, 48H, N-CH₂-, Stp), 4.07 – 4.16 (m, 1H, O=C-C(R)H-NH-, Lys), 4.17 – 4.26 (m, 1H, O=C-C(R)H-NH-, Lys) ppm.

Sequence: HO-K-Stp₄-K-MyrA₂

#: **21**

Molecular formula:

C₈₈H₁₇₈N₂₄O₁₃

M_w 1780.51

MALDI:

1782.7

1781.5 [M+H] calc.

NMR:

¹H-NMR (400 MHz, D₂O, 16.8 °C): δ = 0.72 – 0.85 (m, 6H, -CH₃, MyrA), 1.07 – 1.29 (m, 40H, -CH₂-, MyrA), 1.26 – 1.88 (m, 16H, δ -CH₂/ γ -CH₂/ β -CH₂, Lys; O=C-CH₂-CH₂-, MyrA), 2.10 – 2.29 (m, 4H, O=C-CH₂, MyrA), 2.40 – 2.52 (m, 14H, O=C-CH₂-, Stp), 2.52 – 2.63 (m, 2H, O=C-CH₂-, Stp), 2.87 – 2.97 (t, $J=7.8$ Hz, 2H, ϵ -CH₂, Lys), 3.06 – 3.14 (m, 2H, ϵ -CH₂, Lys), 3.13 – 3.28 (m, 16H, N-CH₂-, Stp), 3.28 – 3.56 (m, 48H, N-CH₂-, Stp), 4.06 – 4.22 (m, 1H, O=C-C(R)H-NH-, Lys) ppm.

Sequence: HO-K-Stp₄-K-OleA₂

#: **22**

Molecular formula:

C₉₆H₁₉₀N₂₄O₁₃

M_w 1888.69

MALDI:

1888.6

1888.5 [M+H] calc.

NMR:

¹H-NMR (400 MHz, D₂O, 16.9 °C): δ = 0.67 – 0.83 (m, 6H, -CH₃, OleA), 0.99 – 1.30 (m, 40H, -CH₂-, OleA), 1.32 – 1.91 (m, 24H, β -CH₂/ δ -CH₂/ γ -CH₂, Lys; -CH₂-CH=CH-CH₂, O=C-CH₂-CH₂-, OleA), 1.92 – 1.99 (m,

4H, O=C-CH₂, OleA), 2.41 - 2.52 (m, 14H, O=C-CH₂-, Stp), 2.52 - 2.60 (m, 2H, O=C-CH₂-, Stp), 2.87 - 2.96 (m, 2H, ε-CH₂, Lys), 2.99 - 3.11 (m, 2H, ε-CH₂, Lys), 3.11 - 3.26 (m, 16H, N-CH₂-, Stp), 3.30 - 3.55 (m, 48H, N-CH₂-, Stp), 4.07 - 4.24 (m, 2H, O=C-C(R)H-NH-, Lys) ppm.

Sequence: HO-K-Stp₅-K-H

#: **23**

Molecular formula:

C₇₂H₁₅₁N₂₉O₁₃

M_w 1631.15

MALDI:

1634.1

1631.2 [M+H] calc.

NMR:

¹H-NMR (400 MHz, D₂O, 17.1 °C): δ = 1.28 - 1.49 (m, 4H, γ-CH₂-, Lys), 1.49 - 1.88 (m, 8H, δ-CH₂-/β-CH₂-, Lys), 2.40 - 2.52 (m, 18H, O=C-CH₂-, Stp), 2.52 - 2.60 (m, 2H, O=C-CH₂-, Stp), 2.87 - 2.95 (t, J=7.6 Hz, 4H, ε-CH₂, Lys), 3.13 - 3.26 (m, 20H, N-CH₂-, Stp), 3.35 - 3.55 (m, 60H, N-CH₂-, Stp), 3.89 - 3.99 (t, J=6.64 Hz, 1H, O=C-C(R)H-NH-, Lys), 4.20 - 4.25 (dd, J=5.2, 8.8, 1H, O=C-C(R)H-NH-, Lys) ppm.

Sequence: HO-K-Stp₅-K-AraA₂

#: **25**

Molecular formula:

C₁₁₂H₂₂₇N₂₉O₁₅

M_w 2220.19

MALDI:

Not determined

NMR:

¹H-NMR (400 MHz, D₂O, 17.0 °C): δ = 0.71 - 0.86 (m, 6H, -CH₃, AraA), 1.04 - 1.30 (m, 72H, -CH₂-, AraA), 1.31 - 1.98 (m, 16H, δ-CH₂/γ-CH₂/β-CH₂, Lys; O=C-CH₂-CH₂-, AraA), 2.10 - 2.29 (m, 4H, O=C-CH₂, AraA), 2.40 - 2.52 (m, 18H, O=C-CH₂-, Stp), 2.52 - 2.60 (m, 2H, O=C-CH₂-, Stp), 2.87 - 2.97 (t, J=7.8 Hz, 2H, ε-CH₂, Lys), 3.03 - 3.14 (m, 2H, ε-CH₂, Lys), 3.13 - 3.28 (m, 20H, N-CH₂-, Stp), 3.31 - 3.57 (m, 60H, N-CH₂-, Stp), 4.06 - 4.26 (m, 2H, O=C-C(R)H-NH-, Lys) ppm.

Sequence: HO-K-Stp₅-K-MyrA₂

#: **26**

Molecular formula:

C₁₀₀H₂₀₃N₂₉O₁₅

M_w 2051.87

MALDI:

Not determined

NMR:

¹H-NMR (400 MHz, D₂O, 17.1 °C): δ = 0.72 - 0.83 (m, 6H, -CH₃, MyrA), 1.07 - 1.25 (m, 40H, -CH₂-, MyrA), 1.26 - 1.88 (m, 16H, δ-CH₂/γ-CH₂/β-CH₂, Lys; O=C-CH₂-CH₂-, MyrA), 2.10 - 2.29 (m, 4H, O=C-CH₂, MyrA), 2.40 - 2.52 (m, 18H, O=C-CH₂-, Stp), 2.52 - 2.60 (m, 2H, O=C-CH₂-,

Stp), 2.88 – 2.97 (t, $J=7.8$ Hz, 2H, ϵ -CH₂, Lys), 3.04 – 3.14 (m, 2H, ϵ -CH₂, Lys), 3.14 – 3.26 (m, 20H, N-CH₂-, Stp), 3.27 – 3.56 (m, 60H, N-CH₂-, Stp), 4.06 – 4.26 (m, 2H, O=C-C(R)H-NH-, Lys) ppm.

Sequence: HO-K-Stp₅-K-OleA₂

#: **27**

Molecular formula: C₁₀₈H₂₁₅N₂₉O₁₅

M_w 2160.05

MALDI: Not determined

NMR: ¹H-NMR (400 MHz, D₂O, 16.9 °C): δ = 0.65 – 0.83 (m, 6H, -CH₃, OleA), 1.02 – 1.30 (m, 40H, -CH₂-, OleA), 1.31 – 1.87 (m, 24H, β -CH₂/ δ -CH₂/ γ -CH₂, Lys; -CH₂-CH=CH-CH₂, O=C-CH₂-CH₂-, OleA), 1.92 – 1.99 (m, 4H, O=C-CH₂, OleA), 2.40 – 2.52 (m, 18H, O=C-CH₂-, Stp), 2.52 – 2.64 (m, 2H, O=C-CH₂-, Stp), 2.86 – 2.97 (m, 2H, ϵ -CH₂, Lys), 3.04 – 3.12 (m, 2H, ϵ -CH₂, Lys), 3.13 – 3.27 (m, 20H, N-CH₂-, Stp), 3.30 – 3.54 (m, 60H, N-CH₂-, Stp), 4.04 – 4.25 (m, 2H, O=C-C(R)H-NH-, Lys) ppm.

Sequence: HO-C-Stp₁-K-CapA₂

#: **30**

Molecular formula: C₃₇H₇₂N₈O₇S

M_w 773.08

FAB: 773.4 773.5 [M+H] calc.

NMR: ¹H-NMR (400 MHz, D₂O, 22.8 °C): δ = 0.78 – 0.92 (m, 6H, -CH₃, CapA), 1.20 – 1.32 (m, 16H, -CH₂-, CapA), 1.32 – 1.96 (m, 16H, δ -CH₂/ γ -CH₂/ β -CH₂, Lys; O=C-CH₂-CH₂-, CapA), 2.18 – 2.25 (m, 2H, O=C-CH₂, CapA), 2.25 – 2.40 (m, 2H, O=C-CH₂, CapA), 2.51 – 2.59 (m, 2H, O=C-CH₂-, Stp), 2.60 – 2.73 (m, 2H, O=C-CH₂-, Stp), 2.89 – 3.01 (m, 2H, β -CH₂-, Cys), 3.12 – 3.20 (t, $J=5.4$ Hz, 2H, ϵ -CH₂, Lys), 3.24 – 3.34 (m, 4H, N-CH₂-, Stp), 3.43 – 3.65 (m, 12H, N-CH₂-, Stp), 4.14 – 4.25 (m, 1H, O=C-C(R)H-NH-, Lys), 4.40 – 4.52 (m, 1H, O=C-C(R)H-NH-, Cys) ppm.

Sequence: HO-C-Stp₁-K-SteA₂

#: **31**

Molecular formula: C₅₇H₁₁₂N₈O₇S

M_w 1053.61

MALDI: 1054.0 1053.8 [M+H] calc.

NMR: ¹H-NMR (400 MHz, MeOD, 23.4 °C): δ = 0.85 – 0.94 (m, 6H, -CH₃, SteA), 1.20 – 1.32 (m, 56H, -CH₂-, SteA), 1.39 – 1.85 (m, 10H, δ -CH₂/ γ -CH₂/ β -CH₂, Lys; O=C-CH₂-CH₂-, SteA), 2.11 – 2.20 (m, 2H, O=C-CH₂,

SteA), 2.21 – 2.32 (m, 2H, O=C-CH₂, SteA), 2.45 - 2.55 (m, 2H, O=C-CH₂-, Stp), 2.56 - 2.73 (m, 2H, O=C-CH₂-, Stp), 2.84 - 2.93 (m, 2H, β-CH₂-, Cys), 3.05 – 3.34 (m, 18H, ε-CH₂, Lys; N-CH₂-, Stp), 4.06 – 4.15 (m, 1H, O=C-C(R)H-NH-, Lys), 4.42 – 4.55 (m, 1H, O=C-C(R)H-NH-, Cys) ppm.

Sequence: HO-K-Stp₂-ButA₁

#: **34**

Molecular formula:

C₃₄H₇₀N₁₂O₇

M_w 759.00

FAB:

759.8

759.6 [M+H] calc.

NMR:

¹H-NMR (400 MHz, D₂O, 17.3 °C): δ = 0.79 – 0.86 (t, J=7.4 Hz, 3H, -CH₃, ButA), 1.34 - 1.45 (m, 2H, γ-CH₂, Lys), 1.46 - 1.56 (m, 2H, -CH₂-, ButA), 1.56 - 1.87 (m, 4H, δ-CH₂/β-CH₂, Lys), 2.14 – 2.23 (t, J=7.4 Hz, 2H, O=C-CH₂, ButA), 2.44 - 2.51 (m, 6H, O=C-CH₂-, Stp), 2.51 - 2.60 (m, 2H, O=C-CH₂-, Stp), 2.87 – 2.96 (t, J=7.8 Hz, 2H, ε-CH₂, Lys), 3.15 – 3.26 (m, 8H, N-CH₂-, Stp), 3.37 – 3.54 (m, 12H, N-CH₂-, Stp), 4.18 – 4.27 (m, 1H, O=C-C(R)H-NH-, Lys) ppm.

Sequence: HO-K-Stp₂-CapA₁

#: **35**

Molecular formula:

C₃₈H₇₈N₁₂O₇

M_w 815.10

FAB:

815.6

815.6 [M+H] calc.

NMR:

¹H-NMR (400 MHz, D₂O, 16.7 °C): δ = 0.73 – 0.82 (m, 3H, -CH₃, CapA), 1.15 – 1.26 (m, 8H, -CH₂-, CapA), 1.34 - 1.44 (m, 2H, γ-CH₂, Lys), 1.45 - 1.56 (m, 2H, δ-CH₂, Lys) 1.57 - 1.66 (m, 2H, O=C-CH₂-CH₂-, CapA), 1.67 - 1.82 (m, 2H, β-CH₂, Lys), 2.15 – 2.24 (t, J=7.4 Hz, 2H, O=C-CH₂, CapA), 2.44 - 2.52 (m, 6H, O=C-CH₂-, Stp), 2.52 - 2.60 (m, 2H, O=C-CH₂-, Stp), 2.88 – 2.96 (t, J=7.8 Hz 2H, ε-CH₂, Lys), 3.16 – 3.25 (m, 8H, N-CH₂-, Stp), 3.37 – 3.51 (m, 24H, N-CH₂-, Stp), 4.16 – 4.25 (m, 1H, O=C-C(R)H-NH-, Lys) ppm.

Sequence: HO-K-Stp₂-MyrA₁

#: **36**

Molecular formula:

C₄₄H₉₀N₁₂O₇

M_w 899.26

ESI:

899.7128

899.7128 [M+H] calc.

NMR:

¹H-NMR (400 MHz, D₂O, 17.6 °C): δ = 0.74 – 0.81 (m, 3H, -CH₃, MyrA),

1.17 – 1.24 (m, 20H, $-\text{CH}_2-$, MyrA), 1.34 – 1.57 (m, 4H, $\delta\text{-CH}_2/\gamma\text{-CH}_2$, Lys), 1.56 – 1.66 (m, 2H, $\text{O}=\text{C}-\text{CH}_2-\text{CH}_2-$, MyrA), 1.67 – 1.83 (m, 2H, $\beta\text{-CH}_2$, Lys), 2.16 – 2.24 (t, $J=7.4$ Hz, 2H, $\text{O}=\text{C}-\text{CH}_2-$, MyrA), 2.44 – 2.52 (m, 6H, $\text{O}=\text{C}-\text{CH}_2-$, Stp), 2.52 – 2.58 (m, 2H, $\text{O}=\text{C}-\text{CH}_2-$, Stp), 2.88 – 2.96 (t, $J=7.8$ Hz, 2H, $\epsilon\text{-CH}_2$, Lys), 3.15 – 3.25 (m, 8H, $\text{N}-\text{CH}_2-$, Stp), 3.37 – 3.52 (m, 24H, $\text{N}-\text{CH}_2-$, Stp), 4.18 – 4.26 (m, 1H, $\text{O}=\text{C}-\text{C}(\text{R})\text{H}-\text{NH}-$, Lys) ppm.

Sequence: HO-K-Stp₂-OleA₁

#: **37**

Molecular formula:

$\text{C}_{48}\text{H}_{96}\text{N}_{12}\text{O}_7$

M_w 953.35

ESI:

953.7721

953.7596 [M+H] calc.

NMR:

^1H -NMR (400 MHz, D_2O , 16.1 °C): δ = 0.71 – 0.83 (m, 3H, $-\text{CH}_3$, OleA), 1.16 – 1.29 (m, 18H, $-\text{CH}_2-$, OleA), 1.31 – 1.82 (m, 12H, $\beta\text{-CH}_2$, $\delta\text{-CH}_2/\gamma\text{-CH}_2$, Lys; $-\text{CH}_2-\text{CH}=\text{CH}-\text{CH}_2-$, $\text{O}=\text{C}-\text{CH}_2-\text{CH}_2-$, OleA), 2.13 – 2.25 (m, 2H, $\text{O}=\text{C}-\text{CH}_2-$, OleA), 2.41 – 2.52 (m, 6H, $\text{O}=\text{C}-\text{CH}_2-$, Stp), 2.52 – 2.61 (m, 2H, $\text{O}=\text{C}-\text{CH}_2-$, Stp), 2.86 – 2.97 (m, 2H, $\epsilon\text{-CH}_2$, Lys), 3.12 – 3.25 (m, 8H, $\text{N}-\text{CH}_2-$, Stp), 3.36 – 3.53 (m, 24H, $\text{N}-\text{CH}_2-$, Stp), 4.16 – 4.24 (m, 1H, $\text{O}=\text{C}-\text{C}(\text{R})\text{H}-\text{NH}-$, Lys) ppm.

Sequence: HO-K-Stp₁-ButA₁

#: **38**

Molecular formula:

$\text{C}_{22}\text{H}_{45}\text{N}_7\text{O}_5$

M_w 487.64

MALDI:

488.5

488.4 [M+H] calc.

NMR:

^1H -NMR (400 MHz, D_2O , 17.3 °C): δ = 0.79 – 0.86 (t, $J=7.4$ Hz, 3H, $-\text{CH}_3$, ButA), 1.30 – 1.46 (m, 2H, $\gamma\text{-CH}_2$, Lys), 1.46 – 1.57 (m, 2H, $-\text{CH}_2-$, ButA), 1.58 – 1.85 (m, 4H, $\delta\text{-CH}_2/\beta\text{-CH}_2$, Lys), 2.14 – 2.21 (t, $J=7.4$ Hz, 2H, $\text{O}=\text{C}-\text{CH}_2$, ButA), 2.42 – 2.51 (m, 2H, $\text{O}=\text{C}-\text{CH}_2$, Stp), 2.51 – 2.62 (m, 2H, $\text{O}=\text{C}-\text{CH}_2$, Stp), 2.88 – 2.97 (t, $J=7.8$ Hz, 2H, $\epsilon\text{-CH}_2$, Lys), 3.15 – 3.26 (m, 4H, $\text{N}-\text{CH}_2$, Stp), 3.35 – 3.58 (m, 12H, $\text{N}-\text{CH}_2$, Stp), 4.10 – 4.18 (dd, $J=5.3, 8.8$, 1H, $\text{O}=\text{C}-\text{C}(\text{R})\text{H}-\text{NH}-$, Lys) ppm.

Sequence: HO-K-Stp₁-CapA₁

#: **39**

Molecular formula:

$\text{C}_{26}\text{H}_{53}\text{N}_7\text{O}_5$

M_w 543.74

FAB/ESI:

544.5/544.4174

544.5/544.4172 [M+H] calc.

NMR: $^1\text{H-NMR}$ (400 MHz, D_2O , 16.5 °C): δ = 0.73 – 0.82 (m, 3H, $-\text{CH}_3$, CapA), 1.15 – 1.25 (m, 8H, $-\text{CH}_2^-$, CapA), 1.32 – 1.56 (m, 4H, $\delta\text{-CH}_2/\gamma\text{-CH}_2$, Lys), 1.57 – 1.66 (m, 2H, $\text{O}=\text{C}-\text{CH}_2-\text{CH}_2^-$, CapA), 1.68 – 1.85 (m, 2H, $\beta\text{-CH}_2$, Lys), 2.15 – 2.25 (t, $J=7.4$ Hz, 2H, $\text{O}=\text{C}-\text{CH}_2$, CapA), 2.44 – 2.52 (m, 2H, $\text{O}=\text{C}-\text{CH}_2^-$, Stp), 2.52 – 2.62 (m, 2H, $\text{O}=\text{C}-\text{CH}_2^-$, Stp), 2.87 – 2.96 (t, $J=7.8$ Hz, 2H, $\varepsilon\text{-CH}_2$, Lys), 3.15 – 3.26 (m, 4H, $\text{N}-\text{CH}_2^-$, Stp), 3.36 – 3.55 (m, 12H, $\text{N}-\text{CH}_2^-$, Stp), 4.13 – 4.21 (dd, $J=5.4$, 8.8, 1H, $\text{O}=\text{C}-\text{C}(\text{R})\text{H}-\text{NH}-$, Lys) ppm.

Sequence: HO-K-Stp₁-MyrA₁

#: 40

Molecular formula:

$\text{C}_{32}\text{H}_{65}\text{N}_7\text{O}_5$

M_w 627.90

MALDI:

628.6

628.5 [M+H] calc.

NMR: $^1\text{H-NMR}$ (400 MHz, D_2O , 17.6 °C): δ = 0.76 – 0.84 (m, 3H, $-\text{CH}_3$, MyrA), 1.15 – 1.28 (m, 20H, $-\text{CH}_2^-$, MyrA), 1.35 – 1.57 (m, 4H, $\delta\text{-CH}_2/\gamma\text{-CH}_2$, Lys), 1.58 – 1.67 (m, 2H, $\text{O}=\text{C}-\text{CH}_2-\text{CH}_2^-$, MyrA), 1.68 – 1.85 (m, 2H, $\beta\text{-CH}_2$, Lys), 2.18 – 2.25 (t, $J=7.4$ Hz, 2H, $\text{O}=\text{C}-\text{CH}_2$, MyrA), 2.45 – 2.53 (m, 2H, $\text{O}=\text{C}-\text{CH}_2^-$, Stp), 2.54 – 2.64 (m, 2H, $\text{O}=\text{C}-\text{CH}_2^-$, Stp), 2.89 – 2.99 (t, $J=7.8$ Hz, 2H, $\varepsilon\text{-CH}_2$, Lys), 3.18 – 3.27 (m, 4H, $\text{N}-\text{CH}_2^-$, Stp), 3.39 – 3.59 (m, 12H, $\text{N}-\text{CH}_2^-$, Stp), 4.12 – 4.19 (dd, $J=5.4$, 8.8, 1H, $\text{O}=\text{C}-\text{C}(\text{R})\text{H}-\text{NH}-$, Lys) ppm.

Sequence: HO-K-Stp₁-OleA₁

#: 41

Molecular formula:

$\text{C}_{36}\text{H}_{71}\text{N}_7\text{O}_5$

M_w 681.99

FAB:

682.5

682.5 [M+H] calc.

NMR: $^1\text{H-NMR}$ (400 MHz, D_2O , 17.1 °C): δ = 0.9 – 0.85 (m, 3H, $-\text{CH}_3$, OleA), 0.99 – 1.3 (m, 18H, $-\text{CH}_2^-$, OleA), 1.31 – 1.82 (m, 12H, $\beta\text{-CH}_2/\delta\text{-CH}_2/\gamma\text{-CH}_2$, Lys; $-\text{CH}_2-\text{CH}=\text{CH}-\text{CH}_2$, $\text{O}=\text{C}-\text{CH}_2-\text{CH}_2^-$, OleA), 2.04 – 2.25 (m, 2H, $\text{O}=\text{C}-\text{CH}_2$, OleA), 2.39 – 2.64 (m, 4H, $\text{O}=\text{C}-\text{CH}_2^-$, Stp), 2.86 – 2.97 (m, 2H, $\varepsilon\text{-CH}_2$, Lys), 3.10 – 3.28 (m, 4H, $\text{N}-\text{CH}_2^-$, Stp), 3.32 – 3.58 (m, 12H, $\text{N}-\text{CH}_2^-$, Stp), 4.12 – 4.19 (m, 1H, $\text{O}=\text{C}-\text{C}(\text{R})\text{H}-\text{NH}-$, Lys), 6.63 – 6.94 (m, 2H, $-\text{CH}=\text{CH}-$) ppm.

Sequence: HO-C-Stp₃-C-K-MyrA₂

#: 45

Molecular formula: $C_{76}H_{151}N_{19}O_{12}S_2$ M_w 1587.26
 FAB: 1587.6 1587.1 [M+H] calc.
 NMR: 1H -NMR (400 MHz, D_2O , 17.2 °C): δ = 0.71 – 0.85 (m, 6H, $-CH_3$, MyrA), 1.05 – 1.31 (m, 40H, $-CH_2-$, MyrA), 1.26 – 1.90 (m, 16H, $\delta-CH_2/\gamma-CH_2/\beta-CH_2$, Lys; $O=C-CH_2-CH_2-$, MyrA), 2.08 – 2.33 (m, 4H, $O=C-CH_2$, MyrA), 2.40 – 2.55 (m, 10H, $O=C-CH_2-$, Stp), 2.54 – 2.67 (m, 2H, $O=C-CH_2-$, Stp), 2.80 – 3.10 (m, 6H, $\epsilon-CH_2$, Lys + Cys), 3.12 – 3.28 (m, 12H, $N-CH_2-$, Stp), 3.29 – 3.58 (m, 36H, $N-CH_2-$, Stp), 4.16 – 4.44 (m, 3H, $O=C-C(R)H-NH-$, Lys + Cys) ppm.

Sequence: HO-C-Stp₃-C-K-OleA₂ #: **46**
 Molecular formula: $C_{84}H_{163}N_{19}O_{12}S_2$ M_w 1695.44
 FAB: 1809.6 1808.2 [M+TFA] calc.
 NMR: 1H -NMR (400 MHz, D_2O , 17.3 °C): δ = 0.63 – 0.82 (m, 6H, $-CH_3$, OleA), 1.01 – 1.33 (m, 40H, $-CH_2-$, OleA), 1.34 – 1.89 (m, 18H, $\delta-CH_2/\gamma-CH_2/\beta-CH_2$, Lys; $-CH_2-CH=CH-CH_2$, $O=C-CH_2-CH_2-$; OleA), 1.90 – 1.97 (m, 4H, $O=C-CH_2$, OleA), 2.40 – 2.55 (m, 10H, $O=C-CH_2-$, Stp), 2.54 – 2.65 (m, 2H, $O=C-CH_2-$, Stp), 2.80 – 3.10 (m, 6H, $\epsilon-CH_2$, Lys + Cys), 3.12 – 3.28 (m, 12H, $N-CH_2-$, Stp), 3.29 – 3.61 (m, 36H, $N-CH_2-$, Stp), 4.16 – 4.45 (m, 3H, $O=C-C(R)H-NH-$, Lys + Cys) ppm.

Sequence: HO-C-Stp₂-K(K-MyrA₂)Stp₂-C-H #: **48**
 Molecular formula: $C_{94}H_{188}N_{26}O_{15}S_2$ M_w 1986.4
 MALDI: 1986.4 1986.4 [M+H] calc.
 NMR: 1H -NMR (400 MHz, D_2O , 16.7 °C): δ = 0.72 – 0.86 (m, 6H, $-CH_3$, MyrA), 1.07 – 1.29 (m, 40H, $-CH_2-$, MyrA), 1.29 – 1.95 (m, 16H, $\delta-CH_2/\gamma-CH_2/\beta-CH_2$, Lys; $O=C-CH_2-CH_2-$, MyrA), 2.08 – 2.28 (m, 4H, $O=C-CH_2-$, MyrA), 2.39 – 2.67 (m, 16H, $O=C-CH_2-$, Stp), 2.83 – 3.15 (m, 8H, $\epsilon-CH_2-$, Lys + Cys), 3.15 – 3.30 (m, 16H, $N-CH_2-$, Stp), 3.30 – 3.68 (m, 48H, Stp) 4.03 – 4.19 (m, 2H, $O=C-C(R)H-NH-$, Cys), 4.28 – 4.40 (m, 2H, $O=C-C(R)H-NH-$, Lys) ppm.

Sequence: HO-C-Stp₂-K(K-OleA₂)-Stp₂-C-H #: **49**

Molecular formula: $C_{102}H_{200}N_{26}O_{15}S_2$ M_w 2094.98
MALDI: 2094.9 2094.5 [M+H] calc.
NMR: 1H -NMR (400 MHz, D_2O , 16.7 °C): δ = 0.71 – 0.88 (m, 6H, $-CH_3$, OleA), 1.06 – 1.31 (m, 40H, $-CH_2-$, OleA), 1.31 – 1.92 (m, 10H, δ - CH_2/γ - CH_2/β - CH_2 , Lys; $-CH_2-CH=CH-CH_2$, $O=C-CH_2-CH_2-$; OleA), 2.05 – 2.27 (m, 2H, $O=C-CH_2-$, OleA), 2.40 – 2.69 (m, 16H, $O=C-CH_2-$, Stp), 2.81 – 3.14 (m, 8H, ϵ - CH_2 , Lys + Cys), 3.14 – 3.30 (m, 16H, $N-CH_2-$, Stp), 3.30 – 3.68 (m, 48H, $N-CH_2$ -Stp), 4.04 – 4.21 (m, 2H, $O=C-C(R)H-NH-$, Cys), 4.25 – 4.38 (m, 2H, $O=C-C(R)H-NH-$, Lys) ppm.

Sequence: HO-K-Stp₄-K-AraA₂ #: **50**
Molecular formula: $C_{100}H_{202}N_{24}O_{13}$ M_w 1948.83
MALDI: Not determined
NMR: 1H -NMR (400 MHz, D_2O , 17.0 °C): δ = 0.73 – 0.86 (m, 6H, $-CH_3$, AraA), 1.04 – 1.30 (m, 72H, $-CH_2-$, AraA), 1.31 – 1.98 (m, 16H, δ - CH_2/γ - CH_2/β - CH_2 , Lys; $O=C-CH_2-CH_2-$, AraA), 2.10 – 2.29 (m, 4H, $O=C-CH_2$, AraA), 2.38 – 2.52 (m, 14H, $O=C-CH_2-$, Stp), 2.52 – 2.62 (m, 2H, $O=C-CH_2-$, Stp), 2.87 – 2.98 (m, 2H, ϵ - CH_2 , Lys), 3.03 – 3.14 (m, 2H, ϵ - CH_2 , Lys), 3.09 – 3.30 (m, 16H, $N-CH_2-$, Stp), 3.31 – 3.57 (m, 48H, $N-CH_2-$, Stp), 4.04 – 4.24 (m, 2H, $O=C-C(R)H-NH-$, Lys) ppm.

Sequence: HO-C-Stp₃-C-K-H #: **51**
Molecular formula: $C_{48}H_{99}N_{19}O_{10}S_2$ M_w 1166.55
MALDI: 1167.3 1167.5 [M+H] calc.
NMR: 1H -NMR (400 MHz, D_2O , 17.3 °C): δ = 1.37 – 1.49 (m, 2H, δ - CH_2 , Lys), 1.59 – 1.71 (m, 2H, δ - CH_2 , Lys), 1.80 – 1.97 (m, 2H, β - CH_2 , Lys), 2.44 – 2.55 (m, 10H, $O=C-CH_2-$, Stp), 2.55 – 2.66 (m, 2H, $O=C-CH_2-$, Stp), 2.81 – 2.99 (m, 4H, ϵ - CH_2 , Lys + Cys), 3.13 – 3.29 (m, 12H, $N-CH_2-$, Stp), 3.33 – 3.58 (m, 36H, Stp), 3.96 – 4.05 (m, 1H, $O=C-C(R)H-NH-$, Lys), 4.33 – 4.46 (m, 2H, $O=C-C(R)H-NH-$, Lys) ppm.

Sequence: HO-C-Stp₂-K(CapA)-Stp₂-C-H #: **56**
Molecular formula: $C_{68}H_{138}N_{24}O_{13}S_2$ M_w 1564.11

MALDI: 1564.4 1564.1 [M+H] calc.

NMR: $^1\text{H-NMR}$ (400 MHz, D_2O , 16.6 $^\circ\text{C}$): δ = 0.73 – 0.83 (m, 3H, $-\text{CH}_3$, CapA), 1.13 – 1.28 (m, 8H, $-\text{CH}_2$ -, CapA), 1.29 – 1.92 (m, 8H, $\delta\text{-CH}_2/\gamma\text{CH}_2/\beta\text{-CH}_2$, Lys; $\text{O}=\text{C}-\text{CH}_2-\text{CH}_2$ -, CapA), 2.11 – 2.20 (t, $J=7.3$ Hz, 2H, $\text{O}=\text{C}-\text{CH}_2$ -, CapA), 2.42 – 2.68 (m, 16H, $\text{O}=\text{C}-\text{CH}_2$ -, Stp), 2.84 – 3.14 (m, 6H, $\epsilon\text{-CH}_2$, Lys + Cys), 3.14 – 3.29 (m, 16H, $\text{N}-\text{CH}_2$ -, Stp), 3.30 – 3.59 (m, 48H, Stp), 4.09 – 4.18 (m, 2H, $\text{O}=\text{C}-\text{C}(\text{R})\text{H}-\text{NH}$ -, Cys), 4.28 – 4.39 (m, 1H, $\text{O}=\text{C}-\text{C}(\text{R})\text{H}-\text{NH}$ -, Lys) ppm.

Sequence: HO-C-Stp₂-K(Myra)-Stp₂-C-H #: **57**

Molecular formula: $\text{C}_{74}\text{H}_{150}\text{N}_{24}\text{O}_{13}\text{S}_2$ M_w 1648.26

MALDI: 1648.4 1648.1 [M+H] calc.

NMR: $^1\text{H-NMR}$ (400 MHz, D_2O , 16.6 $^\circ\text{C}$): δ = 0.73 – 0.83 (m, 3H, $-\text{CH}_3$, Myra), 1.11 – 1.22 (m, 20H, $-\text{CH}_2$ -, Myra), 1.23 – 1.92 (m, 8H, $\delta\text{-CH}_2/\gamma\text{CH}_2/\beta\text{-CH}_2$, Lys; $\text{O}=\text{C}-\text{CH}_2-\text{CH}_2$ -, Myra), 2.11 – 2.20 (t, $J=7.3$ Hz, 2H, $\text{O}=\text{C}-\text{CH}_2$ -, Myra), 2.41 – 2.70 (m, 16H, $\text{O}=\text{C}-\text{CH}_2$ -, Stp), 2.84 – 3.13 (m, 6H, $\epsilon\text{-CH}_2$, Lys + Cys), 3.15 – 3.29 (m, 16H, $\text{N}-\text{CH}_2$ -, Stp), 3.29 – 3.68 (m, 48H, Stp), 4.09 – 4.20 (m, 2H, $\text{O}=\text{C}-\text{C}(\text{R})\text{H}-\text{NH}$ -, Cys), 4.26 – 4.39 (m, 1H, $\text{O}=\text{C}-\text{C}(\text{R})\text{H}-\text{NH}$ -, Lys) ppm.

Sequence: HO-C-Stp₂-K(OleA)-Stp₂-C-H #: **58**

Molecular formula: $\text{C}_{78}\text{H}_{156}\text{N}_{24}\text{O}_{13}\text{S}_2$ M_w 1702.35

MALDI: 1702.6 1702.4 [M+H] calc.

NMR: $^1\text{H-NMR}$ (400 MHz, D_2O , 16.7 $^\circ\text{C}$): δ = 0.73 – 0.83 (m, 3H, $-\text{CH}_3$, OleA), 1.10 – 1.31 (m, 20H, $-\text{CH}_2$ -, OleA), 1.32 – 1.99 (m, 10H, $\delta\text{-CH}_2/\gamma\text{CH}_2/\beta\text{-CH}_2$, Lys; $-\text{CH}_2-\text{CH}=\text{CH}-\text{CH}_2$, $\text{O}=\text{C}-\text{CH}_2-\text{CH}_2$ -, OleA), 2.10 – 2.20 (t, $J=7.3$ Hz, 2H, $\text{O}=\text{C}-\text{CH}_2$ -, OleA), 2.40 – 2.66 (m, 16H, $\text{O}=\text{C}-\text{CH}_2$ -, Stp), 2.84 – 3.13 (m, 6H, $\epsilon\text{-CH}_2$, Lys + Cys), 3.14 – 3.30 (m, 16H, $\text{N}-\text{CH}_2$ -, Stp), 3.31 – 3.61 (m, 48H, Stp), 4.10 – 4.18 (m, 2H, $\text{O}=\text{C}-\text{C}(\text{R})\text{H}-\text{NH}$ -, Cys), 4.32 – 4.45 (m, 1H, $\text{O}=\text{C}-\text{C}(\text{R})\text{H}-\text{NH}$ -, Lys) ppm.

Sequence: HO-C-Stp₂-K(AraA)-Stp₂-C-H #: **59**

Molecular formula: $\text{C}_{80}\text{H}_{162}\text{N}_{24}\text{O}_{13}\text{S}_2$ M_w 1732.43

MALDI: 1732.4 1732.2 [M+H] calc.

NMR: $^1\text{H-NMR}$ (400 MHz, D_2O , 16.6 $^\circ\text{C}$): δ = 0.73 – 0.83 (m, 3H, $-\text{CH}_3$, AraA), 1.12 – 1.31 (m, 36H, $-\text{CH}_2-$, AraA), 1.32 – 1.99 (m, 8H, $\delta\text{-CH}_2/\gamma\text{CH}_2/\beta\text{-CH}_2$, Lys; $\text{O}=\text{C-CH}_2\text{-CH}_2-$, AraA), 2.11 – 2.20 (t, $J=7.4$ Hz, 2H, $\text{O}=\text{C-CH}_2-$, AraA), 2.42 – 2.68 (m, 16H, $\text{O}=\text{C-CH}_2-$, Stp), 2.83 – 3.13 (m, 6H, $\epsilon\text{-CH}_2$, Lys + Cys), 3.14 – 3.30 (m, 16H, N-CH_2- , Stp), 3.31 – 3.64 (m, 48H, Stp), 4.10 – 4.18 (m, 2H, $\text{O}=\text{C-C(R)H-NH-}$, Cys), 4.32 – 4.45 (m, 1H, $\text{O}=\text{C-C(R)H-NH-}$, Lys) ppm.

Sequence: HO-C-Stp₂-K(K-AraA₂)-Stp₂-C-H #: **62**

Molecular formula: $\text{C}_{106}\text{H}_{212}\text{N}_{26}\text{O}_{15}\text{S}_2$ M_w 2155.11

MALDI: 2152.2 2156.1 [M+H] calc.

NMR: $^1\text{H-NMR}$ (400 MHz, D_2O , 16.6 $^\circ\text{C}$): δ = 0.73 – 0.83 (m, 6H, $-\text{CH}_3$, AraA), 1.12 – 1.31 (m, 72H, $-\text{CH}_2-$, AraA), 1.32 – 1.99 (m, 16H, $\delta\text{-CH}_2/\gamma\text{CH}_2/\beta\text{-CH}_2$, Lys; $\text{O}=\text{C-CH}_2\text{-CH}_2-$, AraA), 2.11 – 2.20 (m, 4H, $\text{O}=\text{C-CH}_2-$, AraA), 2.42 – 2.68 (m, 16H, $\text{O}=\text{C-CH}_2-$, Stp), 2.83 – 3.13 (m, 6H, $\epsilon\text{-CH}_2$, Lys + Cys), 3.14 – 3.30 (m, 16H, N-CH_2- , Stp), 3.31 – 3.64 (m, 48H, Stp), 4.10 – 4.18 (m, 2H, $\text{O}=\text{C-C(R)H-NH-}$, Cys), 4.32 – 4.45 (m, 1H, $\text{O}=\text{C-C(R)H-NH-}$, Lys) ppm.

Sequence: HO-C-Stp₂-K(K-CapA₂)-Stp₂-C-H #: **66**

Molecular formula: $\text{C}_{82}\text{H}_{164}\text{N}_{26}\text{O}_{15}\text{S}_2$ M_w 1818.48

MALDI: 1816.6 1818.2 [M+H] calc.

NMR: $^1\text{H-NMR}$ (400 MHz, D_2O , 16.7 $^\circ\text{C}$): δ = 0.73 – 0.83 (m, 6H, $-\text{CH}_3$, CapA), 1.13 – 1.28 (m, 16H, $-\text{CH}_2-$, CapA), 1.29 – 1.92 (m, 16H, $\delta\text{-CH}_2/\gamma\text{CH}_2/\beta\text{-CH}_2$, Lys; $\text{O}=\text{C-CH}_2\text{-CH}_2-$, CapA), 2.11 – 2.20 (t, $J=7.4$ Hz, 2H, $\text{O}=\text{C-CH}_2\text{-CH}_2-$, CapA), 2.11 – 2.20 (m, 2H, $\text{O}=\text{C-CH}_2\text{-CH}_2-$, CapA), 2.42 – 2.68 (m, 16H, $\text{O}=\text{C-CH}_2-$, Stp), 2.84 – 3.14 (m, 8H, $\epsilon\text{-CH}_2$, Lys + Cys), 3.14 – 3.29 (m, 16H, N-CH_2- , Stp), 3.30 – 3.59 (m, 48H, Stp), 4.09 – 4.18 (m, 2H, $\text{O}=\text{C-C(R)H-NH-}$, Cys), 4.28 – 4.39 (m, 1H, $\text{O}=\text{C-C(R)H-NH-}$, Lys) ppm.

Sequence: HO-C-Stp₂-K-MyrA₂ #: **67**

Molecular formula: $C_{61}H_{121}N_{13}O_9S$ M_w 1212.76
MALDI: 1213.4 1213.7 [M+H] calc.
NMR: 1H -NMR (400 MHz, D_2O , 16.7 °C): δ = 0.70 – 0.84 (m, 6H, $-CH_3$, MyrA), 1.08 – 1.32 (m, 40H, $-CH_2-$, MyrA), 1.32 – 1.97 (m, 10H, δ - CH_2/γ - CH_2/β - CH_2 , Lys; $O=C-CH_2-CH_2-$, MyrA), 2.11 – 2.32 (m, 4H, $O=C-CH_2$, MyrA), 2.41 – 2.55 (m, 6H, $O=C-CH_2-$, Stp), 2.55 – 2.67 (m, 2H, $O=C-CH_2-$, Stp), 2.83 – 2.97 (m, 2H, β - CH_2- , Cys), 3.04 – 3.17 (m, 2H, ϵ - CH_2 , Lys), 3.14 – 3.29 (m, 8H, $N-CH_2-$, Stp), 3.29 – 3.60 (m, 24H, $N-CH_2-$, Stp), 4.07 – 4.24 (m, 1H, $O=C-C(R)H-NH-$, Lys), 4.24 – 4.40 (m, 1H, $O=C-C(R)H-NH-$, Cys) ppm.

Sequence: HO-C-K-Stp₂-K-MyrA₂ #: **68**
Molecular formula: $C_{67}H_{133}N_{15}O_{10}S$ M_w 1340.93
MALDI: 1341.3 1341.0 [M+H] calc.
NMR: 1H -NMR (400 MHz, D_2O , 16.7 °C): δ = 0.70 – 0.84 (m, 6H, $-CH_3$, MyrA), 1.08 – 1.32 (m, 40H, $-CH_2-$, MyrA), 1.32 – 1.97 (m, 10H, δ - CH_2/γ - CH_2/β - CH_2 , Lys; $O=C-CH_2-CH_2-$, MyrA), 2.11 – 2.32 (m, 4H, $O=C-CH_2$, MyrA), 2.41 – 2.55 (m, 6H, $O=C-CH_2-$, Stp), 2.55 – 2.67 (m, 2H, $O=C-CH_2-$, Stp), 2.83 – 2.97 (m, 2H, β - CH_2- , Cys), 3.04 – 3.17 (m, 2H, ϵ - CH_2 , Lys), 3.14 – 3.29 (m, 8H, $N-CH_2-$, Stp), 3.29 – 3.60 (m, 24H, $N-CH_2-$, Stp), 4.07 – 4.24 (m, 1H, $O=C-C(R)H-NH-$, Lys), 4.24 – 4.40 (m, 1H, $O=C-C(R)H-NH-$, Cys) ppm.

Sequence: HO-C-K-Stp₂-K-OleA₂ #: **69**
Molecular formula: $C_{75}H_{145}N_{15}O_{10}S$ M_w 1449.11
MALDI: 1449.5 1449.1 [M+H] calc.
NMR: 1H -NMR (400 MHz, MeOD, 16.8 °C): δ = 0.78 – 0.88 (m, 6H, $-CH_3$, OleA), 1.12 – 1.35 (m, 40H, $-CH_2-$, OleA), 1.34 – 1.89 (m, 18H, δ - CH_2/γ - CH_2/β - CH_2 , Lys; $-CH_2-CH=CH-CH_2$, $O=C-CH_2-CH_2-$; OleA), 1.90 – 1.97 (m, 4H, $O=C-CH_2$, OleA), 2.40 – 2.55 (m, 10H, $O=C-CH_2-$, Stp), 2.54 – 2.65 (m, 2H, $O=C-CH_2-$, Stp), 2.80 – 3.10 (m, 6H, ϵ - CH_2 , Lys + Cys), 3.12 – 3.28 (m, 12H, $N-CH_2-$, Stp), 3.29 – 3.61 (m, 36H, $N-CH_2-$, Stp), 4.16 – 4.45 (m, 3H, $O=C-C(R)H-NH-$, Lys + Cys) ppm.

Sequence: HO-C-Stp₂-K-OleA₂#: **70**

Molecular formula:

C₆₉H₁₃₃N₁₃O₉SM_w 1320.94

MALDI:

1321.3

1321.0 [M+H] calc.

NMR:

¹H-NMR (400 MHz, MeOD, 16.8 °C): δ = 0.85 – 0.96 (m, 6H, -CH₃, OleA), 1.21 – 1.40 (m, 40H, -CH₂-, OleA), 1.41 – 1.92 (m, 10H, δ-CH₂/γ-CH₂/β-CH₂, Lys; -CH₂-CH=CH-CH₂, O=C-CH₂-CH₂-, OleA), 1.93 – 2.07 (m, 4H, O=C-CH₂, OleA), 2.41 – 2.57 (m, 6H, O=C-CH₂-, Stp), 2.57 – 2.74 (m, 2H, O=C-CH₂-, Stp), 2.85 – 3.08 (m, 2H, β-CH₂-, Cys), 3.08 – 3.19 (m, 2H, ε-CH₂, Lys), 3.19 – 3.72 (m, 32H, N-CH₂-, Stp), 4.04 – 4.17 (m, 1H, O=C-C(R)H-NH-, Lys), 4.14 – 4.57 (m, 1H, O=C-C(R)H-NH-, Cys) ppm.

Sequence: C-Stp₁-K(K-MyrA₂)-Stp₁-C-H#: **71**

Molecular formula:

C₇₀H₁₃₈N₁₆O₁₁S₂M_w 1444.07

MALDI:

Not determined

NMR:

¹H-NMR (400 MHz, MeOD, 17.0 °C): δ = 0.86 – 0.95 (m, 6H, -CH₃, MyrA), 1.22 – 1.38 (m, 40H, -CH₂-, MyrA), 1.29 – 1.95 (m, 16H, δ-CH₂/γ-CH₂/β-CH₂, Lys; O=C-CH₂-CH₂-, MyrA), 2.13 – 2.20 (m, 2H, O=C-CH₂-, MyrA), 2.20 – 2.30 (m, 2H, O=C-CH₂-, MyrA), 2.43 – 2.71 (m, 8H, O=C-CH₂-, Stp), 2.84 – 3.10 (m, 8H, ε-CH₂-, Lys + Cys), 3.11 – 3.64 (m, 32H, N-CH₂-, Stp), 3.94 – 4.25 (m, 2H, O=C-C(R)H-NH-, Cys), 4.44 – 4.56 (m, 2H, O=C-C(R)H-NH-, Lys) ppm.

Sequence: HO-C-Stp₁-K(K)-Stp₁-C-H#: **72**

Molecular formula:

C₄₂H₈₆N₁₆O₉S₂M_w 1023.36

MALDI:

1024.5

1024.4 [M+H] calc.

NMR:

¹H-NMR (400 MHz, D₂O, 17.0 °C): δ = 1.37 – 1.97 (m, 12H, δ-CH₂/γ-CH₂/β-CH₂, Lys), 2.41 – 2.64 (m, 8H, O=C-CH₂-, Stp), 2.84 – 3.11 (m, 8H, ε-CH₂, Lys + Cys), 3.17 – 3.29 (m, 8H, N-CH₂-, Stp), 3.35 – 3.70 (m, 24H, Stp), 4.10 – 4.17 (m, 2H, O=C-C(R)H-NH-, Cys), 4.38 – 4.48 (m, 2H, O=C-C(R)H-NH-, Lys) ppm.

Sequence: HO-C-Stp₁-K(K-SteA₂)-Stp₁-C-H#: **73**

Molecular formula: $C_{78}H_{154}N_{16}O_{11}S_2$ M_w 1556.28
MALDI: 1554.4 1556.1 [M+H] calc.
NMR: 1H -NMR (400 MHz, MeOD, 17.0 °C): δ = 0.86 – 0.97 (m, 6H, $-CH_3$, SteA), 1.20 – 1.43 (m, 56H, $-CH_2-$, SteA), 1.43 - 1.97 (m, 20H, δ - CH_2/γ - CH_2/β - CH_2 , Lys; O=C- CH_2 - CH_2- , SteA), 2.11 – 2.36 (m, 4H, O=C- CH_2- , SteA), 2.42 - 2.74 (m, 8H, O=C- CH_2- , Stp), 2.83 – 3.11 (m, 8H, ϵ - CH_2- , Lys + Cys), 3.11 – 3.64 (m, 32H, N- CH_2- , Stp), 3.94 – 4.06 (m, 1H, O=C-C(R) \underline{H} -NH-, Cys), 4.08 – 4.25 (m, 1H, O=C-C(R) \underline{H} -NH-, Cys) 4.42 – 4.57 (m, 2H, O=C-C(R) \underline{H} -NH-, Lys) ppm.

Sequence: HO-C-Stp₁-K(K-OleA₂)-Stp₁-C-H #: **74**
Molecular formula: $C_{78}H_{150}N_{16}O_{11}S_2$ M_w 1552.25
MALDI: 1552.5 1552.1 [M+H] calc.
NMR: 1H -NMR (400 MHz, D₂O, 16.7 °C): δ = 0.86 – 0.95 (m, 6H, $-CH_3$, OleA), 1.01 – 1.40 (m, 40H, $-CH_2-$, OleA), 1.41 - 1.92 (m, 24H, δ - CH_2/γ - CH_2/β - CH_2 , Lys; $-CH_2$ -CH=CH- CH_2 , O=C- CH_2 - CH_2- ; OleA), 2.12 – 2.32 (m, 4H, O=C- CH_2- , OleA), 2.44 - 2.73 (m, 16H, O=C- CH_2- , Stp), 2.81 – 3.22 (m, 8H, ϵ - CH_2 , Lys + Cys), 3.22 – 3.63 (m, 32H, N- CH_2- , Stp), 3.99 – 4.25 (m, 2H, O=C-C(R) \underline{H} -NH-, Cys), 4.45 – 4.60 (m, 2H, O=C-C(R) \underline{H} -NH-, Lys), 7.05 – 7.33 (m, 4H, $-CH=CH-$, OleA) ppm.

Sequence: HO-C-Stp₃-K(K-MyrA₂)-Stp₃-C-H #: **75**
Molecular formula: $C_{118}H_{238}N_{36}O_{19}S_2$ M_w 2529.51
MALDI: 2529.3 2528.8 [M+H] calc.
NMR: 1H -NMR (400 MHz, D₂O, 17.3 °C): δ = 0.72 – 0.84 (m, 6H, $-CH_3$, MyrA), 1.10 – 1.30 (m, 40H, $-CH_2-$, MyrA), 1.31 - 1.96 (m, 16H, δ - CH_2/γ - CH_2/β - CH_2 , Lys; O=C- CH_2 - CH_2- , MyrA), 2.12 – 2.27 (m, 4H, O=C- CH_2- , MyrA), 2.41 - 2.66 (m, 24H, O=C- CH_2- , Stp), 2.85 – 3.15 (m, 8H, ϵ - CH_2- , Lys + Cys), 3.15 – 3.30 (m, 24H, N- CH_2- , Stp), 3.30 – 3.63 (m, 72H, N- CH_2- , Stp) 4.03 – 4.20 (m, 2H, O=C-C(R) \underline{H} -NH-, Cys), 4.28 – 4.39 (m, 2H, O=C-C(R) \underline{H} -NH-, Lys) ppm.

Sequence: HO-C-Stp₃-K(K)-Stp₃-C-H #: **76**

Molecular formula: $C_{90}H_{186}N_{36}O_{17}S_2$ M_w 2108.80
MALDI: 2108.8 2109.8 [M+H] calc.
NMR: 1H -NMR (400 MHz, D_2O , 17.0 °C): δ = 1.28 - 1.92 (m, 12H, δ -CH₂/ γ -CH₂/β-CH₂, Lys), 2.41 - 2.66 (m, 24H, O=C-CH₂-, Stp), 2.84 - 3.11 (m, 8H, ε-CH₂, Lys + Cys), 3.17 - 3.29 (m, 24H, N-CH₂-, Stp), 3.35 - 3.70 (m, 72H, Stp) 4.10 - 4.20 (m, 2H, O=C-C(R)H-NH-, Cys), 4.38 - 4.48 (m, 2H, O=C-C(R)H-NH-, Lys) ppm.

Sequence: HO-C-Stp₃-K(K-SteA₂)-Stp₃-C-H #: **77**
Molecular formula: $C_{126}H_{254}N_{36}O_{19}S_2$ M_w 2641.72
MALDI: 2641.4 2640.9 [M+H] calc.
NMR: 1H -NMR (400 MHz, D_2O , 17.1 °C): δ = 0.72 - 0.86 (m, 6H, -CH₃, SteA), 1.06 - 1.31 (m, 56H, -CH₂-, SteA), 1.31 - 1.94 (m, 16H, δ -CH₂/ γ -CH₂/β-CH₂, Lys; O=C-CH₂-CH₂-, SteA), 2.09 - 2.27 (m, 4H, O=C-CH₂-, SteA), 2.40 - 2.68 (m, 24H, O=C-CH₂-, Stp), 2.80 - 3.13 (m, 8H, ε-CH₂-, Lys + Cys), 3.31 - 3.29 (m, 24H, N-CH₂-, Stp), 3.31 - 3.68 (m, 72H, N-CH₂-, Stp), 4.06 - 4.20 (m, 2H, O=C-C(R)H-NH-, Cys), 4.30 - 4.44 (m, 2H, O=C-C(R)H-NH-, Lys) ppm.

Sequence: HO-C-Stp₃-K(K-OleA₂)-Stp₃-C-H #: **78**
Molecular formula: $C_{126}H_{250}N_{36}O_{19}S_2$ M_w 2637.69
MALDI: 2635.8 2638.7 [M+H] calc.
NMR: 1H -NMR (400 MHz, D_2O , 17.3 °C): δ = 0.74 - 0.86 (m, 6H, -CH₃, OleA), 1.06 - 1.33 (m, 40H, -CH₂-, OleA), 1.33 - 1.99 (m, 24H, δ -CH₂/ γ -CH₂/β-CH₂, Lys; -CH₂-CH=CH-CH₂, O=C-CH₂-CH₂-, OleA), 2.07 - 2.30 (m, 4H, O=C-CH₂-, OleA), 2.40 - 2.66 (m, 24H, O=C-CH₂-, Stp), 2.83 - 3.14 (m, 8H, ε-CH₂, Lys + Cys), 3.14 - 3.30 (m, 24H, N-CH₂-, Stp), 3.30 - 3.65 (m, 72H, N-CH₂-, Stp) 4.04 - 4.14 (m, 2H, O=C-C(R)H-NH-, Cys), 4.29 - 4.41 (m, 2H, O=C-C(R)H-NH-, Lys)

Sequence: HO-C-Stp₄-K(K-MyrA₂)-Stp₄-C-H #: **79**
Molecular formula: $C_{142}H_{288}N_{46}O_{23}S_2$ M_w 3072.23

MALDI: 3069.9 3071.2 [M+H] calc.

NMR: $^1\text{H-NMR}$ (400 MHz, D_2O , 17.1 °C): δ = 0.72 – 0.83 (m, 6H, $-\text{CH}_3$, MyrA), 1.11 – 1.29 (m, 40H, $-\text{CH}_2-$, MyrA), 1.29 – 1.95 (m, 16H, $\delta\text{-CH}_2/\gamma\text{CH}_2/\beta\text{-CH}_2$, Lys; $\text{O}=\text{C-CH}_2\text{-CH}_2-$, MyrA), 2.10 – 2.28 (m, 4H, $\text{O}=\text{C-CH}_2-$, MyrA), 2.42 – 2.65 (m, 32H, $\text{O}=\text{C-CH}_2-$, Stp), 2.85 – 3.15 (m, 8H, $\epsilon\text{-CH}_2-$, Lys + Cys), 3.15 – 3.30 (m, 32H, N-CH_2- , Stp), 3.30 – 3.60 (m, 96H, N-CH_2- , Stp) 4.03 – 4.20 (m, 2H, $\text{O}=\text{C-C(R)H-NH-}$, Cys), 4.26 – 4.38 (m, 2H, $\text{O}=\text{C-C(R)H-NH-}$, Lys) ppm.

Sequence: HO-C-Stp₄-K(K)-Stp₄-C-H #: **80**

Molecular formula: $\text{C}_{112}\text{H}_{234}\text{N}_{48}\text{O}_{21}\text{S}_2$ M_w 2653.50

MALDI: Not determined

NMR: $^1\text{H-NMR}$ (400 MHz, D_2O , 17.0 °C): δ = 1.27 – 1.90 (m, 12H, $\delta\text{-CH}_2/\gamma\text{CH}_2/\beta\text{-CH}_2$, Lys), 2.40 – 2.67 (m, 24H, $\text{O}=\text{C-CH}_2-$, Stp), 2.84 – 3.04 (m, 8H, $\epsilon\text{-CH}_2$, Lys + Cys), 3.10 – 3.27 (m, 32H, N-CH_2- , Stp), 3.35 – 3.70 (m, 96H, Stp) 4.07 – 4.19 (m, 2H, $\text{O}=\text{C-C(R)H-NH-}$, Cys), 4.28 – 4.38 (m, 2H, $\text{O}=\text{C-C(R)H-NH-}$, Lys) ppm.

Sequence: HO-C-Stp₄-K(K-SteA₂)-Stp₄-C-H #: **81**

Molecular formula: $\text{C}_{150}\text{H}_{304}\text{N}_{46}\text{O}_{23}\text{S}_2$ M_w 3184.44

MALDI: 3188.5 3185.4 [M+H] calc.

NMR: $^1\text{H-NMR}$ (400 MHz, D_2O , 17.1 °C): δ = 0.74 – 0.85 (m, 6H, $-\text{CH}_3$, SteA), 1.08 – 1.30 (m, 56H, $-\text{CH}_2-$, SteA), 1.29 – 1.95 (m, 16H, $\delta\text{-CH}_2/\gamma\text{CH}_2/\beta\text{-CH}_2$, Lys; $\text{O}=\text{C-CH}_2\text{-CH}_2-$, SteA), 2.09 – 2.27 (m, 4H, $\text{O}=\text{C-CH}_2-$, SteA), 2.39 – 2.66 (m, 32H, $\text{O}=\text{C-CH}_2-$, Stp), 2.80 – 3.12 (m, 8H, $\epsilon\text{-CH}_2-$, Lys + Cys), 3.12 – 3.29 (m, 32H, N-CH_2- , Stp), 3.29 – 3.62 (m, 96H, Stp) 4.01 – 4.19 (m, 2H, $\text{O}=\text{C-C(R)H-NH-}$, Cys), 4.20 – 4.38 (m, 2H, $\text{O}=\text{C-C(R)H-NH-}$, Lys) ppm.

Sequence: HO-C-Stp₄-K(K-OleA₂)-Stp₄-C-H #: **82**

Molecular formula: $\text{C}_{148}\text{H}_{298}\text{N}_{48}\text{O}_{23}\text{S}_2$ M_w 3182.39

MALDI: 3182.4 3182.5 [M+H] calc.

NMR: $^1\text{H-NMR}$ (400 MHz, D_2O , 17.3 °C): δ = 0.73 – 0.87 (m, 6H, $-\text{CH}_3$, OleA),

1.10 – 1.36 (m, 40H, -CH₂-, OleA), 1.36 - 1.99 (m, 24H, δ-CH₂/γ-CH₂/β-CH₂, Lys; -CH₂-CH=CH-CH₂, O=C-CH₂-CH₂-; OleA), 2.07 – 2.29 (m, 4H, O=C-CH₂-, OleA), 2.40 - 2.70 (m, 32H, O=C-CH₂-, Stp), 2.72 – 3.13 (m, 8H, ε-CH₂, Lys + Cys), 3.14 – 3.30 (m, 32H, N-CH₂-, Stp), 3.30 – 3.65 (m, 96H, N-CH₂-, Stp) 4.01 – 4.21 (m, 2H, O=C-C(R)H-NH-, Cys), 4.21 – 4.40 (m, 2H, O=C-C(R)H-NH-, Lys) ppm.

Sequence:	HO-IVNQPTYGYWHY-Stp ₂ -H	#:	GE11-Stp ₂
Molecular formula:	C ₉₉ H ₁₄₇ N ₂₇ O ₂₃	M _w	2083.4
MALDI:	2084.9	2084.4 [M+H] calc.	t _r =24.34 min

Sequence:	HO-IVNQPTYGYWHY-H	#:	GE11
Molecular formula:	C ₇₅ H ₉₇ N ₁₇ O ₁₉	M _w	1540.7
MALDI:	1541.6	1541.6 [M+H] calc.	t _r =16.39 min

8.8 Publications

Original Papers

Schaffert D, Dohmen C, Wagner E, *Polymers for Nucleic Acid Delivery*, European Patent Application (EP10165502.5) in cooperation with Roche Kulmbach

Schaffert D, Kiss M, Roedl W, Shir A, Levitzki A, Ogris M, Wagner E, *Poly(l:C) mediated tumor growth suppression in EGF-receptor overexpressing tumors using EGF-polyethylene glycol-linear polyethyleneimine as carrier*, Pharm. Res., in press

Schloßbauer A, Schaffert D, Knecht J, Wagner E, Bein T; *Click Chemistry for High-Density Biofunctionalization of Mesoporous Silica*, J. Am. Chem. Soc. 130, 12558, 2008

Klutz K, Schaffert D, Willhauck MJ, Knoop K, Grünwald GK, Rödl W, Wunderlich N, Zach C, Gildehaus FJ, Senekowitsch-Schmidtke R, Göke B, Wagner E, Ogris M, Spitzweg C, *Radioiodine Therapy following Systemic Sodium Iodide Symporter Gene Transfer in Hepatocellular Carcinoma using EGF Receptor-targeted Nonviral Gene Delivery*, submitted

Schlossbauer A, Dohmen C, Schaffert D, Wagner E, Bein T, *pH-Responsive Release of Acetal-Linked Mellitin from SBA-15 Mesoporous Silica*, submitted to J. Am. Chem. Soc.

Reviews

Schaffert D, Wagner E; *Gene Therapy: progress and prospects: synthetic polymer-based systems*, Gene Therapy 2008, 15, 1131, 2008

Manuscripts in Preparation

Schaffert D, Badgujar N, Wagner E; *Novel, Fmoc-Polyamino Acids for Solid-Phase Synthesis of Defined Polyamidoamines*, in preparation

Schaffert, D, Troiber C, Wagner E; *Modular constructed Polyamidoamines for Gene Delivery*, in preparation

Kasper JC, Schaffert D, Ogris M, Wagner E, Friess W, *Up-scaled Preparation and Development of a Lyophilized Formulation with Long-Term Stability for Plasmid/LPEI Polyplexes – A Step Closer from Promising Technology to Clinical Application*, in preparation

Poster Presentations

Schaffert D, Kiss M, Roedl W, Shir A, Ogris M, Wagner E, *Poly-IC mediated killing of glioblastoma cells with novel, EGF-receptor targeted conjugates based on polyethyleneimine*, Poster Presentation at Cellular Delivery of Therapeutic Macromolecules 2008, Cardiff

Schaffert D, Kiss M, Roedl W, Shir A, Ogris M, Wagner E, *Poly-IC mediated tumor growth suppression using novel, targeted polyethyleneimine based carriers in an EGF-receptor overexpressing therapeutic model*, Poster Presentation at the Nanoman Summarizing Workshop 2009, Venice

8.9 Curriculum Vitae

Personal Details

Address: David Schaffert
Montenstr. 2
80639 Munich, Germany

Date of birth: 12/04/1980

Place of birth: Wesel

Nationality: German

Marital status: not married

Professional Experience

Ludwig-Maximilians-University, Faculty of Chemistry & Pharmacy, Munich
Dept. Pharmaceutical Biology & Nanomedicine
Scientific Associate/PhD student 02/07 – 08/10

Pharmacy “Max-Weber-Platz-Apotheke”, Munich 04/08 – 04/10

- Part-time pharmacist

International Ludwigs-Pharmacy, Munich 05/06 – 10/06

- Practical training as pharmacist

Scil Technology, Martinsried 11/05 – 04/06

- Practical training as pharmacist

Education

Licensure as pharmacist 12/06

Studies of pharmacy 10/00 – 10/05

Ludwig-Maximilians-University, Munich.

A-levels (Abitur) 9/91 – 06/00

“Nepomucenum”, Coesfeld

8.10 Acknowledgements

Most people believe that a PhD thesis is a solitary expression of a single mind (and generally something only done by funny people). They are wrong. Utterly. A thesis is always a more or less short story of a group of people struggling for scientific truth (or vocational survival). I have to express my thanks to a lot of people and the following list is short of being complete, but I did my best.

I have to thank my supervisor Prof. Dr. Ernst Wagner for giving me the opportunity to perform this work in his research group. I want to express my appreciation for the scientific freedom he granted me and his support for my sometimes absurd ideas. Many thanks for all the support and helpful discussions.

Furthermore I have to thank the “Last Kärntener” Dr. Manfred Ogris for his big repertoire of tasteless jokes (even surpassing mine) and his endless patience whenever the chemist used the FACS machine.

Special thanks go to the members of the IndieLab (Nicole, Markus, Gelja, Miriam) for providing shelter to me and their patience in listening to what they called the worst mixture of music ever. Additionally, I have to thank Nicole for helping me out with the everyday questions when I started.

To the best technicians ever: Melinda and Wolfgang for their patience and assistance during our shared projects. Ursula, Anna for their constant concern regarding my food intake and their encouraging spirit. Marcus for being the funniest German-Croatian mixed blood I ever met. To Olga for her help with the pleasures of university bureaucracy.

Christian D. for numerous hangovers, some of the most frustrating Spicker games in my life and for party-crashing Venice. Christian M. for, hangovers (again), and for introducing me to the Frequency festival (St. Pölten, Austria) and numerous pool rounds in the Bavaria casino. Special thanks go to my “meatbuddy” Arzu for BBQ support and “funny times” and to Rebekka for being a voice of reason in an otherwise mad environment. Prajakta for adopting me and her freshers guide to Indian customs (especially food). Irene for being the best Spanish visiting scientist ever (Qué raro!) and her patience in teaching me the correct pronunciation of Spanish swearwords. Martina for never giving up on me in cultural and in opera related topics. To Naresh (king of the dudes) for his “laid back” attitude – science was fun with you. Thomas I have to thank for performing countless siRNA transfections and his enthusiasm in doing so.

To Dr. Lars Allmendinger and the members of the Analytical Department, without their help this thesis would never have ended.

Thanks to the workgroup of Prof. Wanner personified by Jörg, Thomas and Lars for accepting me as “synthetic biologist” and their help in numerous work and non-work related issues. I have to express my gratitude to Roche Kulmbach for numerous MALDI related experiments and the opportunity to discuss nucleic acid-chemistry related topics with them.

To the newbies (Alex, Claudia, Laura, Raphaela, Flo, Daniel, Uli) - may your stay in the lab be short and productive. To Andi for discussions and some really good concerts. Stefan Prill for his help with the beloved MALDI machine. My master/bachelor/internship students Andrea, Christina, Dana, Johanna, Miriam, Nidhi, Ben, Michi, Nils, Matthias, Stasi for their work, without your help (especially Christinas and Andreas) this thesis would not exist.

Eva for being there. On every day. During every result.

Special thanks go to the “Herzogliches Brauhaus Tegernsee” for liquid support during my thesis and to the Zündfunk for providing the soundtrack to it.

